

University of Kentucky

UKnowledge

Theses and Dissertations--Molecular and Cellular Biochemistry

Molecular and Cellular Biochemistry

2023

PROTEIN S IN COAGULATION AND INFLAMMATION

Martha Mega Silvia Sim

University of Kentucky, bal0nz@yahoo.com

Author ORCID Identifier:

 <https://orcid.org/0000-0002-6966-1494>

Digital Object Identifier: <https://doi.org/10.13023/etd.2023.269>

[Right click to open a feedback form in a new tab to let us know how this document benefits you.](#)

Recommended Citation

Sim, Martha Mega Silvia, "PROTEIN S IN COAGULATION AND INFLAMMATION" (2023). *Theses and Dissertations--Molecular and Cellular Biochemistry*. 66.

https://uknowledge.uky.edu/biochem_etds/66

This Doctoral Dissertation is brought to you for free and open access by the Molecular and Cellular Biochemistry at UKnowledge. It has been accepted for inclusion in Theses and Dissertations--Molecular and Cellular Biochemistry by an authorized administrator of UKnowledge. For more information, please contact UKnowledge@lsv.uky.edu.

STUDENT AGREEMENT:

I represent that my thesis or dissertation and abstract are my original work. Proper attribution has been given to all outside sources. I understand that I am solely responsible for obtaining any needed copyright permissions. I have obtained needed written permission statement(s) from the owner(s) of each third-party copyrighted matter to be included in my work, allowing electronic distribution (if such use is not permitted by the fair use doctrine) which will be submitted to UKnowledge as Additional File.

I hereby grant to The University of Kentucky and its agents the irrevocable, non-exclusive, and royalty-free license to archive and make accessible my work in whole or in part in all forms of media, now or hereafter known. I agree that the document mentioned above may be made available immediately for worldwide access unless an embargo applies.

I retain all other ownership rights to the copyright of my work. I also retain the right to use in future works (such as articles or books) all or part of my work. I understand that I am free to register the copyright to my work.

REVIEW, APPROVAL AND ACCEPTANCE

The document mentioned above has been reviewed and accepted by the student's advisor, on behalf of the advisory committee, and by the Director of Graduate Studies (DGS), on behalf of the program; we verify that this is the final, approved version of the student's thesis including all changes required by the advisory committee. The undersigned agree to abide by the statements above.

Martha Mega Silvia Sim, Student

Dr. Jeremy Paul Wood, Major Professor

Dr. Trevor Creamer, Director of Graduate Studies

PROTEIN S IN COAGULATION AND INFLAMMATION

DISSERTATION

A dissertation submitted in partial fulfillment of the
requirements for the degree of Doctor of Philosophy in the
College of Medicine
at the University of Kentucky

By

Martha Mega Silvia Sim

Lexington, Kentucky

Co- Directors: Dr. Jeremy Paul Wood, Assistant Professor of Internal Medicine
and Dr. Sidney Waldo Whiteheart, Professor of Molecular and Cellular Biochemistry

Lexington, Kentucky

2023

Copyright © Martha Mega Silvia Sim 2023
<https://orcid.org/0000-0002-6966-1494>

ABSTRACT OF DISSERTATION

PROTEIN S IN COAGULATION AND INFLAMMATION

Protein S (PS) is a key regulator, which links inflammation and coagulation and performs multiple proposed functions in both processes. PS exists in the blood as a free soluble form (~40%), bound to complement component 4b-binding protein/ C4BP (~60%), and packaged in platelet α -granules (~2.5%). Subendothelial tissue factor (TF), upon exposure to blood, initiates coagulation, a proteolytic cascade which results in the activation of thrombin, the enzyme responsible for formation of a fibrin clot. PS is a critical anticoagulant that inhibits multiple steps of this process. Only the free fraction of PS has full anticoagulant properties, as C4BP blocks this activity. PS also negatively regulates complement system activation via its association with C4BP, and is a ligand for the anti-inflammatory TAM (Tyro3, Axl, and Mer) tyrosine kinase receptors expressed by monocytes, macrophages and other cell types. Congenital deficiency of PS is rare in the general population and is associated with increased thrombotic risk, whereas acquired PS deficiency commonly occurs secondary to several viral infections, including HIV-1 and SARS-CoV-2, both of which are associated with an increased risk of life-threatening thrombotic events. The mechanisms of this deficiency and its association with thrombosis are unclear.

HIV-1-infected individuals have an ~10-fold increased risk for thromboembolic diseases, and antiretroviral therapy does not reduce this risk. While HIV-1 infection is associated with various hematological changes, acquired PS deficiency is the most common coagulation abnormality, occurring in up to 76% of infected individuals. PS deficiency correlates with disease progression, and both total and free plasma PS are decreased. However, despite this high prevalence, its pathologic consequences were unclear because PS concentration does not correlate with plasma thrombin generation *ex vivo*. We developed a PS-sensitive plasma thrombin generation assay, utilized it to measure thrombotic potential in HIV-1 patient plasmas, and showed that plasma PS negatively correlates with and contributes to the thrombotic risk in this population.

SARS-CoV-2 infection (COVID-19) is associated with a much higher thrombotic risk than HIV-1, occurring in up to 30% of hospitalized patients. We identified a specific deficiency of free PS in COVID-19 patients, which was not explained by known PS-binding proteins, such as C4BP. We next determined that this free PS deficiency is caused by a shear-dependent interaction with von Willebrand Factor (VWF), a previously unrecognized PS-binding protein. Using mass spectrometric and immunoblotting analyses we showed that PS binding to VWF is increased >10,000,000-fold by shear-induced unfolding of VWF, and that sheared VWF dose-dependently inhibits free PS, but not total PS, antigen measurements and interferes with PS anticoagulant activity. Thus, we identified a novel mechanism of acquired PS deficiency, which occurs in COVID-19 patients, reducing the available anticoagulant pool and

shifting the hemostatic balance. This mechanism also likely contributes to PS deficiency in other inflammatory conditions where vascular shear flow is elevated, including viral infections and autoimmune diseases.

The goal of this thesis is to identify the molecular and cellular mechanisms of anticoagulant PS deficiency and its contribution to virus-associated thrombotic risk, using HIV-1 and SARS-CoV-2 as models. In addition, we also evaluated the contribution of procoagulant Tissue Factor (TF), which is the initiator of coagulation often elevated during inflammation, to thrombotic risk, not only in viral infections but also in traumatic brain injury. This study, which utilizes novel assays including PS-sensitive thrombin generation, provides new insights into the molecular mechanisms of thrombosis in viral infections in general and in HIV-1 and SARS-CoV-2 specifically, and informs on the potential of PS as a biomarker, and on potential therapeutic approaches. We provided the first description of VWF-dependent PS deficiency and are now working to fully understand its physiological and pathological implications. Based on our results, it is likely that this interaction contributes to the thrombotic events that are among the leading causes of death in this pandemic, and may contribute to thrombosis in many other inflammatory conditions that share similar features to COVID-19. Finally, the implications extend beyond pathological conditions. VWF is exposed to shear and unfolds at injury sites as part of the normal hemostatic response, so the VWF-PS interaction may represent a regulatory step in normal clot formation, which we are only now beginning to recognize.

KEYWORDS: Protein S deficiency, immunothrombosis, viral infection, HIV, SARS-CoV-2, von Willebrand Factor, traumatic brain injury

Martha Mega Silvia Sim

05/05/2023

Date

PROTEIN S IN COAGULATION AND INFLAMMATION

By
Martha Mega Silvia Sim

Jeremy Paul Wood

Co-Director of Dissertation

Sidney Waldo Whiteheart

Co-Director of Dissertation

Trevor Creamer

Director of Graduate Studies

05/05/2023

Date

DEDICATION

To my family

ACKNOWLEDGMENTS

First and foremost, I would like to express my utmost gratitude and my deepest respect to my mentor, Dr. Jeremy Wood, for his expertise and support in helping me with the work presented in this dissertation. He has been incredibly patient and understanding with my training, with an enviably positive outlook and infectious enthusiasm for science. It has been my absolute privilege to receive guidance from such an excellent scientist and communicator, and I genuinely appreciate the encouragement he gave me when making career decisions. I am incredibly grateful to all members of my dissertation committee; my co-mentor Dr. Wally Whiteheart, Dr. Rebecca Dutch, Dr. Beth Garvy, and the late Dr. Susan Smyth. Their multidisciplinary expertise and wisdom assisted me tremendously in this project. I will never forget the life advice Dr. Smyth gave me during our last committee meeting. Special thanks for Dr. Val Adams for being my outside examiner, Dr. Trevor Creamer for all the help I received as a graduate student in the department, and Dr. Erin Garcia for her mentorship during my master's program.

I am thankful to past and present lab members of the Wood and Whiteheart lab. I want to give special thanks to Dlovan D.Mahmood, Xiaohong Song, and Dr. Xian Li, for your support and contribution for my project. I am incredibly thankful to Shravani Prakhya and Dr. Daniëlle Coenen for helping me with the microfluidics experiments and Dr. Meenakshi Banerjee, Hammodah Alfar, and Chi Peng for helping me with sample collection, processing, and experiments for this project. I am thankful to all the collaborators who

made the work in this dissertation possible. I am thankful to Dr. José López and his lab members in the University of Washington and Bloodworks Northwest Research Institute for their support and expertise, Dr. Molly Mollica for performing the microfluidics, and Dr. Dominic Chung for performing the nano-LC-MS/MS for this project. I am thankful to all the collaborators in the University of Kentucky College of Medicine Virus-Induced Thrombosis Alliance (VITAL), Melissa Hollifield, Siva Gandhapudi, and Dr. Jerold Woodward in the Department of Microbiology, Immunology and Molecular Genetics, Dr. Zach Porterfield and Ryan Weeks in the division of Infectious Disease, and Dr. Kenneth Campbell, Dr. Jamie Sturgill, Gail Sievert, and Marietta Barton-Baxter in the Center of Clinical and Translational Science, for assisting with patient recruitment, sample collection, and various experiments related to this project. I am thankful to the members of the Saha Cardiovascular Research Center Smyth and Morris lab, Li lab, Daugherty lab, and Dr. Congqing Wu, and to the members of the Versiti Blood Research Institute and Medical College of Wisconsin Cheesehead Clotters Club, Dr. Alan Mast, and Dr. Ze Zheng, for supporting this project with their expertise and technical contributions. I learned so much from all of you.

Finally, thank you to my friends and family members for your prayers and support over the years. Special thanks to the University of Kentucky Badminton Club members. Lastly, I would also like to thank the American-Indonesian Exchange Foundation and the Fulbright program, for I would not have accomplished this without them.

TABLE OF CONTENTS

ACKNOWLEDGMENTS	iii
LIST OF TABLES	ix
LIST OF FIGURES	x
LIST OF ABBREVIATIONS.....	xii
CHAPTER 1. INTRODUCTION	1
1.1 Coagulation system overview.....	1
1.1.1 Primary hemostasis.....	1
1.1.2 Secondary hemostasis.....	2
1.1.3 Anticoagulation	5
1.1.3.1 PS cofactor activity with TFPI.....	7
1.1.3.2 PS cofactor activity with APC	8
1.1.3.3 PS direct anticoagulant activity.....	10
1.1.4 Other regulators of coagulation	10
1.2 PS roles in coagulation and inflammation	11
1.2.1 PS biology.....	12
1.2.1.1 PS synthesis and regulation	14
1.2.1.2 Structural features of PS	17
1.2.1.3 Congenital PS deficiency	19
1.2.2 PS non-anticoagulant functions	22
1.2.2.1 PS with C4BP	22
1.2.2.2 PS with TAM receptors	23
1.3 Immunothrombosis overview.....	30
1.3.1 Interplay between coagulation and inflammation	30
1.3.2 Immunothrombosis mechanisms in inflammatory conditions	31
1.3.2.1 Immunothrombosis in HIV-1 infection.....	32
1.3.2.2 Immunothrombosis in SARS-CoV-2 infection.....	35
1.3.2.3 Immunothrombosis in traumatic brain injury	37
1.3.3 Acquired PS deficiency secondary to inflammation	38
1.3.3.1 Acquired PS deficiency in HIV-1 infection	39
1.3.3.2 Acquired PS deficiency in SARS-CoV-2 infection	40
1.3.4 TF biology.....	49
1.3.4.1 TF structure and function	49
1.3.4.2 TF synthesis and regulation	51
1.3.4.3 TF roles in immunothrombosis	55

1.3.5	VWF biology	56
1.3.5.1	VWF structure and function.....	59
1.3.5.2	VWF synthesis and regulation.....	60
1.3.5.3	VWF roles in immunothrombosis	62
1.4	The focus of this dissertation.....	63
CHAPTER 2. MATERIALS AND METHODS.....		64
2.1	Materials	64
2.2	Methods	64
2.2.1	Human subject study approval and blood collection	64
2.2.2	Plasma tissue factor activity.....	66
2.2.3	Plasma thrombin generation.....	67
2.2.4	Enzyme-linked Immunosorbent Assays.....	68
2.2.5	Spike protein IgG measurement.....	69
2.2.6	Flow cytometry	69
2.2.7	Thioflavin T staining	70
2.2.8	Native PAGE and immunoblotting.....	71
2.2.9	SDS PAGE and immunoblotting.....	71
2.2.10	VWF multimer analysis.....	72
2.2.11	Identification of VWF-binding proteins	73
2.2.12	VWF cleavage by ADAMTS13	74
2.2.13	VWF/PS complex ELISA	74
2.2.14	Microfluidics.....	75
2.2.15	Animal study approval and mouse TBI experiments	76
2.2.16	Mouse Factor VIIa activation.....	78
2.2.17	Platelet activation	78
2.2.18	Factor Xa activity assay	79
2.2.19	Continuous thrombin generation assay	79
2.2.20	Discontinuous thrombin generation assay.....	80
2.2.21	FVa cleavage by APC.....	80
2.2.22	Statistical analysis	81
CHAPTER 3. TOTAL PLASMA PROTEIN S IS A PROTHROMBOTIC MARKER IN PEOPLE LIVING WITH HIV		82
3.1	Introduction.....	83
3.2	Results.....	86
3.2.1	Study population	86
3.2.2	Total plasma PS is reduced in untreated PLWH.....	90
3.2.3	Free PS and PC show trends toward depletion	94
3.2.4	Development of a PS-sensitive TG assay	97
3.2.5	Plasma PS deficiency correlates with increased TG.....	100
3.2.6	Antiretroviral treatment has no direct effect on plasma TG	107

3.2.7	Plasma TF activity does not correlate with TG	111
3.3	Conclusions.....	115
CHAPTER 4. VON WILLEBRAND FACTOR CONTRIBUTES TO FREE PROTEIN S DEFICIENCY IN COVID-19		116
4.1	Introduction.....	118
4.2	Results	119
4.2.1	Study population	119
4.2.2	Thromboinflammatory markers in COVID-19 patients.....	121
4.2.3	Free PS deficiency cannot be explained by known PS-binding proteins..	125
4.2.4	Free PS deficiency correlates with higher thrombotic potential	128
4.2.5	Protein S has multiple binding partners in plasma	133
4.2.6	VWF is elevated in COVID-19 patients.....	136
4.2.7	VWF interacts with PS in a shear-dependent manner	139
4.2.8	PS/VWF complex is stable under arterial flow conditions	147
4.2.9	VWF/PS complex forms under flow, in a calcium-sensitive manner	149
4.3	Conclusions.....	154
CHAPTER 5. TISSUE FACTOR RELEASE FOLLOWING TRAUMATIC BRAIN INJURY CONTRIBUTES TO THROMBOSIS IN MICE		155
5.1	Introduction.....	156
5.2	Results	158
5.2.1	Development of mouse plasma TF activity assay	158
5.2.2	Post-TBI plasma TG is not altered when exogenous TF is added.....	160
5.2.3	Post-TBI TG is not mediated by increased PL	162
5.2.4	Acute TF release post-TBI drives TG	164
5.2.5	Early increase in TF is observed in mild TBI model	167
5.3	Conclusions.....	169
CHAPTER 6. DISCUSSION		170
6.1	Part I: Total Protein S Deficiency in HIV Infection	170
6.2	Part II: Free Protein S Deficiency in COVID-19 Infection	174
6.3	Part III: Tissue Factor Release in TBI-Associated Inflammation.....	179
CHAPTER 7. SUMMARY AND FUTURE DIRECTIONS		182
7.1	Summary	182
7.2	Significance.....	184
7.3	Future Directions	188

APPENDICES	191
APPENDIX I. SHEARED VWF PARTIALLY INTERFERES WITH PS ANTICOAGULANT COFACTOR ACTIVITY.....	191
Introduction	191
Results and discussion	191
1. Sheared VWF interferes with TFPI α -cofactor activity of PS.....	191
2. Sheared VWF has minimal effect on APC/PS prothrombinase inhibitory activity.....	193
3. The effect of sheared VWF on FVa-cleavage by APC/PS might be context dependent.....	196
4. The effect of sheared VWF on APC/PS prothrombinase inhibition on activated platelet surface shows donor variability	198
Conclusions.....	201
APPENDIX II. LONGITUDINAL OBSERVATIONS OF COVID-19 PATIENT STUDY.....	202
Introduction	202
Results and discussion	203
1. Reduction in free PS recovers after three months, except in a subset of outpatients.....	203
2. Elevation of the ETP ratio recovers after three months	205
Conclusions.....	207
REFERENCES	208
VITA	236

LIST OF TABLES

Table 1.1. Phenotypes of relevant transgenic mice.....	21
Table 3.1. Description of HIV-1 study population.....	88
Table 3.2. Therapeutic regiment of ART-treated patients	89
Table 4.1. Description of COVID-19 study population	120

LIST OF FIGURES

Figure 1.1. Overview of the coagulation cascade	4
Figure 1.2. Protein S anticoagulant functions.....	6
Figure 1.3. Diverse functions of Protein S.....	13
Figure 1.4. Domain configuration of PS and predicted interaction sites	18
Figure 1.5. Protein S-Mer tyrosine kinase receptor signaling pathways.....	27
Figure 1.6. Possible mechanisms of acquired PS deficiency in COVID-19	43
Figure 1.7. Possible causes of specific free Protein S deficiency in COVID-19	48
Figure 1.8. Domain organization and multimerization of VWF monomer	58
Figure 3.1. Schematic of protein S role in APC pathway.....	85
Figure 3.2. Total plasma PS is deficient in PLWH	91
Figure 3.3. Analyses of age-dependent PS differences.....	93
Figure 3.4. Free PS and PC show similar trend toward depletion	95
Figure 3.5. Development of PS-sensitive TG assay	98
Figure 3.6. Plasma PS deficiency correlates with increased TG	102
Figure 3.7. There is no correlation between total PS and lag time when TM is supplemented	104
Figure 3.8. Free PS and PC negatively correlate with plasma TG when TM is supplemented	105
Figure 3.9. ART had no direct effect on plasma TG in PLWH	108
Figure 3.10. ART had no direct effect on plasma TG in healthy plasma <i>in vitro</i>	109
Figure 3.11. Plasma TF activity is not increased in PLWH	112
Figure 3.12. Plasma TF activity does not correlate with TG unless no exogenous TF is added	114
Figure 4.1. COVID-19 inpatients show signs of immunothrombosis.....	123
Figure 4.2. Free PS deficiency in COVID-19 patients is not explained by increases in known PS-binding proteins	126
Figure 4.3. Free PS deficiency contributes to higher thrombotic potential in COVID-19 patients	129
Figure 4.4. Plasma TG in COVID-19 inpatients shows less APC/PS activity	131

Figure 4.5. Native gel electrophoresis shows that PS has many binding partners in plasma	134
Figure 4.6. Plasma VWF is higher in patients with severe COVID-19	137
Figure 4.7. VWF interacts with PS in a shear-dependent manner	141
Figure 4.8. PS co-migrates with lower molecular weight VWF multimers.....	143
Figure 4.9. Sheared VWF interferes with free PS measurements.....	144
Figure 4.10. Shearing does not interfere with VWF ELISA measurements	146
Figure 4.11. PS/VWF complex is stable under arterial flow conditions	148
Figure 4.12. VWF interacts with PS under flow in a calcium-dependent manner.....	150
Figure 4.13. Time-lapse images of VWF interaction with PS under flow	152
Figure 5.1. Development of mouse plasma TF activity assay	159
Figure 5.2. Post-TBI plasma TG is not altered when exogenous TF is added	161
Figure 5.3. Post-TBI TG is not mediated by increased PL.....	163
Figure 5.4. Acute TF release post-TBI drives TG in severe TBI model	165
Figure 5.5. Early increase in TF is observed in mild TBI model	168
Figure 7.1. The roles of PS/VWF shear-dependent interaction in hemostasis and thrombosis	187
Figure 8.1. Sheared VWF dose dependently reverses FXa inhibition by TFPI α /PS.....	192
Figure 8.2. Sheared VWF had minimal impact on APC/PS prothrombinase inhibitory activity.....	194
Figure 8.3. The impact of sheared VWF on FVa cleavage by APC/PS might be context dependent.....	197
Figure 8.4. The effect of sheared VWF on APC/PS prothrombinase inhibition on platelet surface shows donor variability.....	199
Figure 8.5. Longitudinal observation of free PS in COVID-19 outpatients	204
Figure 8.6. Longitudinal observation of ETP ratio in COVID-19 outpatients	206

LIST OF ABBREVIATIONS

ADAMTS13	A disintegrin and metalloprotease with thrombospondin motif, member 13
AIDS	Acquired Immunodeficiency Syndrome
APC	Activated Protein C
ART	Antiretroviral treatment
C3	Complement component 3
C4BP	Complement component 4b-binding protein
C5a	Complement component 5a
CAT	Calibrated Automated Thrombography
COVID-19	Coronavirus Disease 2019
CCI	Controlled Cortical Impact
CHI	Closed Head Injury
DVT	Deep vein thrombosis
EC	Endothelial cell
EGF	Epidermal Growth Factor
EPCR	Endothelial Cell Protein C Receptor
ETP	Endogenous Thrombin Potential
EV	Extracellular vesicles
FII	Coagulation factor II (also prothrombin)
FV	Coagulation factor V
FVII	Coagulation factor VII

FVIII	Coagulation factor VIII
FIX	Coagulation factor IX
FX	Coagulation factor X
Gas6	Growth arrest-specific factor 6
LG	Laminin G
PAI	Plasminogen Activator Inhibitor
PAR	Protease-Activated Receptor
PBDMs	Peripheral blood-derived macrophages
PBMCs	Peripheral blood mononuclear cells
PC	Protein C
PL	Phospholipids (phospholipid vesicles)
PLA	Platelet-leukocyte aggregation
PLWH	People Living with HIV
PPP	Platelet-poor plasma
PS	Protein S
PtdSer	Phosphatidylserine
PZ	Protein Z
SARS-CoV-2	Severe Acute Respiratory Syndrome Coronavirus 2
SHBG	Sex Hormone Binding Globulin
TAFI	Thrombin-Activatable Fibrinolysis Inhibitor
TAM	Tyro3, Axl, Mer
TBI	Traumatic Brain Injury

TF	Tissue Factor
TFPI	Tissue Factor Pathway Inhibitor
TG	Thrombin generation
TM	Thrombomodulin
tPA	Tissue-type Plasminogen Activator
TSR	Thrombin Sensitive Region
uPA	Urokinase-type Plasminogen Activator
VTE	Venous thromboembolism
VWD	von Willebrand Disease
VWF	von Willebrand Factor
WPBs	Weiber-Palade bodies
ZPI	Protein Z-dependent Protease Inhibitor

CHAPTER 1. INTRODUCTION

1.1 Coagulation system overview

The average human adult has about 5 liters of blood in his or her body. Blood consists of cells (red blood cells, white blood cells, and platelets; ~45%), suspended in plasma (~55%), surrounded by a wall of endothelial cells (ECs). Plasma consists of ~90% water along with various proteins, including an array of coagulation factors. Blood coagulation or clotting occurs as soluble fibrinogen is converted to an insoluble fibrin clot, changing blood from a liquid to gelatinous form. This process involves both cellular components (platelets) and protein components (coagulation factors). Hemostasis, derived from the Greek *haima* (blood) and *stasis* (stopping), is the bodily response to stop bleeding and the loss of blood. As a response to blood vessel injury, primary and secondary hemostasis processes occur, involving platelet and coagulation cascade activation, with the goal of patching the injury site with a platelet and fibrin clot, or thrombus, in order to stop the bleeding [1]. Thrombosis is the formation of a thrombus within a blood vessel, which may partially or completely block the flow of blood.

1.1.1 Primary hemostasis

Primary hemostasis promptly occurs within seconds to minutes after injury. This involves platelet plug formation, generated via platelet adhesion, activation, and aggregation [2]. Platelets are anucleate cellular fragments derived from megakaryocytes in the bone marrow, which circulate in the blood at $150\text{-}450 \times 10^6$ platelets/mL. Platelets contain three types of secretory organelles: (1) α -granules, which store various proteins including coagulation factors V and Va (FV/Va), FXI, Protein S (PS), and von Willebrand Factor

(VWF); (2) dense granules, which store ADP and calcium, among other small molecules and ions; and (3) lysosomes, which store hydrolases. Upon vascular injury, platelets adhere to exposed subendothelial collagen, VWF, and other components of the extracellular matrix, which serve as initial agonists for their activation. As platelets activate, they secrete their granule contents, such as ADP and thromboxane A₂, which activate additional platelets and grow the platelet clot. This also results in the activation of the integrin $\alpha_{IIb}\beta_3$. Fibrinogen then binds to activated $\alpha_{IIb}\beta_3$ receptor on platelets, forming fibrinogen bridges to aggregate platelets, resulting in an unstable platelet clot [2]. The clot is stabilized through secondary hemostasis.

1.1.2 Secondary hemostasis

Secondary hemostasis, also called the coagulation cascade, occurs concurrently with primary hemostasis, with the goal of fibrin generation on the surfaces of platelets and endothelium within the injury site, which then crosslinks platelets and traps other blood cells, creating a more stable fibrin clot (Figure 1.1).

Under hemostatic conditions, the extrinsic or tissue factor pathway is initiated by exposure of the extravascular membrane protein Tissue Factor (TF) to flowing blood [3]. TF binds circulating coagulation factor VIIa (FVIIa), forming *extrinsic tenase*, and promotes the activation of factors IX and X to factors IXa (FIXa) and Xa (FXa), respectively [4]. FIXa, in complex with factor VIIIa (FVIIIa), forming *intrinsic tenase*, activates additional FXa. In the alternative contact pathway, sequential activation of FXII, FXI, and FIX also leads to the *intrinsic tenase* formation [5]. The contact pathway is activated when blood comes into contact with negatively charged surfaces such as artificial biomaterials or microbial

surfaces [5]. FXa forms the *prothrombinase* complex with factor Va (FVa), which generates thrombin from its precursor prothrombin [6]. Thrombin is the serine protease that converts fibrinogen to fibrin, among other functions. In the initiation phase of coagulation, TF-FVIIa activity leads to a small amount of thrombin generation at the site of injury. In the propagation or amplification phase, this initial thrombin primes subsequent coagulation reactions through feedback activation of FV, FVII, FVIII, and FXI along with activation of platelets [7]. Activated platelets, ECs, and other cell types, as well as plasma membrane-derived microvesicles, express phosphatidylserine (PtdSer), providing the negatively charged phospholipid membranes necessary for coagulation reactions to take place; calcium ions bind to the negatively charged phospholipids and enable the assembly of the coagulation complexes. Thrombin activates circulating fibrinogen by cleavages at the ends of fibrinogen A and B chains, allowing fibrin to polymerize and aggregate laterally [7]. Thrombin also activates FXIII in a proteolytic reaction that is enhanced by fibrin. Fibrin molecules self-associate to form a fibrin clot and are covalently cross-linked by the transglutaminase factor XIIIa, generating a stable fibrin clot [8].

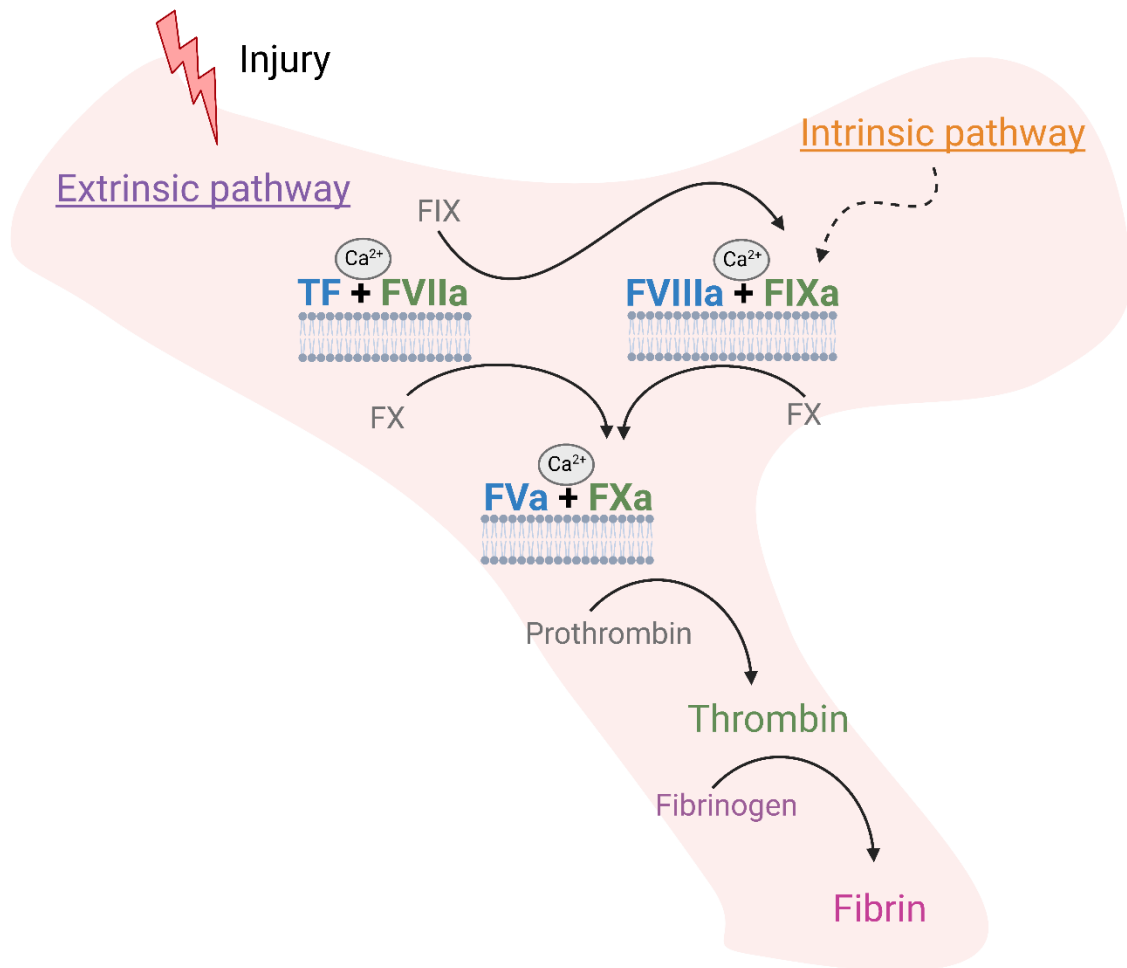


Figure 1.1. Overview of the coagulation cascade

Overview of the coagulation cascade, showing basic components of extrinsic and intrinsic tenase, prothrombinase complex, with the goal of thrombin activation and fibrin generation. The zymogens (shown in grey): FIX = factor IX; FX = factor X; and prothrombin (FII) The serine proteases (shown in green): FVIIa = factor VIIa; FIXa = factor IXa; FXa = factor Xa. The cofactors (shown in blue): TF = Tissue Factor; FVa = factor Va; FVIIIa = factor VIIIa. Image created with BioRender.com.

1.1.3 Anticoagulation

As excessive or insufficient thrombin generation leads to thrombosis or bleeding, respectively, the coagulation system is tightly regulated by anticoagulants, including TF pathway inhibitor (TFPI), activated Protein C (APC), and Protein S (PS) [3] (Figure 1.2). We will be focusing on the many anticoagulant functions of PS, as a cofactor for TFPI and APC and through direct anticoagulant activity.

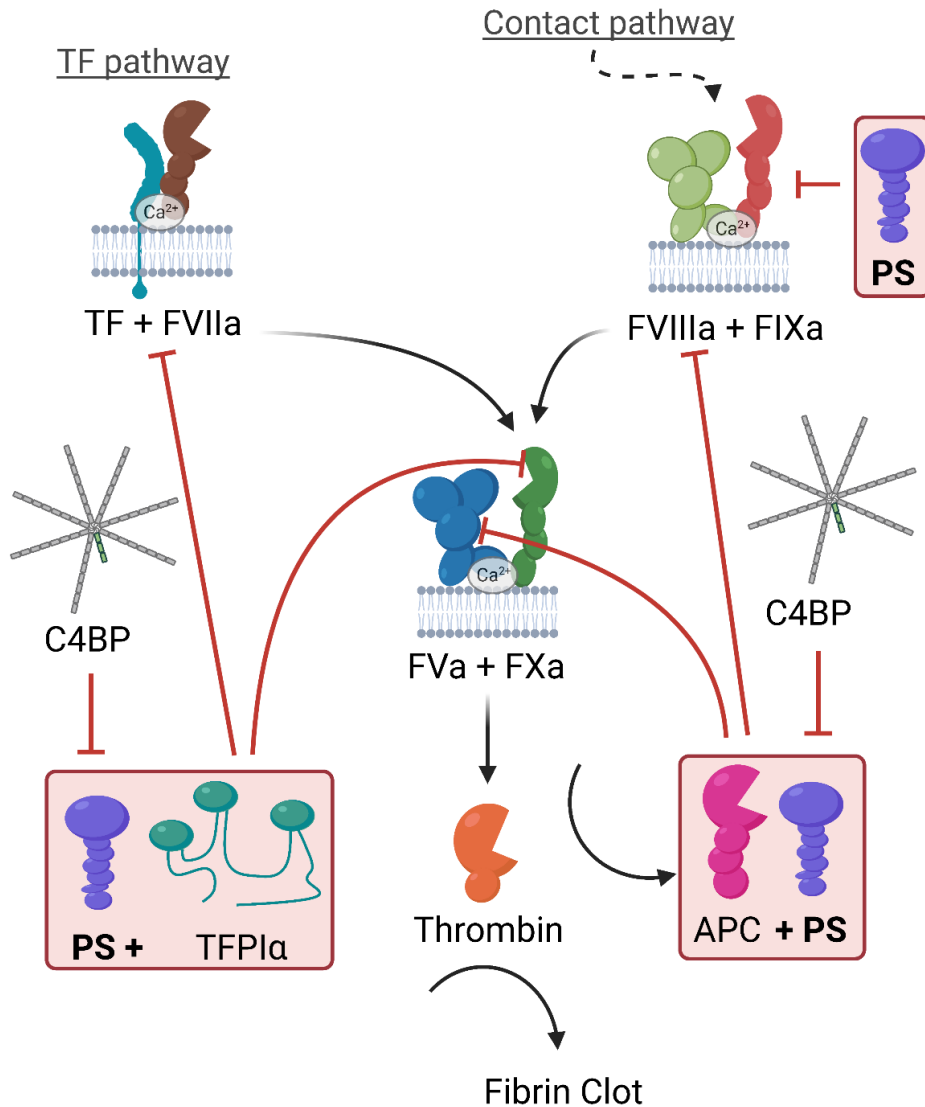


Figure 1.2. Protein S anticoagulant functions.

Protein S anticoagulant functions. Protein S is a master anticoagulant regulating all three coagulation complexes, via its cofactor function with Tissue Factor Pathway Inhibitor- α (TFPI α) and activated Protein C (APC), and its direct anticoagulant activity. (TF = Tissue Factor; FVIIa = factor VIIa; FVIIIa = factor VIIIa; FIXa = factor IXa; FVa = factor Va; FXa = factor Xa; C4BP = complement component 4b-binding protein). Image created with BioRender.com.

1.1.3.1 PS cofactor activity with TFPI

The anticoagulant TFPI is the main inhibitor of the extrinsic pathway of coagulation. It inhibits VIIa and FXa by binding to the TF/FVIIa/FXa ternary complex [9]. TFPI is produced by endothelial cells (ECs) as two major isoforms, TFPI α and TFPI β . TFPI β , containing Kunitz-1 (K1), K2, and glycosylphosphatidylinositol (GPI)-anchor-encoding domains, is the major form, and exists as a membrane-associated protein, anchored to cell surfaces via GPI linkages [10]. Out of ~2 nM total TFPI in plasma, ~10-20% is the full-length TFPI α isoform, consisting of K1-K2-K3 domains, which circulates as a free soluble form and as a content of platelet granules [10]. PS binds K3 and is a cofactor for TFPI α , but not TFPI β [11]. Both TF expression and TFPI inhibitory action are constitutive; TFPI rapidly inhibits low levels of TF expressed on activated ECs and monocytes, preventing uncontrolled intravascular thrombosis under a certain physiological threshold [12]. TFPI α , but not TFPI β , is also an early prothrombinase (FVa/FXa) inhibitor [13]. Several studies suggested that the role of PS as cofactor is to bring TFPI α into proximity of the FXa active site on phospholipid surfaces, thereby decreasing the required concentration of TFPI α needed for efficient inhibition of FXa. [14]. PS enhances TFPI α direct inhibition of FXa by ~10 fold [11] and TFPI α inhibition of TF/FVIIa-mediated FXa generation, as well as FXa-dependent inhibition of FIXa generation, by ~9 fold [15].

TFPI also has non-anticoagulant activity, as TFPI α and TFPI β have been reported to exert anti-apoptotic effects and to inhibit angiogenesis, tumor growth, and metastasis [16, 17]. As these effects seem to pertain mainly to TFPI β which does not bind PS, PS may not play a role in these activities.

1.1.3.2 PS cofactor activity with APC

Activated protein C (APC) is another endogenous anticoagulant that is essential for the downregulation of coagulation in the propagation phase of thrombin generation. It does this by inactivating FVa and FVIIIa, the cofactors in the prothrombinase and the intrinsic tenase complexes, respectively. Protein C (PC) and low levels of APC circulate in plasma at ~70 nM and <40 pM concentrations, respectively. PC is a vitamin K-dependent protein homologous to factors VII, IX, and X. PC activation requires the thrombin/thrombomodulin complex and endothelial protein C receptor (EPCR) [18].

Thrombomodulin (TM) is an integral membrane protein expressed on the surface of ECs which binds to thrombin and alters its substrate specificity, blocking the exosites for procoagulant substrates and PAR1, such that thrombin can then bind and activate PC into APC [19]. TM is a required cofactor, amplifying PC activation >1,000-fold. When complexed with TM, thrombin activity in activating fibrinogen, FV, FVII, or platelet protease-activated receptors (PARs) is reduced, and it is inactivated 20 times faster by plasma protease inhibitors. The thrombin-TM complex is also responsible for the activation of thrombin-activatable fibrinolysis inhibitor (TAFI), which interferes with fibrinolysis by modifying fibrin. PC activation by thrombin-TM is further enhanced by ~20-fold via PC binding with EPCR, a PC cell surface receptor expressed by ECs, monocytes, neutrophils, and dendritic cells. Platelet factor 4 (PF4) may augment PC activation further by inducing a conformational change in PC which increases its affinity for thrombin-TM [18].

Once activated, APC dissociates from EPCR and binds PS on phospholipid surfaces, such as on activated platelets and ECs where it inactivates FVa and FVIIIa. APC inactivates FVa by cleavages at Arg306, Arg506, and Arg679; Arg506 cleavage by APC rapidly occurs, whereas Arg306 cleavage is slower but required for complete inactivation [20]. PS enhances APC enzymatic function of FVa inactivation by increasing its binding to negatively charged phospholipids by 2-14-fold, depending on the presence of its substrate FVa [21]. PS increases the rate of proteolysis at Arg306 by 20-30-fold, compared to a 1-5-fold modest enhancement for Arg506 [22]. Factor V Leiden, caused by a single nucleotide polymorphism of Arg506Gln, prevents efficient inactivation of FVa by APC, leading to hypercoagulability [23]. For APC-mediated FVIIIa inactivation, which occurs by cleavages at Arg336 and Arg562 in FVIIIa, PS moderately enhances the rate of reaction by ~1.5 fold, with less clearly defined molecular mechanisms [24]. FV appears to also be a synergistic cofactor for APC/PS inactivation of FVa [25] and FVIIIa [26].

APC also promotes fibrinolysis by neutralizing plasminogen activator inhibitor-1 (PAI-1), the main inhibitor of tissue-type- (tPA) and urokinase-type plasminogen activators (uPA), an activity shown to be dependent on PS, phospholipid, and calcium ions [27]. The APC/EPCR complex also signals through PAR-1 activation, stimulating an anti-inflammatory cytoprotective effect, with other PARs (-2 and -3) participating in different contexts [28]. TM is also expressed by various other cell types, including monocytes, neutrophils, platelets, mesothelial cells, and keratinocytes and during development [18]. Via its lectin-like domain, TM also directly downregulates inflammation by preventing neutrophil adhesion with the ECs, dampening complement activation, and exerting anti-

apoptosis and pro-survival activity via suppression of the MAPK-ERK1/2 pathway [18]. The role of PS in these other activities is unknown.

1.1.3.3 PS direct anticoagulant activity

In addition to being a cofactor for APC and TFPI α , PS also exhibits direct prothrombinase (FVa/FXa) and intrinsic tenase (FVIIIa/FIXa) inhibitor activity. For inhibition of intrinsic tenase, PS might directly impair the assembly of the complex by interacting with FIXa [29]. FIXa, in the absence or presence of FVIIIa, interacts with PS with a K_d of 40 nM, and PS inhibits FX activation by the intrinsic tenase [30]. PS inhibits FIXa in vivo by associating with the FIXa heparin-binding exosite, which requires residues K132, K126 and R170 [31]. These studies demonstrated a role for PS in regulating the propagation step of thrombin generation. Furthermore, a K132A/R170A FIXa mutant, which does not bind PS, causes an increased rate of thrombus formation in Hemophilia B (FIX-deficient) mice, showing the physiological relevance of these mechanisms in maintaining hemostasis and preventing thrombosis [31].

1.1.4 Other regulators of coagulation

The coagulation cascade is a complex, delicately balanced, and tightly regulated process involving dozens of proteins and molecules in the blood, platelets, ECs, and surrounding tissues. Several other regulators of thrombin generation exist. Antithrombin (also called antithrombin III) is a serine protease inhibitor which inactivates the serine proteases thrombin, FVIIa, FIXa, and FXa, and binding to its targets is greatly enhanced by the anticoagulant drug heparin [32]. Inactivation of the proteases results from irreversible binding with antithrombin in which the active site serine of the protease becomes

covalently bonded to antithrombin. This antithrombin-protease complex is then rapidly removed from the circulation by hepatocytes [33]. Another anticoagulant pathway is the protein Z (PZ) and PZ-dependent protease inhibitor (ZPI). PZ is a vitamin K-dependent protein cofactor of ZPI, which inhibits prothrombinase [34]. ZPI inhibits FXa through a similar mechanism as antithrombin and the presence of PZ enhances this process by 1,000-fold; however, many of the details remain to be elucidated [35].

The various components of the fibrinolysis system are also interconnected with the pro- and anticoagulant pathways, determining clot density, stability, and clearance [8]. Fibrin is digested by plasmin, which is activated from the inactive zymogen plasminogen by tissue plasminogen activator (tPA) and urokinase (uPA). Plasminogen, tPA, and uPA circulate in the blood and become incorporated into a growing thrombus due to their affinity for lysine residues on fibrin. This binding can be inhibited by thrombin-activatable fibrinolysis inhibitor (TAFI), which removes lysine plasmin-binding residues on fibrin. Fibrin degradation is also regulated by plasminogen activator inhibitor-1 (PAI-1), which inhibits tPA and uPA activity by active site binding and enhancing their degradation [8]. When cross-linked fibrin is degraded by plasmin, a distinct set of molecular products, including a fragment known as D-dimer, is released [8].

1.2 PS roles in coagulation and inflammation

In 1977, PS was discovered as a new vitamin K-dependent plasma glycoprotein in Seattle, and hence, named after the city of its discovery [36]. PS is an important natural

anticoagulant with multiple proposed functions in regulating coagulation and inflammation [14, 37-40] (Figure 1.3). Here, PS is described in more detail.

1.2.1 PS biology

PS is a Vitamin K-dependent glycoprotein that circulates in plasma as a free soluble form (~40% or ~5-15 mg/L or ~150 nM) or as part of a high-affinity complex with complement component 4b-binding protein/ C4BP (~60% or ~10-20 mg/L or ~300 nM) – bringing the total plasma PS to 15-35mg/L – and is also packaged in platelet alpha-granules (~2.5%) and released upon platelet activation [41-43]. Platelet PS is derived from megakaryocyte expression, resembles plasma PS, and was demonstrated to limit platelet activation and thrombin generation in venous but not arterial thrombosis [43].

PS lacks enzymatic activity and functions primarily as an anticoagulant cofactor by enhancing binding to negatively charged membranes. Here, we review synthesis and regulation of PS, as well as its structural features.

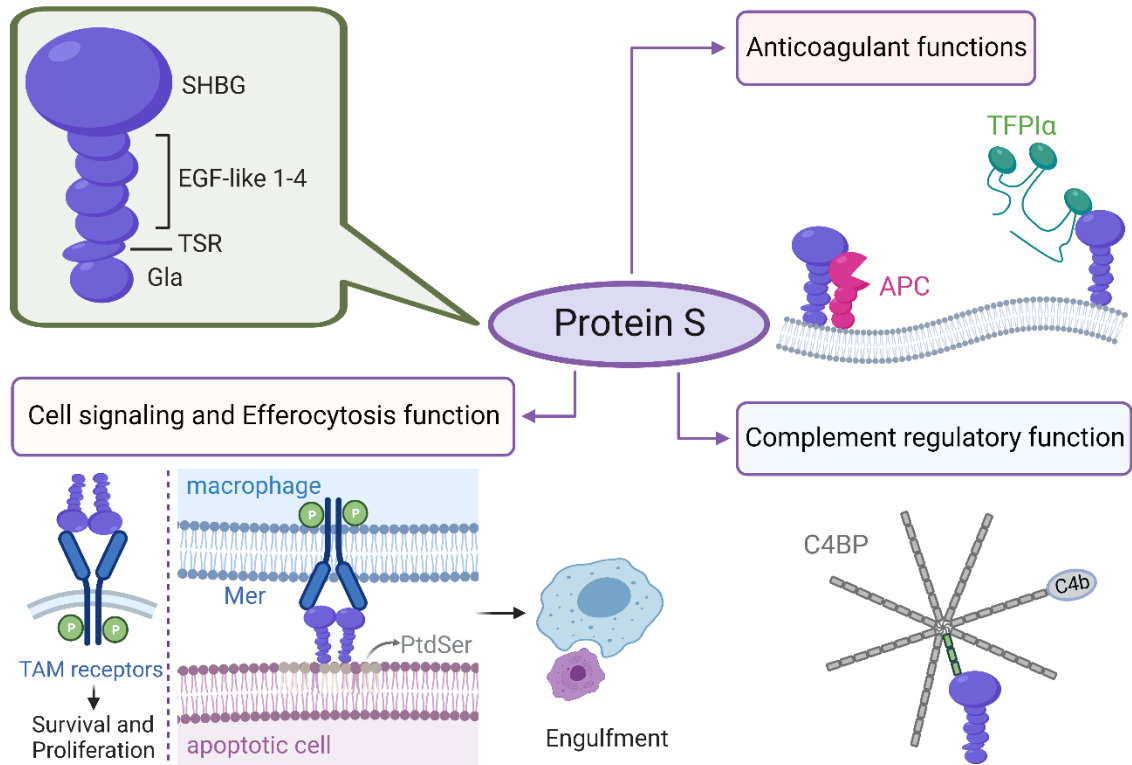


Figure 1.3. Diverse functions of Protein S

Protein S consists of an N-terminal Gla domain, a thrombin sensitive region (TSR), four Epidermal Growth Factor (EGF)-like domains, and a sex hormone binding globulin (SHBG)-like region. These domains provide Protein S with functions in regulating coagulation, complement activation, cell signalling, and efferocytosis. APC = activated Protein C; TFPI α = tissue factor pathway inhibitor- α ; TAM = Tyro3, Axl, Mer; PtdSer = phosphatidylserine; C4BP = complement component 4b-binding protein; C4b = complement component 4b.

Image created with BioRender.com.

1.2.1.1 PS synthesis and regulation

Human PS is a single-chain (75 kDa) glycoprotein of 635 amino acids in its mature form, resulting from post-translational modifications of a 676 amino acids precursor [44]. The human genome contains two PS genes; the active gene *PROS1* or α PS and a pseudogene *PROS2* or β PS, located on chromosome 3 at position 3q 11.1-3q 11.2 [44]. Human PS is encoded by the *PROS1* gene which is composed of 15 exons [44]. Exons 1 and 2 code for a 24-amino acid (aa 1-24) signal peptide, containing a hydrophobic sequence for its targeting to the rough endoplasmic reticulum, and a 16 amino acid (aa 25-41)-propeptide for its carboxylase recognition, which are both removed by proteolytic cleavage prior to secretion. The secreted mature protein contains the Gla domain (aa 42-86 or residues 1-37) encoded by both exon 2 and 3, which contains 11 post-translationally modified γ -carboxyglutamic acid residues which bind to calcium ions [45]. Gla domain carboxylation is required for binding to negatively charged phospholipids and is important for all known functions of PS. Like other vitamin K-dependent proteins (FII, FVII, FIX, FX, PC, and Protein Z), PS Gla-domain carboxylation occurs mainly in the liver, involving γ -glutamyl carboxylase and a reduced form of vitamin K produced by vitamin K epoxide reductase [45]. Exon 4 codes the thrombin sensitive region (TSR; aa 87-113 or residues 46-72), a domain not found in other vitamin K-dependent proteins. The TSR contains two cysteine residues (residues 47 and 72) linked by a disulphide bridge forming a thumb loop motif, with three peptide bonds sensitive to cleavage by thrombin and FXa [46-48]. Cleavage of PS at this region results in the Gla domain remaining linked to the rest of the molecule by a disulphide bond, yet unable to adopt the calcium-dependent conformation required for

phospholipid binding, resulting in a loss of APC cofactor activity [46]. Exons 5 to 8 encode four epidermal growth factor (EGF)-like domains (aa 114-283 or residues 76-242) in tandem, which assist in Ca^{2+} binding by virtue of post-translationally modified amino acids [49]. The first EGF domain contains β -hydroxylated Asp residue while the next three contain β -hydroxylated Asn. Ca^{2+} binding induces conformational changes in these domains that enhance PS anticoagulant functions [49]. In contrast to other vitamin K-dependent coagulation proteins, exons 9 to 15 of PS code for a large domain homologous to sex hormone-binding globulin (SHBG) (aa 284-676), consisting of two laminin G-like modules often found in extracellular matrix components such as laminin and perlecan, and in signaling molecules such as Gas6 and SHBG [50]. This domain contains N-linked glycosylation sites at Asn499, 509, and 530, which are important determinants of PS half-life [51]. PS remains challenging to crystallize, and the only structural determination available to date is limited to the EGF3 and 4 domains, obtained by nuclear magnetic resonance (NMR) [52]. Theoretical models of Gla-TSR-EGF1 and SHBG-like domains have been constructed by computer modelling, based on structural homologies with domains of other vitamin K-dependent coagulation factors and with Gas6, respectively [19, 53].

Functional PS in plasma is mainly synthesized by hepatocytes, although other cells such as megakaryocytes, ECs, Leydig and Sertoli cells, osteoblasts, dendritic cell, macrophages, T cells, vascular smooth muscle cells, and tumor cells also synthesize and secrete PS [40]. As plasma PS circulates as either a free or C4BP- β -bound form, PS concentration is regulated by factors affecting the concentration of either protein. PS synthesis is strongly influenced by hormonal state, liver function, and the presence of intravascular

coagulation consumption, inflammation, or hypoxia. The *PROS1* proximal promoter region contains four consensus binding sites for the transcription factor Sp1, which acts to activate *PROS1* transcription, and two binding sites for Sp3, which may repress transcription [54]. Sp1/Sp3 binding to the *PROS1* promoter might play important dual roles in PS transcription regulation. Estrogen E2 (17beta-estradiol) has been shown to repress *PROS1* transcription via an Sp1-dependent mechanism [55]. Estrogen receptor alpha interacts with Sp1 and recruits nuclear factor receptor-interacting protein 140 (RIP140), which associates with the HDAC3 complex, leading to deacetylation of histones in the *PROS1* promoter, which turns off gene expression [55]. The repressive effect of estrogen is consistent with the general observation that PS concentration is lower in premenopausal females compared to males and is reduced during pregnancy and oral contraceptive use, as well as with higher thrombosis risk seen in these conditions [56]. On the other hand, progestins directly upregulate *PROS1* transcription [57]. Signal transducer and activator of transcription (STAT3) transcription factor is another important activator of the *PROS1* promoter [58]. STAT3 induces transcription by binding to the interleukin (IL)-6 responsive element within the promoter. IL-6, a proinflammatory cytokine upregulated as a part of systemic inflammatory responses, locally stimulates cell survival via STAT3 and PS synthesis within the inflammation site [40, 59]. More recently, hypoxia inducible factor 1 α (HIF1 α), a transcription factor upregulated by hypoxia, has been shown to directly downregulate PS expression in the liver, and to contribute to decreased PS in patients with diabetes [60, 61].

1.2.1.2 Structural features of PS

PS contains an N-terminal Gla domain, a thrombin sensitive region (TSR), four epidermal growth factor (EGF)-like domains, and a sex hormone binding globulin (SHBG)-like region, which consists of two laminin G-type (LG) domains [14] (Figure 1.4). These domains provide PS with functions in the coagulation and inflammatory responses. The Gla domain mediates interaction with membrane phosphatidylserine and is critical for all known functions of PS. TSR renders PS susceptible to cleavage by FXa and thrombin, which abolishes PS activity [62]. The EGF domains bind APC, and the LG domains bind C4BP- β , TFPI α , TAM receptors, and FIXa [14]. Most of the domains of PS have been shown to be important for the APC-cofactor function of PS, with all four EGF domains shown to be involved in their interaction [63-67]. For FV-dependent APC inactivation of FVIIIa, the second laminin G domain was shown to be important [65, 66]. For the inhibition of prothrombinase, it is suggested that residues in the Gla domain are implicated in the interaction with FVa [68] and the TSR region in the interaction with FXa [69], with an unclear mechanism which involves retention of zinc particularly by zinc-containing protein S [70]. The laminin G domains of PS are involved in C4BP [71] and FIX interactions [72] and specifically the first laminin G domain has been shown to mediate TFPI α [73, 74] and TAM receptor interactions [53, 75]. TFPI cofactor function has been shown to be competitively regulated by C4BP [74]. In contrast to APC and TFPI α cofactor activity of PS, PS direct inhibition of prothrombinase is unaffected by C4BP-binding [76]. However, C4BP binding blocks most PS anticoagulant function, and thus free PS is considered to be the anticoagulant pool [77, 78].

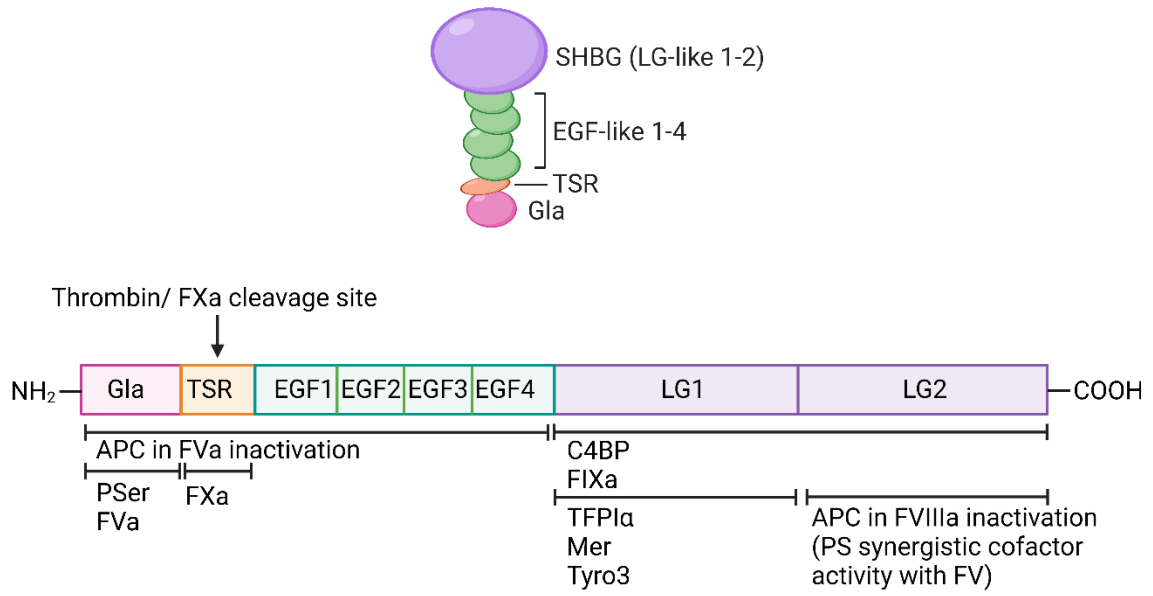


Figure 1.4. Domain configuration of PS and predicted interaction sites

Domain configuration of PS and predicted molecular interaction sites. PS = Protein S; SHBG = sex-hormone binding globulin; EGF = epidermal growth factor; TSR = thombin sensitive region; FXa = factor Xa; LG = laminin G; APC = activated Protein C; FVa = factor Va; P Ser = phosphatidylserine; C4BP = complement component 4b-binding protein; FIXa = factor IXa; TFPI α = tissue factor pathway inhibitor- α ; FVIIIa = factor VIIIa. Image created with BioRender.com.

1.2.1.3 Congenital PS deficiency

PS is a key anticoagulant regulator, congenital deficiency of which is associated with increased thrombotic risk [79]. To date, there are over 360 reported mutations of the *PROS1* gene, resulting in missense or nonsense substitutions, splice site mutations, insertions, or deletions, which might lead to PS deficiency [80]. Homozygous PS deficiency is associated with life-threatening purpura fulminans shortly after birth and heterozygous with a 5-11.5-fold increased risk of thrombosis, most commonly in the form of lower extremity deep vein thrombosis and pulmonary embolism [81, 82]. Hereditary PS deficiency manifests as an autosomal dominant trait and is classified into three subtypes: type I (decreased total PS and free PS concentrations, and PS activity), type II (normal total PS and free PS concentrations, decreased PS activity), and type III (normal total PS, decreased free PS concentration and PS activity). The majority (95%) of patients with hereditary PS deficiency develop type I or III. Genetic studies involving a number of thrombophilic Danish families with PS deficiency type I and III were one of the most robust characterizations of hereditary PS deficiency, uncovering an array of pathogenic to likely-benign variants, with the c.1168G>A mutation in exon 11 resulting in Glu390Lys substitution identified to be the founder variant, present in ~26% of study participants. Another relatively common polymorphism among subjects of European ancestry is PS Herleen (Ser460Pro), which results in reduction of half-life and a type III deficiency [83]. PS Tokushima (Lys155Glu) has also been described, resulting in a slightly higher molecular weight PS with no cofactor activity and a type II deficiency [84].

While genetic PS deficiency in the general population is relatively rare (~0.03-0.13% allelic frequency) [85], it is more prevalent in East Asian populations, and in populations with familial history of venous thrombosis [86]. Several biological factors also influence plasma PS concentration: men have higher free PS and total PS than women, neonates have lower total PS but higher free PS than adults, and total PS increases further with age [87]. Acquired PS deficiency is discussed further in section (1.3.3). Phenotypes of transgenic mouse models relevant to PS [88] and PS functions; Gas6 [89], TAM receptors [90], PC [91], and TFPI [92] are summarized in Table 1.1.

Genotype	Characteristics
PS ^{-/-} (global)	Embryonic lethality (at E.17.5 to full term) by coagulopathy with macroscopic blood clots and extensive hemorrhages, defective vascular development.
PS ^{+/-} (global)	~44% decrease in PS levels, defective vascular development, undescribed effect on inflammation.
PS ^{+/-} (tissue specific)	Hepatocytes PS ^{+/-} mice show 55% decrease in PS level, fibrin deposition in blood vessels. Endothelial and hematopoietic cells PS ^{+/-} mice show 43% decrease in PS level and less severe fibrin deposition. Undescribed effect on inflammation.
Gas6 ^{-/-} (global)	Normal mice without spontaneous bleeding, have defects in platelet aggregation, activation, secretion, and clot stability, protected against venous and arterial thrombosis with reduced clot size and stability, and have pronounced anti-inflammatory phenotype: reduced inflammation upon liver injury, reduced leukocyte and macrophages infiltration, increased fibrosis, with enhanced autoimmunity.
Mer ^{-/-} (global)	Reduced thrombus formation and clot stability, SLE-like autoimmunity, efferocytosis defects leading to blindness (due to impaired phagocytosis of photoreceptor outer segment by retinal pigment epithelial cells), infertility (due to defective spermatogenesis), and enlarged spleen.
Tyro3,Axl,Mer ^{-/-} (global)	More severe phenotype than Mer ^{-/-} , with recurrent thrombosis and bleeding (associated with antiphospholipid antibodies), thrombocytopenia (due to defective megakaryopoiesis), neural degeneration with seizure and paralysis in aged mice.
PC ^{-/-} (global)	Stillbirth or fatal perinatal consumptive coagulopathy, normal development, microvascular thrombosis in the brain and liver.
PC ^{+/-} (global)	Normal phenotype, ~63% PC compared to WT at adult age.
TFPI(K1) ^{-/-} (global)	~60% embryonic lethality (at E9.5-E11.5) with yolk sac hemorrhage, perinatal lethality in survivors beyond E11.5; organ development is normal, central nervous system hemorrhage.
TFPI(K1) ^{+/-} (global)	Normal phenotype, ~50% TFPI activity compared to WT.

Table 1.1. Phenotypes of relevant transgenic mice

Phenotypic characteristics of various relevant knockout mice. PS = protein S; PC = protein C, TFPI(K1) = Tissue Factor Pathway Inhibitor lacking Kunitz domain-1 which is required for TF/FVIIa inhibition; WT = wild type.

1.2.2 PS non-anticoagulant functions

PS also possesses anti-inflammatory functions in addition to its role as an anticoagulant. Here, PS regulatory roles with the complement pathway and anti-inflammatory TAM (Tyro3, Axl, and Mer) receptors are discussed.

1.2.2.1 PS with C4BP

Approximately 60% of plasma PS circulates in a noncovalent high-affinity complex with C4BP, as shown by Dahlbäck and Stenflo using barium citrate adsorption (a method often used to purify vitamin K-dependent plasma proteins) and ion exchange chromatography in 1981 [93]. Only the free fraction of plasma PS has full anticoagulant properties, as C4BP blocks APC and TFPI α cofactor activity of PS [77, 78]. Due to the high affinity interaction (K_d of ~ 0.1 nM), the concentration of free PS is largely dictated by the plasma concentration of C4BP β -chain, the PS-binding component [41, 94, 95]. C4BP is a 570 kDa protein composed of seven α -chains that are the binding sites for C4b and one β -chain that binds PS, held together by disulfide bonds. C4BP is synthesized mainly in the liver with a plasma concentration of ~ 200 mg/L (300 nM) and several isoforms: 7 α -chains and 1 β -chain (the most abundant; 80% or ~ 160 mg/L), 6 α -chains and 1 β -chain, and 6 α or 7 α -chains without β -chain [94, 96]. *In vitro*, successful secretion of C4BP β -chain depends on its intracellular complex formation with PS in the endoplasmic reticulum [94]. C4BP inhibits the C3 convertase, the C4b2b complex of the complement system, by promoting degradation of C4b. C4BP is an acute phase protein and its level may increase up to 4-fold during an inflammatory response [41]. This rise in C4BP largely pertains to an increase in α -chain synthesis, while synthesis of the β -chain is less affected, due to differential

regulation of expression by cytokines [96]. As such, an increase in C4BP during inflammation will not necessarily result in a decrease of free PS.

While the exact function of the PS-C4BP complex is largely unknown, PS is proposed to regulate the complement system by localizing C4BP to negatively charged phospholipids present on the surface of apoptotic cells [97]. PS has been shown to enhance C4BP binding to neutrophils and to control complement activation at sites where coagulation is activated [98]. Cell surface-associated PS-C4BP can bind to C4b and inhibit phagocytosis [99]. C4BP also binds to necrotic cells via PS-PtdSer binding [100]. Furthermore, C4BP binds DNA via a patch of positively charged amino acids on the second component control domain of its α -chains, limiting DNA release from necrotic cells and inhibiting DNA-mediated complement activation *in vitro* [100]. It is unclear whether PS binding affects the C4BP/DNA interaction. Overall, however, the PS/C4BP complex reduces the pro-inflammatory state.

1.2.2.2 PS with TAM receptors

In addition to its functions with C4BP, PS has C4BP-independent anti-inflammatory activity, which is mediated through its SHBG domain. PS and its homolog, growth arrest-specific factor 6 (Gas6), are ligands of TAM (Tyro3, Axl, and Mer) receptor tyrosine kinases, key modulators of the innate immune system and part of an important anti-inflammatory signaling axis [101]. Gas6 is a homolog of PS with identical domain composition and 43% sequence identity. It is widely expressed by endothelium, fibroblasts, and smooth muscle cells and its synthesis can be induced by growth arrest or

serum starvation. It is not expressed by the liver and its plasma concentration is 1,000-fold lower than PS. PS activates Tyro3 and Mer, with limited evidence of effect on Axl, while Gas6 binds to all three TAM receptors [102]. Both proteins interact with the TAM receptors via their SHBG-like region. TAM receptor activation leads to intracellular signaling pathways regulating cell differentiation, metastasis, angiogenesis, and other processes that culminate in cell survival, proliferation, and anti-inflammatory effects [103-106]. PS and Gas6 are also bridging molecules that facilitate binding between exposed phosphatidylserine on apoptotic cells and TAM receptors on macrophages, triggering receptor activation and subsequent cell signaling to promote efferocytosis, the phagocytosis of dead or apoptotic cells, which is essential for normal homeostatic cell-turnover and for clearance of infected cells [107].

Monocytes, macrophages, and all immune cells are shown to express all TAM receptors (Tyro3, Axl, and Mer). All three TAM receptors share structural domains: two extracellular Ig-like domains and fibronectin type III domains, a transmembrane domain, and an intracellular tyrosine kinase domain. Known TAM receptor ligands are: Protein S, Gas6, Tubby, Tubby-like protein-1, and Galectin-3. PS-Mer and Gas6-Axl interactions are of higher affinity and lead to more pronounced effects. New understandings are still emerging for the role of each of these ligands with macrophages.

Signaling pathway of PS-Mer in macrophages (Figure 1.5)

PS-Mer in efferocytosis mediation [107, 108]: A dimer of protein S binds to a homodimer of Mer on macrophages. PS interacts with Mer with its SHBG-domain and with PtdSer on apoptotic cells with its Gla-domain. The binding activates the receptor, causing

autophosphorylation of the intracellular tyrosine kinase domain. The kinase phosphorylates PI3K (phosphatidylinositol-3 kinase), which induces phosphorylation of PIP2 (phosphatidylinositol 4,5-bisphosphate) to PIP3 (phosphatidylinositol 3-4-5-triphosphate), and activation of phospholipase C γ 2 (PLC γ 2), which hydrolyses plasma membrane PIP2 generating diacylglycerol (DAG) and IP3 (inositol 1,4,5-triphosphate). IP3 binds to its receptor on the endoplasmic reticulum and induces calcium cytosolic release, while DAG activates protein kinase C (PKC). This leads to activation of the Rho GTPase Rac1. Activated Mer also directly phosphorylates Vav1, which activates Rac1 and other Rho GTPases Cdc42 and RhoA. Together, these proteins regulate cytoskeleton dynamics and promote engulfment of the apoptotic cell [107].

PS-Mer in anti-inflammatory signaling [109-114]: Mer activation following PS binding leads to the activation of multiple signaling pathways, with certain details still unknown. (1) The tyrosine kinase domain phosphorylates PI3K, which phosphorylates Akt [111]. This leads to glycogen synthase kinase 3 β (GSK3 β) phosphorylation and suppression of NF κ B nuclear translocation. Receptor activation also induces Twist transcriptional repressor activation, which suppresses NF κ B-dependent transcription. The overall cellular outcome is reduced proinflammatory cytokine production and increased anti-inflammatory cytokines by lifting NF κ B inhibition, including stimulating macrophage *GAS6* and *PROS1* expression [112]. (2) Together with Interferon- α/β receptor (IFNAR)/ signal transducer and activator of transcription 1 (STAT1), Mer induces the transcription of suppressor of cytokine signaling protein 1 (SOCS1) and SOCS3, which inhibit cytokine receptor and Toll-Like Receptor (TLR) signaling, resulting in anti-inflammatory effects [110, 114]. (3) Mer

activation also inhibits mitogen activated protein kinase (MAPK), extracellular signal regulated kinase-1 (ERK1)/Erk2, and tumor necrosis factor (TNF)-receptor-associated factor 3 (TRAF3) and TRAF6, which further block NFκB nuclear translocation [109]. Overall, PS- and Gas6-Mer signaling contributes to phenotypic changes or macrophage reprogramming into an M2-like resolution phase phenotype, characterized by a reduction of proinflammatory cytokines and increase in anti-inflammatory cytokines.

Activation of Tyro3 and Mer by PS attenuates the response of macrophages and dendritic cells to pathogens and reduces the secretion of proinflammatory cytokines such as IL-6, TNF, and type 1 interferons [115]. Gas6- or PS-stimulated efferocytosis contains cell death and dampens the innate immune response within the affected tissue, preventing inflammation and autoimmunity and protecting the surrounding healthy tissues [113, 116].

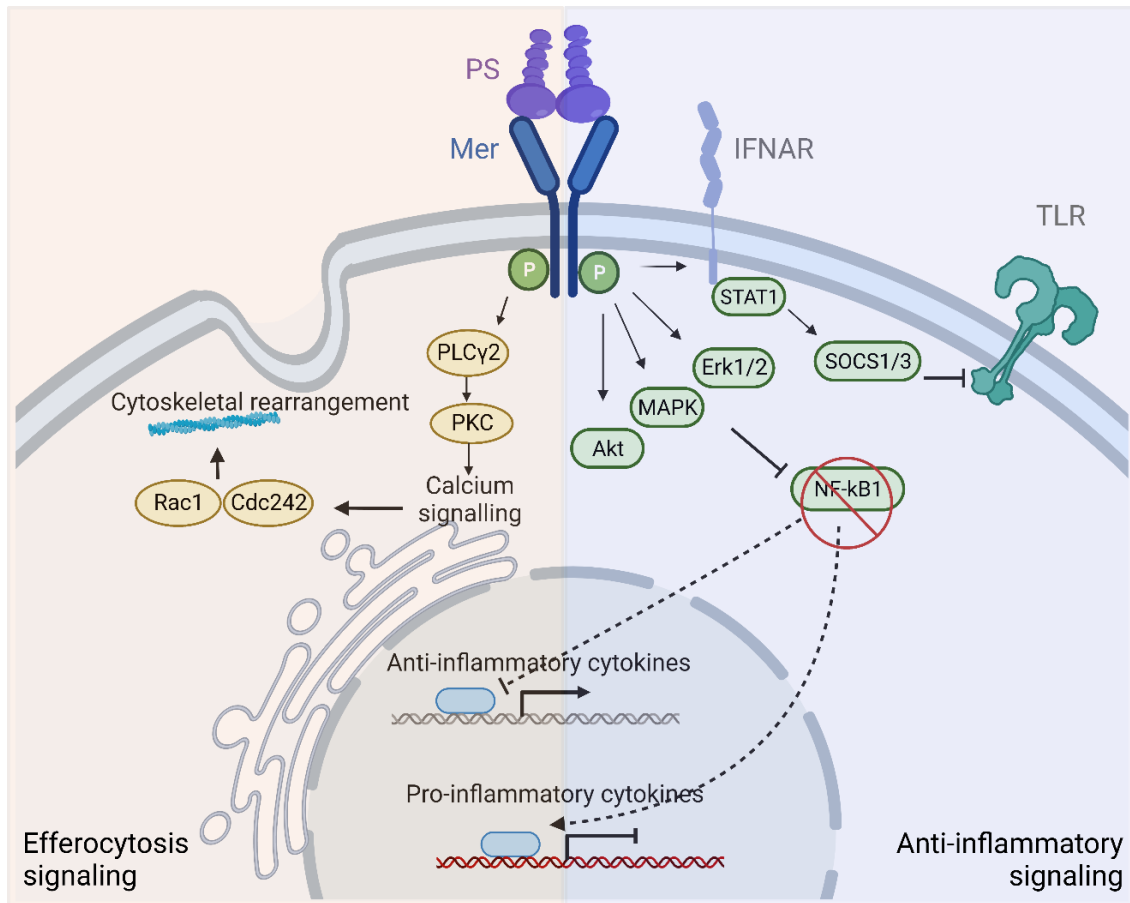


Figure 1.5. Protein S-Mer tyrosine kinase receptor signaling pathways

Current understanding of the signaling pathways involved in PS-Mer efferocytosis (left side) and anti-inflammatory (right side) activity. PLC γ 2 = phospholipase C γ 2; PKC = protein kinase C; IFNAR = Interferon- α/β receptor; TLR = toll-like receptor; STAT1 = signal transducer and activator of transcription-1; SOCS = suppressor of cytokine signaling protein; Erk = extracellular signal regulated kinase; MAPK = mitogen activated protein kinase; NF κ B = Nuclear factor kappa-light-chain-enhancer of activated B cells. Image created with BioRender.com.

In the tumor microenvironment, Gas6 and PS stimulate TAM activation and efferocytosis, promoting tumor growth, metastasis, and evasion of anti-tumor immunity [105]. During resolution of inflammation, macrophages, T cells, and dendritic cells express PS and TAM receptors to limit inflammation and promote efferocytosis [101]. Peritoneal macrophages were shown to upregulate *PROS1*, the PS gene, during the resolution phase of a murine peritonitis model [112]. Selective knockout of *PROS1* in the myeloid lineage downregulated macrophage anti-inflammatory properties and efferocytosis activity [112]. Activated T cells were also shown to produce PS, which signals through the TAM receptors in dendritic cells and down-regulates their immune responses [117]. In a murine model of lipopolysaccharide-(LPS) induced acute lung injury, alveolar macrophages were shown to express Gas6 and promote the efferocytosis of neutrophils in response to IL-4 and IL-13 cytokine signaling by regulatory T cells in a transcription factor signal transducer and activator-6 (STAT-6) dependent manner [116].

The immune system also uses efferocytosis as a way to protect the host from pathogens, by mediating phagocytic clearance of infected cells. For example, PS and Gas6 mediate macrophage efferocytosis of HIV-1-infected T cells by bridging phosphatidylserine exposed on the infected cells to macrophage-expressed Mer tyrosine kinase [118]. In this *in vitro* study, efferocytosis was shown to remove not only dead infected T cells, but also live virus-producing cells [118].

The viral envelope is derived from plasma membrane, as enveloped viruses exit by budding out of intact host cell membrane. Viral infection often leads to the induction of apoptosis and exposure of phosphatidylserine (PtdSer) on infected cells [119].

Additionally, viral particles likely do not have the flippases necessary to reverse the membrane transverse diffusion that causes PtdSer exposure on the outer leaflet. PtdSer exposure is a general apoptotic “eat me” signal that calls for engulfment by patrolling phagocytes [119]. When newly mature virions exit the cell and envelope themselves with host cell membrane, viruses can disguise as apoptotic debris and use phagocytic properties of many types of cells to avoid immune detection and infect other cells. As efferocytosis triggers anti-inflammatory properties and the dampening of immune responses, this viral “apoptotic mimicry” is highly advantageous for perpetuating infection [120]. PS/Gas6 and the TAM receptors have been shown to mediate Dengue, West Nile, and Yellow Fever virus entry *in vitro* [121]. Gla-domainless Gas6 or Axl mutated for the Gas6 binding site did not enhance viral infection [121]. Another study showed that PS/Gas6 enhanced viral transduction of Sindbis virus and various viral vectors in a manner dependent on the presence of the Gla domain and calcium ions, and was reversible by the addition of soluble Axl as a decoy [122]. Gas6 was shown to enhance virus binding in an envelope protein-independent manner, but did not mediate entry, suggesting that the envelope protein is necessary for the fusion step [122]. However, other studies have proposed that TAM receptors are not required for infection [120] and that TAM activation remains beneficial for its anti-inflammatory effects, as TAM receptors, especially Mer, protect mice against the CNS infection of neuroinvasive viruses, protect the blood brain barrier integrity, and relieve brain lesions during encephalitis [123]. The metalloprotease ADAM17 cleaves Mer and Axl to shut down signaling, shedding soluble ectodomains of

Mer (sMer) and Axl (sAxl), which can be measured in circulation as a marker of increased receptor activity in inflammation.

1.3 Immunothrombosis overview

Thrombosis, pathological intravascular blood clot formation, likely occurs through a similar pathway to hemostasis, though the initiator of the process is less clear. Here, we review the interplay between the inflammation and coagulation systems, and the mechanisms of immunothrombosis in specific inflammatory conditions, including HIV-1, SARS-CoV-2, and traumatic brain injury (TBI), with particular focus on the roles of PS, TF, and VWF.

1.3.1 Interplay between coagulation and inflammation

Coagulation and inflammation evolved from a common ancestor, as in lower vertebrates the two systems are unified. Simple organisms have blood cells that carry out the immune response, inflammation and phagocytosis, and coagulation processes. In response to injury, hemostasis is necessary to prevent excessive bleeding while inflammation is important for defending against invading pathogens and clearing tissue damage. As both being the first line of defense against trauma and invaders, and as injuries usually come with infections, extensive cross talk between the two systems has existed throughout evolution. Infection triggers innate immune responses that also lead to activation of coagulation, activated coagulation factors also activate inflammatory cells and the complement system, and the fibrin clot, the main product of coagulation, also limits or traps the spread of infectious pathogens.

1.3.2 Immunothrombosis mechanisms in inflammatory conditions

Infection and inflammation lead to recruitment of cells and molecules which facilitate both innate immune response and coagulation. TF expression and activity is central in this cross-talk. TF cellular expression and microvesicle-associated release by monocytes and other cell types occur under infection and inflammatory conditions, providing a trigger for coagulation initiation [124]. TF and its roles in immunothrombosis are reviewed further in section (1.3.4). Alternatively, thrombin may be produced through the intrinsic or contact pathway, in which exposure of negatively charged molecules, such as DNA, can lead to TF-independent activation of FXIIa [125]. The fibrinolysis system also plays a major role in immunothrombosis. Plasmin generation induces expression of proinflammatory mediators, such as tumor necrosis factor (TNF), IL-1, and IL-6, and plasmin can directly activate the complement system via C3 and C5 cleavage [126]. Lipopolysaccharides, IL-1, TNF, tumor growth factor- β (TGF- β), very low-density lipoprotein (VLDL), lipoprotein(a), and thrombin increase PAI-1 levels without a counteracting increase in tPA or uPA, promoting thrombosis [8]. The complement system is a major contributor to immunothrombosis. The activated products C3a and C5a act as anaphylatoxins, mediating various inflammatory processes by inducing endothelium activation and recruitment, as well as activation of innate immune cells, altering vascular permeability [126]. C5a mediates TF expression on neutrophils and neutrophil extracellular traps (NETs) release by neutrophils, as well as VWF secretion from ECs. NETs contain DNA, histones, proteases, TF, and microbicidal proteins, exerting proinflammatory and procoagulant effects and providing a means of pathogen entrapment [126, 127]. Histones promote platelet and

endothelium activation, induce the release of procoagulant polyphosphate from platelets via toll-like receptor (TLR)-2 or TLR-4-dependent mechanisms [128], and bind to PC and TM inhibiting APC generation [129]. TLRs, expressed by ECs, platelets, and antigen presenting cells such as macrophages and dendritic cells, are pattern recognition receptors that mediate the innate immune response against various molecules [130]. TLR-2 and TLR-4 recognize various microbial antigens, while TLR-9 recognizes microbial DNA [131]. Activation of these TLRs leads to induction of TF expression. Inflammation also induces the production of microvesicles, cell membrane-derived vesicles of 0.05-1 μm diameter shed from many types of cells [132]. Microvesicles may contain TF and other receptors facilitating coagulation and inflammation. In the next subsections, immunothrombosis in HIV-1 and SARS-CoV-2 infections, and in traumatic brain injury (TBI) are discussed in more detail.

1.3.2.1 Immunothrombosis in HIV-1 infection

Human Immunodeficiency Virus (HIV)-1 infection is caused by the HIV-1 virus, which is an enveloped retrovirus of the genus Lentivirus classified as a reverse transcribing virus [133]. The other subtype of HIV virus, HIV-2, has lower infectivity and virulence and is largely confined to West Africa. HIV-1 infects CD4^+ cells: CXCR4^+ T cells or CCR5^+ macrophages and dendritic cells, and is transmitted by contact with certain bodily fluids [133]. The HIV-1 virion contains two copies of single-stranded, positive-sense RNA genome, which may be reverse transcribed into double-stranded DNA and integrated into the host genome during infection [133]. Once integrated, the provirus can become latent for years while avoiding immune detection. HIV-1 infection typically begins with an acute

viremia with flu-like illness following inoculation of the virus, which gradually subsides after ~14 days as the infection becomes latent [134]. To date, there is no cure for HIV-1 and the chronic infection is controlled with lifelong medication, although there have been several reports of an apparent cure using stem cell transplant strategies involving CCR5 receptor deletion [135].

Since the beginning of its epidemic, HIV-1 infection has caused over 35 million deaths worldwide and there are currently 38 million people living with HIV-1 (PLWH) [136]. However, with the advent of the antiretroviral therapy (ART), which cannot cure but can slow down or prevent the progression to acquired immunodeficiency syndrome (AIDS), HIV-1 infection is now a manageable chronic disease with its patients having near normal life expectancy [137]. In this aging patient population, the causes of death have shifted from AIDS-related complications to comorbidities, including cardiovascular disease and cancer [138]. PLWH have a 5-16-fold and 2-8-fold increased risk for venous and arterial thrombosis, respectively, with 0.19%-7.63% yearly venous thromboembolism frequency (compared to ~0.1% in the general population), and this risk does not subside even with long-term ART treatment, suggesting that it is not solely related to viral load [139, 140]. The cause of the thrombophilia has been proposed to be multifactorial; where chronic immune activation, the presence of opportunistic infections, traditional cardiovascular risk factors, and side effects of lifelong medication might all contribute [141]. Increased plasma thrombin generation is a strong predictor of mortality in this population [142], and yet, the exact mechanisms leading to thrombosis are unclear.

HIV infection is associated with various hematological changes: decrease of plasma PC (0-14% in study populations) and PS (27-76%), as well as increases of plasma and cell surface TF, VWF, soluble P-selectin, tPA, PAI-1, and even NETs have all been reported [141, 143]. While antiretroviral therapy has been very effective at achieving clinical viral clearance and preserving CD4+ T cell counts, even long-term ART treatment does not always normalize levels of biomarkers associated with inflammation and coagulation in PLWH, and these individuals remain at greater risk for both venous and arterial thrombosis [138].

PLWH are treated with a combination of several classes of ART drugs: protease inhibitor (PI), nucleoside and non-nucleoside reverse transcriptase inhibitors (NRTI and NNRTI), integrase inhibitor and entry inhibitor. Certain drugs belonging to protease inhibitor (PI) and nucleoside reverse transcriptase inhibitor (NRTI) classes have been shown to exert procoagulant properties in patients [144, 145]. Many of the protease inhibitors are known to induce dyslipidemia and are associated with an increased risk of myocardial infarction [140]. Moreover, even as protease inhibitors inhibit viral aspartyl proteases, it has been suggested that they might cross react with coagulation factor serine proteases and impact their activity. The drug Abacavir, which is an NRTI, is also associated with increased cardiovascular disease risk with compelling evidence for its vascular inflammatory effects [146]. As a purine analog, the drug is thought to interfere with purine signaling pathways leading to EC dysfunction and increased platelet activation [146]. For most of the other drugs, however, it is unclear whether they contribute to thrombosis, nor the mechanisms that may be involved.

Acquired PS deficiency is the most consistently observed coagulation abnormality in PLWH with prevalence up to 74% in study populations and ~12% of these PLWH developing venous thrombosis [147-150]. PS deficiency in HIV infection is found in almost all subjects who develop venous thrombosis and correlates with disease progression. In section (1.3.3.1), we further review acquired PS deficiency in HIV-1 infection. Increased expression of procoagulant TF on circulating monocytes has also been described in PLWH [151]. In infection or inflammation, monocytes may express TF after stimulation by inflammatory cytokines, which may lead to intravascular coagulation and thrombosis [151]. Monocytes also release TF-bearing microvesicles into plasma, which may impact coagulation measurements *ex vivo* [152]. Similarly, EC activation might also occur and contribute to intravascular coagulation and the release of TF-bearing microvesicles. In chapter 3, we delineate the roles of PS deficiency and plasma TF activity in regulating thrombin generation in a cohort of PLWH.

1.3.2.2 Immunothrombosis in SARS-CoV-2 infection

Coronavirus Disease 2019 (COVID-19) is the acute respiratory illness caused by severe acute respiratory syndrome coronavirus 2 (SARS-CoV-2). SARS-CoV-2 is a single-stranded positive-sense RNA virus of the genus Betacoronavirus, the cause of the current pandemic which was first identified in Wuhan, China in 2019 [153]. The virus is transmitted by close contact and via aerosols and respiratory droplets, and infects the respiratory epithelium by binding to angiotensin-converting enzyme 2 (ACE2) receptor [154].

Almost immediately at the beginning of the pandemic, COVID-19 patients were reported to have a markedly increased risk of thrombotic complications associated with poor

prognosis [155, 156], with many different proposed mechanisms. COVID-19 patients have a higher frequency and severity of thrombosis compared to other common respiratory viral infections. Systematic review and meta-analyses reported an incidence of 17-28% for venous thromboembolism (VTE), 7-12.1% for deep vein thrombosis (DVT), and 7.8-19% for pulmonary embolism (PE) among hospitalized patients, and the incidence of VTE was as high as 32-33% when assessed based on ultrasound screening [157-159]. COVID-19 thrombosis manifests as micro- and macrothrombosis and occurs in multiple organs, including lungs, heart, and the brain.

The pathogenesis of COVID-19 thrombosis seems to involve vascular endothelial cell dysfunction, hyper-inflammatory immune response, and hypercoagulability [160]. COVID-19 is associated with elevated plasma concentrations of D-dimer, C-reactive protein, soluble P-selectin, fibrinogen, and an increase in TF expression by activated monocytes, NETs from neutrophils, and complement activation within the lung [161]. Neutrophils of COVID-19 patients showed high TF expression and released NETs carrying active TF, which can be blocked *in vitro* by thrombin or NETosis inhibition or C5aR1 blockade [162]. Increased platelet activation and aggregation is also seen, often accompanied by elevated levels of soluble platelet activation markers, such as platelet factor 4, and increased platelet-leukocyte aggregation [163]. As SARS-CoV-2 binds to ACE2 on lung epithelium, local ACE2 deficiency might occur, resulting in decreased kinin degradation by ACE2 and increased kinin activity and vascular permeability [164]. Vascular inflammation and increased endothelial activation result in elevation of VWF, soluble E-selectin, TM and EPCR [165-167]. Shedding of TM and EPCR may induce

impairment of APC generation and impaired PAR1 and PAR3 anti-inflammatory signaling by APC/EPCR [165, 166].

Approximately 20-30% of COVID-19 survivors develop long COVID or Post-Acute Sequelae of COVID-19 (PASC), in which symptoms including fatigue, shortness of breath, “brain fog,” chest pain, persistent loss of smell or taste, and various other persist or arise months after the acute infection [168]. Viral persistence, autoimmunity, and persistent inflammation have been proposed as overlapping mechanisms that contribute to the pathogenesis of PASC [169], and coagulation activation may play a role [314].

Dysregulation of PS in COVID-19 is reviewed in more detail in section (1.3.3.2). In chapter 4, we evaluate thromboinflammatory markers and coagulation parameters in a cohort of COVID-19 patients and identify a cause of free PS deficiency.

1.3.2.3 Immunothrombosis in traumatic brain injury

Traumatic brain injury (TBI) is caused by a blunt or penetrating head injury which disrupts the normal function of the brain [170]. It is classified as mild, moderate, or severe based on the post-resuscitation Glasgow Coma Scale (GCS) assessment, the duration of post-traumatic amnesia, and the duration of loss of consciousness [170]. In the USA, ~80% of TBI incidences are mild, with moderate and severe TBI each estimated to account for ~10%. TBI is a leading cause of death and disability around the world with 100-600 per 100,000 yearly incidence and the case fatality rate reaching ~21% [171]. About 90% of patients who die from TBI, do so within 48 hours of injury due to the primary injury, while the mortality and morbidity for survivors are mainly due to secondary brain injury

pathologies [171]. Therefore, the prevention and management of secondary brain injury are significant areas of research receiving a lot of attention [172].

TBI leads to a myriad of secondary pathology propagated by the initial injury. Early blood-brain barrier (BBB) disruption initiates mechanisms of thromboinflammation and coagulopathy by releasing brain-derived molecules into the systemic circulation [173, 174]. As tissue injury and shock provoke endothelial, immune system, platelet, and coagulation activation, TBI-induced coagulopathy often manifests as disseminated intravascular coagulation, producing systemic blood clots that can cause secondary ischemic events after TBI [175]. In the early hours post TBI, hypocoagulability typically occurs, resulting in bleeding, whereas later timepoints are characterized by a hypercoagulable and hyperfibrinolytic state associated with VTE, delayed intracranial hemorrhage, and multiple organ failure [176]. TBI-induced coagulopathy is common in penetrating head injuries [177] and has also been reported following blunt head trauma [178]. Studies found a 3-4-fold increased risk of DVT in TBI patients independent of anticoagulant therapy [179]. The presence of coagulopathy following TBI is strongly associated with poor prognosis [180]. In chapter 5, we compare the thrombotic potential of plasma microvesicle-associated TF, which is released into the systemic circulation, in mouse models of mild and severe TBI at early and late timepoints post-TBI.

1.3.3 Acquired PS deficiency secondary to inflammation

Acquired PS deficiency is more common than hereditary deficiency and is associated with conditions such as pregnancy, nephrotic syndrome, liver disease, disseminated intravascular coagulation, certain autoimmune diseases, multiple myeloma, the use of

oral contraceptives, chemotherapy, or vitamin K-antagonists, and certain viral infections [37, 85]. Autoantibodies against PS can be found in antiphospholipid syndrome [148, 181] and are common findings in systemic lupus erythematosus, in which PS deficiency is associated with a hyperinflammatory response [182, 183]. Acquired PS deficiency is a relatively common complication of infection with HIV-1 [141, 184-186], varicella [187], dengue [188], and SARS-CoV-2 [189, 190], all of which are associated with an increased risk of thrombosis. PS deficiency with autoantibodies against PS and severe thrombosis is occasionally observed following varicella infection in children [187], while dengue infection is associated with PC and PS deficiency of unclear mechanism, and thrombocytopenia and bleeding are the hallmarks of dengue hemorrhagic fever [188]. Here, we will review acquired PS deficiency in HIV-1 and SARS-CoV-2 infections in more detail.

1.3.3.1 Acquired PS deficiency in HIV-1 infection

Acquired PS deficiency is the most common coagulation abnormality in PLWH, with frequency as high as ~76% [141]. It correlates with decreased T-cell count and progression to acquired immunodeficiency syndrome [185]. As Brummel-Ziedins et al. showed that increased thrombin generation correlates with all-cause mortality in PLWH [142], this suggests that PS deficiency is a contributing risk factor [141, 150]. The cause of the acquired PS deficiency is unknown, but may involve decreased synthesis by ECs, hepatocytes, and megakaryocytes which could be affected in HIV infection, increased coagulation consumption, production of inhibitory PS autoantibodies, increased C4BP,

efferocytosis, loss due to nephropathy, or a combination of these mechanisms [118, 148, 150, 191].

1.3.3.2 Acquired PS deficiency in SARS-CoV-2 infection

Soon after the identification of thrombotic risk in COVID-19 patients, acquired PS deficiency was hypothesized to be a contributing factor. Since then, multiple studies have described PS deficiency in this population, lending credence to this hypothesis. In chapter 4 of this dissertation, we propose a novel mechanism of acquired PS deficiency, as we investigated the cause of specific free PS deficiency in a cohort of COVID-19 patients. Here, we review the existing literature in greater detail for the evidence of PS deficiency in COVID-19 and discuss the mechanisms that have been proposed for this dysregulation. Stoichitoiu et al. reported a decrease in PS activity in 65% of a 91-inpatient cohort at admission [189], which was confirmed to be secondary due to COVID-19 by a follow up measurement at ~2.5 months post infection [190]. This deficiency correlated with the extent of pulmonary damage, disease severity and mortality. Ferrari et al. found a 20% prevalence of PS deficiency in a cohort of 89 hospitalized COVID-19 patients [192]. A case report by Ali et al. discussed a patient with PS deficiency and COVID-19 infection presenting with a recurrent stroke [193]. Lemke et al. suggested that procoagulant activity and immune hyper-reaction in COVID-19 might be exacerbated by PS deficiency [194].

Martín-Rojas et al. [195] reported a free PS reduction (median 56.6%) in 206 hospitalized COVID-19 patients, with 33% of patients showing levels below 50%. The lowest levels of free PS were observed in patients receiving low-flow oxygen therapy ($p < 0.001$) [195].

Panigada et al. measured free PS antigen in eleven ICU patients with mechanical ventilation and saw a marginal decrease (69 IU/dL; reference range 60-140) as well. On the other hand, Voicu et al. [196] measured PS activity and free PS antigen concentrations in their cohort of 82 mechanically ventilated COVID-19 patients and found a slightly reduced activity (58 IU/dL; reference range 50-130) with preserved antigen level (79 IU/dL; reference range 50-130). Here, they compared the PS activity or antigen level to the absence or presence of venous thromboembolic event and found no statistical difference [196].

In a cohort of thirty ICU patients, Corrêa et al. [197] reported low free PS at baseline that occurred to a similar extent in patients with SOFA (Sequential Organ Failure Assessment) scores ≤ 10 or > 10 . The low free PS was observed to recover over time up to 14 days post-ICU admission [197]. Sehgal et al. [198] showed that free PS is reduced in a cohort of eighty hospitalized patients, but is not different between the non-survivors and survivors, between those with SOFA scores of 0 or ≥ 1 , or between those with or without Acute Respiratory Distress Syndrome. Free PS concentration was in the 60-70% range (reference range 60-140%) and remained so through day 7 and at discharge [198]. Hardy et al. [199], on the other hand, followed ICU stay of 21 severe patients and observed that free PS antigen levels were still within normal range, albeit lower at day 1-10 (median 80%), compared to either day 11-20 (median 114%) or day 21-30 (median 110%) of care [199]. White et al. [200] also looked at free PS antigen and compared it between 34 noncritical and 75 critical COVID-19 patients and observed similar extents of reduction (mean 52.1 vs 54.5 IU/dL; reference range 65-135). Fan et al. [201] also looked at PS activity between

10 mild and 10 severe patients and found mild reduction, but no difference between mild and severe patients (median 74% vs 71%; reference range 55-130%). Bauer et al. [202] analysed 58 hospitalized adult patients with clinically suspected COVID-19 and reported no statistical difference in PS activity in 41 non-COVID-19 (mean 93%) and 17 COVID-19 (mean 74%) patients ($p = 0.06$), with 22% of non-COVID-19 and 35% of COVID-19 patients being below reference range [202].

Overall, these studies demonstrate a mild to moderate decrease in either free PS antigen or PS activity in COVID-19 patients. This decrease is dependent on infection, but appears in many studies to be independent of disease severity. This suggests that, while PS deficiency may make a patient more susceptible to thrombosis, a second procoagulant hit is required for a thrombotic event to occur.

Possible mechanisms of acquired PS deficiency

There are many potential causes of acquired PS deficiency, which vary depending on whether Total PS or only free PS is reduced. Total PS deficiency (Figure 1.6) may result from increased consumption, clearance, or degradation, or from decreased synthesis. By contrast, free PS deficiency is caused by binding of PS to another protein, generally presumed to be C4BP.

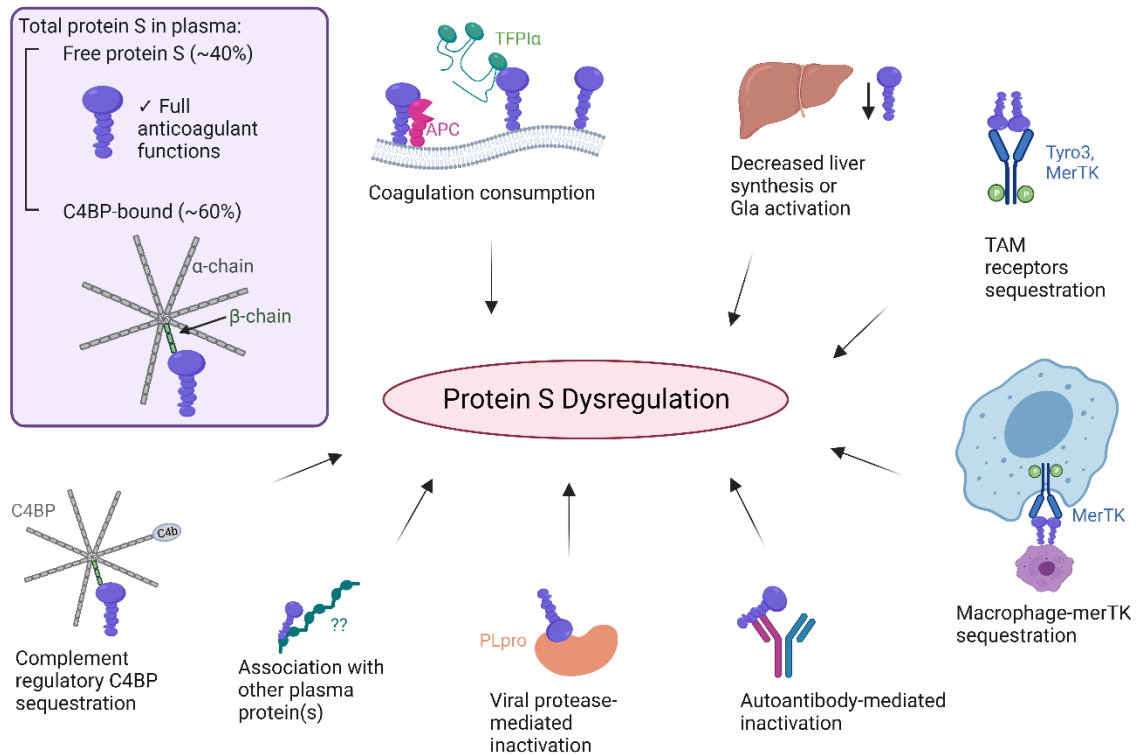


Figure 1.6. Possible mechanisms of acquired PS deficiency in COVID-19

Plasma PS can be dysregulated through coagulation consumption, decreased liver synthesis or Gla activation, sequestration by the TAM (Tyro3, Axl, Mer) receptors or by complement component 4b-binding protein (C4BP), inactivation by autoantibody or by viral papain-like protease (PLpro), or by increased association with other plasma protein(s). Image created with BioRender.com.

1. Loss due to consumption

PS may be consumed through any of its described functions, all of which are relevant to COVID-19 pathology. COVID-19 has been associated with macro- and microthrombosis, along with disseminated intravascular coagulation-like pathophysiology [203, 204]. Dysregulation of coagulation factors has been widely reported, as well as consumption of fibrinogen in severely ill patients [205], indicating that PS may be consumed through its actions as an anticoagulant.

COVID-19 is also associated with a local and systemic hyperinflammatory response, which includes dysregulation of the PS/Gas6-TAM receptor tyrosine kinase axis and activation of the complement system. Morales et al. found that higher plasma Gas6 and Axl were predictive of COVID-19 severity and mortality [206]. In a more recent study, Tonello et al. showed that baseline plasma Gas6 concentration was higher in patients with adverse outcomes while soluble Mer was lower in patients who had quicker resolution of the disease [207]. While both studies did not look at PS, the contribution of PS as a ligand for TAM receptors in COVID-19 has been acknowledged [194, 208]. In COVID-19, hyperactivation of the complement system is also evident [209, 210]. Patients with severe COVID-19 have high circulating levels of complement activation markers C5a and C5b-9, which correlate with disease severity [211, 212]. Complement component C5 and C5a receptor activation on ECs, neutrophils, monocytes and macrophages and the resulting release of TF on neutrophil extracellular traps are recognized to be important drivers of COVID-19 thromboinflammation [162, 213]. Data from the University of Kentucky Biobank indicate single-nucleotide variants in the gene encoding the C4BP α chain as risk

factors for morbidity and death from SARS-CoV-2 infection [214]. More studies are needed to understand the extent of PS depletion that might result from activation of TAM receptors and the efferocytic process, along with complement dysregulation.

2. Loss due to degradation by viral protease

Studies have also suggested that PS may be degraded directly by a SARS-CoV-2 protease. Group IV and VI viral cysteine proteases specifically recognize conserved cleavage site sequences of ~6-8 amino acids and have been shown to target approximately 40 host proteins [215]. SARS coronaviruses, including CoV-2, encode two cysteine proteases: 3C-like protease and papain-like protease [216]. The papain-like protease of SARS-CoV-2 has been shown to target PS *in vitro*. Ruzicka et al. identified a prospective cleavage site in the first laminin G domain, which would result in removal of ~80% of the SHBG domain from PS, likely eliminating most of its function [217]. Reynolds et al. showed cleavage of PS following prolonged treatment with the papain-like protease (65-72 h at room temperature) [215]. By contrast, treatment of pooled human serum with the protease did not result in readily detected cleavage products [215]. Thus, it is not clear whether PS may be proteolytically degraded by the papain-like protease *in vivo*.

3. Loss through antibody-mediated clearance

Acquired PS deficiency with autoantibodies against PS has been observed in varicella infection [187], and has been suggested to contribute to PS deficiency in HIV-1 patients [148]. While autoantibodies against PS have not been demonstrated with COVID-19,

there is evidence of other autoantibody formation. The persistent presence of lupus anticoagulant, anti-cardiolipin or β 2-glycoprotein antibodies are risk factors for thrombosis in patients with antiphospholipid syndrome and have been associated with coagulation abnormalities and hyperinflammation in COVID-19 [218]. Antiphospholipid antibodies (aPL) target phospholipids and phospholipid-binding proteins, including proteins involved in coagulation, such as prothrombin, thrombomodulin, antithrombin III, protein C, and PS [218, 219]. Oosting et al. investigated IgG fractions from patients with aPL who suffered thrombotic complications, and found subpopulations of IgG directed to prothrombin, APC, and PS, and confirmed the inhibitory effects of these antibodies [181]. Ferrari et al. found a 20% prevalence of PS deficiency and 72% prevalence of antiphospholipid antibodies, mainly lupus anticoagulant, in a cohort of 89 hospitalized COVID-19 patients. However, these findings did not correlate with abnormal coagulation activation markers [192].

4. Loss due to decreased synthesis

Apart from increased consumption or clearance, decreased total PS could be caused by reduced synthesis, resulting from the inflammatory and respiratory nature of COVID-19. Chatterjee et al. showed that hypoxia and interleukin-6 downregulate PS hepatic expression via stabilization of transcription factor hypoxia inducible factor 1 [60, 220]. Mast, et al. [221] showed evidence of downregulation of PS gene expression (~54-fold transcript reduction) in broncho alveolar lavage fluid samples of COVID-19 patients. Dofferhoff et al. found evidence of extrahepatic vitamin K insufficiency in a cohort of

hospitalized COVID-19 patients, which was related to poor outcome [222]. Vitamin K is necessary for synthesis of PS. As vitamin K is preferentially transported to the liver for the activation of vitamin K-dependent procoagulant factors, including PS, this mechanism might result in a loss of PS activity [223, 224]. Finally, it is possible that PS is co-translationally processed by the papain-like protease, resulting in either intracellular degradation or secretion of an inactive protein [215].

Specific free PS deficiency (Figure 1.7)

The majority of studies that have reported PS deficiency in COVID-19 patients have either reported free PS or PS activity, a measure of the APC cofactor activity of free PS [189, 190, 192-202]. It is possible for total PS antigen to remain normal but free PS, and PS anticoagulant activity, to decrease. Indeed, we recently reported specific free PS deficiency in a cohort of 82 COVID-19 patients, including mild and severe patients [225]. Due to its diverse functions, PS interacts with many proteins discussed above, including C4BP, APC, TFPI α , FIX, Tyro3, and Mer. C4BP is known to block PS anticoagulant activity and is commonly increased during infection. This increase can lead to a shift between the free and bound PS pools and result in reduced PS anticoagulant function, as was shown in an HIV-1-infected patient cohort [191]. In that study, Bello et al. showed that free PS deficiency correlated with elevated C4BP. The patients also showed evidence of thrombophilia, as indicated by a prolonged euglobulin clot lysis time compared to controls [191]. Conversely, C4BP deficiency can result in increased PS activity, as reported by Mulder et al., in a patient with ischemic retinopathy, who had increased free PS and decreased C4BP and PS-C4BP complex [226].

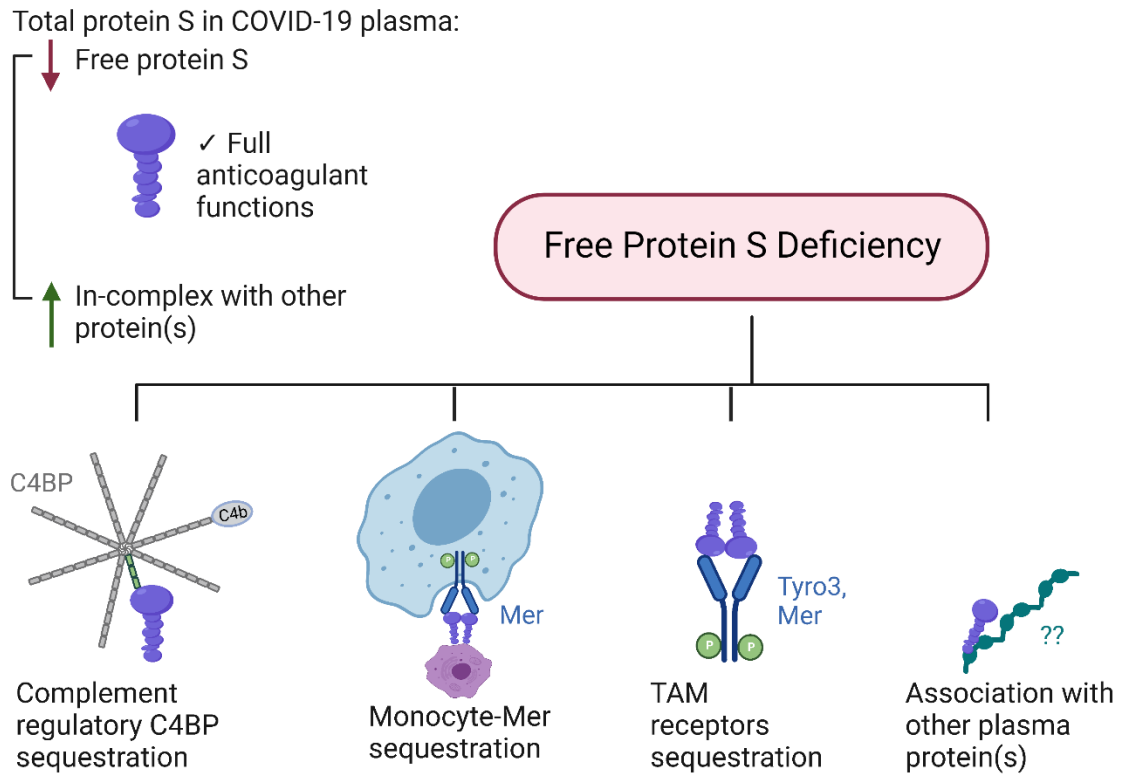


Figure 1.7. Possible causes of specific free Protein S deficiency in COVID-19

Free PS deficiency can occur through increased sequestration of plasma PS by either complement component 4b-binding protein (C4BP), TAM (Tyro3, Axl, Mer) receptors, or by increased association with other plasma protein(s). Image created with BioRender.com.

C4BP is well-described to decrease free PS and block anticoagulant activity, but other as-yet-unidentified proteins could have similar effects. In chapter 4, we identified VWF as a PS binding protein and showed how it contributes to a specific free PS deficiency.

1.3.4 TF biology

Tissue Factor (TF, also coagulation factor III, CD142, or thromboplastin) is a member of the originally hypothesized 4-factor coagulation system, which exists in primitive species, with four components consisting of fibrinogen (FI), prothrombin (FII), thromboplastin (FIII), and calcium ion (FIV) [227]. Indeed in 1904, placental tissue-derived reagents, termed thromboplastin, were shown to induce the conversion of plasma prothrombin to thrombin and were used to measure prothrombin time [228]. Studies in the 1960s determined that the protein component of thromboplastin requires phospholipid for its activity [229, 230], and in 1970, TF was purified [231, 232]. TF is a transmembrane protein that serves as a receptor for coagulation factor VIIa (FVIIa), forming the TF/FVIIa complex, which is the primary initiator of the coagulation cascade [233]. Here, details regarding TF structural and functional features, as well as its synthesis and regulation, are discussed.

1.3.4.1 TF structure and function

TF is a type I integral membrane protein, consisting of a single polypeptide chain of 263 amino acids [234-236]. It is a member of the class 2 cytokine receptor superfamily. TF structural analysis shows homology in sequence and topology with characteristic antiparallel beta-sandwich fold with a Greek key, a motif found in the extracellular domains of receptor family proteins such as interferon- α/β and the immunoglobulin

superfamily [234-236]. The first 219 residues of the N-terminal part represent the extracellular domain which contains two fibronectin type III modules critical for its membrane and ligand binding function (with FVIIa and FX) [236]. Each module spans approximately 100 amino acid residues [235]. They also contain two disulfide bridges at position Cys⁴⁹-Cys⁵⁷ and Cys¹⁸⁶-Cys²⁰⁹, the latter of which is a characteristic allosteric disulfide bond critical in the encryption and decryption of TF [237], which is discussed further in the next section (1.3.4.2).

TF is a transmembrane glycoprotein cofactor that serves as a high affinity receptor and promotes the catalytic activity of FVIIa [238]. Upon vascular injury, TF becomes exposed to blood and binds circulating FVIIa to initiate coagulation by activating both FX and FIX [239]. TF also binds to FVII; which triggers its activation to FVIIa by various coagulation proteases, mainly via autoactivation by trace amounts of FVIIa. The TF/FVIIa complex also has signaling activity via PAR2, a member of the G protein-coupled receptor family [240]. TF/VIIa signaling activity is mainly studied in cancer, where PAR2 activation by TF/FVIIa has been shown to induce proangiogenic and immune modulating cytokine expression [241].

TF is essential for survival, as deletion of TF in mice leads to universal embryonic lethality. For a while, TF was the only coagulation factor for which a human genetic defect had never been described, until Schulman et al. [242] described a heterozygous frameshift variant with an abnormal bleeding haploinsufficiency phenotype. They estimate that heterozygous TF deficiency is present in at least 1 in 25,000 individuals [242].

1.3.4.2 TF synthesis and regulation

TF is encoded by the *F3* gene consisting of six exons, of which exons 2 to 5 translate for the extracellular domain and exon 6 translates for the transmembrane and cytoplasmic domains [243]. An alternatively spliced TF, in which exon 5 is skipped, lacks the transmembrane domain and was shown to be secreted and functional [243]. However, more recent studies have contradicted that report and concluded that this soluble TF is not normally secreted and is coagulant inactive [244], although it may have a role in tumor cell angiogenesis [245].

TF is constitutively expressed by many types of cells surrounding the blood vessels, such as pericytes, smooth muscle cells, stromal cell, fibroblasts, and keratinocytes of the skin. However, many types of cells such as monocytes, neutrophils, ECs - either healthy or inflammatory - and tumor cells, can be stimulated by various agents - such as LPS, certain cytokines, and oxygen free radicals - to express detectable levels of TF [246-250]. These cells might also release TF into the circulation, either as the soluble extracellular form or as full-length protein incorporated into microvesicles [247, 250]. Mouse and human studies show that circulating TF is important for thrombosis and fibrin formation, and its activation is implicated in microvascular and large artery as well as venous thrombosis [251-255].

To date, there are numerous inconsistencies regarding the synthesis and expression of TF on blood cells and within the plasma as a soluble protein or on circulating microparticles. In part, this is due to the low physiological concentration of TF in tissues where sub-picomolar concentrations of TF can lead to efficient clotting within minutes, and is

possibly further complicated by sample collection artifacts and the sensitivity of assays used to measure it. It is commonly accepted that the concentration of active TF in healthy human plasma is very low and does not exceed 20 fM [256, 257]. As there is a discrepancy between antigen expression and procoagulant activity of cell surface TF, it has been proposed that circulating TF and most of cell surface TF is encrypted or coagulation inactive [258]. Activation of TF from the encrypted to the de-encrypted form is thought to involve a conformational change induced by rearrangement of an allosteric disulfide bond and the mechanism remains controversial [259]. An allosteric bond controls protein function by triggering conformational changes depending on its reduction or oxidation state. Cys¹⁸⁶ and Cys²⁰⁹ have been observed in several redox states on the cell surface: as free thiols, disulfide bonded, S-nitrosylated, or in mixed disulfide bond with glutathione or with protein disulfide isomerase (PDI) [259, 260]. Formation of this disulfide bond was shown to correspond with the active conformation of TF, whereas free thiol or thiol-modified forms correspond with encryption [259]. Exact mechanisms of the encryption process are unclear. In vitro, encryption may involve reduction and maintenance of the reduced free-thiol form by thioredoxin or the thioredoxin reductase (TR)/NADPH system and the natural asymmetrical phospholipid environment, as well as cell surface level control by active dynamin-mediated TF internalization [261, 262]. On the other hand, the chaperoning and redox activity of extracellular PDI and procoagulant PtdSer exposure are also implicated in the de-encryption process [263].

Different pathways leading to de-encryption have been described. Stimulation of purinergic receptor 7 (P2X7) stimulation by ATP de-encrypts cell surface TF on human

monocytes stimulated by LPS and increases the release of TF-bearing microparticles [264]. The de-encryption can be inhibited by thiol blocker 5,5'-dithiobis-(2-nitrobenzoic) acid (DNTB) and nitric oxide. The microparticle release can be inhibited by anti-PDI antibody and the procoagulant potential of the microparticles is attenuated by DNTB [264]. Another reported mechanism involves anti-thymocyte globulin potentially de-encrypting TF on monocytic cells, which depends on lipid raft integrity and complement C5 activation resulting in cell-surface PDI oxidation [265]. The de-encryption by anti-thymocyte globulin is inhibited by thiol alkylators, anti-PDI antibody and PDI inhibitor, and does not require maximal PtdSer membrane exposure [265]. It is generally accepted that exposure of phosphatidylserine (PtdSer) is required for maximal TF activity. However, PtdSer exposure by itself is insufficient and the details of a PtdSer-independent mechanism in de-encryption are still unclear, but are shown to involve thiol-disulfide exchange and protein disulfide isomerase (PDI) action on specific cysteine residues in the membrane proximal of the extracellular domain [266]. Furthermore, in some cell types, TF associates with caveolae, or areas of the cell surface with altered lipid composition, and forms dimers or oligomers which are proposed to reduce its activity [267, 268].

In pancreatic cancer, which is considered to be the most prothrombotic cancer type, there is a clear correlation between TF activity of cancer-derived microvesicles with the risk of DVT, and tumor microvesicles can induce thrombosis in animal models [269]. However, it was shown that TF on microvesicles is not sufficient by itself to cause DVT and synergistic EC-expressed TF is required. Furthermore, the procoagulant properties of the pancreatic

cancer-derived microvesicles surprisingly depend on surface exposure of the phospholipid phosphatidylethanolamine (PEth) and not PtdSer [269].

Other traditional stimuli that lead to TF de-encryption include cell disruption, TFPI inhibition, and calcium ionophore and oxidizing agent (for example HgCl₂) treatment. TF procoagulant activation can also be triggered by numerous signals in the disease process. Degradation of TFPI by neutrophil proteases, activation of complement factors, extracellular PDI released by injured cells, and NETs can trigger TF activation [270, 271]. Neutrophils release NETs which consist of DNA, histones, and granular enzymes through a programmed cell death pathway, and this may serve as a solid-state reactor by sequestering circulating platelets and coagulation factors, including TF, from the circulation. NET-associated effectors also induce EC expression of TF through interleukin 1 α and cathepsin G-dependent pathway [272].

TF procoagulant activity is also regulated by other factors. Krüppel-like factor-11, a transcription factor known as maturity-onset diabetes mellitus of the young type 7, with mutations implicated in early-onset type 2 diabetes mellitus, has anti-inflammatory effects in ECs [273]. KLF11 binds to the F3 promoter to inhibit its transcription. In basal conditions, endogenous KLF11 is abundant enough to maintain low levels of TF in vascular smooth muscle cells and ECs. Vascular smooth muscle-specific TF knockout inhibited thrombus formation in the ferric chloride model, while smooth muscle-specific *Klf11* KO mice have increased TF and a prothrombotic phenotype. Overexpression of *Klf11* potently inhibited TNF- α induced TF expression in human umbilical vein ECs at both the mRNA and protein levels [273].

TF binding affinity to FVIIa is greatly increased upon de-encryption ($K_D < 1\text{nM}$), whereas the TF/FVIIa complex binding and cleavage of its substrate factor X (FX) only meaningfully occurs after de-encryption [270, 271]. In the liver hepatocytes, which are the primary site of synthesis of several coagulation factors including FVII(a), have direct exposure to the plasma due to the liver vasculature fenestrated endothelium. Consequently, liver hepatocytes express TF complexed with FVIIa although this complex exists in an encrypted state. Bile acids stimulate the de-encryption of this TF/FVIIa complex in animal cholestasis model, explaining the hypercoagulability seen in patients with liver diseases [274].

The endogenous anticoagulant TFPI is the inhibitor of the TF/FVIIa complex, with action dependent on the presence of FXa [9]. TFPI contains binding sites for FVIIa and FXa and it may either initially bind and inhibit FXa followed by TF/FVIIa or it preferentially binds to the TF/FVIIa/FXa ternary complex resulting in a fully inhibited complex [9]. TFPI is produced mainly by ECs and megakaryocytes and is expressed constitutively. Both TF expression and TFPI inhibitory action are constitutive: TFPI rapidly inhibits low levels of TF expressed on activated ECs and monocytes preventing uncontrolled intravascular thrombosis unless a threshold of stimulus is reached [12].

1.3.4.3 TF roles in immunothrombosis

As TF is normally only expressed by perivascular tissues, it is proposed that TF serves as a hemostatic envelope around blood vessels [275], allowing for rapid activation of coagulation after injury. Due to its high procoagulant activity in coagulation initiation and hemostasis, intravascular procoagulant TF is present only at very low levels and is tightly

regulated or inhibited [246, 256]. Studies have suggested that intravascular TF may contribute more to thrombosis than hemostasis [251]. TF is involved in both arterial and venous thrombosis [276]. Monocyte TF contributes to thrombosis in many diseases [151, 249]. Other intravascular TF sources include macrophages in atherosclerotic plaques, TF-bearing microvesicles which are mostly monocyte/ macrophage-derived, neutrophil extracellular traps (NETs), activated endothelium, and perivascular cells that are exposed due to an increase in vascular permeability during inflammation [124, 152, 162, 252]. C5a and platelet-derived thrombin induce both neutrophil TF expression and generation of NETs carrying active TF, in a C5aR1 and PAR1 dependent manner, respectively [162]. Monocyte TF activation can be induced by complement C5 activation, which requires cell surface PDI oxidation as well as complement C7-dependent PtdSer expression [277]. Antiphospholipid antibodies, implicated in antiphospholipid syndrome which causes thrombosis, upregulate cell surface TF activation in a complement C3-dependent manner [278]. Overall, TF expression and activation play a central role in linking coagulation activation and the inflammatory response.

1.3.5 VWF biology

Von Willebrand Factor (VWF) is named after Professor Erik Adolf von Willebrand, an internist who first described an inherited form of bleeding disorder, “a new form of hemophilia,” which bears his name (von Willebrand Disease, VWD) in 1925 [279]. In 1971, Zimmerman and collaborators identified a newly discovered protein, VWF, as the cause of the bleeding diathesis in these patients [280, 281]. VWF is a multimeric glycoprotein present in plasma, in storage granules of platelets (α -granules) and ECs (Weibel-Palade

bodies, WPBs), and in the subendothelial matrix [282] (Figure 1.8). It is best known for its hemostatic role in serving as a bridge linking platelets to exposed subendothelial matrix components, such as collagen, following vascular injury [283]. Here, more details regarding VWF structural and functional features, as well as synthesis and regulation of its activity, are discussed.

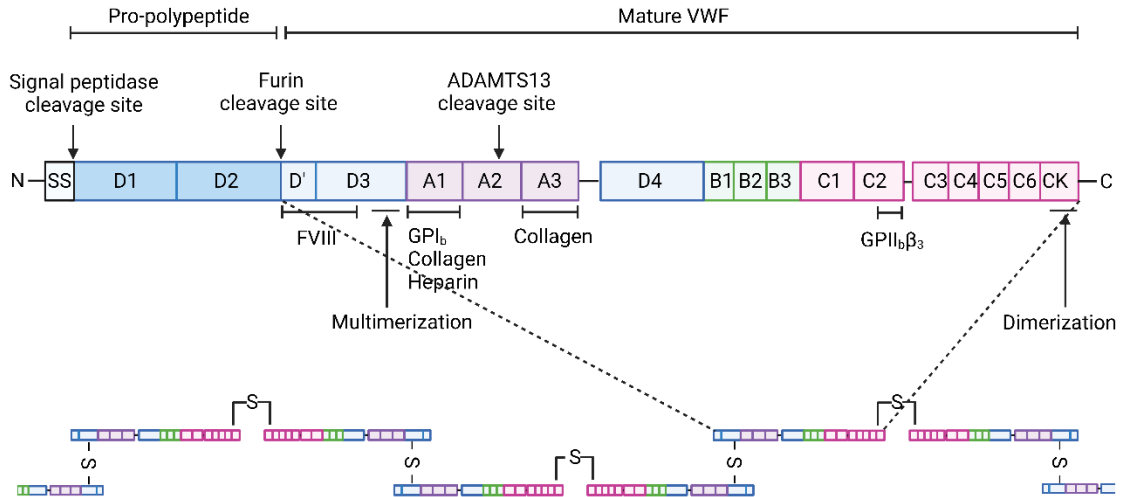


Figure 1.8. Domain organization and multimerization of VWF monomer

Domain organization of von Willebrand Factor (VWF) monomer, with protease cleavage sites and protein binding sites indicated. VWF monomers dimerize between the cystine knot (CK) domains and multimerize between the D3 domains by disulfide bonds. Image created with BioRender.com.

1.3.5.1 VWF structure and function

The VWF monomer (molecular mass of ~270 kDa) consists of four repeated domains (A, B, C, and D) present in tandem copies of each and arranged in the following order: D1-D2-D'-D3-A1-A2-A3-D4-B1-B2-B3-C1-C2-C3-C4-C5-C6-CK [283]. The A domains of VWF are homologous to segments in complement factor B, complement factor C2, and cartilage matrix protein, whereas the C domains are homologous to thrombospondin and $\alpha 11$ -procollagen type I and III [284]. The A domains of VWF contain regions which are sensitive to vascular shear; in particular the A2 domain, which undergoes a proline *cis-trans* isomerization and is not protected from unfolding by medium- or long-range disulfide bonds [285]. Circulating VWF is found as a series of multimers (from low molecular weight to high molecular weight, or ultra-large) ranging in size from about ~500 to 20,000 kDa (or up to ~100 monomers), with the larger multimers being more hemostatically active [284]. VWF participates in hemostasis by stabilizing coagulation factor VIII (FVIII) and by recruiting platelets to the injured vessel wall via GPIb and $\alpha_{IIb}\beta_3$ binding [283, 284]. VWF protects FVIII from proteolytic clearance, prolonging its half-life while also localizing it to the site of vascular injury [286].

VWF-mediated platelet adhesion is dependent on fluid shear stress. In low-shear conditions and in intact blood vessels, VWF circulates in a globular form; however, in high shear rates (above $5,000\text{ s}^{-1}$) VWF rapidly unfolds, elongates into a long thread conformation, and self-associates [287]. At lower shear rates of veins and intact arteries, platelet adhesion is not stimulated by VWF. At higher shear rates (above $1,000\text{ s}^{-1}$ threshold) and upon vascular injury, platelet adhesion is strongly dependent on VWF as

the VWF-GPIb interaction enables platelet rolling on damaged endothelium to establish a preliminary adhesive interaction [288]. The slow rolling action allows time for the activation of $\alpha_{IIb}\beta_3$ integrin, which in turn binds to VWF, fibrin(ogen), and various extracellular matrix proteins resulting in a more stable platelet adhesion and aggregation [289].

Via binding sites in the A1 and A3 domains, VWF binds to fibrillar collagen types I and III, which also facilitate platelet adhesion and aggregation [290, 291]. VWF has been observed to bind to other ECM components, such as fibronectin, vitronectin, sulfatides, and heparin, and is predicted to interact with various other plasma proteins, including P-selectin, prothrombin, and coagulation factor IX [284]. VWF has also been shown to facilitate leukocyte recruitment, rolling, adhesion, and extravasation on ECs via interaction with leukocyte β_2 -integrins [292]. As the shear sensitive-A2 domain is homologous to complement factor B, unfolded VWF binds to the activated complement component C3b, which promotes alternative complement pathway activation [293].

1.3.5.2 VWF synthesis and regulation

VWF is synthesized by ECs and megakaryocytes and is encoded on the short arm of chromosome 12 (12p13.31) [284]. The *VWF* gene, 180 kb in length, contains 52 exons which code for a 2,813-residue precursor referred to as pre-pro-VWF [283]. Among these residues, 234 (8.3%) are cysteines, which are conserved in mammals and abundant in all domains except in the A domains, which altogether contain only six cysteine residues [294]. The monomers dimerize in a tail-to-tail fashion between the cystine knot (CK) domains in the endoplasmic reticulum and multimerize in the Golgi and post-Golgi

compartments by disulfide bonds between the D3 domains [284]. This precursor can then be cleaved into mature VWF and the pro-polypeptide (~97 kDa). The pro-polypeptide, termed VWF antigen II, is secreted into plasma with unknown function, and has been shown to assist in multimer assembly of mature VWF [295]. Mature multimers of VWF are packaged in helicoidal structures and stored in WPBs in ECs and α -granules in megakaryocytes and platelets [296]. In ECs, VWF is the main cargo and is secreted from WPBs in both a constitutive and regulated (i.e. via endothelial activation) manner. VWF secretion by ECs can be stimulated by a variety of agents, such as histamine, thrombin, fibrin, certain cytokines, and calcium ionophores [292]. In platelets, platelet activation is necessary for VWF secretion from α -granules and no observed constitutive release occurs [297]. The multimeric size of VWF, the main determinant of its activity, is regulated by the plasma metalloprotease, a disintegrin and metalloprotease with thrombospondin type 1 motif, member 13 (ADAMTS13), which cleaves it at a single site (Tyr1605-Met1606) in the A2 domain [298].

VWD is an autosomally inherited genetic bleeding disorder with abnormal primary hemostasis and bleeding time prolongation caused by a deficiency of functional VWF [299]. There are four types of hereditary VWD: type I (reduced VWF antigen, the most common), type II (reduced VWF activity), type III (absence of VWF due to being homozygous for a defective gene; one per million frequency) [299], and platelet-type VWD, an autosomal dominant type of pseudo-VWD caused by gain of function platelet GPIIb α mutations, which lead to abnormally high GPIIb α -VWF binding affinity [300].

1.3.5.3 VWF roles in immunothrombosis

In response to inflammatory stimulus, ECs activate and release the content of the WPBs via exocytosis [292]. VWF is a positive acute phase reactant and a universal marker for EC activation in systemic inflammation and metabolic disorders like diabetes and obesity [301]. On the other hand, ADAMTS13 is a negative acute phase reactant; its activity declines in systemic inflammation [302]. Inflammatory mediators promote an increase in VWF by various mechanisms; IL-8 and TNF stimulate the release of ultra-large VWF by ECs, while IL-6 inhibits cleavage of the ultra-large multimers by ADAMTS13 [303]. Increased high molecular weight multimers results in higher VWF activity at lower shear threshold and leads to thrombosis. Increased VWF activity or ADAMTS13 deficiency may result in microvascular obstruction and thrombotic microangiopathy [304].

The increase in plasma VWF is predominantly EC-dependent, as the contribution of platelets is limited by the much lower VWF content in platelets and the necessity of platelet activation for VWF release [292]. Multiple studies have reported correlations of VWF total antigen concentration, ratio of VWF antigen to VWF pro-polypeptide, and VWF activity with clinical severity and mortality in acute systemic inflammatory conditions, such as sepsis, acute respiratory distress syndrome (ARDS), or systemic inflammatory response syndrome (SIRS) [292, 305].

In COVID-19, elevated plasma VWF concentration is strongly associated with thrombotic complications and may be a predictor of disease severity [306]. Systematic review and meta-analysis showed over 300% higher VWF:Ag (antigen), VWF:Ac (activity), and VWF:RCo (ristocetin cofactor activity), and lower ADAMTS13 activity (~60% of healthy

controls) in ICU patients [306]. Plasma VWF is associated with mechanical ventilation need and is higher in intensive care unit patients [304]. Longitudinal observations found normalization of plasma VWF in mild patients six months post hospitalization, while patients with respiratory sequelae still had increased VWF and thrombotic complications [307].

1.4 The focus of this dissertation

This dissertation focuses on the roles of PS and TF in thrombosis, which occurs secondary to inflammation. The overarching hypothesis of this dissertation is that PS deficiency, secondary to viral infections, significantly contributes to thrombotic mechanisms in HIV-1 and SARS-CoV-2 patients, and that increased plasma TF activity significantly contributes to thrombosis in TBI. To test this hypothesis, we utilized cohorts of HIV-1 and SARS-CoV-2 human patients and mouse models of mild and severe TBI. In chapters 3 and 4, we examine the contributions of PS and TF to thrombin generation potential and thrombotic risk in HIV-1 and SARS-CoV-2 patients. In chapter 4, we describe a previously unrecognized role for VWF as a PS-binding protein, and evaluate the contribution of this interaction to acquired PS deficiency. In chapter 5, we examine the contribution of TF and extracellular vesicles released post-TBI to thrombin generation potential in mouse models of different severity of TBI.

CHAPTER 2. MATERIALS AND METHODS

2.1 Materials

Pooled normal human plasma (control plasma N) and human tissue factor (Dade Innovin) were from Siemens Healthineers (Erlangen, Germany). Human VWF from Haematologic Technologies, VT, USA (HCVWF-0191). Human thrombomodulin was from PeproTech (NJ, USA). Human PS, FVIIa and FX were from Enzyme Research Laboratories (IN, USA). Phosphatidylcholine (PCho), phosphatidylethanolamine (PEth), phosphatidylserine (PtdSer) were from Avanti Polar Lipids (AL, USA) and were used to prepare PCho:PEth:PtdSer (40:40:20) vesicles (phospholipids, PL) according to the protocol of Morrissey [308]. PS-, PC-, and Fibrinogen-depleted plasma were from Affinity Biologicals (Ontario, Canada). Thrombin calibrator and FluCa substrate for Calibrated Automated Thrombography (CAT) were from Diagnostica Stago (Asnières-sur-Seine, France). o-Phenylenediamine dihydrochloride substrate was from Sigma Aldrich (P-6912; Darmstadt, Germany), and Spectrozyme FXa and Spectrozyme TH were from BioMedica Diagnostics (CT, USA). Recombinant mouse tissue factor (mTF) and factor VII (mFVII), and bacterial thermolysin were from R&D systems (MN, USA). 1,10-Phenanthroline was from Sigma Aldrich (Darmstadt, Germany). Brij-35 was from Milipore Sigma (MA, USA).

2.2 Methods

2.2.1 Human subject study approval and blood collection

Human subject studies were approved by the Institutional Review Board of the University of Kentucky. Written informed consent was received from subjects prior to participation.

Blood was collected and platelet-poor plasma (PPP) and washed platelets were isolated. Whole blood was collected into 3.2% buffered sodium citrate from donors by venipuncture. Blood was diluted with PBS (NaCl 137 mM, KCl 2.7 mM, Na₂HPO₄ 10 mM, KH₂PO₄ 1.8 mM, pH 7.4), supplemented with 0.2 U/mL apyrase (A6410; Sigma Aldrich, St. Louis, MO, USA) and 10 ng/mL prostaglandin I₂ (18220; Cayman Chemical, Ann Arbor, Michigan, USA) or prostaglandin E₁ (Enzo Life Sciences, Framingdale, New York, USA), and centrifuged (190 x *g*, 15 m) to generate platelet-rich plasma (PRP), which was centrifuged again (700 x *g*, 15 m) to yield PPP and platelets. PPP was freshly frozen at -80°C. Washed platelets were counted with a Beckman Coulter Z2 Particle Counter (Beckman Coulter, IN, USA).

For HIV-1 related projects, blood was collected from consenting healthy control donors and HIV-1+ patients. The patients were in good general health at the time of blood draw, and patients with history of cardiovascular disease or cigarette smoking were excluded. Subjects were grouped into either healthy controls (n = 9), naïve (patients on first diagnosis prior to receiving treatment, n = 17) or ART (patients on antiretroviral treatment, n = 13). A portion of the whole blood utilized for flow-cytometric measurement of platelet-leukocyte aggregation (PLA) and washed platelets lysates were prepared for immunoblotting. The cohort has been partially described in a published study by Banerjee et al. [309].

For SARS-CoV-2-related projects, blood samples were collected from consenting adults: SARS-CoV-2 negative controls (n=38, 56% male, age 59.9±14.1 y) and SARS-CoV-2 positive outpatients (patients with mild or no symptoms, post-quarantine) (n=52, 31% male, age

48.4±15.5 y) and inpatients (ICU patients) (n=30, 69% male, age 61.5±14.2 y). A portion of the whole blood was utilized for flow-cytometric measurement of platelet-leukocyte aggregation (PLA), preparation of platelets lysates for immunoblotting, and peripheral blood derived mononuclear cells isolation for the flow-cytometric measurement of monocyte tissue factor expression. Biosafety cabinets were used for manipulation of potentially infectious samples when aerosol generation was deemed probable.

2.2.2 Plasma tissue factor activity

TF activity was measured using a spectroscopic Factor Xa generation assay, adapted from the protocol of Hisada and Mackman [310, 311]. For human studies, 50 µL PPP was diluted with 1 mL HBSA (HEPES-buffered saline supplemented with 0.1% bovine serum albumin/BSA) and centrifuged (20,000 x *g*, 45 min, 4°C) to isolate plasma microvesicle-associated TF. The pellet was washed by centrifugation with HBSA and resuspended in 100 µL HBSA. FXa activity assay was measured immediately following isolation. 50 µL of each sample were added into 96-well plate microplate wells. Standards of TF (0-500 fM) were prepared. 12.5 nM of FVIIa and 375 nM of FX in HBSA buffer supplemented with 10 mM CaCl₂ were added into every well, with final addition of 0.5 mM chromogenic substrate of FXa (Spectrozyme FXa). Cleavage of Spectrozyme FXa was monitored at 405 nm for 2 h at 37°C and compared to a TF standard curve to calculate TF activity, using nonlinear regression (GraphPad Prism v.8.0.2). Results were normalized to plasma total protein.

For mouse experiments, PBS-diluted PPP as described in (2.2.15) was diluted with 1 mL HBSA, pelleted by centrifugation (20,000 x *g*, 45 min, 4°C), and washed by recentrifugation as described with human PPP. Immediately following isolation, samples

were incubated with mFVIIa (12.5 nM) and 0.5 mM Spectrozyme FXa, and reactions initiated by addition of hFX (375 nM in HBSA with 10 mM CaCl₂), and FXa activity monitored at 405 nm for 2 h at 37°C. Results were compared to standards of hTF (0-500 fM) to calculate TF functional concentration. Initial experiments determined that human FVIIa (12.5 nM) does not function with mouse TF, necessitating the need to use mouse FVIIa for subsequent experiments. Standard curves generated using mFVIIa (2.5 nM) with mouse or human TF revealed that the standards were more sensitive and reproducible using human TF. Thus, experimental data using mouse samples are presented as the equivalent human TF activity.

2.2.3 Plasma thrombin generation

Thrombin generation was measured in PPP using Calibrated Automated Thrombography (CAT), as described [13], with modifications. For human studies, 40 µL PPP was incubated with 10 µL of (a) thrombin calibrator; (b) phospholipid vesicles (4 µM final concentration), (c) phospholipid vesicles and TF (1 pM), or (d) phospholipid vesicles, TF and thrombomodulin (20 nM). Samples were incubated for 10 min at 37°C, and thrombin generation was initiated with the addition of 10 µL of a mixture of calcium and fluorogenic thrombin substrate. Results were the average of three measurements. Thrombin activity was measured for up to 2 h using a Fluoroskan Ascent Microplate Reader (Thermo Scientific) and quantified using Thrombinoscope software (Diagnostica Stago).

For mouse experiments, CAT was performed using PBS-diluted PPP as described in section (2.2.15). Forty microliters of diluted-PPP were incubated with 10 µL of (a) thrombin calibrator; (b) phospholipid vesicles (4 µM final concentration), (c) TF (1 pM), or (d)

phospholipid vesicles and TF, subsequent steps were identical to the protocol with human samples described here, with thrombin activity measured for up to 1 h.

2.2.4 Enzyme-linked Immunosorbent Assays

Total PS (PS-EIA; Enzyme Research Laboratories), PC (PC-EIA; Enzyme Research Laboratories), free PS (REAADS monoclonal free protein S kit; Corgenix, CO, USA), C4BP- β (LS-F22498; Lifespan Biosciences, WA, USA), soluble Mer (Human Mer DuoSet; R&D Systems, MN, USA), C5a (Human C5a DuoSet; R&D Systems), D-dimer (Asserachrom D-dimer; Diagnostica Stago, Asnières-sur-Seine, France), myeloperoxidase (DY3174; R&D Systems), soluble E-selectin (DY724; R&D Systems), and VWF (DY2764-05 by R&D Systems and VWF-EIA by Enzyme Research Laboratories) were measured by ELISA, following manufacturer's instructions. Plasma IL-6 and TNF- α were measured using Milliplex MAP Kit (Millipore Sigma). Total PS, PC, and VWF-EIA (Enzyme Research Laboratories matched-pair antibody set) measurements were compared to standards of control plasma N (Siemens Healthineer), whereas all the other ELISAs used standards provided with the kits. Results were normalized to plasma total protein concentration determined by bicinchoninic assays (BCA; by bioWORLD, Dublin, OH, USA or by Pierce, IL, USA) of each sample to account for dilution during processing, and further normalized to the average of controls.

For some experiments, purified VWF was mixed with purified PS, or into control plasma N, with or without vortex-induced shearing (~2,500 rpm at RT for 30 s). For some experiments, 5 mM CaCl₂ was added to plasma samples after 1 mM hirudin (Sigma Aldrich, St. Louis, MO, USA) and 5 mM GPRP (GenScript Biotech, Piscataway, NJ, USA)

peptide addition. For some experiments, 2 mg/mL Ristocetin A sulfate (MP Biomedicals, Irvine, CA, USA) was mixed with plasma.

2.2.5 Spike protein IgG measurement

Antibodies against SARS-CoV-2 spike protein were measured using an ELISA based on that of the Krammer group [312, 313]. Briefly, purified spike protein was synthesized by the University of Kentucky Protein Core Facility utilizing plasmid provided by Florian Krammer. Nunc-Immulon plates were coated with spike protein (2 µg/mL), washed, blocked, and heat-inactivated (56°C, 1 h) serum (1:10² to 1:10⁵ dilutions) was added to wells (2 h, RT). Plates were washed, and HRP-conjugated goat anti-human IgG antibody was added (1 h, RT). Plates were washed, developed for 10 min using OPD substrate with acid stop, and read on a SpectraMax (Molecular Devices, San Jose, CA, USA) microplate reader at 490 nm. Endpoint titer was determined as the last dilution producing a signal +3SD background.

2.2.6 Flow cytometry

Peripheral blood derived mononuclear cells were freshly isolated from whole blood using the RosetteSep Human Monocyte Enrichment Cocktail kit (Stemcell Technologies, Vancouver, Canada) per manufacturer's protocol. Briefly, 15 mL of Lymphoprep density gradient medium was prepared in a labeled 50 mL conical for each blood sample. 10 mL of EasySep Buffer was added to each blood sample with a 25 mL pipet and mixed, and then gently transferred to the top of the Lymphoprep. The conical was then centrifuged at 1200 x *g* for 20 min at 20°C with brake acceleration set at 5/9 and deceleration at 0/9. The resulting upper plasma layer was then removed to isolate the buffy coat containing

the cells of interest. The isolated buffy coat was then brought up to 10 mL volume with EasySep buffer and spun down at 300 x *g* for 10 min at 20°C with both brake acceleration and deceleration at 9/9, incubated with 1 mL ACK (ammonium-chloride-potassium) for 1m, washed with 10 mL HBSS (Hanks' Balanced Salt Solution) with 1200 rpm for 10 min at 10°C, and further washed with 10 mL PBSA (PBS, 0.5% BSA). The cells were then counted using trypan blue staining and hemocytometer. Flow cytometry was performed using the Cytoflex flow cytometer by Beckman Coulter (Brea, CA, USA). Briefly, cells were incubated with 5 µL primary antibodies for 20 min at 4°C in the dark, washed with 1 mL PBSA at 1200 rpm for 10 min at 10°C, fixed with formalin for 20 min at RT in the dark, further washed with 2 min L PBSA at 1200 rpm for 10 min at 10°C, and finally resuspended in 1 mL HBSS to run on the flow cytometer. Antibodies used were anti-CD11b-PerCP, anti-CD163-PE-Cy7, anti-CD64-APC, anti-CD206-(MR)-e450, anti-CD14-Sb600, and anti-CD16-SB780 from Life Technologies (Carlsbad, CA, USA), and anti-TF-PE by Abcam (Cambridge, UK).

2.2.7 Thioflavin T staining

Thioflavin T fluorescent staining was utilized to measure fibrin amyloid microclots in PPP, using a protocol adapted from Pretorius, et al [314], and modified to run in a microplate format. Briefly, fibrinogen-immunodepleted plasma or PPP samples were incubated with 5 µM Thioflavin T for 30 min at RT, protected from light. Five microliters of samples was then diluted with HBS-PEG (20 mM HEPES, 150 mM NaCl, 0.1% PEG8000, pH 7.4) to 50 µL and plated onto a 96-well plate. Total fluorescence with excitation at 450 to 488 nm and emission at 499 to 529 nm was then measured using a BioTek Cytation 5 fluorescence

plate reader and Gen5 software (Agilent Technologies, Santa Clara, CA, USA). Results were normalized to the fluorescence value of fibrinogen-immunodepleted plasma as a negative control and to total protein. All samples were measured in triplicate.

2.2.8 Native PAGE and immunoblotting

Human protein S (HPS; Enzyme Research Laboratories, IN, USA) and plasma in native sample buffer were subjected to SDS-PAGE on 4-20% Mini-PROTEAN TGX precast protein gels (BioRad, Laboratories, CA, USA) and transferred to nitrocellulose membrane, using a Mini-PROTEAN Tetra Cell system (Bio-Rad) per manufacturer recommendations. Immunoblotting was performed using 2 µg/mL sheep anti-human PS (CL20105A; Cedarlane Laboratories, Burlington, Canada), sheep anti-human PC (PAHPC-S; Haematologic Technologies, Essex Junction, VT, USA), mouse anti-human Mer (MAB8911; R&D Systems, MN, USA), rabbit anti-human-C4BPβ (Abcepta, San Diego, CA, USA), rabbit anti-human-TFPI (ProteinTech, Rosemont, IL, USA), mouse-anti-human-FV HC+LC monoclonal antibodies (Haematologic Technologies, Essex Junction, VT, USA), or 1 µg/mL sheep anti-human VWF (Abcam, Cambridge, UK) primary antibodies, with 0.5 µg/mL HRP-conjugated donkey anti-sheep IgG (Jackson ImmunoResearch, West Grove, PA, USA), horse anti-mouse IgG (Vector Laboratories, Newark, CA, USA), and goat anti-rabbit IgG (Vector Laboratories, Newark, CA, USA) secondary antibodies.

2.2.9 SDS PAGE and immunoblotting

Platelet lysate samples were subjected to SDS-PAGE on 4-20% polyacrylamide gel and transfer to nitrocellulose membranes, using a Mini-PROTEAN Tetra Cell system (Bio-Rad Laboratories, CA, USA) per recommended protocol. Immunoblotting was performed using

sheep anti-human PS (CL20105A; Cedarlane Laboratories, Burlington, Canada) and rabbit anti-human RabGDI [309] primary antibodies, with secondary antibodies donkey anti-sheep IgG (Jackson ImmunoResearch, PA, USA) and goat anti-rabbit IgG (Vector Laboratories, CA, USA), respectively. Computational densitometric analyses were performed using the Image Lab software (Bio-Rad Laboratories, CA, USA).

2.2.10 VWF multimer analysis

Plasma VWF multimer distribution was assayed by SDS-agarose gel electrophoresis and immunoblotting, adapted from protocols by Thomazini, et al [315] and Ott, et al [316]. Electrophoresis and membrane transfer were using the Mini-PROTEAN Tetra electrophoresis system and Mini Trans-Blot electrophoretic transfer cell (Bio-Rad, Hercules, CA, USA). Briefly, buffers for SDS-agarose gel electrophoresis were prepared for a 0.8-1.6% (w/v; stacking-resolving) discontinuous gel electrophoresis using Seakem HGT Agarose (Lonza, Basel, Switzerland). Gel glass cassette and stand, gel comb, and serological pipet were prewarmed (50°C, 15 m) prior to pouring of the microwave-heated gel solutions into the gel cassette, then the comb was inserted onto the stacking gel, and maintained at RT until solidification. Agarose gels were then kept at 4°C for 30 m. Plasma samples were normalized by the VWF:Ag ELISA results with agarose sample buffer to reach a final concentration of 1 µg/mL in 10 µL loading per well, whereas purified PS was 25 ng and VWF 10 ng. Shearing of samples was performed by vortexing at ~2,500 rpm for 30 s. Recalcification of plasma entailed the addition of 1 mM hirudin (Sigma Aldrich, St. Louis, MO, USA), 5 mM GPRP peptide (GenScript, Piscataway, New Jersey, USA), and 5 mM CaCl₂. Freshly prepared samples were heated at 56°C for 30 min prior to loading.

Electrophoresis of the samples was then conducted at 10 mA constant current at 9°C using precooled electrode buffer until the dye front had migrated to the bottom of the gels. To increase transfer efficiency of the higher multimers, the gel was incubated in 1 mM β -mercaptoethanol in transfer buffer for 30 m. Transfer to nitrocellulose membrane was conducted at constant 120 V and 4°C for 1 h. Immunoblotting was performed with either the LiCor system with IRdye antibodies (LiCor Biosciences, Lincoln, NE, USA) or the BioRad enhanced chemiluminescence with horse radish peroxidase (HRP)-conjugated antibodies, as described previously in section (2.2.9). Primary antibodies used were sheep anti-human PS (Cedarlane Laboratories, Burlington, Canada), mouse anti-human-VWF-A2 (R&D Systems), and rabbit anti-human C4BP- α (LifeSpan Biosciences, Seattle, WA, USA) IgG at 2 μ g/mL. Secondary antibodies used were IRdye 800CW donkey anti-goat, IRdye 680LT donkey anti-mouse, and IRdye 800CW donkey anti-rabbit IgG (LiCor Biosciences, Lincoln, NE, USA) at 0.1 μ g/mL, and HRP-conjugated donkey anti-sheep (Jackson ImmunoResearch, PA, USA) and horse anti-mouse IgG (Vector Laboratories, CA, USA) at 0.5 μ g/mL. Images were taken using either Image Studio (LiCor Biosciences) or ChemiDoc MP (BioRad).

2.2.11 Identification of VWF-binding proteins

Recombinant biotinylated VWF, expressed by stably transfected HEK293 cells, was immobilized onto streptavidin magnetic beads (New England Biolabs) [317]. The VWF-bound beads were exposed to pooled or single-donor human plasma, under static conditions and under shear (vortexing at 37°C for 30 min) in the presence of 10 mM EDTA. The beads were washed five times with PBS then subjected to on-bead trypsin digestion

and the released peptides were analyzed by nano-liquid chromatography coupled with tandem mass spectrometry (nano-LC-MS/MS), as described [318]. Proteins were identified by the presence of at least two tryptic peptides and the average peak area of the three most abundant unique peptides was used to calculate abundance of the captured protein, expressed as the shear-to-static ratio. Bead-bound proteins were electrophoresed on reducing 4-20% SDS-PAGE gels, transferred to nitrocellulose, and probed with antibodies against PS, C4BP- β , and C4BP- α .

2.2.12 VWF cleavage by ADAMTS13

VWF cleavage by recombinant ADAMTS13 was assayed with constant shearing (~2,500 rpm) at RT for 60 min with a tabletop mixer followed by immunoblotting, following protocol adapted from Han, et al [319]. Briefly, for each well, one microliter of control plasma N was diluted to 20 μ L and supplemented with 150 nM purified VWF, 5 mM GPRP peptide, 2 mM AEBSF (Thermo Scientific, Waltham, MA, USA), 5 mM CaCl₂, with or without 20mM EDTA, 50 nM recombinant ADAMTS13 (Novus Biologicals, Centennial, CO, USA), or 150 nM PS, in 0.2 mL PCR tubes. Samples were then sheared for 60 min using Retsch MM301 mixer mill (Glen Mills, Clifton, NJ, USA), mixed with agarose sample buffer, heated at 56°C for 30 min, and SDS-agarose electrophoresis, transfer, and immunoblotting performed according to the previously described procedure in section (2.2.9).

2.2.13 VWF/PS complex ELISA

A VWF/PS complex ELISA was developed, using goat anti-human VWF (Enzyme Research Laboratories) as the capture antibody and HRP-conjugated goat anti-human PS (Enzyme

Research Laboratories) as the detecting antibody. 96-well microplates were coated overnight with anti-VWF and blocked for 2 h with 2.5% casein (Sigma Aldrich, St. Louis, MO, USA). Purified protein samples in HBSA buffer or control plasma N, with or without shearing (~2,500 rpm for 30 s) or the addition of 1 mM hirudin, 5 mM GPRP peptide, and 5 mM CaCl₂, were added to the wells and incubated for the indicated times. After quick removal of the samples, the wells were washed five times with HBSAT (20 mM HEPES, 150 mM NaCl, 1% BSA, 0.1% Tween20) wash buffer, incubated with anti-PS for 90 min at RT, further washed five times, and finally mixed with freshly prepared OPD substrate. Color development was allowed to occur for 5-15 min and stopped with the addition of 50 µL of 2.5 M H₂SO₄.

2.2.14 Microfluidics

Microfluidic experiments were conducted using two systems. First, BioFlux 200 system by Fluxion Biosciences (Oakland, CA, USA) was utilized to visualize thrombus formation under flow. A 48-well (0-200 dyne/cm²) bioflux plate was incubated and coated with 40 µg/mL collagen (Chrono-Log Corporation, Havertown, PA, USA) for 1 h at RT, prior to blocking with PBSA. Freshly drawn whole blood was supplemented with 10 µg/mL Alexa Fluor 555-conjugated VWF and 200 nM Alexa Fluor 488-conjugated PS, either with or without prior shearing at ~2,500 rpm for 30 s. Alexa Fluor 555 and 488 were from Thermo Fisher Scientific (Waltham, MA, USA). Samples were then anticoagulated with 4 U/mL hirudin (Sigma Aldrich, St. Louis, MO, USA), recalcified with 1 mM CaCl₂, and perfused into the channel at 35 dyn/cm². After PBSA washing, images were taken with a Nikon Eclipse Ti2 microscope using the NIS elements software (Nikon, Tokyo, Japan).

Second, a polydimethylsiloxane (PDMS) microfluidic device was utilized to visualize PS binding to self-associated VWF. The PDMS microfluidic channel had a width of 60 μm and a 30 x 30 μm block in the center of the channel, as to previously described [320]. PDMS microfluidic channels were fabricated by casting Sylgard 184 (prepared at a 10:1 base to curing agent ratio by weight, Dow Corning) onto a silicon master structure. Devices were cured in a 110°C oven for 30 mins. Channel inlet and outlets were punched and the device was sealed onto a plasma-treated coverslip.

VWF was diluted in Tris-buffered saline (TBS, with or without 2 mM CaCl_2) to 7.5 $\mu\text{g}/\text{mL}$ and was flowed through the channel at a flow rate of 0.02 mL/min, resulting in VWF self-associated over the PDMS block. PS (80% unlabeled, 20% labeled with Alexa Fluor-488) was diluted to 7.5 $\mu\text{g}/\text{mL}$ (in TBS with or without 2 mM CaCl_2) and flowed into the channel. VWF self-association was visualized with differential interference contrast (DIC) microscopy and PS binding was visualized with epifluorescence microscopy. Z-stacks extending the height of the channel were captured after VWF and PS had been flowed through the channel; PS binding was quantified by creating a background-subtracted maximum intensity-projection and summing pixel intensity. Area of VWF self-association was quantified by manually outlining the DIC image.

2.2.15 Animal study approval and mouse TBI experiments

Animal studies were approved by the University of Kentucky Institutional Animal Care and Use Committee (IACUC), in compliance with the guidelines of the Association for the Assessment and Accreditation for Laboratory Animal Care, International and the NIH Guide for the Care and Use of Laboratory Animals [321].

All experiments were conducted using male C57BL/6J mice (2-3 months old; Jackson Laboratories, Bar Harbor, ME). The animals were housed 5 per cage, maintained in a 14h light/ 10h dark cycle, fed a balanced diet *ad libitum*. Animals were randomly assigned to groups and all data analyses were performed blinded to treatment groups. Experimental groups were euthanized at either 6 or 24 h after TBI or sham injury. For all outcomes, experiments were conducted with biological replicates of n=5-8/ group.

Controlled Cortical Impact (CCI)

The CCI procedure was performed according to past studies [322, 323]. Briefly, anesthetized (2.5% isoflurane) mice were fixed with ear bars in a stereotaxic frame. After scalp incision, a 3 mm craniotomy was performed lateral to midline and mice received a pneumatic impact (TBI-0310 Impactor, Precision Systems and Instrumentation, Fairfax, VA, USA: 1.0 mm depth; 3.5 m/sec velocity; 500 msec dwell) directly to brain using a 2 mm impactor tip. Sham animals received a craniotomy but no impact. Following impact, the craniotomy was covered with absorbable hemostat (Surgicel) and a plastic cap. Mice recovered on a heating pad until the animals were fully responsive.

Closed Head Injury (CHI)

Mice were subjected to CHI based on previous studies [324, 325]. Briefly, anesthetized mice (2.5% isoflurane) were fixed in a stereotaxic frame with non-rupture Zygomar ear cups (Kopf Instruments, Tujunga, CA). A scalp incision was made and mice received an impact at midline between bregma and lambda sutures using a pneumatic impactor (TBI-

0310 Impactor: 2.0 mm depth; 3.5 m/sec velocity; 500 msec dwell) fitted with a silicone tip. Sham-injured mice received all procedures except impact.

Isolation of Platelet Poor Plasma (PPP)

At either 6 h or 24 h post-injury, animals were asphyxiated with CO₂ and up to 1 mL blood was collected via cardiac puncture. Blood was harvested using 0.38% sodium citrate solution (supplemented with 0.2 U/mL apyrase and 10 ng/mL prostacyclin (Cayman Chemical, Cat #18220)) in a 26 G 3/8 syringe. Whole blood was centrifuged according to Hubbard, et al. [326]. Isolated platelet-rich plasma (PRP) was diluted 1:10 with prostacyclin (prepared at 1 mg/mL in 50 mM Tris, pH 9.5) in phosphate/glucose buffer (50 mL PBS, 45 mg glucose (5 mM)). The samples were centrifuged at 2,000 x *g* for 6 min at RT. The supernatant (PPP) was used for subsequent analyses.

2.2.16 Mouse Factor VIIa activation

Recombinant mouse FVII was activated using bacterial thermolysin. Briefly, mFVII was incubated at 100 µg/mL with 10 µg/mL Thermolysin in TNBC activation buffer (50 mM Tris, 10 mM CaCl₂, 150 mM NaCl, 0.05% (w/v) Brij-35, pH 7.5). After incubation, the reaction was stopped with 1,10-phenanthroline at a final concentration of 10 mM in activation buffer. The reaction mixture was further incubated at 37°C for 5 min, and the final concentration of mFVIIa was 2 µM.

2.2.17 Platelet activation

Washed platelets were prepared from whole blood withdrawn from healthy human donors as in (2.2.1). 2x10⁸/mL of washed platelets in HEPES-buffered Tyrode's (HT)

solution were activated with 50 nM α -thrombin (Enzyme Research Laboratories) in the presence of 5 mM RGDS peptide and 2 mM GPRP peptide for 2 min at 37°C, stopped with 75 nM hirudin, pelleted by centrifugation (700 x *g*, 15 min), and resuspended in HT supplemented with 5 mM RGDS peptide.

2.2.18 Factor Xa activity assay

Factor Xa activity was assayed using a chromogenic method in a 96-well plate. One nanomolar of TFPI α , 100 nM PS, and/or 10 μ g/mL VWF, with or without shear, were incubated in HBS-PEG-Ca for 20 min, with 20 μ M phospholipid vesicles, prior to initiating the reactions with 5 nM FXa and Spectrozyme FXa, a chromogenic substrate for FXa. Shearing of PS/VWF was done by vortexing for 30 s at \sim 2,500 rpm, at RT. Color development at 405 nm was monitored for 15 min using a SpectraMax plate reader.

2.2.19 Continuous thrombin generation assay

Continuous thrombin generation or prothrombinase activity was assayed using a chromogenic method in a 96-well plate. One nanomolar of APC, 100 nM PS, and/or 10 μ g/mL VWF, with or without shear, and 20 μ M phospholipid vesicles or 2×10^8 /mL washed platelet for some experiments, were incubated in HBS-PEG-Ca buffer for 15 min, prior to the addition of 1.4 μ M prothrombin, Spectrozyme TH, a chromogenic substrate for thrombin, and 5 nM FXa. Shearing of PS/VWF was done by vortexing for 30 s at \sim 2,500 rpm, at RT. Color development at 405 nm was monitored for 30 min using a SpectraMax plate reader.

2.2.20 Discontinuous thrombin generation assay

Discontinuous thrombin generation or prothrombinase activity was assayed using a chromogenic method in a 96-well plate. To assay APC/PS activity on FVa cleavage, we used a limiting FVa concentration and initiated the reaction with excess FXa. Twenty micromolar PL, 3 μ M DAPA (dansylarginine N-(3-ethyl-1,5-pentanediy)amide; Haematologic Technologies), 0.5 nM FVa, 1 nM APC, 100 nM PS, and/or 10 μ g/mL VWF, with or without shear, were incubated in HBS-PEG-Ca buffer for 15 min at RT, prior to initiating the reaction with 1.4 μ M prothrombin and 5 nM FXa. FXa-uninitiated reactions served as the zero timepoint. At the indicated times (20, 40, 60, 80, 100, and 120 s), reactions were stopped by mixing with HBS-PEG-EDTA (HBS-PEG solution supplemented with 50 mM EDTA, pH 7.4). Thrombin activity was measured as (2.2.19), using 20 μ L of each samples and 80 μ L of 0.4 mM Spectrozyme TH. Thrombin activity standards were generated using half dilutions of a 200 nM thrombin stock solution in HBS-PEG-EDTA. Thrombin concentration was extrapolated using nonlinear regression and the slope of thrombin concentration kinetics was calculated using GraphPad Prism.

2.2.21 FVa cleavage by APC

FVa cleavage was assayed with immunoblotting. Synthetic phospholipid vesicle (20 μ M) or 2×10^8 /mL activated platelets were incubated with 100 nM PS and/or 10 μ g/mL VWF, with or without shearing, in HT buffer for 10 min at RT, and reactions were initiated with the addition of 1 nM APC. At indicated times (1, 3, 5, 10, and 30 min), reactions were stopped with 50 mM EDTA and 1x protease inhibitor cocktail (EZBlock EDTA-free, BioVision, Milpitas, CA, USA). Platelet pellets were removed with centrifugation at 700 x

g for 10 min, and supernatants were added with 1x SDS-PAGE sample buffer. The samples were boiled for 10 min at 80°C. SDS-PAGE and immunoblotting was carried out as previously described in section (2.2.9).

2.2.22 Statistical analysis

Power analysis was conducted for experimental data a priori based on effect size and expected data variance. All experiments were performed in triplicate and results are presented as mean \pm standard deviation (SD). Statistical analyses were performed using GraphPad Prism version 8.0.2 (GraphPad Software, CA, USA). Differences between two groups were assessed by unpaired nonparametric Mann-Whitney test. For multiple comparisons, nonparametric Kruskal-Wallis with Dunn multiple comparison test was carried out. Correlation coefficients were calculated according to the method of Spearman. For all analyses, the significance of differences was set at $p < 0.05$.

CHAPTER 3. TOTAL PLASMA PROTEIN S IS A PROTHROMBOTIC MARKER IN PEOPLE LIVING WITH HIV

A part of this chapter has been published in *Journal of Acquired Immune Deficiency Syndrome*, 2022;90(4):463-471. The following is the manuscript and the author information:

Total Plasma Protein S is a Prothrombotic Marker in People Living with HIV

Martha M.S. Sim, MS¹, Meenakshi Banerjee, PhD¹, Thein Myint, MD^{2,3}, Beth A. Garvy, PhD⁴, Sidney W. Whiteheart, PhD¹, and Jeremy P. Wood, PhD^{1,5,6}

¹Department of Molecular and Cellular Biochemistry, University of Kentucky, Lexington, KY

²Division of Infectious Diseases, Department of Internal Medicine, University of Kentucky, Lexington, KY

³Bluegrass Care Clinic, Kentucky Clinic, University of Kentucky, Lexington, KY

⁴Department of Microbiology, Immunology and Molecular Genetics, University of Kentucky, Lexington, KY

⁵Lexington Veterans' Affairs Healthcare System, Lexington, KY

⁶Gill Heart and Vascular Institute, Division of Cardiovascular Medicine, Department of Internal Medicine, University of Kentucky, Lexington, KY

⁷Saha Cardiovascular Research Center, University of Kentucky, Lexington, KY

3.1 Introduction

Human Immunodeficiency Virus (HIV)-1 infection has caused over 35 million deaths worldwide, and there are currently 37 million people living with HIV-1 (PLWH) [136]. However, with the advent of antiretroviral therapy (ART), HIV-1 infection is now a manageable chronic disease where PLWH have near normal life expectancy [137]. The causes of death in HIV-1-infected individuals have shifted from Acquired Immunodeficiency Syndrome (AIDS)-related complications to comorbidities, including cardiovascular disease [138, 327]. PLWH have higher risk of venous (5-16-fold) and arterial (2-8-fold) thrombosis, and this risk does not completely reverse even with long-term ART treatment, suggesting that it is not solely related to viral load [139, 140]. The thrombophilia has been proposed to be multifactorial in origin, potentially including: chronic immune activation, opportunistic infections, traditional cardiovascular risk factors, and the side effects of lifelong medication [141]. However, the exact mechanisms leading to thrombosis are unclear.

HIV-1 infection is associated with many different types of procoagulant changes: (1) decreased plasma anticoagulants protein S (PS), protein C (PC), tissue factor pathway inhibitor (TFPI), and antithrombin III; (2) increased procoagulants tissue factor (TF) (cell surface and microvesicle-associated), fibrinogen, factor VIII, and von Willebrand factor; (3) platelet hyperactivity; and (4) increased neutrophil extracellular traps (NETs) [150]. Acquired PS deficiency is the most common coagulation abnormality in PLWH, with frequency as high as ~76% [141], and correlates with disease progression [185]. Congenital homozygous PS deficiency is associated with life threatening thrombosis

shortly after birth [41] and heterozygous PS deficiency with a 5-10-fold increased risk of thrombosis [81], suggesting that PS deficiency could contribute to the thrombotic risk in PLWH.

PS circulates as a free protein (~40%) or bound to the β -chain of complement factor C4b-binding protein (C4BP- β ; ~60%), and in the α -granules of platelets (~2.5%) (Figure 3.1A). Both total and free plasma PS are reduced in PLWH [139, 150]. Free PS is a critical anticoagulant cofactor for activated PC (APC) and the alpha isoform of TFPI (TFPI α), promoting inhibition of coagulation factors Va (FVa) and Xa (FXa), respectively [11, 328, 329]. FVa and FXa activate thrombin, the enzyme that converts fibrinogen into an insoluble fibrin clot [6]. Regulation of thrombin generation is essential, as excess thrombin produces potentially fatal occlusive thrombi. A recent study, which did not look at PS, showed that increased *ex vivo* plasma thrombin generation is predictive of all-cause mortality in PLWH, and that the best predictors of increased thrombin generation were PC and factor V, the target of APC/PS [142]. Despite the high prevalence of PS deficiency in HIV-1 infection [150], its pathologic consequences are unclear because PS concentration does not correlate with *ex vivo* plasma thrombin generation in the standard assay [23]. We hypothesized that this is due to a lack of PC activation. PC is activated through a negative feedback loop, and requires that thrombin bind the EC receptor thrombomodulin [18] (Figure 3.1B). Consistent with our hypothesis, we have previously shown that an inhibitory antibody against APC has no effect on plasma thrombin generation unless exogenous APC is added to the sample [23].

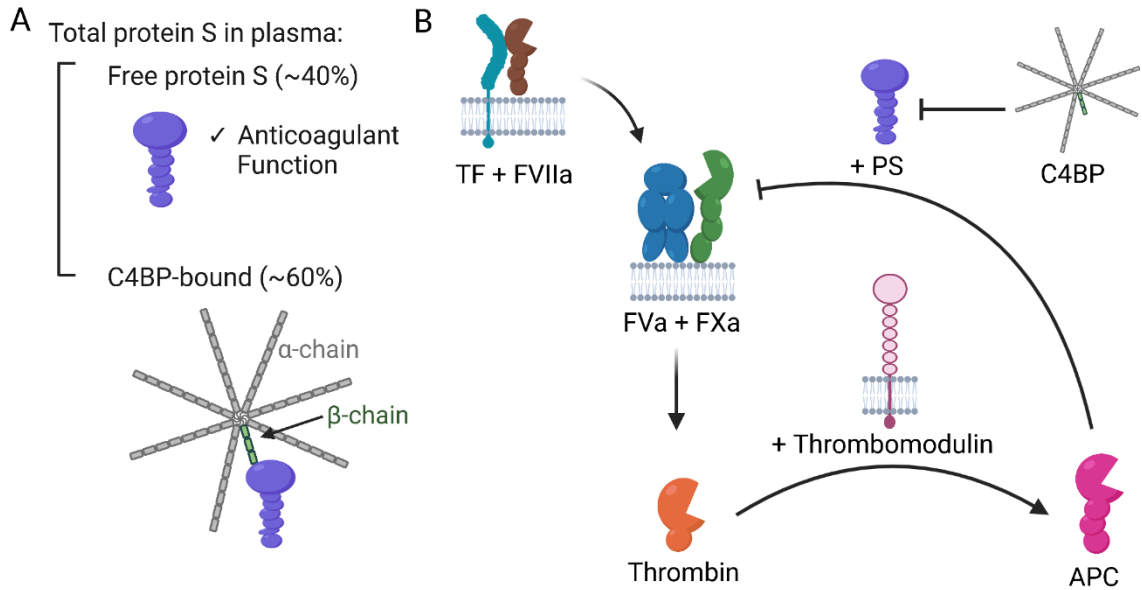


Figure 3.1. Schematic of protein S role in APC pathway

Schematic of (A) PS distribution in plasma and (B) PS role as cofactor for APC in prothrombinase (FVa+FXa) inhibition. As thrombin binds to thrombomodulin, PC is activated to APC, and together with PS inhibit prothrombinase activity in generating thrombin. C4BP binding inhibits APC cofactor activity of PS. (TF = Tissue Factor, FVIIa = factor VIIa, FVa = factor Va, FXa = factor Xa, APC = activated protein C, C4BP = C4b-binding protein). Image created with BioRender.com.

Increased expression of TF on circulating monocytes has also been reported in PLWH [151]. TF binds circulating factor VIIa (FVIIa) and initiates coagulation [4]. However, the contribution of increased TF expression on circulating monocytes to thrombin generation in PLWH has never been established. While monocytes are not present in plasma-based thrombin generation assays, they can release TF-bearing microvesicles, which would be present [152]. In addition, recent *in vitro* studies have shown that Herpes Simplex Virus virions can incorporate TF into their envelope [330]. If this same process occurs with HIV, then the virions represent an additional source of TF in the assay. As increased plasma thrombin generation is a strong predictor of mortality in PLWH [142], we sought to define the contributions of PS and TF to *ex vivo* plasma thrombin generation in this population.

Here, we present a refined PS-sensitive thrombin generation assay and show that PS deficiency strongly correlates with increased thrombin generation. We did not observe any increase in plasma TF, suggesting that it does not significantly contribute to *ex vivo* plasma thrombin generation in the population studied.

3.2 Results

3.2.1 Study population

The study population were previously described, in part, by Banerjee et al [309]. Subjects were classified as either healthy control (n = 9), naïve (PLWH on first diagnosis prior to receiving treatment, n = 17), or ART (PLWH on antiretroviral treatment, n = 13) (Table 3.1, Table 3.2). Due to the PLWH population seen in the Kentucky Clinic, the cohort is mostly male, with only 2 female PLWH recruited.

Group	Control	Naïve	ART-treated
Number	9	17	13
Male/Female	7/2	15/2	13/0
Age	35.2 ± 10.2	27.3 ± 6.1	49.5 ± 8.7
Race or ethnicity (A/AA/C/H)	3/1/5/0	2/5/8/2	0/3/10/0
Viral Load (copies x10 ³ /mL)	N.D.	413.6 ± 1080.1	12 of 13 subjects were B.D.L., one subject was 7.4
Platelet Count (x10 ³ /μL)	N.D.	225.1 ± 75.6	226.0 ± 53.0

Table 3.1. Description of HIV-1 study population

Abbreviations: Asian (A), African American (AA), Caucasian (C), Hispanic (H); ART: antiretroviral therapy; N.D.: not determined; B.D.L.: below detection limit. Data are in mean ± SD.

Subject	ART regimen
1	FTC (NRTI), TDF (NRTI), DRV (PI), RTV (PI)
2	ABC (NRTI), DTG (II), 3TC (NRTI)
3	FTC (NRTI), TAF (NRTI), DTG (II)
4	ABC (NRTI), DTG (II), 3TC (NRTI), MVC (EI)
5	FTC (NRTI), TDF (NRTI), RAL (II)
6	EVG (II), FTC (NRTI), TAF (NRTI)
7	ABC (NRTI), DTG (II), 3TC (NRTI), RPV (NNRTI)
8	FTC (NRTI), TDF (NRTI), RAL (II)
9	FTC (NRTI), TDF (NRTI), RAL (II)
10	EFV (NNRTI), FTC (NRTI), TDF (NRTI)
11	FTC (NRTI), RPV (NNRTI), TAF (NRTI)
12	BIC (II), FTC (NRTI), TAF (NRTI)
13	EVG (II), FTC (NRTI), TAF (NRTI)

Table 3.2. Therapeutic regimen of ART-treated patients

Nucleoside Reverse Transcriptase Inhibitors (NRTI): emtricitabine (FTC), tenofovir disoproxil fumarate (TDF), abacavir (ABC), lamivudine (3TC), tenofovir alafenamide (TAF); Protease Inhibitor (PI): darunavir (DRV), ritonavir (RTV); Integrase Inhibitor (II): dolutegravir (DTG), raltegravir (RAL), elvitegravir (EVG), bictegravir (BIC); Entry Inhibitor (EI): maraviroc (MVC); Non-Nucleoside Reverse Transcriptase Inhibitor (NNRTI): rilpivirine (RPV), efavirenz (EFV).

3.2.2 Total plasma PS is reduced in untreated PLWH

We measured total plasma PS (Figure 3.2A) and found that it was significantly reduced in PLWH compared to healthy controls ($P = 0.009$), with 50% of PLWH (15 of 30) having clinical deficiency (below 70% reference value) ($100 \pm 25.57\%$ in controls vs $69.59 \pm 35.29\%$ in PLWH). The deficiency was particularly pronounced in naïve PLWH samples, 58.8% of which (10 of 17) were below 70% (average $58.87 \pm 23.99\%$ total PS, $P = 0.0093$, relative to healthy controls). By contrast, only 38.5% (5 of 13) of ART-treated PLWH had clinical PS deficiency, and the average PS concentration in this group was not different than healthy controls ($83.6 \pm 43.21\%$, $P = 0.3911$). These data suggest that ART treatment restores PS deficiency in most, but not all, PLWH, consistent with previous reports [139]. PS concentration did not correlate with PLA ($P = 0.6005$) (Figure 3.2B), platelet count ($P = 0.3991$) (Figure 3.2C), or viral load in naïve PLWH samples ($P = 0.3774$) (Figure 3.2D). The ART-treated PLWH were older than the naïve PLWH (Table 3.1), total PS concentration did not significantly change with age, and there was no difference in the slopes of total PS with age between groups ($P = 0.14$; Figure 3.3A), consistent with the report of Ellery et al, who observed that PS increases with age in females but not males [87].

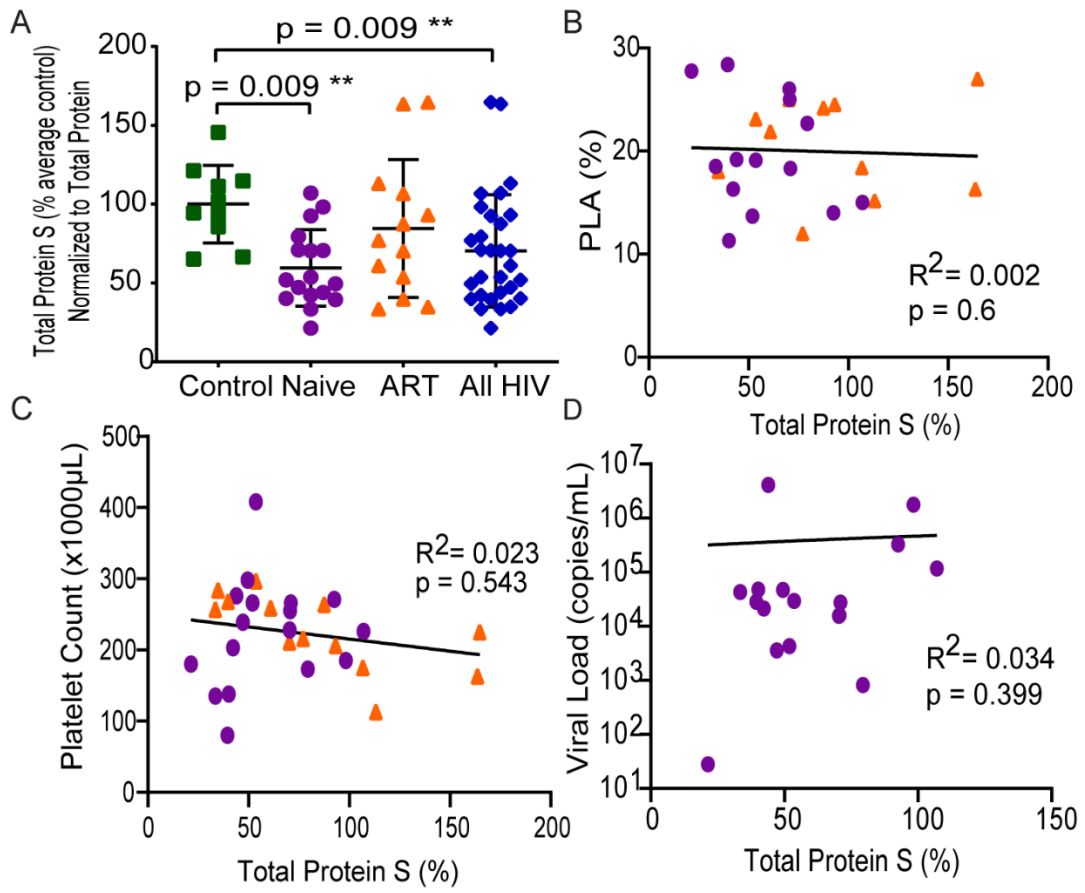
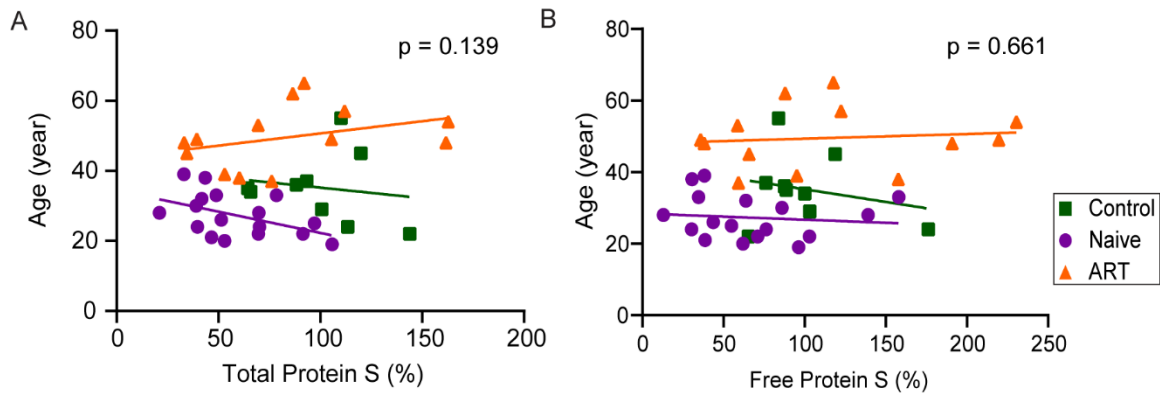


Figure 3.2. Total plasma PS is deficient in PLWH

Figure 3.2. Total plasma PS is deficient in PLWH

(A) Total plasma PS of 9 healthy controls, 13 PLWH on first diagnosis prior to treatment (naïve), and 17 PLWH on antiretroviral treatment (ART) in citrated platelet poor plasma measured by ELISA (mean \pm SD). Values were compared to a standard curve of control plasma. (B-D) Total plasma PS plotted against (B) platelet-leukocyte aggregation (PLA) measured by flow cytometric analyses, (C) platelet count measured by particle counter method, and (D) viral load of naïve PLWH derived from medical record. Every data point is the average of three measurements. Every data point is the average of three measurements. *P*-values are according to Mann-Whitney and Kruskal-Wallis with Dunn's multiple comparison test in panel A. *P*-values and correlation coefficients are according to Spearman correlation analysis in panel B-D. (**, $p < 0.01$)

PLA flow cytometric analyses and platelet count measurements were conducted by Dr. Meenakshi Banerjee. The study population were previously described, in part, by Banerjee et al [309].



3.2.3 Free PS and PC show trends toward depletion

We also measured free plasma PS (Figure 3.4A), which were lower in HIV-1 patients, albeit not reaching significance (controls vs PLWH, $P = 0.1695$; controls vs naïve, $P = 0.1022$; naïve vs ART, $P = 0.0973$; and controls vs ART, $P > 0.9999$). Free and total plasma PS measurements show significant positive correlation (Figure 3.4B), and the ratio of free to total plasma PS was not different between groups (Figure 3.4C), indicating an overall depletion of PS rather than a shift between free and C4BP-bound pools. Therefore, we proceeded with a focus on total PS as the main component of analysis. C4BP- β was unchanged in PLWH (Figure 3.4D), and PC trended towards a decrease in naïve PLWH, though this was not statistically significant ($P = 0.1204$; Figure 3.4E). ART-treated PLWH had higher PC than naïve PLWH ($P = 0.0437$).

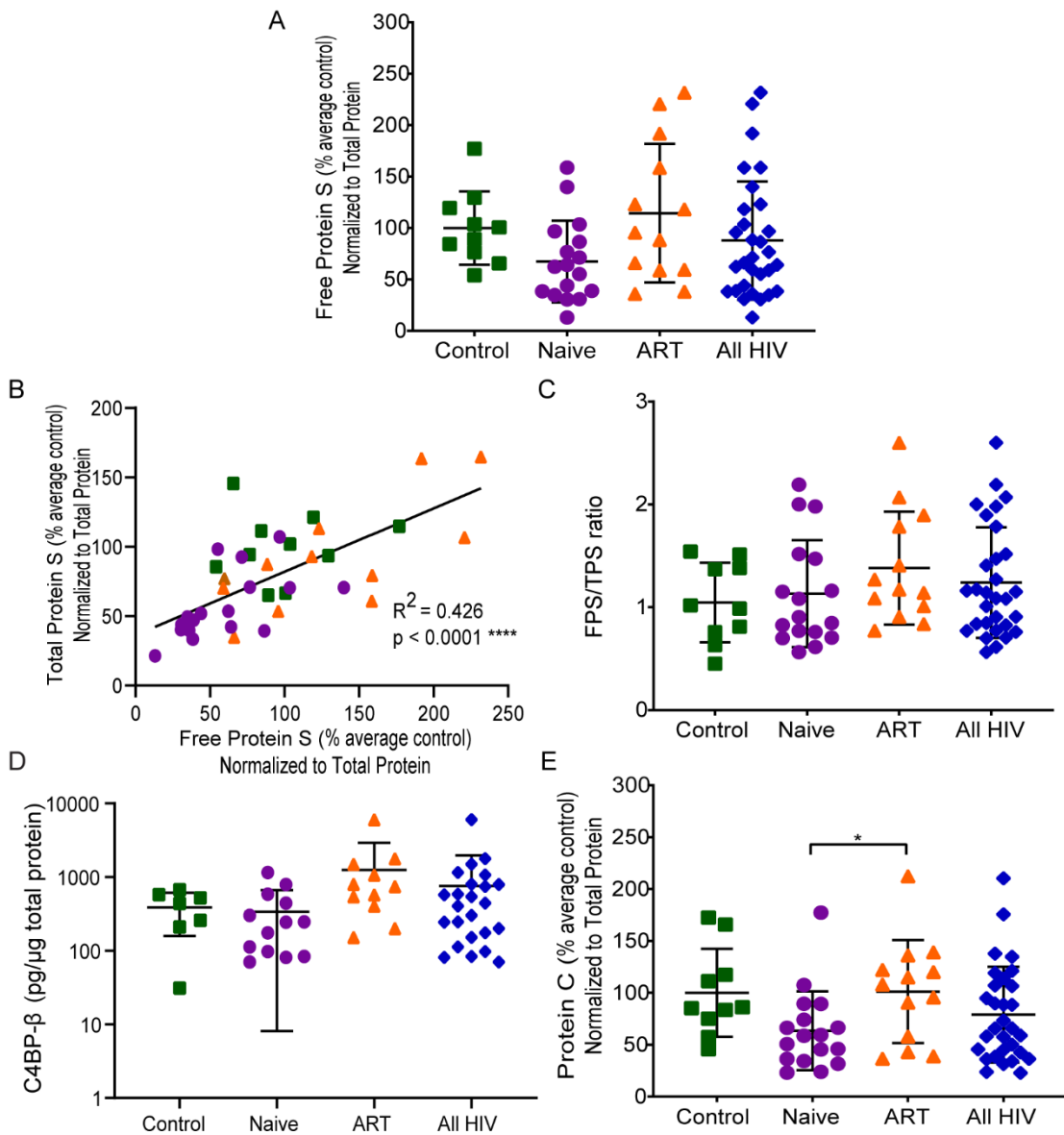


Figure 3.4. Free PS and PC show similar trend toward depletion

Figure 3.4. Free PS and PC show trends toward depletion

(A) Free PS measured by ELISA, (B) Free PS plotted against total PS, (C) Ratio of free to total PS. (D) C4b-binding protein- β measured by ELISA, (E) Protein C measured by ELISA. Every data point is the average of three measurements. *P*-values are according to Kruskal-Wallis with Dunn's multiple comparison test in panel A and C-E. *P*-values and correlation coefficients are according to Spearman correlation analysis in panel B. (*, $p < 0.05$; ****, $p < 0.0001$).

3.2.4 Development of a PS-sensitive TG assay

Despite the high prevalence of PS deficiency in HIV-1 infection [150], its pathologic consequences are unclear because PS concentration does not correlate with plasma thrombin generation *ex vivo* [23]. We hypothesized that the standard plasma thrombin generation assay could be insensitive to PS, because PC activation requires EC thrombomodulin (TM) [18]. Consistent with this, addition of 150 nM exogenous PS to PS-depleted plasma had very little effect on TF-initiated thrombin generation, causing only an 8% decrease in peak thrombin and a 12% decrease in total thrombin produced (Figure 3.5A). We next supplemented the assay with 20 nM recombinant human soluble TM, which contains the extracellular region of TM required for thrombin-mediated PC activation. In the absence of PS, TM had little effect on thrombin generation (Figure 3.5B). However, we observed a dose-dependent decrease in thrombin generation when the plasma was supplemented with PS. As PS concentration increased, peak thrombin (Figure 3.5C) and endogenous thrombin potential (ETP) (Figure 3.5D) decreased, with 150 nM PS causing 75% and 74% decreases, respectively. By contrast, the lag time was unaffected (Figure 3.5E), consistent with the need for some thrombin generation before PC can be activated. We confirmed the importance of APC in this assay using PC-depleted plasma, in which TM-supplementation had little or no effect (Figure 3.5F).

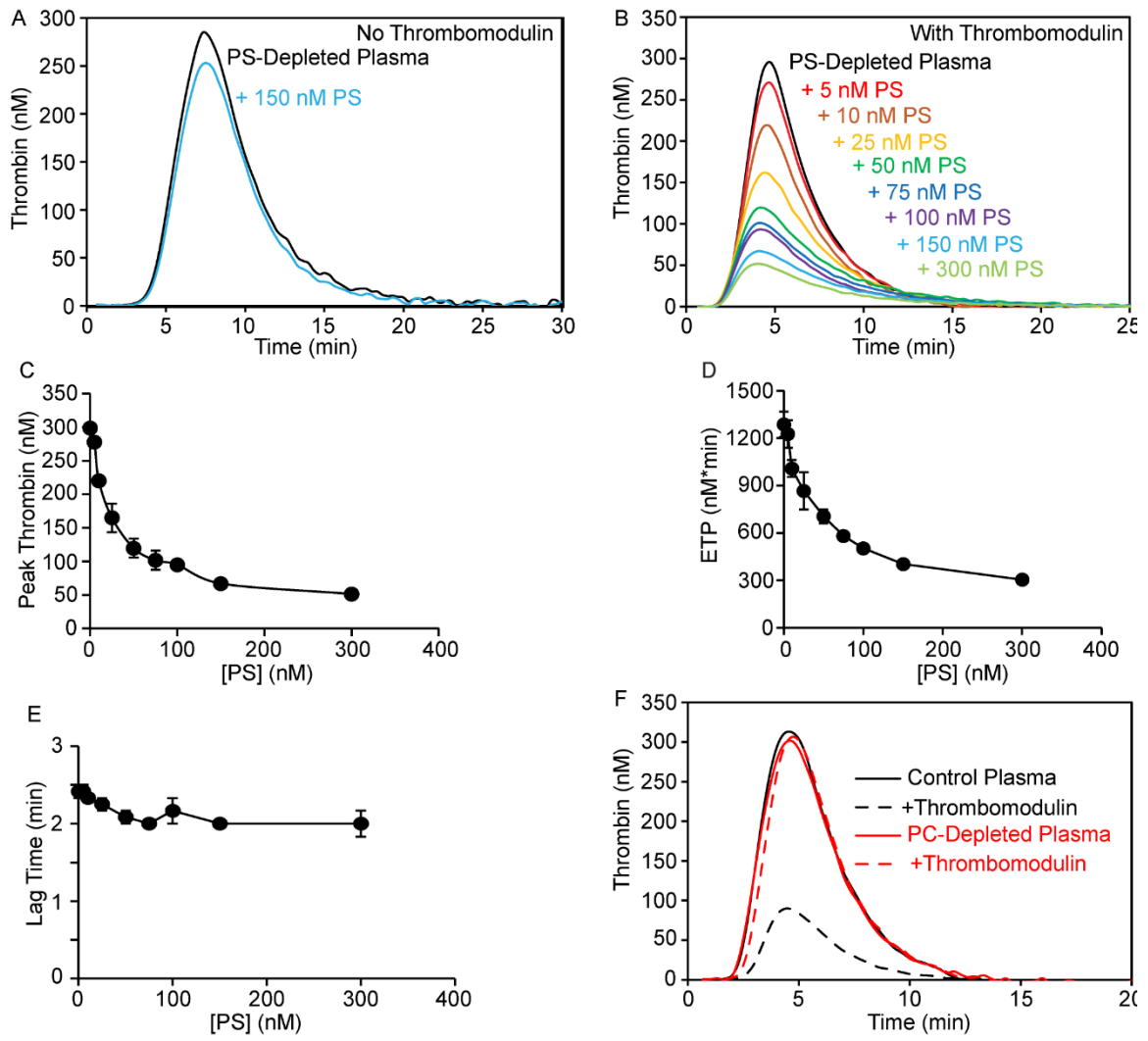


Figure 3.5. Development of PS-sensitive TG assay

Figure 3.5. Development of PS-sensitive TG assay

(A, B) Plasma thrombin generation in respect to time, measured using fluorogenic substrate to thrombin according to the Calibrated Automated Thrombography (Thrombinoscope) method (Diagnostica Stago) (A) of PS-depleted plasma without thrombomodulin supplementation and (B) of PS-depleted plasma with 20 nM thrombomodulin supplementation, initiated with 1 pM Tissue factor and 4 pM phospholipid (PE:PC:PS = 40:40:20) vesicles, in the absence or presence of purified PS. (C-E) Concentration of supplemented PS plotted against (C) peak thrombin concentration, (D) endogenous thrombin potential (ETP), and (E) lag time (mean \pm SD, n = 3). (F) Plasma thrombin generation in respect to time of control plasma and protein C-depleted plasma, with and without 20 nM thrombomodulin supplementation. Every data point is the average of three measurements.

3.2.5 Plasma PS deficiency correlates with increased TG

We utilized this modified assay to measure PS-independent and PS-dependent thrombin generation in PLWH samples. We measured plasma thrombin generation under three conditions: (1) initiated with phospholipids alone; (2) initiated with TF and phospholipids; and (3) initiated with TF and phospholipids in the presence of TM. In PLWH samples, total plasma PS did not correlate with phospholipids-initiated thrombin generation (peak thrombin and ETP: $P = 0.8419$ and $P = 0.5220$, respectively) (Figure 3.6A-B) or TF-initiated thrombin generation in the absence of TM ($P = 0.2659$ and $P = 0.4033$) (Figure 3.6C-D), consistent with previous reports [23]. In the presence of TM, there was a negative correlation, with decreased PS associated with increased peak thrombin (Figure 3.6E) ($R^2 = 0.1338$, $P = 0.003$) and ETP (Figure 3.6F) ($R^2 = 0.1643$, $P = 0.0025$). Total PS did not correlate with lag time of thrombin generation when no exogenous TF was added ($P = 0.2413$) (Figure 3.7A) or when TF and TM were added ($P = 0.6126$) (Figure 3.7B). However, there was a positive correlation between PS and lag time when thrombin generation was initiated with exogenous TF without TM ($R^2 = 0.1411$, $P = 0.0153$) (Figure 3.7C). This may reflect the TFPI cofactor activity of PS [11], or the recently described anti-factor IXa activity [294], which may be masked when the full anticoagulant system is present. Finally, raw thrombin generation curves of PLWH with highest (mean = 91.37%) and lowest (mean = 25.83%) values of plasma PS showed that there was no trend seen in thrombin generation when TM was not added (Figure 3.7D), whereas, when TM was added, thrombin generation of PLWH with the lowest PS showed a decreased sensitivity to TM compared to PLWH with higher PS (Figure 3.7E). This finding was true for both naïve

and ART-treated PLWH samples. Thus, total plasma PS deficiency did contribute to increased thrombin generation in this PLWH population, in an assay sensitive to PS. Similarly, free PS and PC negatively correlated with plasma thrombin generation when TM was present (Figure 3.8).

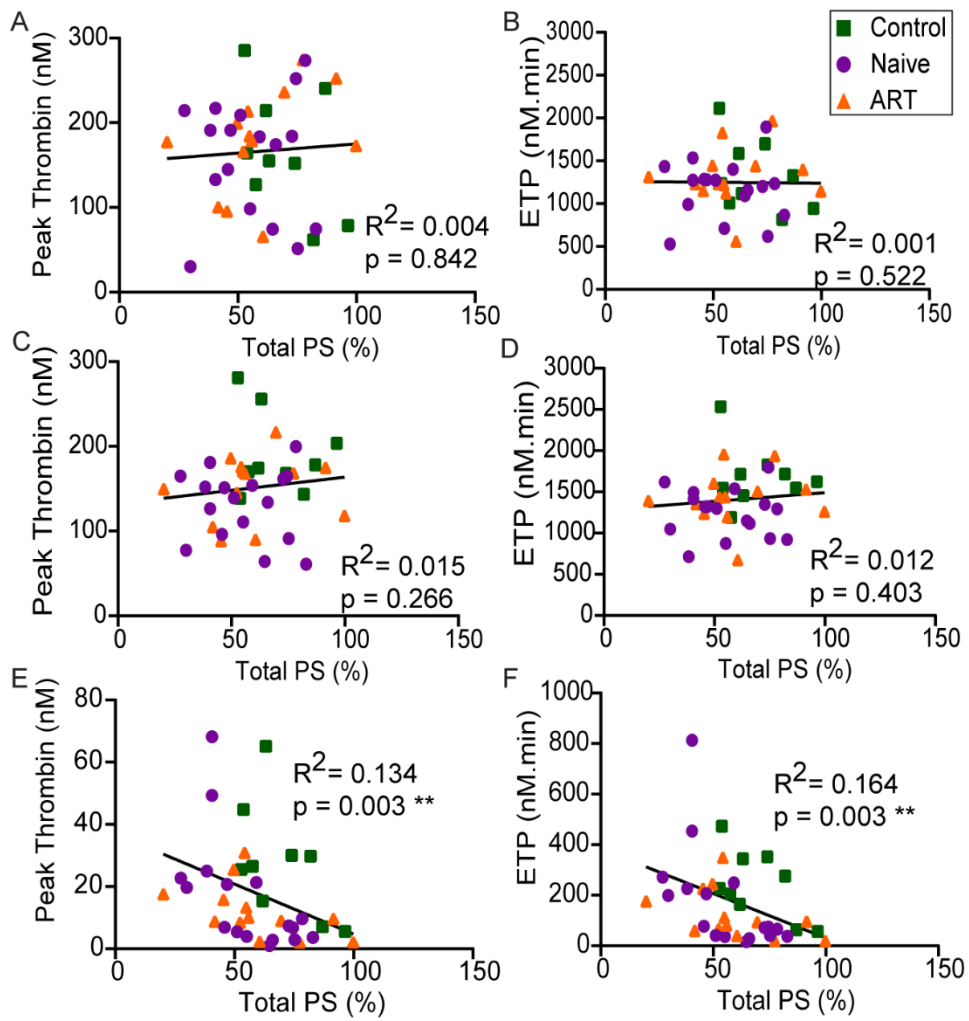


Figure 3.6. Plasma PS deficiency correlates with increased TG

Figure 3.6. Plasma PS deficiency correlates with increased TG

(A-F) Total plasma PS plotted against (A) peak thrombin concentration and (B) endogenous thrombin potential (ETP) in phospholipids (4 pM)-initiated; (C) peak thrombin concentration and (D) ETP in phospholipids (4 pM)/TF (1 pM)-initiated; and (E) peak thrombin concentration and (F) ETP in phospholipids/TF-initiated with 20 nM thrombomodulin supplementation; plasma thrombin generation measurements. Every data point is the average of three measurements. *P*-values and correlation coefficients are according to Spearman correlation analysis (**, $p < 0.01$).

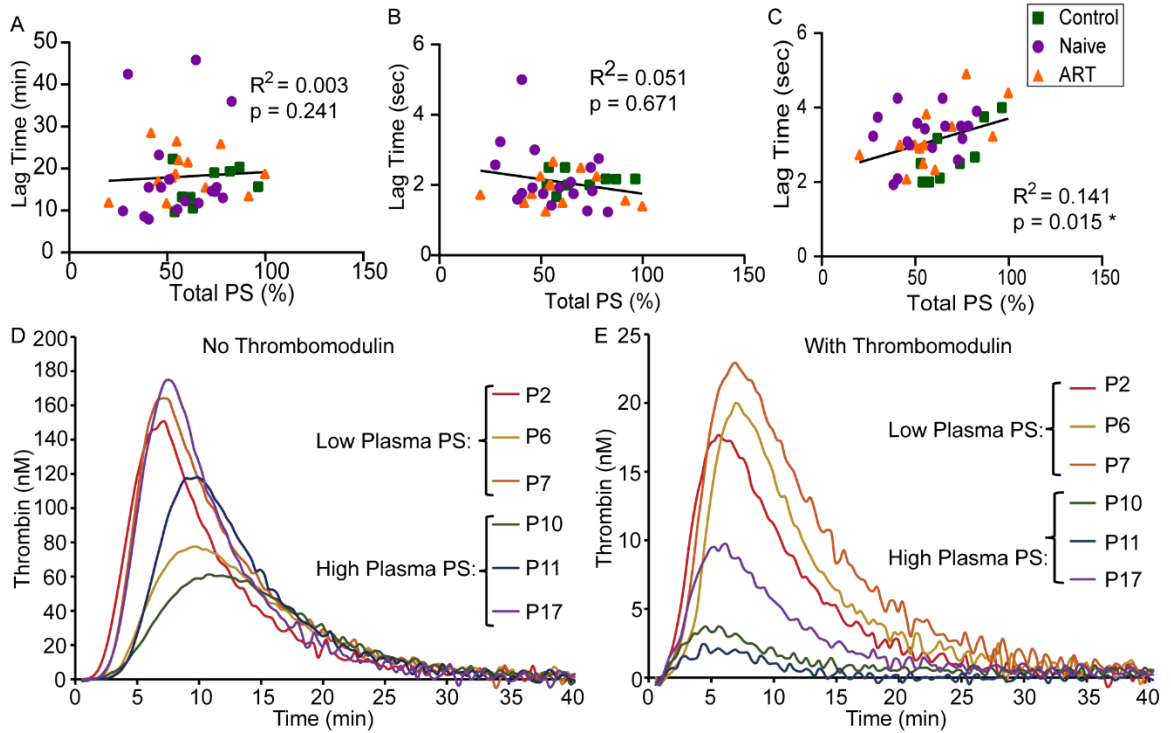


Figure 3.7. There is no correlation between total PS and lag time when TM is supplemented

(A-C) Total plasma PS plotted against lag time of plasma thrombin generation in (A) phospholipids-initiated, (B) phospholipids/Tissue Factor (TF)-initiated with 20 nM thrombomodulin supplementation, and (C) phospholipids/TF-initiated assays. (D, E) Thrombin generation in respect to time, of three patient plasma samples with low plasma PS (P2, P6, P7; mean = 25.83%) and high plasma PS (P10, P11, P17; mean = 91.37%), (D) in the absence and (E) in the presence of 20 nM thrombomodulin supplementation. Every data point is the average of three measurements. *P*-values and correlation coefficients are according to Spearman correlation analysis (*, $p < 0.05$).

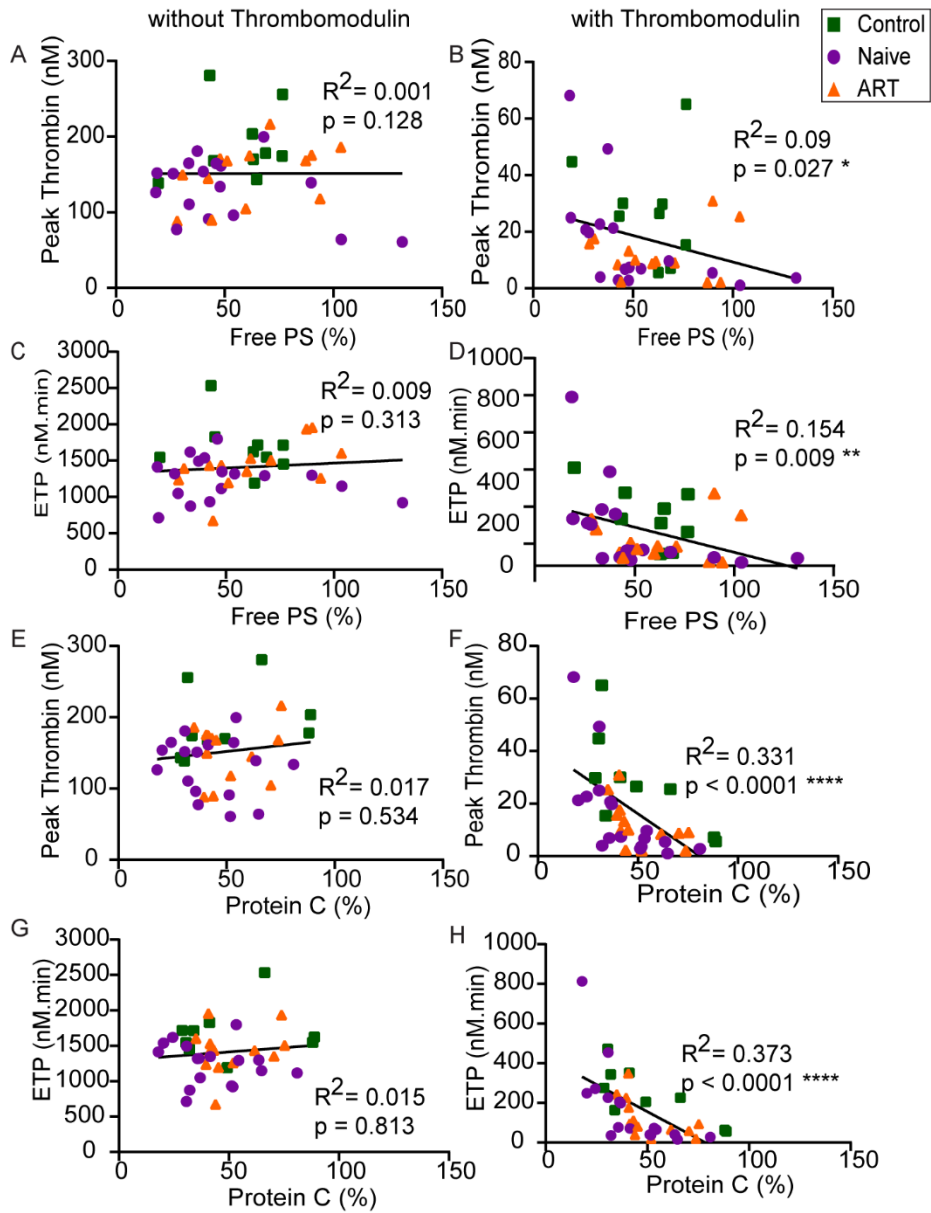


Figure 3.8. Free PS and PC negatively correlate with plasma TG when TM is supplemented

Figure 3.8. Free PS and PC negatively correlate with plasma TG when TM is supplemented (A-D) Free plasma PS and (E-F) protein C plotted against (A-B, E-F) peak thrombin generation and (C-D, G-H) endogenous thrombin potential (ETP) in (A, C, E, G) phospholipids/Tissue Factor (TF)-initiated and (B, D, F, H) phospholipids/TF-initiated with 20 nM thrombomodulin supplementation. Every data point is the average of three measurements. *P*-values and correlation coefficients are according to Spearman correlation analysis.

3.2.6 Antiretroviral treatment has no direct effect on plasma TG

Plasma thrombin generation was not different in ART-treated and naïve PLWH in the absence of TM (peak thrombin = 150.5 ± 39.4 nM vs 131.0 ± 41.3 nM, $P = 0.1833$; and ETP = 1425 ± 326.5 nM*min vs 1247 ± 289.1 nM*min, $P = 0.1227$) (Figure 3.9A-B) or in the presence of TM ($P = 0.9671$ and $P = 0.9671$) (Figure 3.9C-D). Consistent with this, none of the most common ART drugs used by our patient population (Table 3.2) had any direct effect on plasma thrombin generation at therapeutic concentrations (Figure 3.10A-B), with the exception of ritonavir, an inhibitor of the HIV protease, which slightly inhibited thrombin generation, likely indicating an off-target effect on one of the coagulation enzymes (Figure 3.10B).

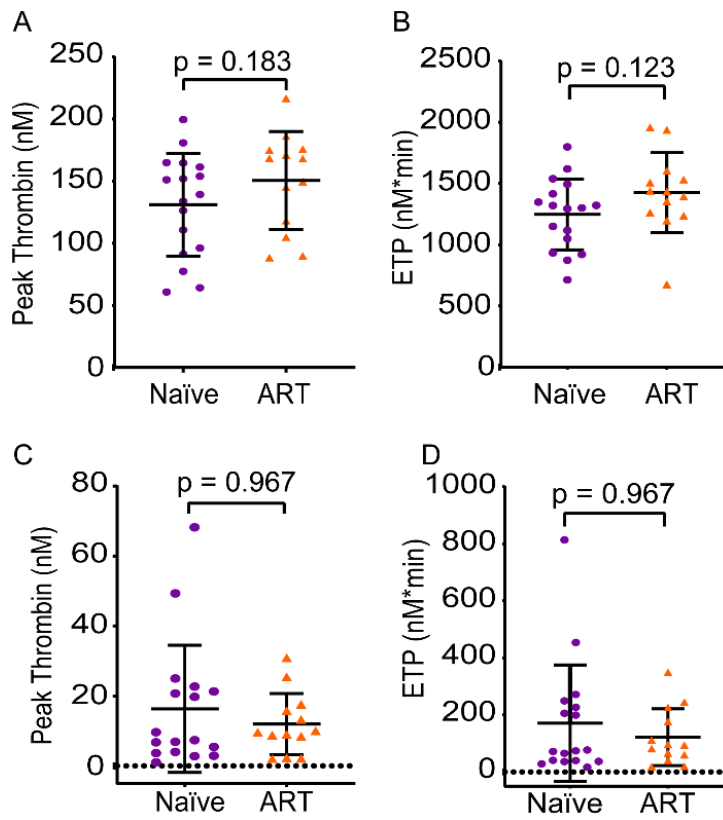


Figure 3.9. ART had no direct effect on plasma TG in PLWH

Plasma thrombin generation parameters; peak thrombin generation and endogenous thrombin potential (ETP), respectively, are shown according to antiretroviral treatment status, in assays that are (A, B) phospholipids/TF-initiated and (C, D) phospholipids/TF-initiated supplemented with 20 nM thrombomodulin. Every data point is the average of three measurements. *P*-values are according to Mann-Whitney test.

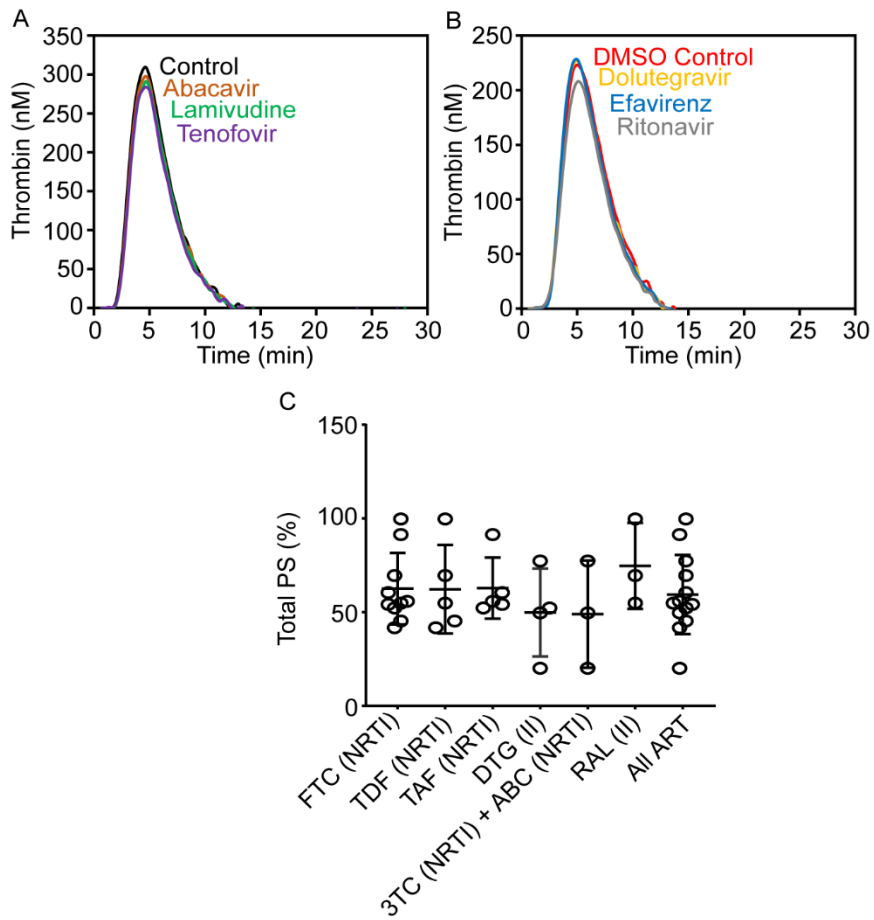


Figure 3.10. ART had no direct effect on plasma TG in healthy plasma *in vitro*

Figure 3.10. ART had no direct effect on plasma TG in healthy plasma *in vitro*

(A, B) Phospholipids/TF-initiated plasma thrombin generation was measured in control plasma N (Siemens Healthineers) after 1 hour incubation with various antiretroviral drugs in separate experiments. (C) Total plasma PS of ART-treated PLWH grouped in an inclusive manner by ART regiment, for drugs with at least n = 3. Every data point is the average of three measurements. ART drug or class abbreviations: Nucleoside Reverse Transcriptase Inhibitors (NRTI): emtricitabine (FTC), tenofovir disoproxil fumarate (TDF), abacavir (ABC), lamivudine (3TC), tenofovir alafenamide (TAF); Protease Inhibitor (PI): darunavir (DRV), ritonavir (RTV); Integrase Inhibitor (II): dolutegravir (DTG), raltegravir (RAL), elvitegravir (EVG); Entry Inhibitor (EI): maraviroc (MVC); Non-Nucleoside Reverse Transcriptase Inhibitor (NNRTI): rilpivirine (RPV), efavirenz (EFV).

3.2.7 Plasma TF activity does not correlate with TG

Monocytes, while not present in these plasma assays, can release TF-bearing microvesicles, which would be present and could contribute to plasma thrombin generation [152]. In addition, based on studies of Herpes Simplex Virus, it is possible that HIV-1 virions may also contribute TF to this assay [330]. We isolated plasma TF with high-speed centrifugation, and measured its activity using an assay sensitive to low femtomolar concentrations (Figure 3.11A). TF activity was not different between PLWH and controls (80.1 ± 60.6 fM vs 108.2 ± 47.4 fM, $P = 0.08$) or between naïve and ART-treated PLWH (75.11 ± 61.5 fM vs 86.58 ± 61.4 fM, $P > 0.9999$) (Figure 3.11B).

There was no correlation between plasma TF and either peak thrombin ($P = 0.4135$) or ETP ($P = 0.7295$) (Figure 3.12A-B), or with any of the thrombin generation parameters when exogenous TF was added (Figure 3.12C-H). Plasma TF did correlate with a shorter lag time for thrombin generation, but only when no exogenous TF was added ($R^2 = 0.1539$, $P = 0.0039$) (Figure 3.11C, Figure 3.12A-B), consistent with the low concentrations of TF detected in the samples.

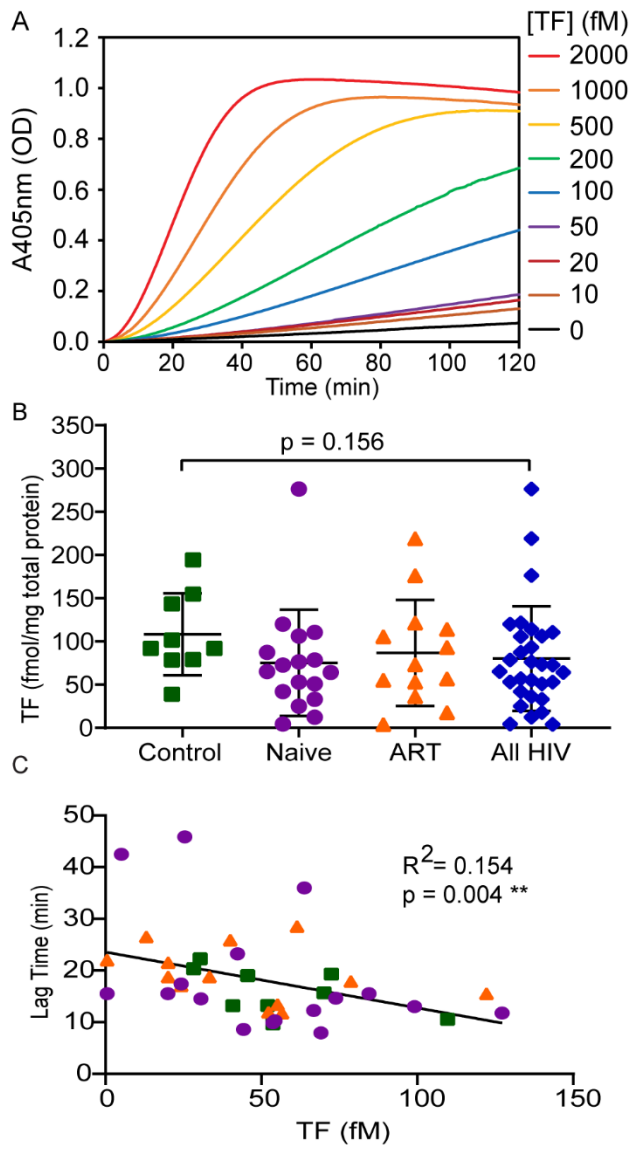


Figure 3.11. Plasma TF activity is not increased in PLWH

Figure 3.11. Plasma TF activity is not increased in PLWH

(A-B) TF activity measured by Factor Xa generation assay, using a chromogenic substrate cleavage monitored by absorbance at 405 nm (optical density). (A) Factor Xa generation and standard curves of recombinant TF in HBSA, shown as absorbance in respect to time (B) Plasma TF activity of healthy controls and PLWH. (C) Lag time of plasma thrombin generation measured in phospholipids-initiated assays. Every data point is the average of three measurements. *P*-values are according to Kruskal-Wallis with Dunn's multiple comparison test in panel B, *P*-values and correlation coefficients are according to Spearman correlation analysis in panel C (**, $p < 0.01$).

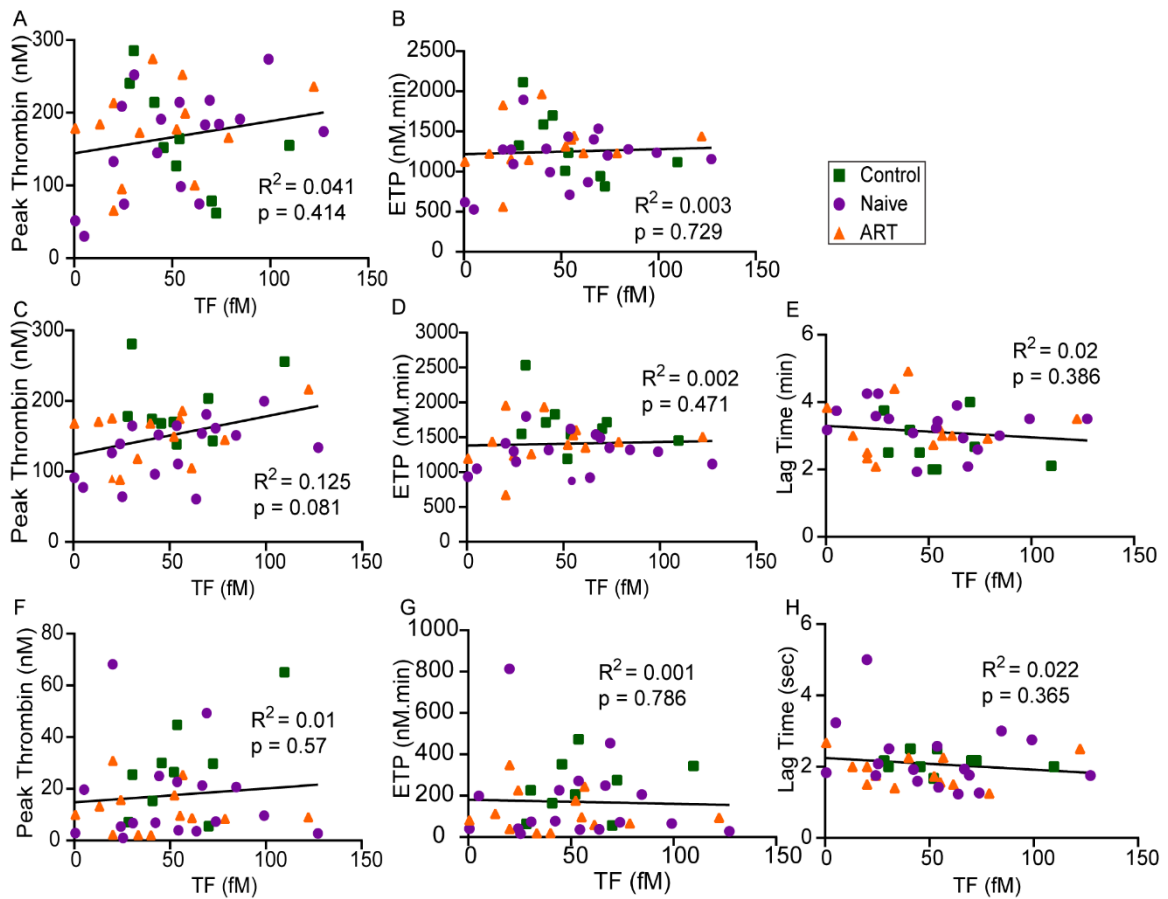


Figure 3.12. Plasma TF activity does not correlate with TG unless no exogenous TF is added. Plasma TF activity plotted against plasma thrombin generation parameters; peak thrombin concentration, endogenous thrombin potential (ETP) and lag time, respectively, in measurements that are (A-B) phospholipids-initiated, (C-E) phospholipids/TF-initiated, or (F-H) phospholipids/TF-initiated supplemented with 20 nM thrombomodulin. Every data point is the average of three measurements. *P*-values and correlation coefficients are according to Spearman correlation analysis.

3.3 Conclusions

In conclusion, we describe here a PS-sensitive plasma thrombin generation assay, and show that PS deficiency in PLWH contributes to increased thrombin generation potential, and likely to increased thrombotic risk. By contrast, we did not observe changes in plasma TF in our patient population. We propose using total plasma PS as a marker to identify and manage individuals with the highest risk of developing thrombotic complications.

CHAPTER 4. VON WILLEBRAND FACTOR CONTRIBUTES TO FREE PROTEIN S DEFICIENCY
IN COVID-19

A part of this chapter has been submitted for publication to the *Circulation Research*. The following are the manuscript and the author information:

Von Willebrand Factor Contributes to Free Protein S Deficiency in Patients with SARS-
CoV-2

Martha M.S. Sim¹, Molly Y. Mollica^{2,3,4}, Hammodah R. Alfar¹, Melissa Hollifield⁵, Dominic W. Chung^{2,6}, Xiaoyun Fu^{2,3}, Siva Gandhapudi⁵, Daniëlle M. Coenen¹, Kanakanagavalli S. Prakhya¹, Dlovan F.D. Mahmood⁷, Meenakshi Banerjee¹, Chi Peng⁸, Xian Li⁷, Alice C. Thornton⁹, James Z. Porterfield^{5,9}, Jamie L. Sturgill⁵, Gail A. Sievert¹⁰, Marietta Barton-Baxter¹⁰, Kenneth S. Campbell¹⁰, Jerold G. Woodward⁵, José A. López^{2,3}, Sidney W. Whiteheart^{1,7}, Beth A. Garvy⁵, and Jeremy P. Wood^{1,7,11}

¹Department of Molecular and Cellular Biochemistry, University of Kentucky, KY

²Bloodworks Northwest Research Institute, WA

³Division of Hematology, School of Medicine, University of Washington, WA

⁴Department of Mechanical Engineering, University of Maryland, Baltimore County, MD

⁵Department of Microbiology, Immunology and Molecular Genetics, University of Kentucky, KY

⁶Department of Biochemistry, University of Washington, WA

⁷Saha Cardiovascular Research Center, University of Kentucky, KY

⁸Department of Pharmacology and Nutritional Sciences, University of Kentucky, KY

⁹Division of Infectious Disease, University of Kentucky, KY

¹⁰Center for Clinical and Translational Science, University of Kentucky, KY

¹¹Division of Cardiovascular Medicine Gill Heart and Vascular Institute, University of
Kentucky, KY

4.1 Introduction

Hemostasis, the process of blood clot formation in response to vascular injury, is initiated by exposure of extravascular TF to the blood, which binds circulating coagulation FVIIa. The TF/FVIIa complex activates factors IX and X to factors IXa and Xa, respectively [4]. FIXa, in complex with FVIIIa, activates additional FXa. FXa with FVa forms the prothrombinase complex, which generates thrombin from circulating prothrombin [6]. Thrombin is the serine protease responsible for the conversion of soluble fibrinogen to an insoluble fibrin clot. Thrombosis, pathological blood clot formation, occurs due to hypercoagulability of the blood. As excessive thrombin generation leads to thrombosis, the coagulation system is tightly regulated by several anticoagulants, including PS, congenital deficiency of which is associated with increased thrombotic risk [79].

PS circulates in plasma and in platelet α -granules [43]. Plasma PS exists in two pools. ~60% circulates bound to the beta chain of complement component 4b-binding protein (C4BP- β) and is thought to promote its anti-inflammatory functions. The remaining ~40% is called "free PS" and is considered the anticoagulant pool [93]. It is a cofactor for the anticoagulants activated protein C (APC), which degrades FVa and FVIIIa [331], and tissue factor pathway inhibitor-alpha (TFPI α), which inhibits FVIIa and FXa [329]. PS also has direct anticoagulant activity inhibiting FIXa [29].

Coronavirus Disease 2019 (COVID-19), caused by severe acute respiratory syndrome coronavirus 2 (SARS-CoV-2) infection, is associated with increased inflammation and coagulation, and an increased risk of thrombotic complications [156], with many different

proposed mechanisms. Acquired PS deficiency has been reported by multiple studies [189, 190, 192-194] and is thought to be a contributing factor.

Due to its functions in regulating the inflammatory and coagulopathic responses, acquired PS deficiency is a common complication of severe viral infections, including human immunodeficiency virus [184-186], varicella [187], and dengue [188] infections, all of which are associated with an increased risk of thrombosis. As we recently reviewed [332], acquired PS deficiency in COVID-19 patients may result from increased consumption [205], antibody-mediated clearance [181, 192, 218, 219], degradation by viral protease [215, 217], decreased synthesis [60, 220, 221, 223, 224], or increased C4BP binding [191], among other mechanisms. Here, we assessed the mechanism of acquired free PS deficiency in COVID-19 patients and identified von Willebrand Factor (VWF) as a previously unrecognized PS-binding protein.

4.2 Results

4.2.1 Study population

Subjects were enrolled between April 2020 and January 2021 through Kentucky Clinic and the University of Kentucky Center for Clinical and Translational Science. Blood samples were collected from adult patients (Table 4.1): SARS-CoV-2 negative controls (n = 38) and SARS-CoV-2 positive (COVID-19) outpatients (patients with mild or no symptoms, post-quarantine) (n = 52) and inpatients (ICU patients) (n = 30).

Group	Control	Outpatients	Inpatients
Number	38	52	30
Male %	53%	31%	69%
Age (year)	55.3 ± 17.4	48.4 ± 15.5	61.5 ± 14.2
Race or ethnicity (A/AA/C/H/U)	3/1/32/2	3/7/20/3/19	0/2/8/20

Table 4.1. Description of COVID-19 study population

Abbreviations: Asian (A), African American (AA), Caucasian (C), Hispanic (H), U (unreported); Data are in mean ± SD.

4.2.2 Thromboinflammatory markers in COVID-19 patients

As expected, COVID-19 patients had elevated anti-spike protein IgG (Endpoint Titer = $18.5 \times 10^3 \pm 23.2 \times 10^3$ in inpatients ($P < 0.0001$) and $14.2 \times 10^3 \pm 22.8 \times 10^3$ in outpatients ($P < 0.0001$), compared to 199 ± 361 in controls; expressed in reciprocal dilution) (Figure 4.1A). Anti-spike IgG was detected in some controls who had received the first dose of the COVID-19 vaccine, while a few patients did not have a detectable IgG response. Inpatients displayed more inflammation, marked by increased TNF (1.33 ± 1.01 pg/mg total protein, $P = 0.006$), than outpatients (0.62 ± 0.56 pg/mg, $P > 0.9999$) or controls (0.78 ± 0.87 pg/mg) (Figure 4.1B), as well as increased IL-6 (2.56 ± 5.18 , $P < 0.0001$; 0.053 ± 0.081 , $P > 0.9999$; vs. 0.043 ± 0.039 pg/mg total protein; in inpatients, outpatients, compared to controls, respectively) (Figure 4.1C). Complement system activation, measured by increased C5a, was also evident, particularly in the inpatients ($1,195 \pm 1,021$ pg/mg, $P < 0.0001$; 271.8 ± 273.3 , $P = 0.222$; vs 179.8 ± 174.6 pg/mg total protein) (Figure 4.1D), as well as increased plasma myeloperoxidase (MPO), indicative of leukocyte activation (15.98 ± 9.19 , $P < 0.0001$; vs 3.02 ± 1.32 , $P > 0.9999$; vs 2.72 ± 1.15 pg/mg total protein) (Figure 4.1E). Plasma tissue factor (TF) activity, enriched by high-speed centrifugation for the extracellular vesicle fraction, was increased in the inpatients (2.55 ± 4.15 , $P = 0.027$; vs 1.14 ± 1.79 , $P > 0.9999$; vs 0.76 ± 0.7 fmol/g total protein) (Figure 4.1F), and monocyte TF expression was similarly increased in the inpatients ($2,360 \pm 1,669$, $P < 0.0001$; vs $1,792 \pm 1,125$, $P = 0.012$; vs $1,259 \pm 403$ MFI) (Figure 4.1G). Moreover, inpatients had elevated D-dimer (72.67 ± 141.7 , $P < 0.0001$; vs. 6 ± 5.67 , $P > 0.9999$; vs. 5.18 ± 4.39 ng FEU/mg total protein) (Figure 4.1H), as well as elevated plasma Thioflavin T staining, a

fluorescent dye which stains aggregated protein and has been shown to detect microclots [314] (0.072 ± 0.092 , $P < 0.0001$; 0.024 ± 0.014 , $P > 0.9999$; 0.03 ± 0.051 ; expressed as ratio to fibrinogen-depleted plasma fluorescence signal) (Figure 4.1l). All of these were consistent with the hypercoagulable and hyperinflammatory state reported in COVID-19 [161, 333-335].

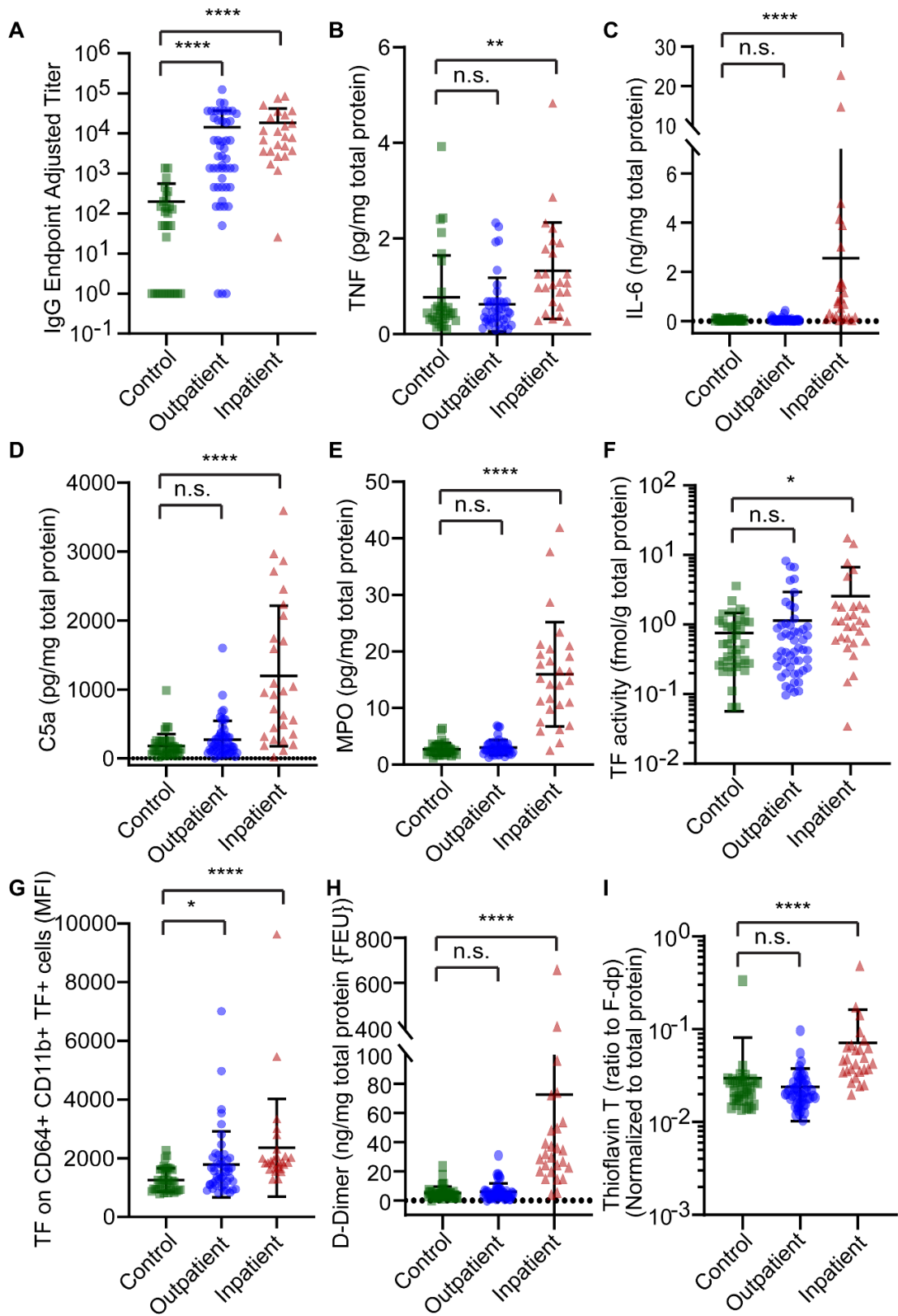


Figure 4.1. COVID-19 inpatients show signs of immunothrombosis

Figure 4.1. COVID-19 inpatients show signs of immunothrombosis

Citrated plasma samples and peripheral blood derived mononuclear cells were collected from healthy controls (n = 38), COVID-19 inpatients (n = 30), and COVID-19 outpatients (n = 52). Due to sample limitations, some measurements could not be performed with all subjects. (A-E, H) Shown are ELISA measurements of plasma (A) anti-spike protein IgG, (B) tumor necrosis factor (TNF), (C) interleukin-6 (IL-6), (D) Complement Component 5a (C5a), (E) Myeloperoxidase (MPO), and (H) D-dimer Fibrinogen Equivalent Units, (F) plasma Tissue Factor (TF) activity as measured by factor Xa activity assay, (G) monocyte TF expression as measured by flow cytometry, and (I) plasma thioflavin T fluorescence staining which measures fibrin as adapted from [314]. Green squares represent controls, blue circles represent COVID-19 outpatients, and red triangles represent COVID-19 inpatients. All data were normalized to total protein. Every data point is the average of three replicates (mean \pm SD). *P*-values are according to Kruskal-Wallis with Dunn's multiple comparison test (n.s., non-significant; *, *P* < 0.05; **, *P* < 0.01; ****, *P* < 0.0001). Anti-spike protein ELISA experiments were conducted by Dr. Siva Gandhapudi; TNF, IL-6, and MPO ELISA were conducted by Hammodah Alfar; Monocyte TF flow cytometry experiments were conducted by Melissa Hollifield.

4.2.3 Free PS deficiency cannot be explained by known PS-binding proteins

Because severe viral infections are associated with acquired PS deficiency [184-190, 192-194], we measured PS in our samples. Total plasma PS was measured with polyclonal antibody-based ELISA, while free PS was measured using a monoclonal capture antibody which does not recognize C4BP-bound PS (Figure 4.2A). Total PS was not different between the three groups ($P = 0.235$) (Figure 4.2B), but free PS (Figure 4.2C) was decreased in both inpatients ($81 \pm 40.6\%$, $P = 0.008$) and outpatients ($81.5 \pm 38.7\%$, $P = 0.001$) compared to controls ($100 \pm 33\%$). A decrease in free, but not total, PS indicates an increase in a PS-binding protein, with C4BP- β usually implicated [191, 226]. However, neither C4BP- β nor PC was elevated in these patients (Figure 4.2D and 4.2E). Soluble Mer tyrosine kinase, a PS-binding receptor shed from macrophages and other cell types [336], was increased in inpatients compared to controls (135.8 ± 80.1 , $P = 0.001$; 90 ± 75.91 , $P > 0.9999$; 77.3 ± 45 pg/mg total protein) (Figure 4.2F), but not nearly enough to explain the decreased free PS as the low picomolar concentration of this protein (~ 70 - 1000 pM in controls and inpatients) makes it unlikely to have a meaningful impact on free PS concentration (normal range 5 - 15 $\mu\text{g}/\text{mL}$ or ~ 150 nM).

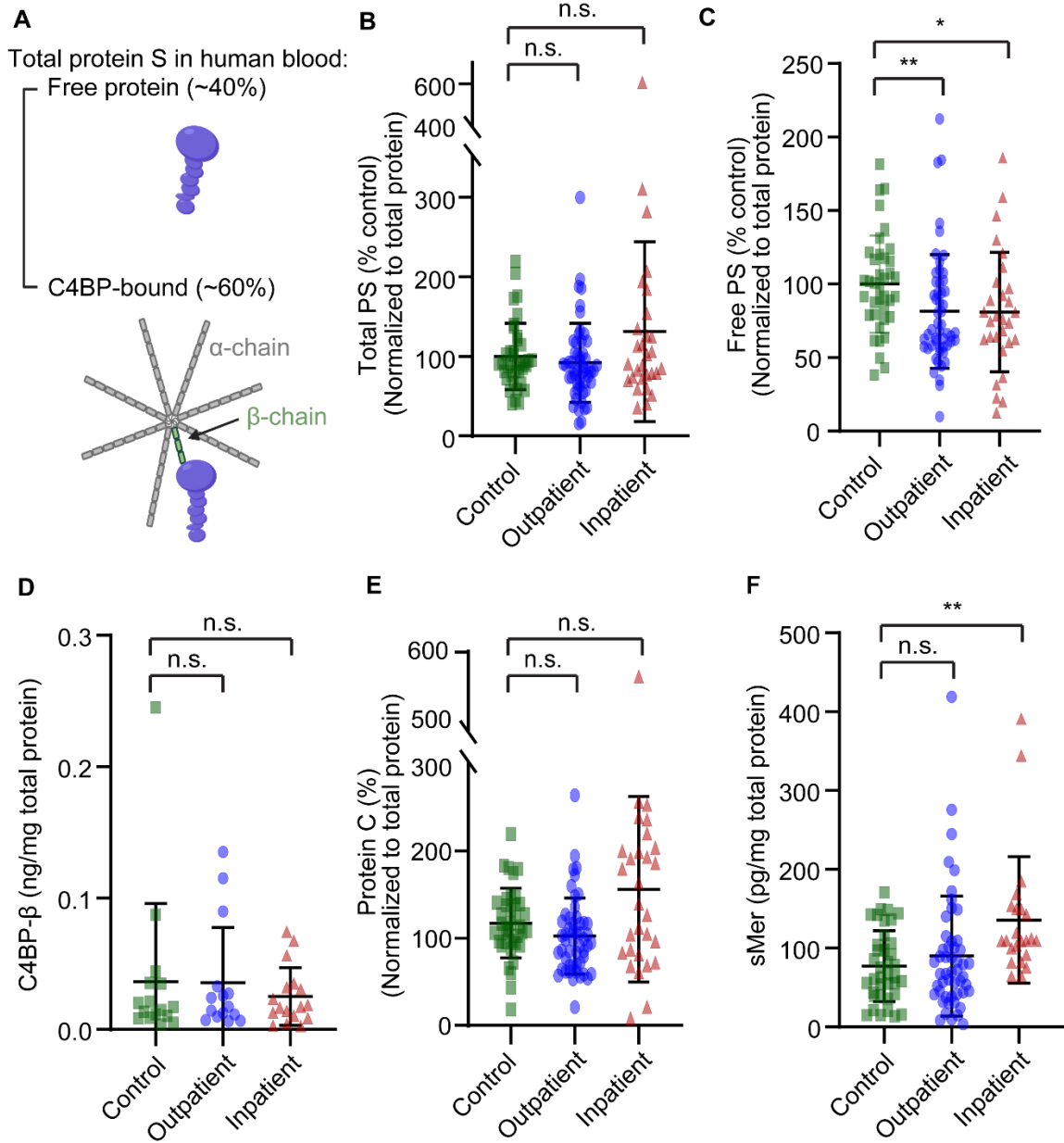


Figure 4.2. Free PS deficiency in COVID-19 patients is not explained by increases in known PS-binding proteins

Figure 4.2. Free PS deficiency in COVID-19 patients is not explained by increases in known PS-binding proteins

Citrated plasma samples were collected from healthy controls (n = 38), COVID-19 inpatients (n = 30), and COVID-19 outpatients (n = 52). Due to sample limitations, some measurements could not be performed with all subjects. Shown are (A) schematic diagram of PS plasma distribution and (B-F) ELISA measurements of plasma (B) total PS, (C) free PS, (D) Complement Component 4b-Binding Protein (C4BP) beta chain, (E) protein C, and (F) shed soluble Mer tyrosine kinase. All data were normalized to total protein. Every data point is the average of three replicates (mean \pm SD). Green squares represent controls, blue circles represent COVID-19 outpatients, and red triangles represent COVID-19 inpatients. *P*-values are according to Kruskal-Wallis with Dunn's multiple comparison test (n.s., non-significant; *, *P* < 0.05; **, *P* < 0.01).

4.2.4 Free PS deficiency correlates with higher thrombotic potential

We then measured the contribution of PS to plasma thrombin generation using calibrated automated thrombography as we have previously published [186]. In this assay, plasma is supplemented with thrombomodulin to allow evaluation of the APC/PS system. Despite several inpatients receiving heparin prophylactic treatment at the time of sample collection, there were significant differences in plasma thrombin generation between groups, especially when TM was supplemented (peak thrombin without TM, $P = 0.047$; peak thrombin with TM, $P = 0.015$; ETP without TM, $P = 0.525$; ETP with TM, $P = 0.045$), with TF-initiated plasma thrombin generation parameters trending higher in COVID-19 inpatients compared to controls (peak thrombin without TM, $P = 0.173$; peak thrombin with TM, $P = 0.017$; ETP without TM, $P > 0.9999$; ETP with TM, $P = 0.057$) (Figure 4.3A-B, Figure 4.4B,4D-E). There was no difference between groups in the absence of exogenous TF (Figure 4.4A, C). Peak thrombin and ETP ratio, defined as the respective value with TM divided by without TM, were also increased in the inpatients compared to controls (peak thrombin ratio; $P = 0.023$; ETP ratio; $P = 0.003$) (Figure 4.3C and Figure 4.4B). These indicate reduced APC/PS pathway activity in the more severe COVID-19 patients. Consistent with our previous report (18), free PS did not correlate with peak thrombin or ETP in the absence of TM (Figure 4.3D-E), but negatively correlated in the presence of TM (peak thrombin, $r = -0.317$, $P = 0.007$; ETP, $r = -0.443$, $P = 0.0002$) (Figure 4.3F-G), indicating a functional consequence of the free PS deficiency.

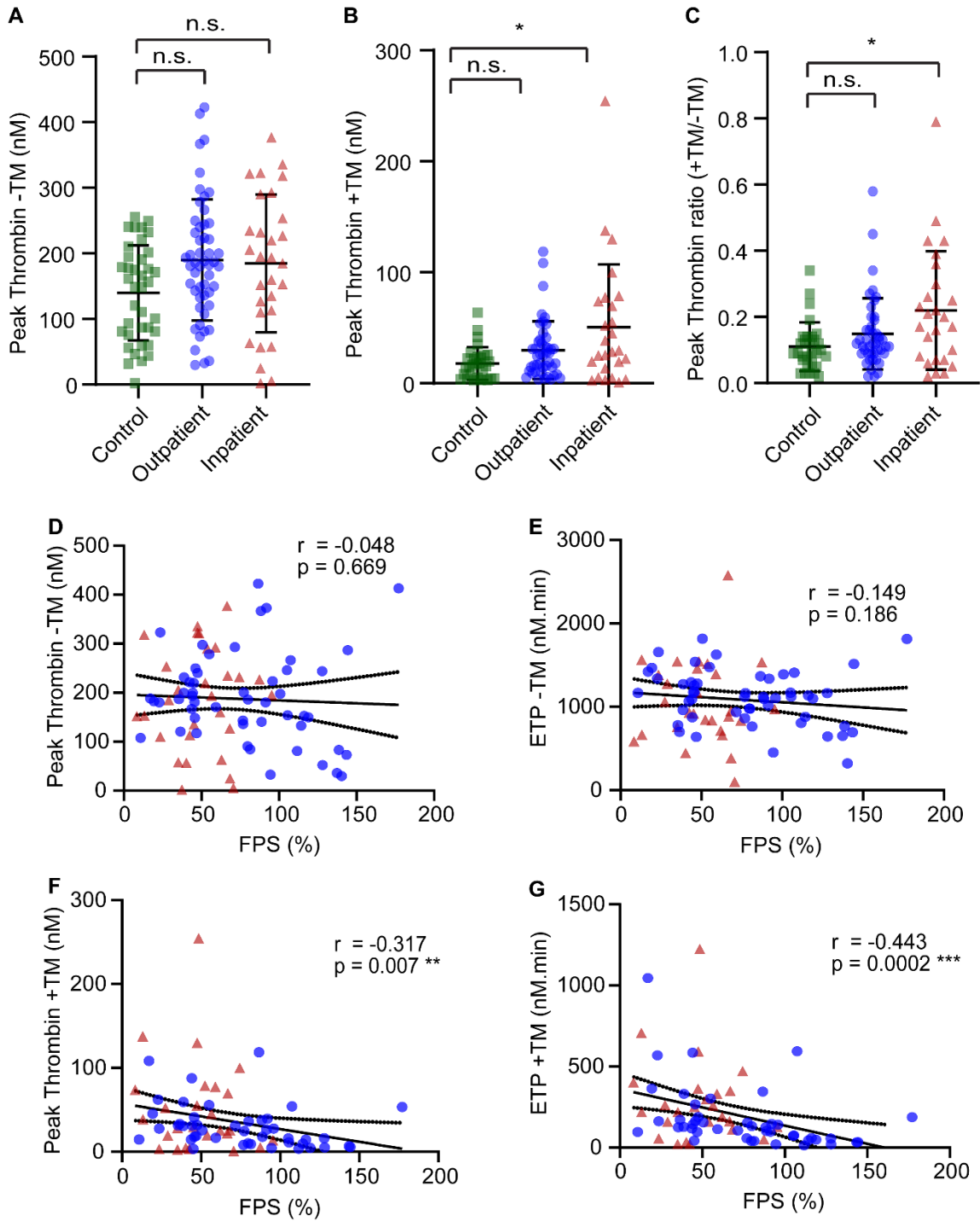


Figure 4.3. Free PS deficiency contributes to higher thrombotic potential in COVID-19 patients

Figure 4.3. Free PS deficiency contributes to higher thrombotic potential in COVID-19 patients

Plasma thrombin generation was measured using fluorogenic substrate to thrombin according to the Calibrated Automated Thrombography (Thrombinoscope) method (Diagnostica Stago) in citrated plasma samples collected from healthy controls (n = 38), COVID-19 inpatients (n = 30), and COVID-19 outpatients (n = 52). Several inpatients were receiving heparin prophylactic dose at the time of blood collection. (A-C) Shown are peak thrombin concentrations in assays initiated with 4 μ M phospholipids and 1 pM tissue factor (TF), (A) without, and (B) with 20 nM thrombomodulin (TM) supplementation to evaluate the contribution of APC/PS activity, and (C) the ratio of peak thrombin concentration (with TM/without TM). Every data point is the average of three replicates (mean \pm SD). P-values are according to Kruskal-Wallis with Dunn's multiple comparison test (n.s., non-significant; *, P < 0.05; **, P < 0.01; ***, P < 0.001). (D-G) Free PS plotted against (D, F) peak thrombin concentration and (E, G) Endogenous Thrombin Potential (ETP) in assays (D-E) without and (F-G) with TM supplementation. P-values and r correlation coefficients are according to Spearman correlation analysis. Green squares represent controls, blue circles represent COVID-19 outpatients, and red triangles represent COVID-19 inpatients.

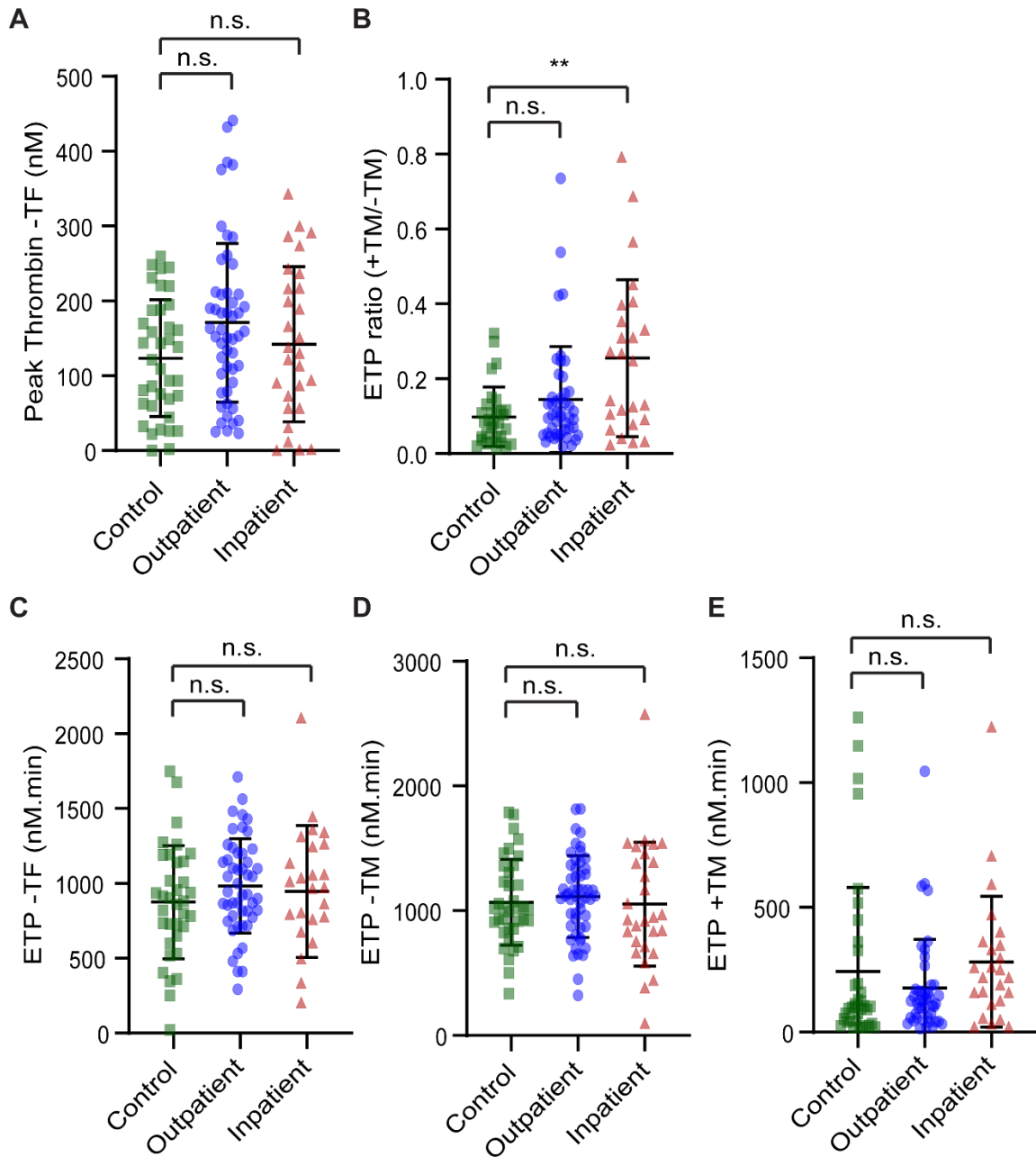


Figure 4.4. Plasma TG in COVID-19 inpatients shows less APC/PS activity

Figure 4.4. Plasma TG in COVID-19 inpatients shows less APC/PS activity

Plasma thrombin generation was measured using fluorogenic substrate to thrombin according to the Calibrated Automated Thrombography (Thrombinoscope) method (Diagnostica Stago) in citrated plasma samples collected from healthy controls (n = 38), COVID-19 inpatients (n = 30), and COVID-19 outpatients (n = 52). Several inpatients were receiving heparin prophylactic dose at the time of blood collection. Shown are (A) peak thrombin concentrations and (C) Endogenous Thrombin Potential (ETP) in assays initiated with 4 μ M phospholipids without tissue factor (TF); and (B) the ratio of ETP (with TM/without TM) and the ETP values in assays (D) without, and (E) with 20 nM thrombomodulin (TM) supplementation, as initiated with 4 μ M phospholipids and 1 pM TF. Every data point is the average of three replicates (mean \pm SD). Green squares represent controls, blue circles represent COVID-19 outpatients, and red triangles represent COVID-19 inpatients. *P*-values are according to Kruskal-Wallis with Dunn's multiple comparison test (n.s., non-significant; **, *P* < 0.01).

4.2.5 Protein S has multiple binding partners in plasma

To understand the cause of free PS deficiency and test for other PS-binding proteins, plasma samples from patients and controls were separated on a native, non-denaturing gel and immunoblotted for PS (Figure 4.5A), with purified PS used as controls. PS self-associates and fully dimerizes at high (17 μM) concentrations [337], far above the plasma concentration of free PS (~ 150 nM), whereas calcium induces monomerization of PS, such that PS dimers or multimers are scarce in plasma [338]. Interestingly, plasma PS migrated differently than purified PS (left 3 lanes), with no bands running at the same apparent size as either the PS monomer (Figure 4.5A, *) or dimer (Figure 4.5A, **). Instead, several new bands appeared, mostly above the monomer, and many toward the top of the gel. The darkest band co-migrated with C4BP- β (Figure 4.5B), consistent with reports that $\sim 60\%$ of PS is bound to C4BP, while some of the other bands appear to co-migrate with Mer (Figure 4.5C), PC (Figure 4.5D) TFPI (Figure 4.5E), VWF (Figure 4.5F), and factor V (Figure 4.5H). We probed for VWF, because it is a large multimeric protein with many protein binding sites that can be exposed under high shear [339], as well as it being a prothrombotic acute phase protein elevated during inflammation, including in COVID-19 [302, 340].

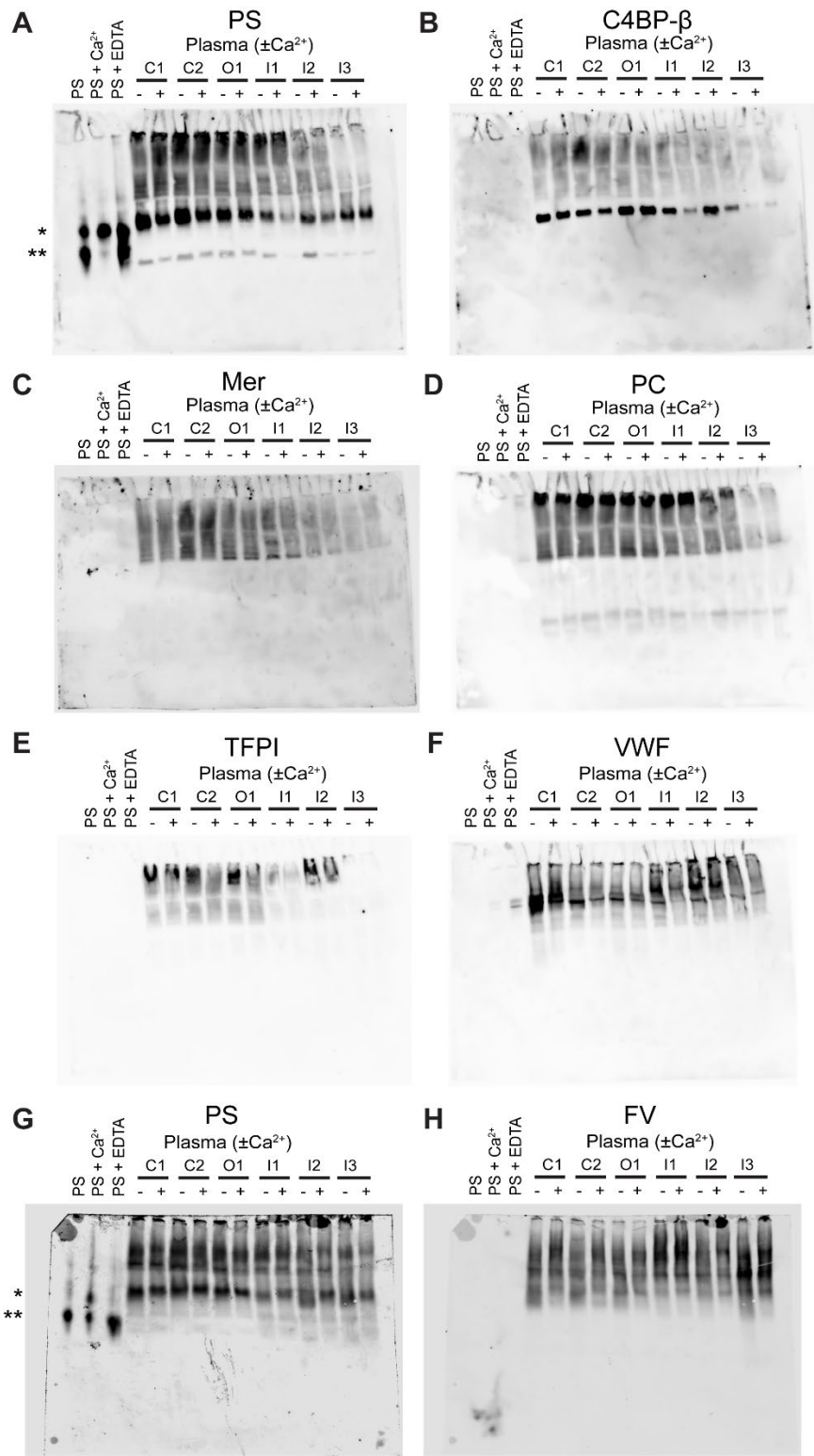


Figure 4.5. Native gel electrophoresis shows that PS has many binding partners in plasma

Figure 4.5. Native gel electrophoresis shows that PS has many binding partners in plasma

Purified PS (50 ng), with either 20 mM CaCl₂ or 5 mM EDTA, or 4 μL citrated plasma (C1-2: healthy controls, O1: COVID-19 outpatient, I1-3: COVID-19 inpatients), with/wo 1 μM Hirudin, 5 mM GPRP peptide, and 20 mM CaCl₂, were separated with native gel electrophoresis and probed with (A) anti-PS, (B) anti-C4BP-β, (C) anti-protein C, (D) anti-TFPI, (E) anti-Mer, (F) anti-VWF antibody. In a separate experiment, the immunoblot was probed with (G) anti-PS and (H) anti-factor V. (*, apparent monomer band; **, apparent dimer band).

4.2.6 VWF is elevated in COVID-19 patients

Plasma VWF antigen concentration (VWF:Ag) was elevated in inpatients ($353 \pm 187\%$, $P < 0.0001$) compared to outpatients ($102 \pm 42\%$, $P > 0.9999$) and controls ($100 \pm 38.2\%$) (Figure 4.6A), as others have reported. Soluble E-selectin (Figure 4.6B) was also elevated in inpatients (191 ± 72.5 vs 123.4 ± 43.4 and 133 ± 32 pg/mg total protein in outpatients and controls, respectively), consistent with increased VWF secretion from activated endothelium. No differences were observed in VWF multimer distribution (Figure 4.6C). VWF:Ag did not correlate with free PS concentration (Figure 4.6D).

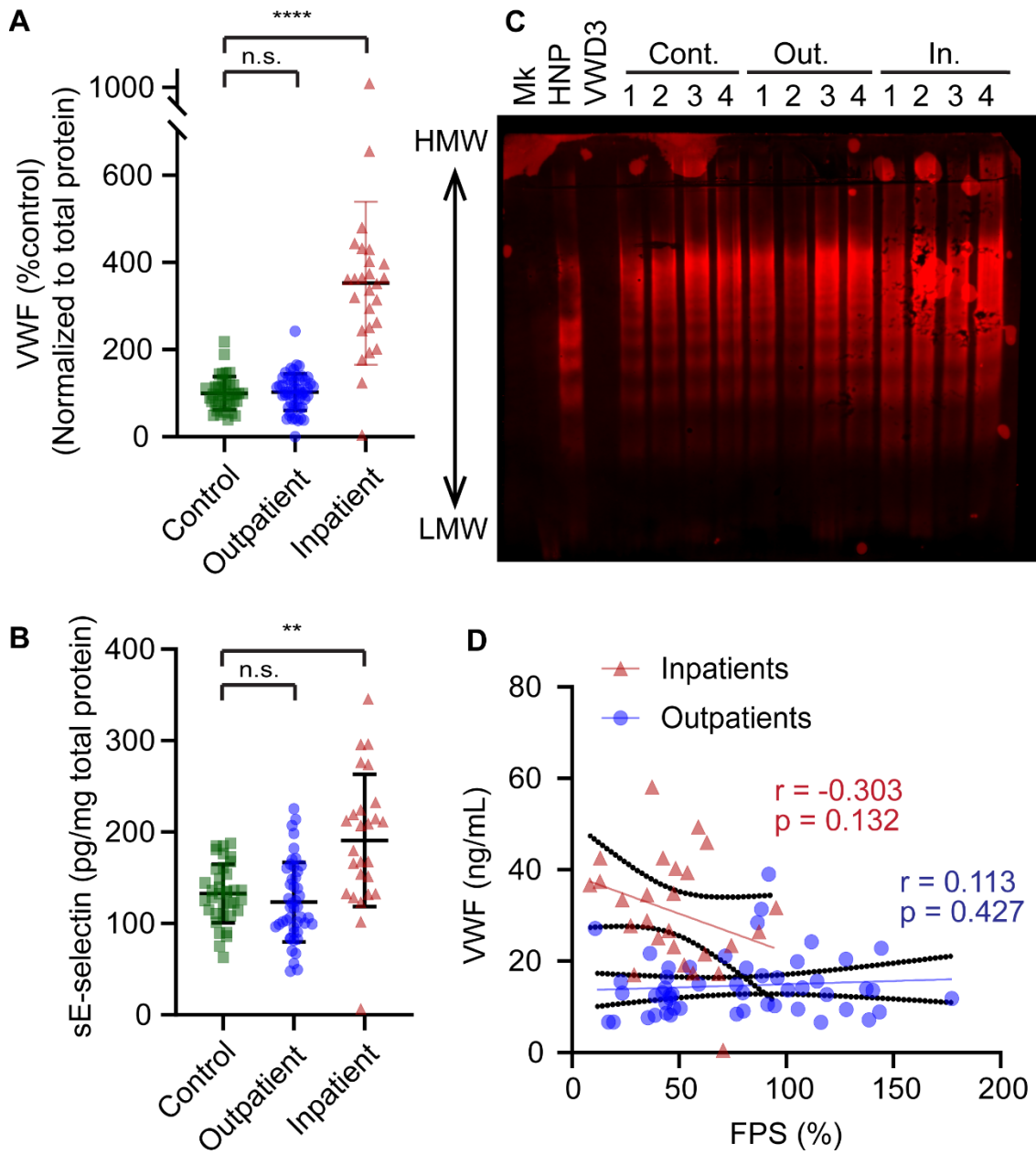


Figure 4.6. Plasma VWF is higher in patients with severe COVID-19

Figure 4.6. Plasma VWF is higher in patients with severe COVID-19

(A) VWF:Ag and (B) E-selectin were measured using ELISA in citrated plasma samples collected from controls (n = 38), COVID-19 inpatients (n = 30), and outpatients (n = 52). Every data point is the average of three replicates (mean \pm SD). P-values are according to Kruskal-Wallis with Dunn's multiple comparison test (n.s., non-significant; **, P < 0.01; ****, P < 0.0001). (C) Healthy normal plasma (HNP) from Siemens and citrated plasmas from VWD type 3 patient (VWD3), healthy controls (Cont.; 1-4), COVID-19 outpatients (Out.; 1-4), and COVID-19 inpatients (In.; 1-4) were normalized to 10 μ g/mL of VWF:Ag, and 1 μ L of each samples were separated for VWF multimer analysis using SDS-agarose gel electrophoresis and anti-VWF probing. (D) Free PS plotted against VWF:Ag. P-values and r correlation coefficients are according to Spearman correlation analysis. Green squares represent controls, blue circles represent COVID-19 outpatients, and red triangles represent COVID-19 inpatients.

4.2.7 VWF interacts with PS in a shear-dependent manner

To directly assess VWF/PS binding, we incubated plasma with VWF-coated beads in the presence or absence of shearing and identified bead-bound proteins by mass spectrometry (MS). In all three samples tested (two pooled plasmas, one single-donor plasma), the quantity of PS bound to VWF increased upon shearing (>10,000,000-fold in 2 of 3 samples), suggesting that shear-induced unfolding of VWF exposes a PS-binding site (Figure 4.7A and B), as it does for platelet glycoprotein Ib (GPIb) (43) or ADAMTS13 (46). C4BP- α was also enriched under shearing conditions (Figure 4.7C), though to a lesser extent than PS, based on MS quantification. However, C4BP- β , the subunit of C4BP which binds PS, was not detected in any pull-down condition, either by immunoblotting or MS. PS (~69 kDa as monomer) was also observed on VWF multimer gels (Figure 4.7F, Figure 4.8A) and ran as a ladder of bands, similar to VWF. While the lowest molecular weight band migrated similarly to C4BP, the remaining bands co-migrated with the low molecular weight VWF multimers (~0.5–20 mDa multimers) (Figure 4.8B). This was apparent regardless of shearing or calcium supplementation, implying either a presence of some pre-existing PS/VWF complex in plasma, or that VWF-unfolding in the presence of SDS allows for PS binding.

Sheared VWF dose-dependently interfered with the detection of free, but not total, PS, using purified protein in plasma (Figure 4.9A). The concentrations of VWF supplementation we used (0, 10, 20, and 40 $\mu\text{g}/\text{mL}$) were chosen to simulate the physiological (~10 $\mu\text{g}/\text{mL}$) to pathological (~40 $\mu\text{g}/\text{mL}$) range of VWF antigen seen in our COVID-19 patients. Furthermore, shearing of plasma reduced free PS measurements

(Figure 4.9B). The effect of shearing was similar either in the absence or presence of calcium, when measured with either purified proteins or plasma (Figure 4.9C). By contrast, shearing did not alter the VWF concentration (Figure 4.10A and B).

The PS interaction site on VWF appears distinct from the site which binds GPIIb. Ristocetin, which exposes the GPIIb binding site on VWF, did not reduce free PS (Figure 4.9D). Furthermore, exogenous PS did not interfere with VWF cleavage by recombinant ADAMTS13 (A Disintegrin And Metalloproteinase with a Thrombospondin type 1 motifs, member 13) (Figure 4.9E). Finally, we developed a PS/VWF complex ELISA in which we capture with a polyclonal anti-human VWF antibody and detect with a polyclonal antibody against PS. In this assay, captured VWF binds PS out of plasma in a time-dependent manner. Interestingly, however, this did not occur with purified proteins, suggesting that an additional plasma component(s) may enhance the PS/VWF interaction (Figure 4.9F). Shearing and calcium had no effect in this detection system, consistent with the hypothesis that immobilizing VWF can induce exposure of protein binding sites [341].

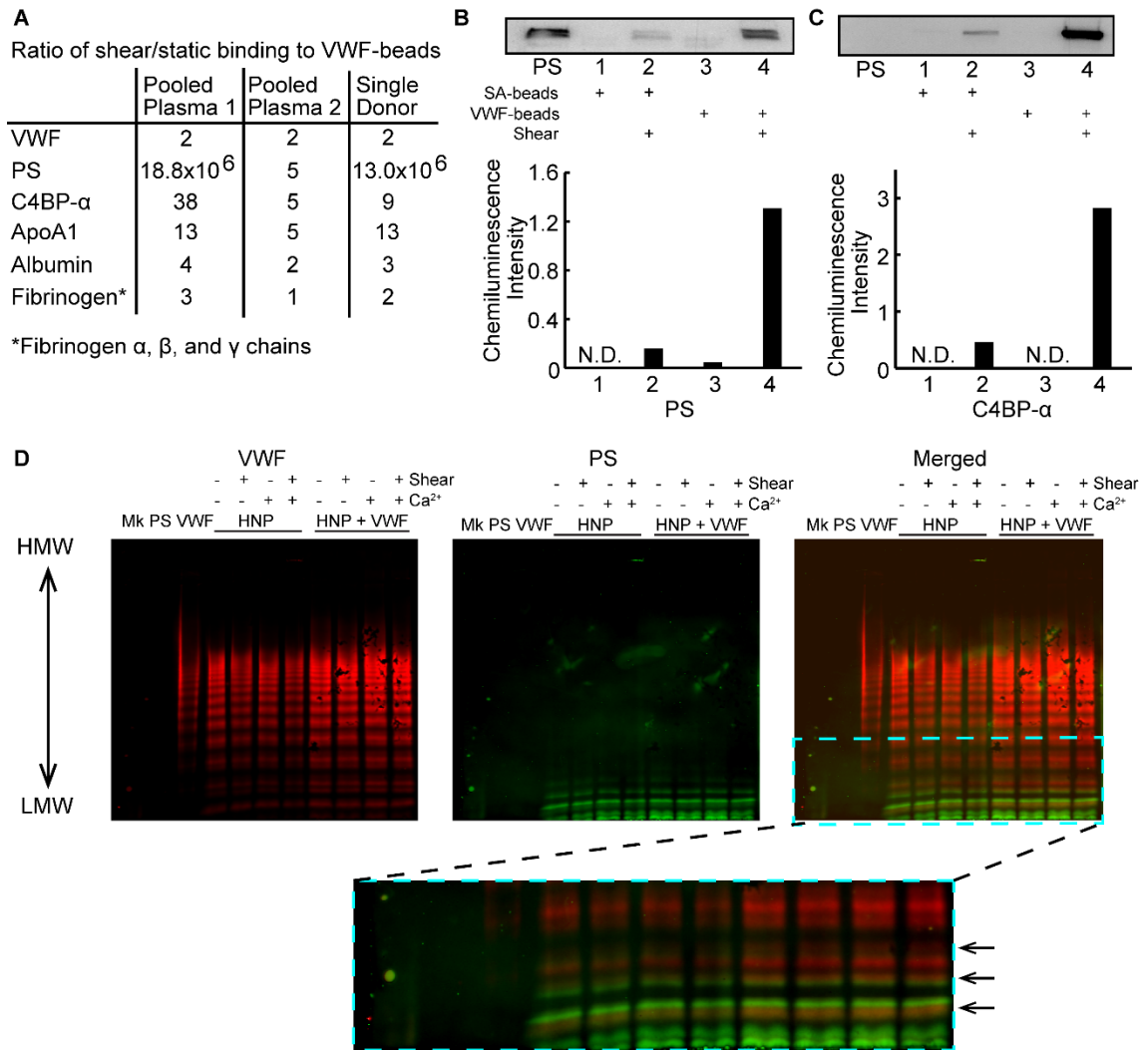


Figure 4.7. VWF interacts with PS in a shear-dependent manner

Figure 4.7. VWF interacts with PS in a shear-dependent manner

Streptavidin beads-immobilized biotinylated VWF were exposed to pooled human plasma or single donor plasma, under static conditions or under shear, and bound proteins were analyzed with nano-LC-MS/MS, and probed for PS and C4BP- α by immunoblot, serum albumin (SA) is used as a control. (A) Mass spectrometry analysis of VWF pull-down in pooled normal plasmas (Pooled plasma 1 from Innovative Research, Pooled plasma 2 from Precision Biologics) and single donor. (B) Western blot of VWF pull-down probed for PS. (C) Reprobing of blot for C4BP- α . (D) 25 ng of PS or 10 ng of VWF purified proteins, and 1 μ L of healthy normal plasma (HNP) from Siemens, with or without shearing (~2,500 rpm for 30 s), or 1 μ M Hirudin, 5 mM GPRP peptide, and 5 mM CaCl₂ supplementation, or additional 10 μ g/mL of purified VWF, were separated for VWF multimer analysis using SDS-agarose electrophoresis. The highest band on the molecular weight marker was 460 kDa. VWF is shown on red channel, PS on green, and zoomed-in inset of the merged image is presented for clarity. N.D.; non-detectible.

VWF plasma pull-down and nano-LC/MS-MS were conducted by Dr. Xiaoyun Fu and Dr. Dominic Chung in the Bloodworks Northwest, Seattle, Washington.

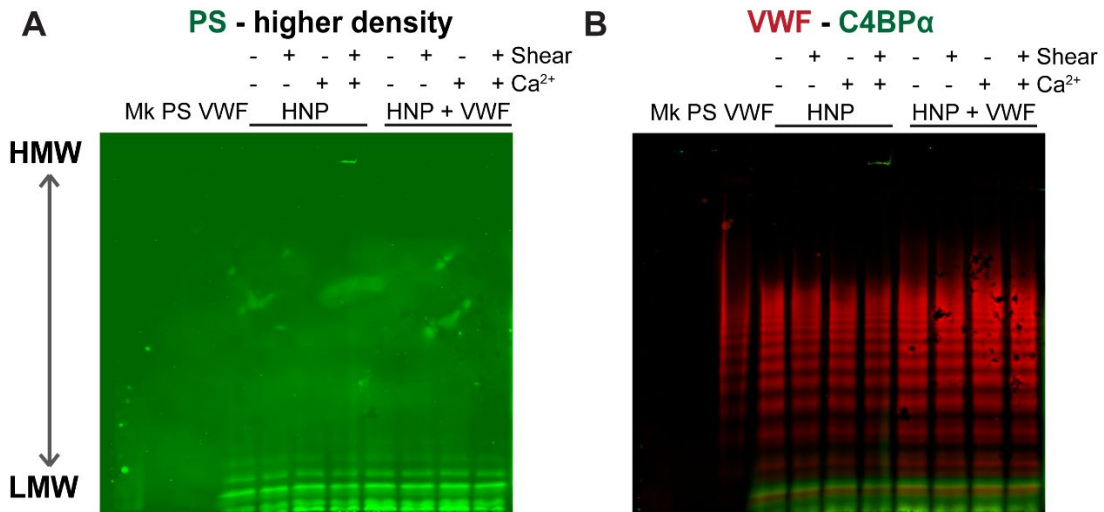


Figure 4.8. PS co-migrates with lower molecular weight VWF multimers

Twenty-five nanograms of PS or 10 ng of VWF purified proteins, and 1 μ L of healthy normal plasma (HNP) from Siemens, with or without shearing (\sim 2,500 rpm vortexing for 30 s), or 1 μ M Hirudin, 5 mM GPRP peptide, and 5 mM CaCl₂ supplementation, or additional 10 μ g/mL of purified VWF, were separated for a VWF multimer analyses using SDS-agarose electrophoresis. The highest band on the molecular weight marker was 460 kDa. (A) Shown is PS in green, tuned up in fluorescence intensity. (B) The same blot reprobed for C4BP- α in green.

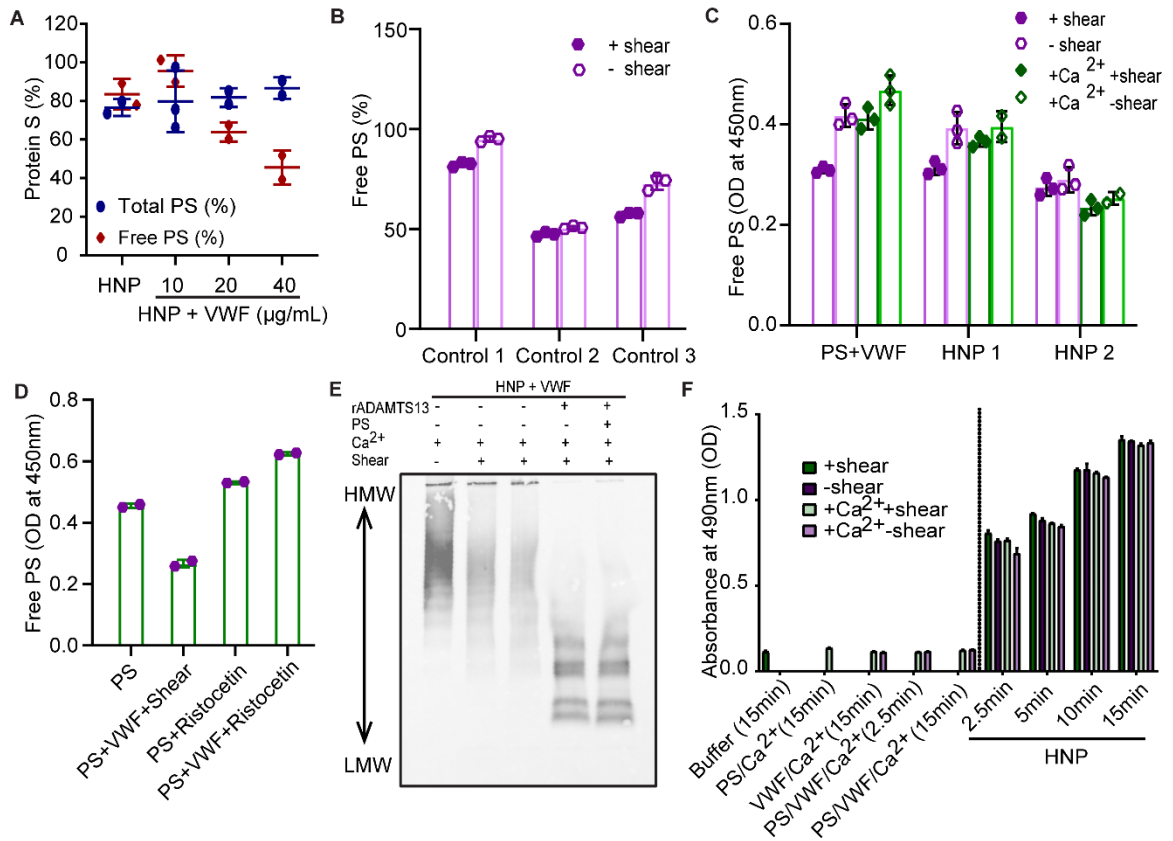


Figure 4.9. Sheared VWF interferes with free PS measurements

Figure 4.9. Sheared VWF interferes with free PS measurements

(A) Free PS and total PS ELISA measurements of healthy normal plasma (HNP) from Siemens, with additions of purified VWF, under shear ($\sim 2,500$ rpm for 30 s). (B) Free PS ELISA measurements of healthy control plasmas (1-3) with or without shear. (C) Free PS ELISA results of purified proteins (200 nM PS and 10 $\mu\text{g}/\text{mL}$ VWF in HBSA), HNP1 (Corgenix), and HNP2 (Siemens), with or without shear or 1 μM Hirudin, 5 mM GPRP peptide, and 5 mM CaCl_2 supplementation. (D) Free PS ELISA results of purified PS (200 nM), with or without purified VWF (10 $\mu\text{g}/\text{mL}$) or 2 mg/mL Ristocetin, with or without shear ($\sim 2,500$ rpm for 30 s). (E) VWF multimer blot of 0.25 μL healthy normal plasma with additional 150 nM purified VWF, with or without 50 nM recombinant ADAMTS13, 200 nM PS, or 1 μM Hirudin, 5 mM GPRP peptide, and 5 mM CaCl_2 , supplementation with or without shear ($\sim 2,500$ rpm for 60 m). (F) PS ELISA results of either purified proteins (200 nM PS, 10 $\mu\text{g}/\text{mL}$ VWF, 5 mM CaCl_2 , as indicated, in HBSA) or healthy normal plasma (HNP) from Siemens, with or without shear or 1 μM Hirudin, 5 mM GPRP peptide, and 5 mM CaCl_2 supplementation, after the indicated incubation time with anti-VWF capture antibody.

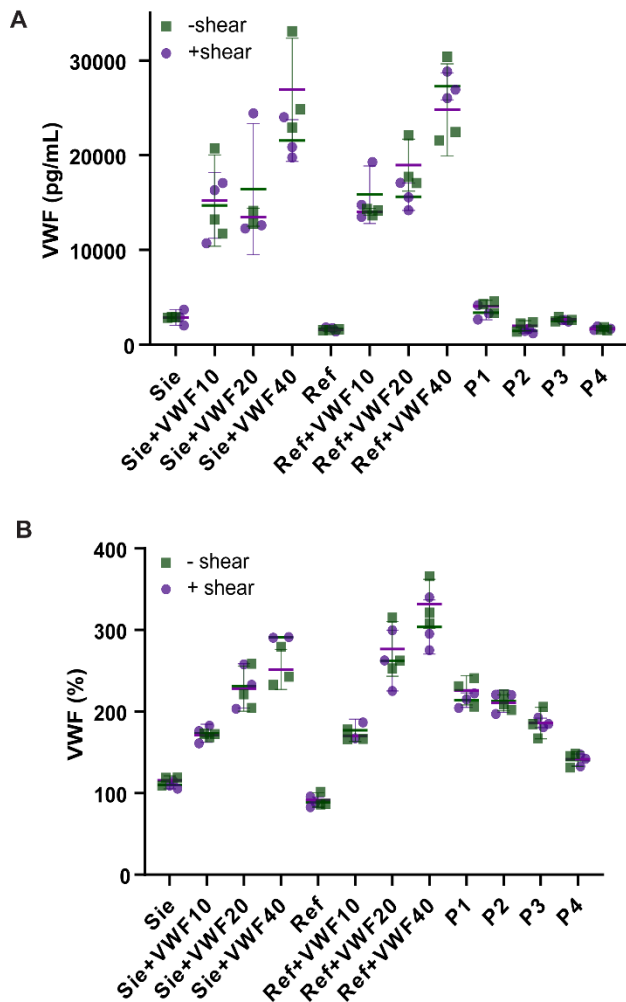


Figure 4.10. Shearing does not interfere with VWF ELISA measurements

VWF:Ag ELISA (A, R&D systems; B, Enzyme Research Labs) results of pooled normal plasmas (Sie, Siemens control plasma from Siemens; Ref, Reference plasma from Corgenix), with additions of purified VWF, and several COVID-19 in- (P1, P2) and outpatients (P3, P4), with or without shear.

4.2.8 PS/VWF complex is stable under arterial flow conditions

Whole blood microfluidics experiments were performed using the BioFlux 200 system in order to visualize thrombus formation under flow. Freshly drawn whole blood was supplemented with fluorescently tagged VWF and PS, either with or without prior shearing, recalcified, and perfused into the channel at 35 dyn/cm^2 (~arterial) flow rate (Figure 4.11). In the absence of shearing, no apparent colocalization of PS and VWF was observed, as PS and VWF were observed to bind independently to different thrombi structures. However, when PS and VWF were sheared to form the complex prior to addition to blood, the two proteins co-localized on platelet thrombi, indicating that the complex, once formed, is stable under flow.

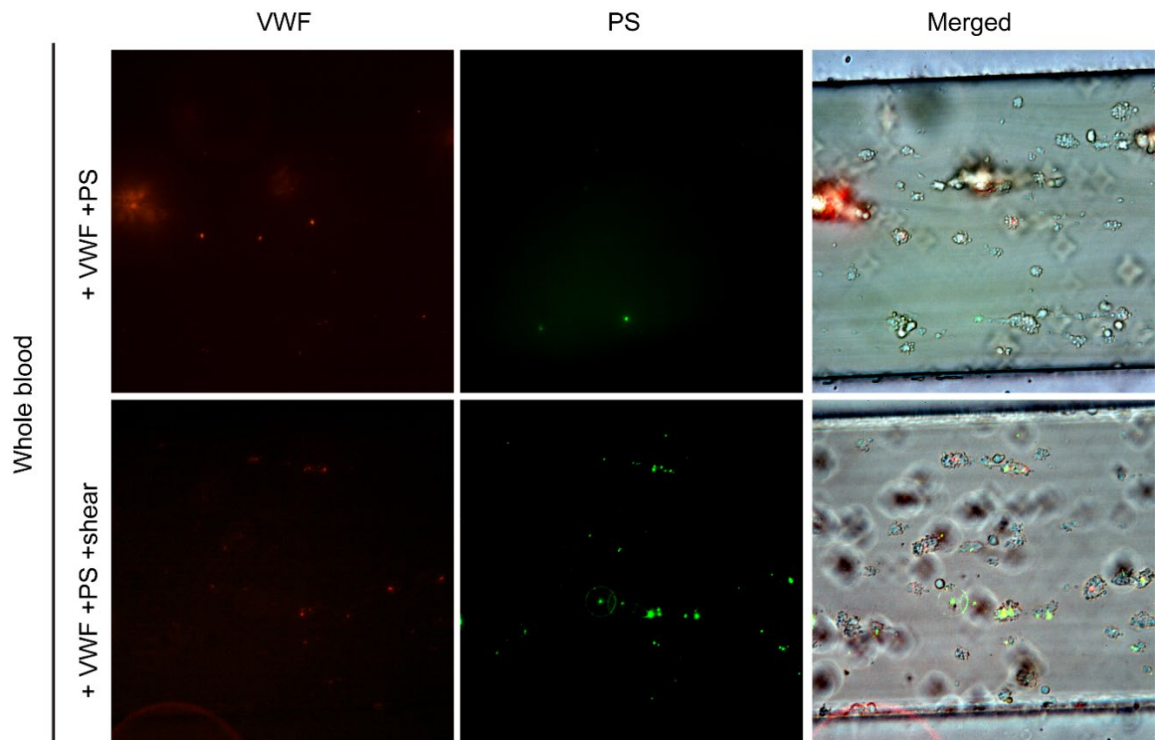


Figure 4.11. PS/VWF complex is stable under arterial flow conditions

Whole blood was supplemented with 10 $\mu\text{g}/\text{mL}$ AlexaFluor555-conjugated VWF and 200 nM AlexaFluor488-conjugated PS and flowed through collagen-coated channels at 35 dyn/cm^2 . Experiments were performed either without or with PS/VWF vortexing. Images taken after flushing with buffer (scale bar = 100 μm).

BioFlux microfluidic experiments were conducted by Dr. Daniëlle Coenen, Shravani Prakhya, Dlovan D. Mahmood, and Martha Sim.

4.2.9 VWF/PS complex forms under flow, in a calcium-sensitive manner

To further investigate VWF/PS binding under shear, we perfused VWF through a polydimethylsiloxane (PDMS) microfluidic device [342] that allows visualization of VWF self-association around a PDMS block (Figure 4.12A). VWF and fluorescently labeled PS were perfused into the PDMS device in the absence (Figure 4.12B, Figure 4.13A) or presence (Figure 4.12C, Figure 4.13B) of 2 mM calcium chloride. We observed PS binding to VWF under shear and found that PS binding was significantly higher in the absence of calcium (Figure 4.12D). As expected, we observed no fluorescence intensity above noise in conditions without VWF (with PS) or without PS (with VWF) (Figure 4.12D, Figure 4.13C), indicating that PS binding was VWF-specific. To account for differences in VWF self-association with and without calcium, we also normalized PS binding for the amount of VWF self-association in each channel. We found that even when accounting for the area of VWF self-association, PS binding was significantly higher in the absence of calcium (Figure 4.12E).

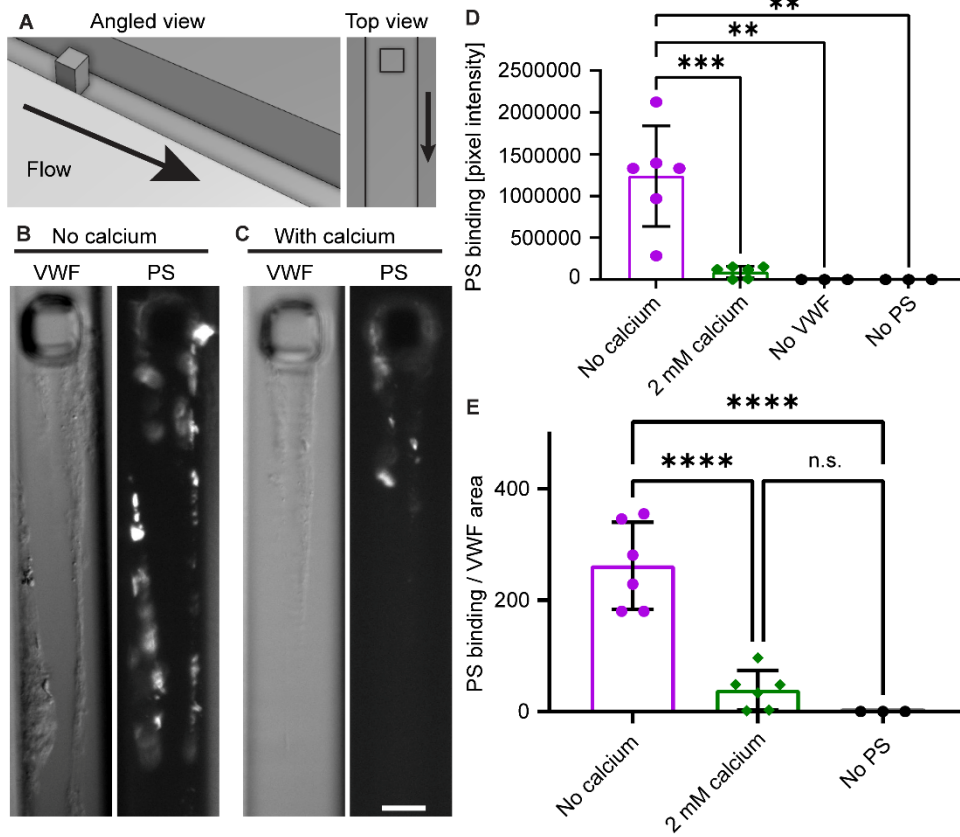


Figure 4.12. VWF interacts with PS under flow in a calcium-dependent manner

Figure 4.12. VWF interacts with PS under flow in a calcium-sensitive manner

(A) VWF and PS were flowed into a PDMS microfluidic device. (B-C) In the absence (B) or presence of 2 mM calcium (C), VWF self-association and Alexa Fluor 488-PS binding were visualized differential interference contrast (non-fluorescence image) and epifluorescence microscopy. (D) Raw pixel intensity above noise was summed for these conditions and controls without VWF (but with PS) and without PS (but with VWF). PS binding was significantly higher in the absence of calcium than all other conditions, (E) when accounting for the area of VWF self-association, PS binding was significantly higher than all other conditions. Error bars are standard deviation. Statistical significance was determined with an ANOVA and Tukey post hoc test (n.s., non-significant; **, $P < 0.01$; ***, $P < 0.001$; ****, $P < 0.0001$). Scale bar = 25 μm .

VWF self-association experiments using a PDMS microfluidic device were conducted by Dr. Molly Mollica in the Bloodworks Northwest, Seattle, Washington.

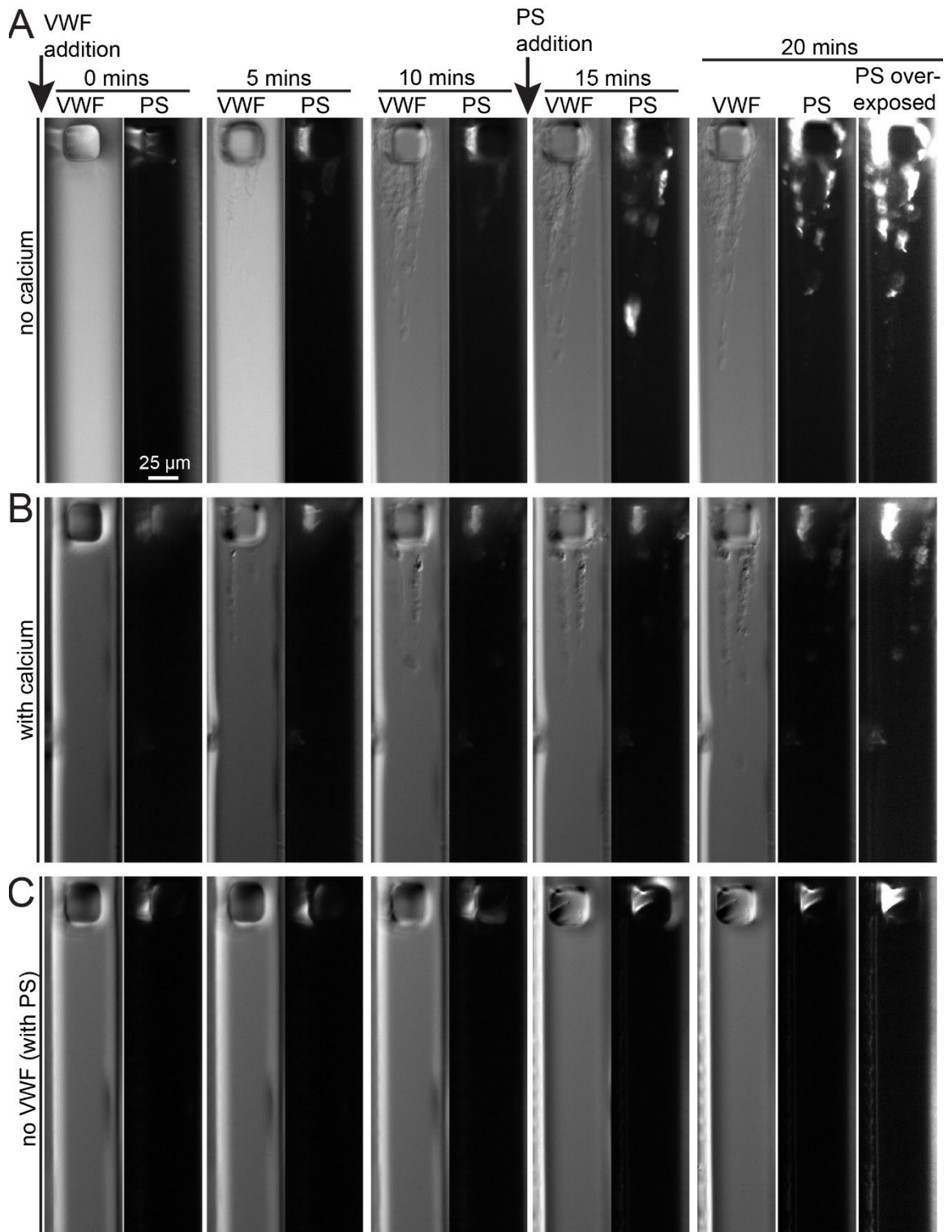


Figure 4.13. Time-lapse images of VWF interaction with PS under flow

Figure 4.13. Time-lapse images of VWF interaction with PS under flow

Representative images captured over time (0 min, 5 min, 10 min, and 20 min) of (A) VWF + PS without calcium, (B) VWF + PS with calcium (2 mM CaCl_2), and (C) PS without VWF (and without calcium). VWF is added at time = 0 and VWF self-association is visible around the block in the DIC images. At time = 10 minutes, fluorescently labeled PS is added and is observed binding to VWF, especially in the absence of calcium (A and B). Intensity in the fluorescent channel is not observed in the absence of VWF (C).

VWF self-association experiments using a PDMS microfluidic device were conducted by Dr. Molly Mollica in the Bloodworks Northwest, Seattle, Washington.

4.3 Conclusions

Collectively, we observed a shear-dependent interaction between PS and VWF in human plasma, which can contribute to acquired free PS deficiency in COVID-19, and correlated with higher thrombotic potential in these patients. This novel mechanism is likely applicable to other inflammatory conditions as elevation of VWF activity and pathological vascular shear are common clinical complications.

CHAPTER 5. TISSUE FACTOR RELEASE FOLLOWING TRAUMATIC BRAIN INJURY
CONTRIBUTES TO THROMBOSIS IN MICE

A part of this chapter has been published in *Research Practice in Thrombosis and Haemostasis*, 2022 Jun 8;6(4):e12734. The following are the manuscript and the author information:

Tissue Factor Release Following Traumatic Brain Injury Drives Thrombin Generation

W. Brad Hubbard^{1,2,3}, Martha M.S. Sim⁴, Kathryn E. Saatman^{2,3}, Patrick G. Sullivan^{1,3,5},

Jeremy P. Wood^{4,6,7}

¹Lexington Veterans' Affairs Healthcare System

²Department of Physiology, University of Kentucky

³Spinal Cord and Brain Injury Research Center, University of Kentucky

⁴Department of Molecular and Cellular Biochemistry, University of Kentucky

⁵Department of Neuroscience, University of Kentucky

⁶Division of Cardiovascular Medicine, the Gill Heart and Vascular Institute, University of
Kentucky

⁷Saha Cardiovascular Research Center, University of Kentucky

5.1 Introduction

Traumatic brain injury (TBI) leads to a myriad of secondary pathology propagated by the initial head insult. Early blood-brain barrier (BBB) disruption initiates mechanisms of thromboinflammation [173] and TBI-induced coagulopathy [174]. Coagulopathy manifests as disseminated intravascular coagulation, producing systemic blood clots that can cause secondary cerebral injury and ischemia after TBI [175]. Patients with TBI are at higher risk of blood clot formation [176]. TBI-induced coagulopathy is common in penetrating head injuries, [177] but there are also reports of coagulopathy following blunt head trauma [178]. The presence of coagulopathy following isolated TBI is strongly associated with poor patient prognosis [180].

Limitations of clinical practice in treating TBI-induced coagulopathy highlight the urgent need to identify new therapies [343]. The creation of experimental models that recapitulate clinical findings will help identify the specific etiology related to delayed thrombosis. Further, understanding of the pathobiology of coagulopathy in these models will inform researchers of potential therapeutic targets to reduce secondary brain injury and improve outcomes following TBI and will aid in identifying biomarkers for predicting which patients are most at-risk for thrombosis.

Following clinical TBI, procoagulant microparticles containing phosphatidylserine (PtdSer) and tissue factor (TF) are released into the blood early after injury [344]. In clinical TBI plasma samples, microparticles derived from ECs are more highly elevated than those from platelets or leukocytes [345]. It has been proposed that TF drives coagulopathy following clinical TBI [177, 346-348]; however, direct evidence to support this claim is

lacking. Tian, et al. showed that brain-derived extracellular vesicles (BDEV) are released following fluid percussion injury (FPI) and that BDEVs have both TF and PtdSer that result in thrombosis [174, 349]. However, there is no clear evidence whether TF or PtdSer is the driving factor.

For this investigation, we utilized two distinct preclinical TBI models to recapitulate coagulopathy of clinical TBI. Neurovascular damage is a major endophenotype of TBI and propagates pathways of coagulopathy. The controlled cortical impact (CCI) model involves impact directly to the dura of the brain producing a relatively defined, focal cortical contusion that results in vascular injury, BBB breakdown, and acute hemorrhage at the site of impact. Intracerebral hemorrhage and vascular damage lead to local immune and inflammatory responses. The closed head injury (CHI) model involves a midline impact to the skull, which generates a relatively diffuse, mild brain injury that produces neuroinflammation and deficits in brain metabolism. CHI is non-hemorrhagic and does not produce overt cell death but can lead to diffuse vascular damage. These models were used to examine thrombin production and TF activity following injury.

A major component of thrombosis following brain injury is release of EVs by damaged neurovasculature. EVs play a role in the pathogenesis of TBI and have been used as brain-specific injury markers [350]. EVs can be procoagulant and contribute to TBI-induced coagulopathy, either through the expression of PtdSer or coagulation proteins, such as TF. Indeed, brain-derived microvesicles are present in plasma after FPI and promote coagulopathy following brain injury [349]. As described by Tian et al. [349], both TF and

PtdSer are expressed on brain-derived EVs following experimental TBI. Here, we assess the role of TF and EVs in TBI-induced thrombosis.

5.2 Results

5.2.1 Development of mouse plasma TF activity assay

Initial experiments determined that human FVIIa (12.5 nM) does not function with mouse TF (Figure 5.1A), necessitating the need to use mouse FVIIa for subsequent experiments. We activated mouse FVIIa using bacterial Thermolysin per recommended protocol. Standard curves generated using mFVIIa (2.5 nM; Figure 5.1B-C) with mouse or human TF revealed that the standards were more sensitive and reproducible using human TF. Thus, experimental data using mouse samples are presented as the equivalent human TF activity.

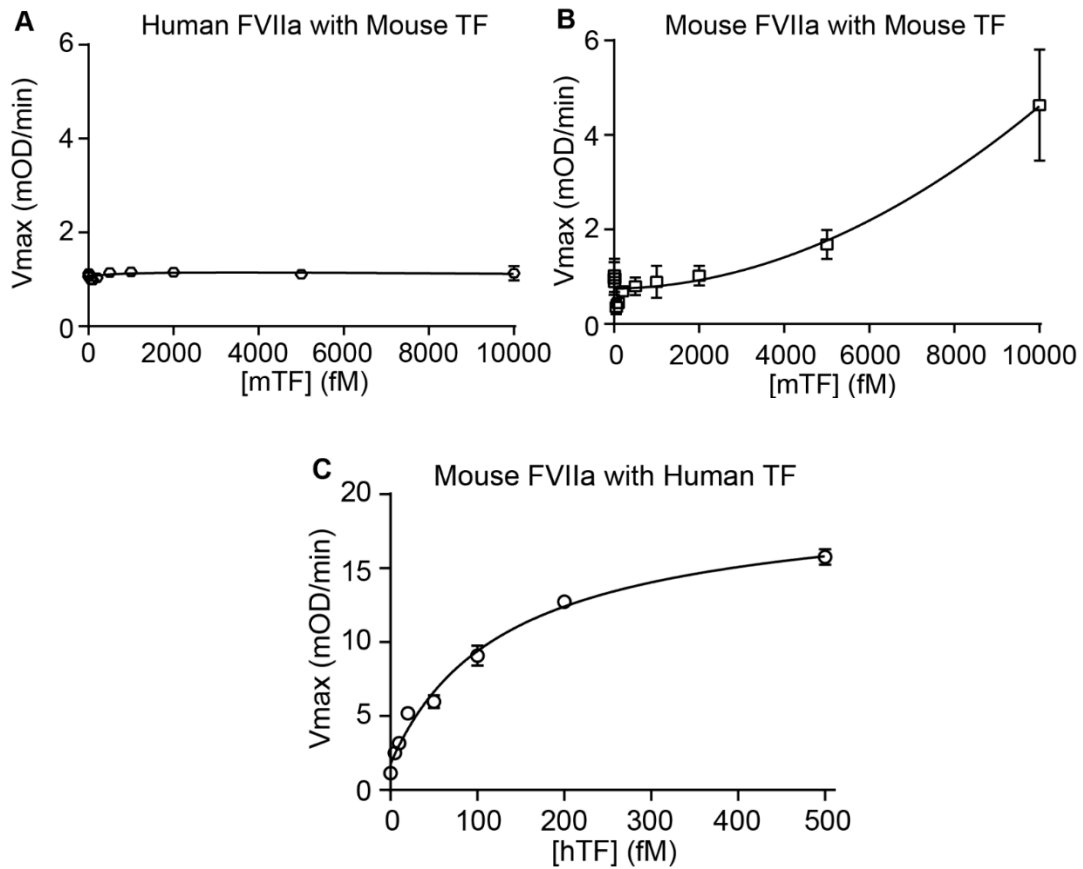


Figure 5.1. Development of mouse plasma TF activity assay

Validation of mouse TF activity and thrombin generation assays. (A-B) mTF was incubated with (A) hFVIIa (12.5 nM) or (B) mFVIIa (2.5 nM). Reactions were initiated by addition of hFX (375 nM), and cleavage of a FXa substrate (500 μ M) was monitored by measuring absorbance at 405 nm for 2 hr at 37°C. The maximum slope of substrate cleavage is presented (Mean \pm S.D.; $n \geq 3$). (C) hTF was incubated with mFVIIa (2.5 nM), and FXa activation was measured as in A.

5.2.2 Post-TBI plasma TG is not altered when exogenous TF is added

We used a model of focal brain injury to investigate the role of TF and PL in TBI-induced coagulopathy. We first assessed whether coagulation factors downstream of TF contributed to thrombin generation after TBI. For this experiment, we measured thrombin generation in the presence of excess TF and PL (Figure 5.2). There were no significant differences between groups in any parameter of thrombin generation at 6 h (Figure 5.2A) or 24 h (Figure 5.2B) post-injury. This suggests that CCI-induced coagulopathy is not mediated primarily by coagulation components downstream of TF.

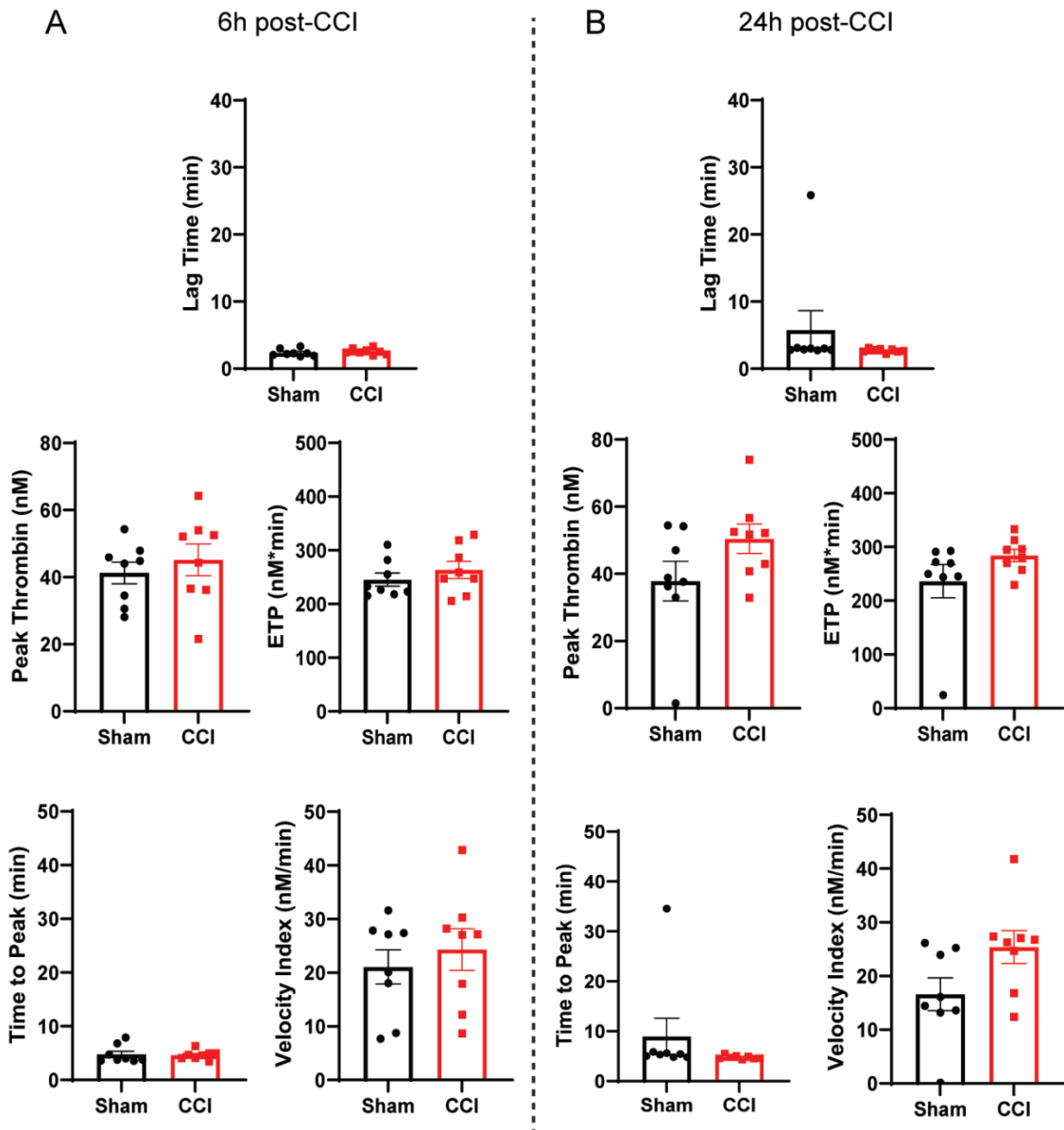


Figure 5.2. Post-TBI plasma TG is not altered when exogenous TF is added

Mice received either sham injury or severe CCI followed by euthanasia at either 6 or 24 h post-injury. PPP was assayed for thrombin generation. Lag time, ETP, peak thrombin, time to peak, and velocity index were calculated under addition of TF+/PL+. CCI does not result in a change in any parameters in the presence of TF+/PL+. n=8/group. Mean \pm SEM and data points.

5.2.3 Post-TBI TG is not mediated by increased PL

We next assessed the contribution of procoagulant phospholipids (PL) by measuring thrombin generation in the presence of excess TF, but no additional PL (Figure 5.3), making the assay dependent on PL present in the plasma samples. Under these conditions, no significant differences were observed between sham and CCI mice, either at 6 h (Figure 5.3A) or 24 h (Figure 5.3B) post-injury, suggesting that increased PL is not the driving force in acute thrombin production following brain injury.

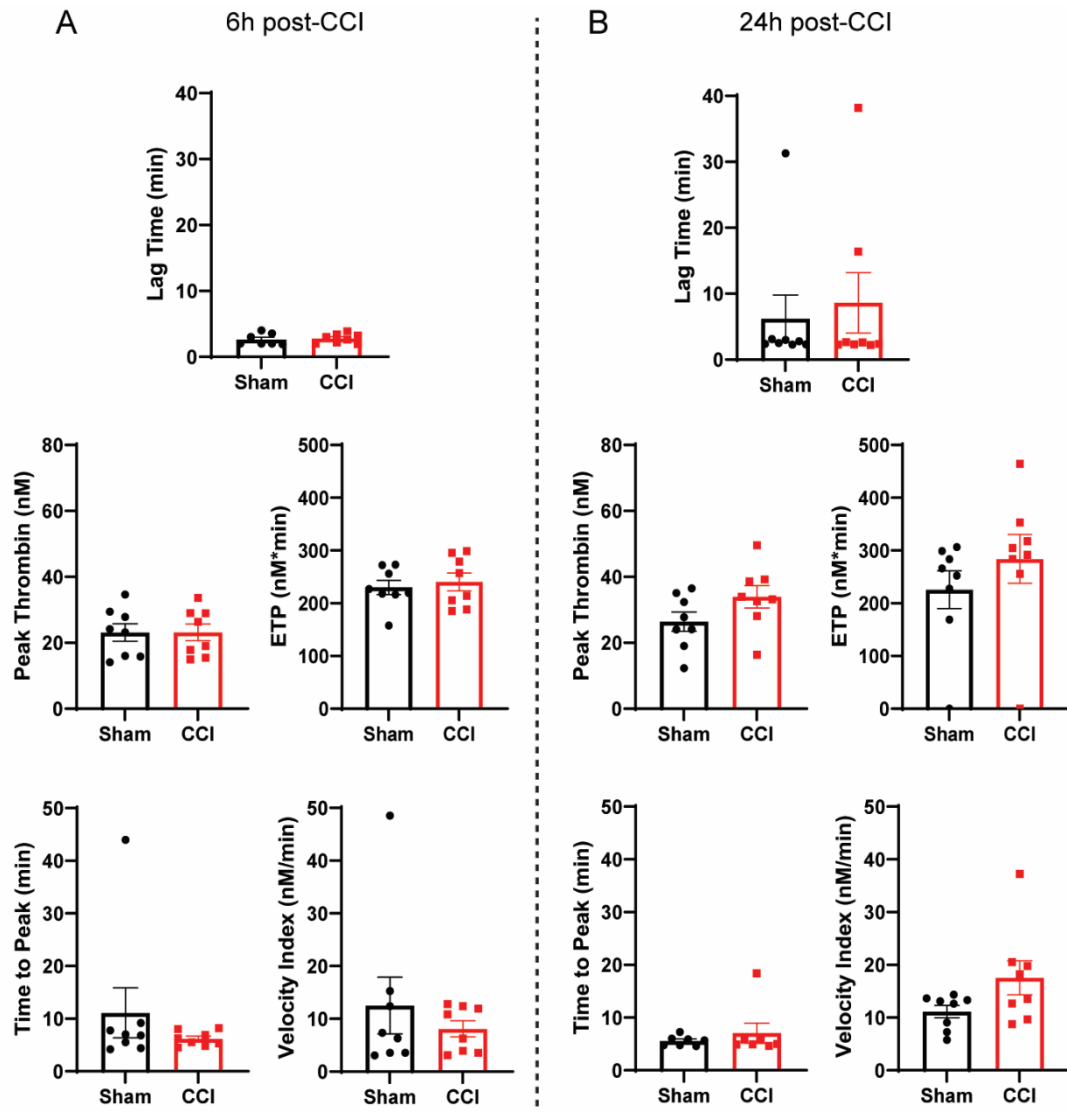


Figure 5.3. Post-TBI TG is not mediated by increased PL

Mice received either sham injury or severe CCI followed by euthanasia at either 6 or 24 h post-injury. PPP was assayed for thrombin generation. Lag time, ETP, peak thrombin, time to peak, and velocity index were calculated under addition of TF+/PL-. CCI does not result in a change in any parameters in the presence of TF+/PL-. n = 8/group. Mean ± SEM and data points.

5.2.4 Acute TF release post-TBI drives TG

We next measured thrombin generation in the presence of excess PL, with no added TF (Figure 5.4). At both 6 h (Figure 5.4A) and 24 h (Figure 5.4B) post-injury, lag time and time to peak were significantly decreased in plasma from CCI mice compared to sham mice. Further, plasma from CCI mice displayed higher ETP 6 h post-injury and higher ETP and velocity index 24 h post-injury compared to sham mice. Overall, thrombin generation was significantly faster and higher following CCI. To confirm the contribution of TF to this mechanism, we determined that plasma TF activity following CCI was increased two-fold at both 6 h and 24 h post-injury and this increase was statistically significant at 24 h post-injury, supporting a TF-driven mechanism of acute coagulopathy following TBI.

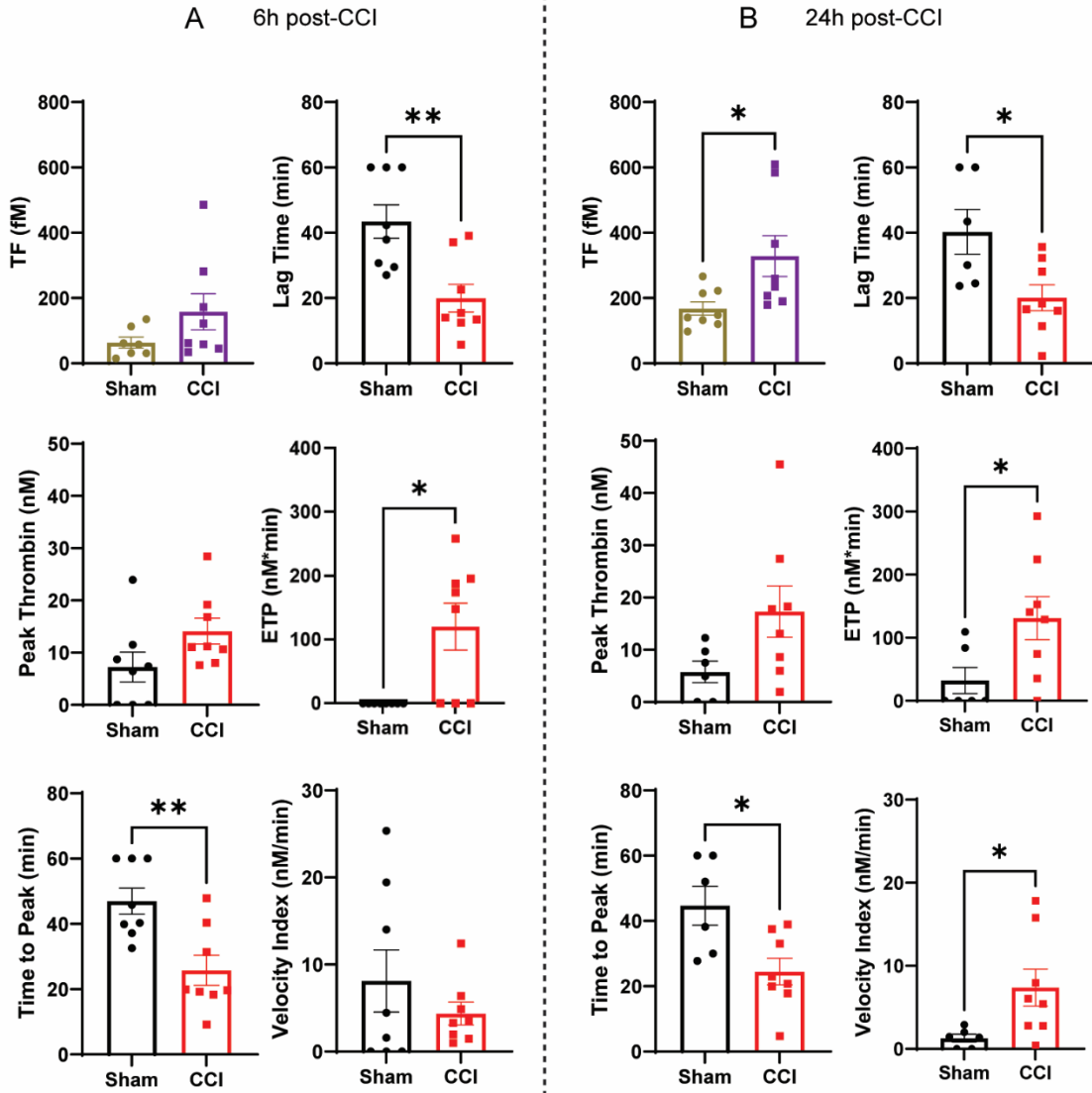


Figure 5.4. Acute TF release post-TBI drives TG in severe TBI model

Figure 5.4. Acute TF release post-TBI drives TG in severe TBI model

Mice received either sham injury or severe CCI followed by euthanasia at either 6 or 24 h post-injury. PPP was assayed for thrombin generation. Lag time, ETP, peak thrombin, time to peak, and velocity index were calculated under addition of TF-/PL+. Tissue factor activity was also measured in the same samples. There was significantly decreased lag time and time to peak in PPP from CCI mice as compared to sham mice at both 6 h and 24 h post-injury. ETP was significantly elevated in PPP from CCI mice as compared to sham mice at both 6 h and 24 h post-injury. There was a significant increase in the velocity index in PPP from CCI mice as compared to that from sham mice at 24 h post-injury. There was a non-significant increase in TF at 6 h post-CCI and significant increase in TF at 24 h post-CCI. 6 h: lag time ** $p = 0.007$; ETP * $p = 0.026$; time to peak * $p = 0.015$. 24 h: lag time * $p = 0.041$; ETP * $p = 0.037$; time to peak * $p = 0.028$; velocity index * $p = 0.039$; TF * $p = 0.028$. $n = 6-8/\text{group}$. Mean \pm SEM and data points.

5.2.5 Early increase in TF is observed in mild TBI model

To fully attribute changes in TF activity to brain damage in a non-hemorrhagic environment, we performed thrombin generation and TF activity assays in a CHI model (Figure 5.5). CHI does not produce overt hemorrhage but can result in diffuse vascular disruption [351]. Plasma from CHI mice generated detectable thrombin in 2/5 mice compared to 0/5 sham at 6 h post-injury (Figure 5.5A). This coincided with significantly elevated plasma TF activity in the CHI group compared to sham, in which mice with >140 fM TF activity producing detectable thrombin. No differences were observed 24 h post-CHI (Figure 5.5B), suggesting a time-dependence to TBI, consistent with reports in patients following TBI or extracranial trauma [346].

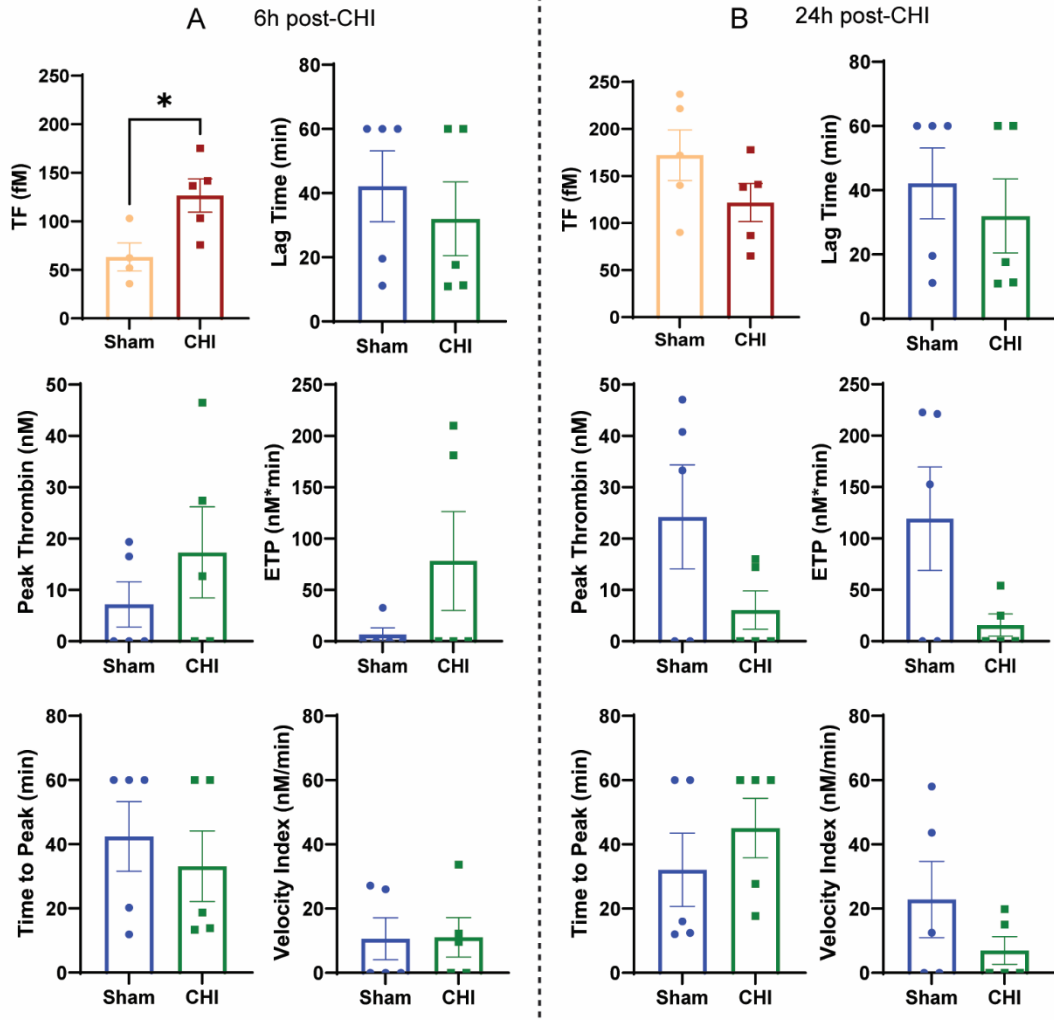


Figure 5.5. Early increase in TF is observed in mild TBI model

Mice received either sham injury or mild CHI followed by euthanasia at either 6 or 24 h post-injury. PPP was assayed for thrombin generation. Lag time, ETP, peak thrombin, time to peak, and velocity index were calculated under addition of TF-/PL+. Tissue factor activity was also measured in the same samples. There is a significant increase in TF in PPP from CHI mice as compared to sham mice at 6 h post-injury. There was no difference in thrombin generation or TF between groups at 24 h post-CHI. * $p = 0.029$. $t = 2.741$. $n=5/\text{group}$. Mean \pm SEM and data points.

5.3 Conclusions

Our data in CCI and CHI models of TBI show that thrombin generation is mediated, at least in part, by increased microvesicle TF, and that the TF increase is transient and dependent on the type or severity of injury. These findings support the clinical hypothesis that TF drives acute coagulopathy after brain injury, and suggests microvesicle TF may be a valuable biomarker for identifying patients most at-risk for thrombotic complications of TBI and for guiding therapeutic interventions.

CHAPTER 6. DISCUSSION

6.1 Part I: Total Protein S Deficiency in HIV Infection

In Chapter 3, we evaluated the contribution of PS deficiency, a commonly occurring hematologic abnormality in PLWH, to increased thrombotic risk seen in this patient population. In these studies, we demonstrated that decreased total PS contributes to increased thrombin generation in PLWH, suggesting that PS deficiency is a direct contributor to thrombotic risk in this population. Clinical PS deficiency occurred in 50% of our PLWH population, including 58.8% of the PLWH for which samples were collected prior to the start of ART treatment. The PS deficiency in our PLWH population is consistent with both the frequency and the extent of acquired PS deficiency in HIV-1 infection reported by previous studies [150, 352]. Acquired PS deficiency has been reported to occur secondary to viral infections, in the case of dengue [188], varicella [187], SARS-CoV-2 [189, 353], and HIV-1 [147, 149]. In HIV, acquired PS deficiency is thought to be caused by decreased synthesis by ECs, hepatocytes, and/or megakaryocytes, antibody-mediated clearance of PS, and loss due to nephropathy, among other possible mechanisms [148-150]. PS deficiency correlates with disease progression to AIDS [185], and both total and free plasma PS are decreased [149, 184]. The variability of PS deficiency reported in PLWH (~27-76%) [150] likely depends on the participant's health prior to initiation of ART, and on the particular ART regimen used [185]. Our study population included PLWH without AIDS, who were otherwise generally healthy at the time of sampling. We observed that PS deficiency was more pronounced in the untreated PLWH, with restoration to normal levels in most ART-treated PLWH. This is consistent with previous studies that suggest the

role of acute inflammation and immunothrombosis mechanisms. However, PS deficiency remained in 5 of 13 ART-treated PLWH, indicating that other pathological mechanisms might also play a role. Others have reported that even long-term ART treatment does not completely normalize the levels of some coagulation biomarkers [354] and treated PLWH remain at greater risk for thrombosis [140].

Acquired PS deficiency is the most common coagulation abnormality found in PLWH [150]. However, despite this high prevalence (~27-76%) [150], its pathologic consequences were unclear because PS concentration had not correlated with plasma thrombin generation *ex vivo* in the standard CAT assay [23]. One recent study, which did not look at PS, showed that the best predictors of increased plasma thrombin generation in PLWH were PC and factor V, the target of APC/PS anticoagulant activity [142]. We hypothesized that PS also contributes, and, therefore, developed a PS-sensitive CAT assay to investigate this hypothesis. We showed that thrombin generation was sensitive to plasma PS when samples are supplemented with TM but not when TM is absent, and that PS concentration negatively correlates with thrombin generation, if measured by a PS-sensitive assay. Hence, plasma PS likely contributes to thrombotic risk in PLWH. It is important to mention that other techniques for assessing PS activity exist, as summarized [355], which are typically clot endpoint-based assays with exogenously added APC in which its activity or promotion by PS is used as a proxy to measure PS activity. By modifying the standard CAT assay, we have developed a PS-sensitive plasma thrombin generation assay that relies on thrombin-thrombomodulin to activate PC, reflecting the

in vivo mechanism, and provides more detailed kinetic insight into the full dynamic range of thrombin generation.

HIV-1-induced expression of TF on circulating monocytes has also been described [151]. In infection or inflammation, blood cells such as monocytes may express TF after stimulation by inflammatory cytokines. Monocytes can release TF-bearing microvesicles into plasma, which could contribute to plasma thrombin generation measurements [152]. In addition, viral particles may incorporate procoagulant TF into their envelope, providing a second possible source for plasma TF in samples from PLWH with active infection [330]. Similarly, EC dysfunction can also contribute to intravascular coagulation and the release of TF-bearing microvesicles [356]. In the HIV population, increases in both the activity and antigen level of TF have been documented, yet the significance to thrombotic risk is unknown. We did not observe any increase in plasma TF in our patient population. The low amount of plasma TF that was detected did contribute to thrombin generation, but only in the absence of exogenous TF, correlating with decreased lag time.

People living with HIV are treated with a combination of several classes of ART drugs: protease inhibitors (PI), nucleoside and non-nucleoside reverse transcriptase inhibitors (NRTI and NNRTI), integrase inhibitors and entry inhibitors. Certain PI and NRTI drugs have been shown to exert procoagulant properties in PLWH [144, 146]. Many of the protease inhibitors are known to induce dyslipidemia and are associated with an increased risk of myocardial infarction [144]. Moreover, even though the protease inhibitors target viral aspartyl proteases, it is plausible that they might cross react with and inhibit coagulation factors. The drug Abacavir, an NRTI, is also associated with increased cardiovascular

disease risk, and has vascular inflammatory effects [146]. And thus, there has been inconsistency in the field in regards to the consequence of ART treatment to thrombotic risk. While ART effectively achieves clinical viral clearance and preserves CD4+ T cell counts, even long-term ART treatment does not completely normalize the levels of some coagulation markers [354]. and these PLWH remain at greater risk for thrombosis [139, 140]. In our patient group, treatment with ART effectively reduced the viral load (undetectable in 12 of 13 treated PLWH) and decreased plasma markers of inflammation to levels observed in healthy controls [309]. However, plasma thrombin generation was not different between naïve PLWH and those on ART, consistent with the inability of treatment to eliminate the thrombotic risk.

We acknowledge limitations with this study. We have only a limited number of female PLWH (n = 2 out of 30 PLWH), which is reflective of the overall PLWH population in the state of Kentucky, but limits our ability to translate our results to female PLWH. Females, on average, have reduced PS compared to males and thus may be more susceptible to an acquired PS deficiency. Other sex-specific coagulation factor differences may also alter the sensitivity of the modified thrombin generation assay to PS concentration. In addition, a larger study would allow us to determine the interaction of PS with other thrombotic risk factors, some of which are sex-dependent, and to assess the potential predictive value of PS for thrombotic events.

6.2 Part II: Free Protein S Deficiency in COVID-19 Infection

In Chapter 4, we described a specific free PS deficiency in a cohort of COVID-19 patients and investigated its possible mechanisms. In this study, we demonstrated an acquired free PS deficiency in COVID-19 patients, which occurs with similar frequency in patients with mild or severe disease, correlates with higher plasma thrombin generation *ex vivo*, and cannot be explained by an increase in well-described PS-binding proteins. Subsequent experiments using mass spectrometry, immunoblotting, ELISA, and microfluidics revealed a shear-dependent interaction between PS and VWF, which we propose as a previously unrecognized mechanism of acquired PS deficiency. Consistently, we detected PS/VWF comigration in control and patient samples by native agarose gel electrophoresis.

Severe viral infections, including HIV-1, dengue, and varicella, are associated with acquired PS deficiency [184-190, 192-194]. Other groups have reported acquired PS deficiency in COVID-19 patients, measuring either free PS antigen or PS activity, an APC activity-based measurement of free PS, and have proposed a variety of potential mechanisms for this deficiency, which we recently reviewed [332]. In this cohort, we did not observe reduction in total PS, suggesting that the deficiency is not due to decreased synthesis, increased consumption, or antibody-mediated clearance, as others have proposed. Instead, we report a specific decrease in free PS, which occurs at a similar frequency in both outpatients and inpatients. This is striking as our outpatients were for the most part mildly symptomatic, whereas all inpatients had severe disease and were under intensive care.

The specific decrease in free PS suggests a concurrent increase in a plasma PS-binding protein, with C4BP- β being the most likely candidate. The major isoform (~80%) of C4BP in plasma consists of 7 α and 1 β chains, with the other isoforms containing either 6 α and 1 β or exclusively 7 α or 6 α [357]. We measure C4BP- β , as this is the chain that binds PS. However, C4BP- β was unchanged in COVID-19 patients, as was PC. PS is also involved in anti-inflammatory signaling and efferocytosis by monocytes/macrophages, as a ligand for the TAM (Tyro3, Axl, Mer) receptors, which are implicated in COVID-19 [194, 208]. While we did see a slight elevation of plasma soluble Mer, the low picomolar concentration of this protein makes it unlikely to have a meaningful impact on free PS concentration (normal range 5-15 $\mu\text{g}/\text{mL}$ or ~ 150 nM).

To understand the cause of free PS deficiency and test for other PS-binding proteins, we visualized PS in plasma from patients and controls by non-denaturing gel electrophoresis and immunoblotting. PS dimerizes at high concentrations [337], and this dimer is disrupted by calcium [338]; therefore, high concentrations (~ 10 μM) of purified PS, dialyzed to calcium-free buffer, with calcium or EDTA supplementation, were used as controls to observe the locations of PS monomer and dimer. While the purified protein separated as the expected monomer and dimer species, a multitude of bands toward the top of the gel were observed in all plasma samples, some of which co-migrated with C4BP- β , PC, TFPI, Mer, factor V, or VWF. VWF was included, as it is an abundant, large multimeric protein with numerous protein binding sites that can be exposed under high shear [339], and a prothrombotic acute phase reactant during inflammation, including in

COVID-19 [302, 340]. Consistent with other studies, we also observed elevation of VWF:Ag in our inpatients, despite no apparent change in multimer distribution.

Mass spectrometry analyses revealed that the amount of PS bound to VWF increases >10,000,000-fold upon exposure to shear. We hypothesize that shear-induced unfolding of VWF exposes a binding site, as it does for platelet GPIb [339] or ADAMTS13 [358], which interacts either directly or indirectly with PS and contributes to acquired free PS deficiency. Consistent with this, addition of sheared VWF to control plasma dose-dependently inhibited free, but not total, PS antigen measurement, and shearing of plasma lowered free PS detection in healthy donor samples. Additionally, PS co-migrated with the lower molecular weight VWF multimers. This comigration was apparent either in the presence or absence of shearing, suggesting that either some of this complex exists normally in plasma or exposure to SDS and electrophoresis induces sufficient VWF unfolding for PS to bind. This also suggests that the PS/VWF interaction is strong enough to withstand electrophoresis. In addition, PS/VWF complexes can be pre-formed by shearing and stably maintained in recalcified whole blood, and co-localize on platelet thrombi under a flow system. Finally, PS binds to VWF after it unfolds and self-associates *in situ* under flow. The calcium sensitivity of the PS-VWF binding under flow could be due to calcium effects on VWF unfolding, VWF self-association, and/or PS monomerization. The lack of sensitivity to calcium when VWF is vortexed suggests that process induces higher effective shear forces than the microfluidic system, which are sufficient to overcome the limitations imposed by calcium.

As shearing reduces free PS in healthy control plasma, and free PS concentration did not correlate with increased VWF antigen, the effect of VWF on free PS is likely mediated primarily by shear-dependent unfolding, rather than changes in VWF antigen. Shear-induced unfolding of VWF increases with elevated wall shear stress and therefore would become progressively greater in the arterial system as the vessels become smaller. Unfolding and self-association of VWF also is favored in regions of flow acceleration as occur in stenotic arteries or valves and in resistance vessels [359], especially during hypertension. It is noteworthy that in two studies published early in the COVID-19 pandemic, hypertension was the most common comorbidity associated with severe disease [360, 361].

The exact PS binding site on VWF is unknown, but appears distinct from the platelet binding site, as treatment with Ristocetin, which exposes the GPIb binding site on VWF, did not reduce free PS. The shear-dependent association between PS and VWF is supported by mass spectrometry and immunoblotting analyses of VWF-interacting proteins, ELISAs, and microfluidics experiments. It is less clear whether any PS circulates bound to VWF in healthy individuals. We observed PS/VWF co-migration by both non-denaturing gel electrophoresis and VWF multimer gels. A VWF/PS complex ELISA also detected this complex in healthy normal plasmas. However, the complex increased rapidly over incubation time. Thus, it is unclear whether the complex pre-exists in plasma or was induced by the experimental conditions. Similarly, electrophoresis may unfold VWF enough to allow for PS association. Regardless, this complex was apparent in plasma

samples but not in studies performed with purified proteins, suggesting that additional plasma component(s) may help mediate the interaction, in the absence of excess shear.

The free PS deficiency that develops in COVID-19 patients appears to be functionally relevant. In a PS-sensitive plasma thrombin generation assay [186], free PS deficiency correlated with increased plasma thrombin generation. TF-initiated thrombin generation was measured in the presence and absence of exogenous thrombomodulin, an endothelial receptor protein necessary for PC activation. Despite prophylactic heparin anticoagulation received by some inpatients, plasma thrombin generation was not decreased in patients and trended toward increased, though this was not statistically significant. In the presence of thrombomodulin, peak thrombin and endogenous thrombin potential were elevated in patients, signifying lower sensitivity to thrombomodulin and reduced APC/PS pathway activity. The inpatients received an array of different therapeutic regimens, including anticoagulant, as the hospital treatment procedures were evolving during the initial phases of the pandemic. As such, we are not able to precisely account for the effect of anticoagulation on thrombin generation. Only one of the inpatients in this study had a clinically identified thrombotic event, a pulmonary embolism which occurred days prior to sample collection. Otherwise, our patient population was similar to other reports, in terms of inflammatory markers, immune response, EC activation, and tissue factor expression [161, 333-335].

In conclusion, these data suggest that shear-induced unfolding of VWF exposes a binding site for PS, localizes PS, and blocks free PS antigen measurement in patients with COVID-19. Thus, elevated shear forces can cause free PS deficiency in a VWF-dependent manner,

which is associated with increased thrombin generation *ex vivo*. We anticipate that this mechanism also contributes to acquired PS deficiency in other inflammatory conditions in which VWF is exposed to elevated vascular shear forces, and that VWF may modulate PS anticoagulant activity under normal hemostatic conditions.

6.3 Part III: Tissue Factor Release in TBI-Associated Inflammation

In Chapter 5, we examined the role of systemic release of TF and EVs in TBI-induced thrombosis mechanisms in mice. A major component of thrombosis following brain injury is release of EVs by damaged neurovasculature. EVs play a role in the pathogenesis of TBI and have been used as brain-specific injury markers [350]. EVs can be procoagulant and contribute to TBI-induced coagulopathy, either through the expression of PtdSer or coagulation proteins, such as TF. As described by Tian et al. [349], both TF and PtdSer are expressed on brain-derived EVs following experimental TBI.

To expand on these findings, we used a model of focal brain injury to investigate the role of TF and PL in TBI-induced coagulopathy. We first assessed whether coagulation factors downstream of TF contributed to thrombin generation after TBI. There were no significant differences between groups in any parameter of thrombin generation at 6 h or 24 h post-injury. This suggests that CCI-induced coagulopathy is not mediated primarily by coagulation components downstream of TF. We next assessed the contribution of procoagulant phospholipids (PL) by measuring thrombin generation in the presence of excess TF, but no additional PL, making the assay dependent on PL present in the plasma samples. Under these conditions, no significant differences were observed between sham

and CCI mice, suggesting that increased PL is not the driving force in acute thrombin production following brain injury.

One limitation of the CCI model is the requirement of a craniotomy procedure, which can induce local blood flows changes and damage to the superficial vessels underlying the skull. To fully attribute changes in TF activity to brain damage in a non-hemorrhagic environment, we performed thrombin generation and TF activity assays in a CHI model. CHI does not produce overt hemorrhage but can result in diffuse vascular disruption [351]. Plasma from CHI mice generated detectable thrombin in 2/5 mice compared to 0/5 sham at 6 h post-injury. This coincided with significantly elevated plasma TF activity in the CHI group compared to sham, in which mice with >140 fM TF activity producing detectable thrombin. No differences were observed 24 h post-CHI, suggesting a time-dependence to TBI, consistent with reports in patients following TBI or extracranial trauma [346].

These results are consistent with our group's observation of early changes in platelet coupling efficiency after CCI, pointing to TBI-induced alteration of platelet metabolism [326]. Thrombin activates platelets and influences platelet metabolism, as shown by Aibibula, et al [362]. In addition, TF+ BDEVs, which can be derived from neurons and astrocytes in the TF-rich brain, can also activate platelets [349]. EVs from ECs were also elevated after TBI in one clinical study [345], suggesting a mechanism of TF release from damaged neurovasculature.

Future directions are poised to examine the on-going and/or chronic nature of thrombin generation in these models. Patients who are admitted to the emergency department can develop coagulopathy over the first several days following brain injury [180], indicating possible delayed mechanisms. Further, early mechanisms that lead to fibrin production could contribute to long-term fibrin(ogen) deposition after brain injury. In clinical and preclinical studies, BBB disruption after TBI leads to fibrin(ogen) deposition in cortical vessels, leading to gliosis, reduced neuronal density, and worsened neurological performance [363-366]. Therefore, fibrin(ogen) can drive poor outcomes and early targeting of thrombin generation could mitigate these outcomes.

Our data in CCI and CHI models of TBI show that thrombin generation is mediated, at least in part, by increased microvesicle TF, and that the TF increase is transient and dependent on the type or severity of injury. These findings support the clinical hypothesis that TF drives acute coagulopathy after brain injury, and suggests microvesicle TF may be a valuable biomarker for identifying patients most at-risk for thrombotic complications of TBI and for guiding therapeutic interventions.

CHAPTER 7. SUMMARY AND FUTURE DIRECTIONS

7.1 Summary

Part I: Total Protein S Deficiency in HIV Infection

1. In the presence of TM, plasma thrombin generation is very sensitive to plasma PS concentration. With this modified CAT assay, we can examine PS-dependent impacts in thrombin generation of donor plasmas, enabling us to evaluate the impact of antigenic or functional PS deficiency in HIV-1 and SARS-CoV-2 infection.
2. In PLWH, despite successful treatment with ART, both total and free PS are reduced, along with PC, indicating an overall depletion of PS and decreased PC/PS pathway activity. Consistent with existing literature, ~50% of PLWH plasmas were deficient in PS, while ART-treatment partially restored total PS, with ~27% patients remaining deficient.
3. PS deficiency, the most common coagulation abnormality in PLWH, contributes to increased thrombin generation, and likely thrombotic risk, observed in this population, despite the opposite observation in a previous study.
4. Reduction of total PS, free PS, and PC in HIV-1, individually correlate with increased thrombin generation potential, therefore, PS and PC may serve as prothrombotic biomarkers that could be monitored in PLWH patients, in order to evaluate thrombotic risk as well as to help determining prophylactic anticoagulant therapeutic needs.
5. Plasma TF activity is unlikely to contribute to the thrombotic risk associated with HIV infection.

Part II: Free PS Deficiency in COVID-19 Infection

1. Unlike HIV-1, SARS-CoV-2 (COVID-19) patients develop free PS, but not total PS deficiency. PS-interacting proteins C4BP- β , PC, and soluble Mer were not sufficiently altered to explain the free PS deficiency.
2. Despite anticoagulation, COVID-19 inpatients had comparable plasma thrombin generation to healthy controls and elevated D-dimer, indicating a prothrombotic state, which is likely exacerbated by the free PS deficiency.
3. Using our COVID-19 patient cohort as a model for specific free PS deficiency, we identified a previously unrecognized shear-dependent and calcium-sensitive interaction between PS and VWF, a prothrombotic acute phase reactant often elevated in COVID-19 and other inflammatory conditions.
4. VWF antigen concentration is markedly elevated mostly in the inpatients, whereas free PS deficiency occurs in the out- and inpatients to a similar extent, suggesting that it is the pathological vascular shear pattern, rather than a particular VWF antigen concentration, that induces the unfolding of VWF, which in turn sequesters PS.
5. We see evidence of co-migration of PS with lower molecular weight multimers of VWF, which is unaffected by calcium or shear, possibly implying either pre-existing PS/VWF complexed in plasma or induced by experimental conditions.

Part III: TF Release in TBI-associated Inflammation

1. In controlled cortical impact (CCI), a mouse model for a severe form of TBI, which causes acute hemorrhage, cortical neurovascular damage, and blood-brain barrier

breakdown, post-TBI coagulopathy is not caused directly by coagulation components downstream of TF nor by an increase in circulating phospholipids. Instead, an acute TF release occurs, with an approximately two-fold increase in plasma TF activity at both 6 h and 24 h post-TBI, which drives faster and higher thrombotic potential. This TF increase is reflective, at least in part, of a release of brain-derived extracellular vesicles, with increased expression and activity of microvesicle-associated TF into the systemic circulation.

2. In closed head injury (CHI), a mouse model for a milder form of TBI, which is non-hemorrhagic but causes diffuse neuroinflammation and brain metabolism deficits, elevated plasma TF activity occurs at 6 h post-TBI, without significant effect on plasma thrombotic potential, and subsides at 24 h post-injury, suggesting a time-dependency. The post-TBI plasma TF activity in CCI mice was notably higher by as much as 5-fold compared to the CHI mice, consistent with the severity of TBI.

7.2 Significance

1. With the modified CAT assay, we can examine PS-dependent impacts on thrombin generation potential of patient samples to evaluate the impact of antigenic or functional PS deficiency in various clinical conditions.
2. Acquired PS deficiency secondary to viral infection occurs with different contributing mechanisms and might differentially affect either total antigenic or free functional PS concentration, supporting the merit of measuring both total and free PS as part of the coagulation panel when evaluating the thrombotic risk in the clinic.

3. Depletion of anticoagulant proteins is a prominent consequence of HIV-1 infection correlating with increased thrombotic risk. Hence, periodic monitoring of anticoagulant proteins should be considered as a part of thrombotic risk assessment in HIV-1 patient care.
4. In COVID-19, we observed free PS deficiency in mildly symptomatic outpatients that is comparable to severe ICU-hospitalized patients, indicating notable and possibly specific mechanisms implicating PS in COVID-19 pathogenesis. While the other mechanisms such as decrease in synthesis, loss due to consumption, viral protease degradation, or autoantibody-mediated clearance might all play a role, the specific loss in free PS indicates that there is a shift of proportion between the free anticoagulant and bound PS pools. This shift in PS fraction could not be explained by an increase in well-described PS-binding proteins, such as by an increase in C4BP-binding which has been previously reported in HIV-1. Here, we describe a novel explanation of specific free PS deficiency, via an increase in VWF-binding, another acute phase reactant with previously unrecognized PS-binding activity.
5. As elevation of VWF antigen and activity via inflammation, endothelial activation, and decreased ADAMTS13 activity is a prominent consequence of severe SARS-CoV-2 infection, the PS/VWF interaction and its effects might be a significant feature in COVID-19 pathogenesis with important physiological consequences in patients affected by this pandemic. There are similarly many other viral infections as well as inflammatory conditions that are associated with VWF elevation and a pathological shear pattern that occurs as a consequence of severe endothelial activation and

- dysfunction in these inflammatory states. The PS/VWF interaction and impacts might be significant in these other conditions as well, leading to acquired free PS deficiency and thrombophilia (Figure 7.1B).
6. The PS/VWF shear-dependent interaction not only affects free (functional anticoagulant) PS measurement, but also at least partially interferes with PS anticoagulant cofactor activity (see Appendix I). This suggests further physiological relevance to this interaction under pathologic conditions. Moreover, based on VWF prothrombotic role in primary hemostasis, it is possible that the PS/VWF interaction is also a part of the normal vascular injury response. As VWF unfolds within the locally elevated or disrupted shear of the injury site and binds to collagen and platelets, VWF might also play an additional role in recruiting PS to where coagulation activation is occurring, and locally regulate anticoagulant activity (Figure 7.1A).
 7. Our ongoing longitudinal data indicates that free PS deficiency persists for up to three months post-infection in some patients (see Appendix II). Thus, we propose that PS deficiency and/or the PS/VWF interaction might play a role not only during the acute phase of infection, but also in the pathogenesis of its sequelae or as a contributing mechanism in long COVID-19 syndrome.
 8. Microvesicle-TF released post-TBI drives thrombin generation in a temporal manner and dependent on the severity of the injury. Measurement of microvesicle-associated TF or plasma TF activity may serve as biomarkers for evaluating thrombotic risk in TBI patients.

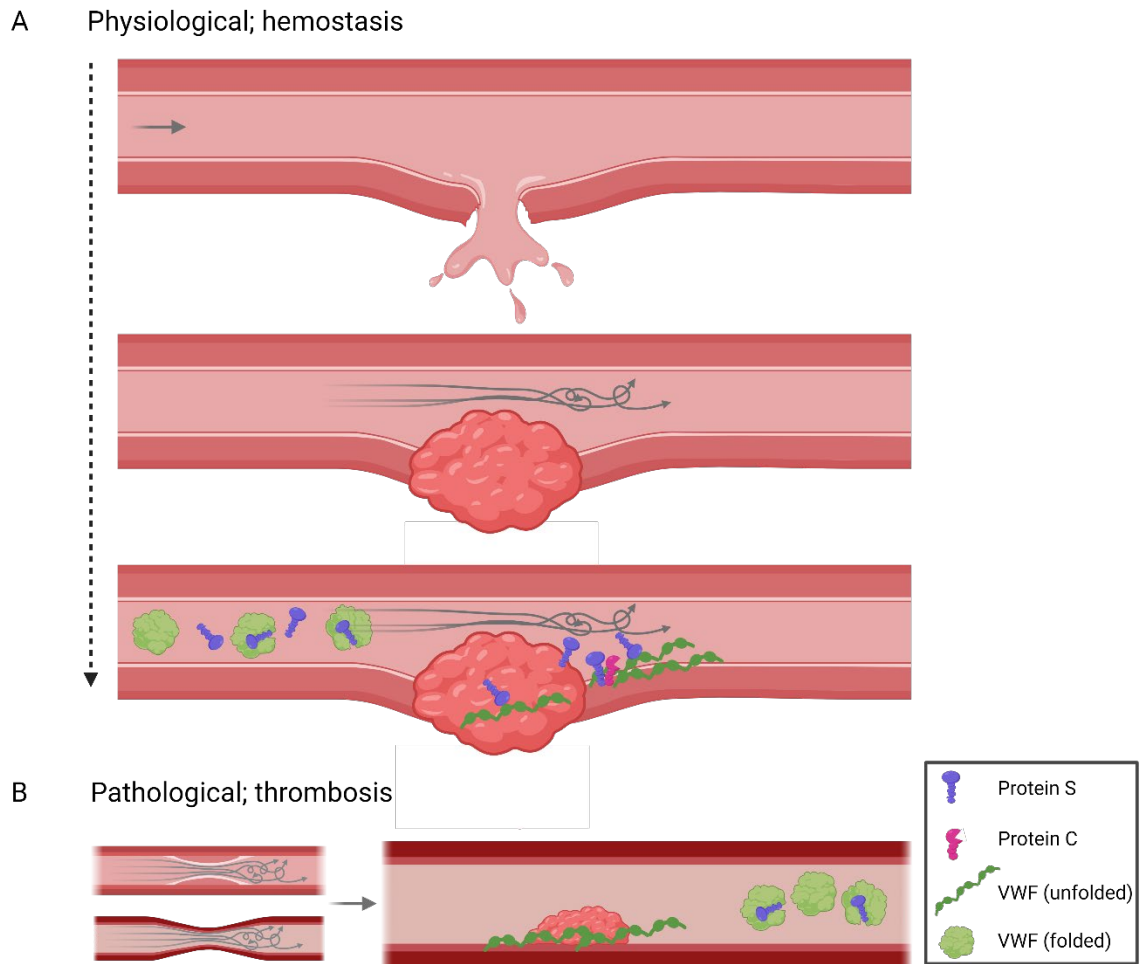


Figure 7.1. The roles of PS/VWF shear-dependent interaction in hemostasis and thrombosis

A postulated model of the roles of PS/VWF interaction in physiological (hemostatic) and pathological (immunothrombotic) conditions. Image created with BioRender.com.

7.3 Future Directions

1. To determine the interaction characteristics of PS/VWF; binding affinity, binding sites on both PS and VWF, calcium sensitivity, shear-dependency, and other determinants.
 - a. One way we have been undertaking this is by utilizing a crosslinking and biotin label transfer method with the Sulfo-SBED (Sulfo-N-hydroxysuccinimidyl-2-(6-[biotinamido]-2-(p-azido benzamido)-hexanoamido) ethyl-1,3'-dithiopropionate) technology. With this method, it is possible to separately label either PS or VWF with NHS-ester and biotin, incubate the labeled protein with plasma, while applying shear or other conditions, induce crosslinking to transfer the biotin label to interacting proteins, and evaluate the results using either immunoblotting or mass spectrometry. This assay is an unbiased approach to confirm PS/VWF binding, identify amino acids near the binding site, and identify other plasma proteins that bind either PS or VWF.
 - b. We have also communicated and established collaborative plans with several research labs to provide us with reagents and expertise in regards to VWF-related experimentations. Through these collaborations, we can gain access to patient plasmas from von Willebrand disease with known domain mutations, a phage display library of various domains of VWF, and various truncations of VWF protein. With these reagents, we can examine further the binding characteristics of PS/VWF.
 - c. Similarly, we have the capacity to purify the EGF1-2 and the Laminin G domains of PS. We also have access to Gla-domainless PS and various binding proteins of PS

(full-length C4BP, C4BP- β , Mer, TFPI α , and PC), each of which having established binding sites on PS. We can utilize these proteins in competition-based assays to study PS/VWF interaction characteristics.

2. To study the functional effects of the PS/VWF interaction on PS anticoagulant activity. We continue to delineate the impact of VWF binding on PS cofactor activity with APC and TFPI α , as well as PS direct FIXa inhibitory activity using enzyme activity assays, with chromogenic as well as with immunoblotting methods. Our preliminary data suggests that sheared VWF at least partially interferes with PS anticoagulant cofactor activity (see Appendix I).
3. To study the functional effects of the PS/VWF interaction on VWF hemostatic functions. We aim to also determine the impact of PS/VWF binding on VWF activity; with collagen binding, platelet binding, and ADAMTS13 activity assays in the presence or absence of PS, shear, calcium, and other determinants.
4. To study this interaction in the platelet environment. Platelet α -granules contain both PS and VWF which are released during platelet activation. Platelet VWF has both similarities and distinct features compared to endothelium-released plasma VWF, and little is known regarding the PS/VWF interaction in platelets. Moreover, there are differences in the activity of the coagulation complexes, as well as the anticoagulants, on the surface of phospholipid vesicular membranes and on platelets.
5. We continue with patient recruitment in both the HIV-1 and COVID-19 project.
 - a. Our lab is part of the VITAL (Virus-Induced Thrombosis Alliance) of the College of Medicine. We have approved IRB protocols in both HIV-1 and COVID-19 patient

recruitment and studies. We aim to also follow our patients longitudinally in order to evaluate the coagulation parameters as well as the long-term thrombotic risk. In an ongoing COVID-19 patient study, we observed a persistence of PS deficiency in a subset of outpatients after three months post-infection (see Appendix II).

- b. For COVID-19, the University of Kentucky and our lab personnels are part of the NIH RECOVER (Researching COVID-19 to Enhance Recovery Initiative) study, which recruits and follows COVID-19 patients in order to study the development and mechanisms of long COVID-19 or PASC (Post-Acute Sequelae of COVID-19).

APPENDICES

APPENDIX I. SHEARED VWF PARTIALLY INTERFERES WITH PS ANTICOAGULANT COFACTOR ACTIVITY

Introduction

We previously observed a shear-dependent interaction between PS and VWF, in which shear-induced VWF unfolding binds PS and blocks free PS antigen measurement. We next aim to delineate the functional effects of the PS/VWF interaction on PS anticoagulant activity. Here, we investigated the impact of sheared VWF on PS cofactor activity with APC and with TFPI α using chromogenic enzyme activity assays, as well as comparing the effect of sheared VWF on FVa cleavage by APC/PS, on synthetic phospholipids and on activated platelets using chromogenic and immunoblotting assays.

Results and discussion

1. Sheared VWF interferes with TFPI α -cofactor activity of PS

We investigated the impact of sheared VWF on FXa inhibitory activity of TFPI α /PS using chromogenic enzyme activity assay. We utilized 10 and 40 $\mu\text{g}/\text{mL}$ concentrations of VWF, to simulate the physiological and pathological conditions, respectively. We observed that sheared VWF reversed FXa inhibition by TFPI α /PS only at higher (40 $\mu\text{g}/\text{mL}$), but not at physiological VWF concentration (Figure 8.1).

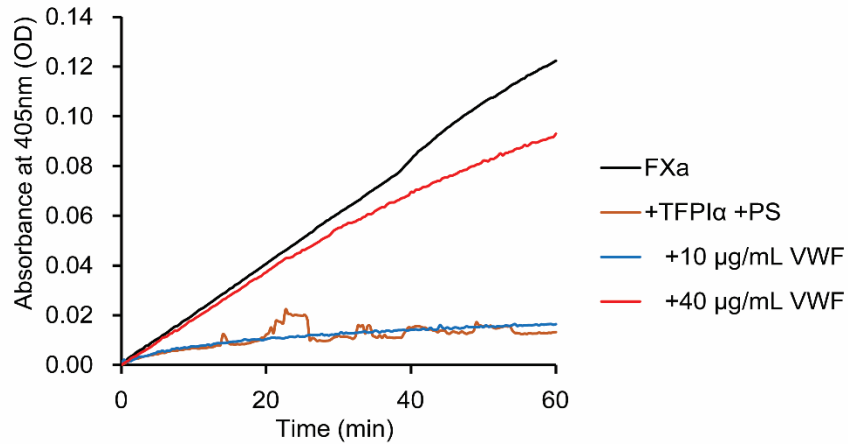


Figure 8.1. Sheared VWF dose dependently reverses FXa inhibition by TFPIα/PS

Shown is 5nM factor Xa (FXa) activity measured by chromogenic substrate cleavage, in respect to time, in the absence or presence of 1 nM TFPIα, 100 nM PS, and 10 or 40 μg/mL VWF, sheared by vortexing (~2,500 rpm for 30 s). Every data point is the average of three replicates. Shown is representative image of at least three independent experiments.

2. Sheared VWF has minimal effect on APC/PS prothrombinase inhibitory activity

We next investigated the impact of sheared VWF on prothrombinase inhibitory activity of APC/PS using chromogenic enzyme activity assays. We utilized 10 and 40 $\mu\text{g}/\text{mL}$ concentrations of VWF, to simulate the physiological and pathological conditions, respectively. In a continuous TG assay (Figure 8.2A), sheared VWF had no effect on prothrombinase activity. Assessing the kinetics further with a discontinuous TG assay, we observed a slight reversal of prothrombinase inhibitory kinetics during the early phase of TG, especially with the higher (40 $\mu\text{g}/\text{mL}$), but not at physiological VWF concentration (Figure 8.2B-C). Overall, sheared VWF had minimal effect on APC/PS prothrombinase inhibitory activity.

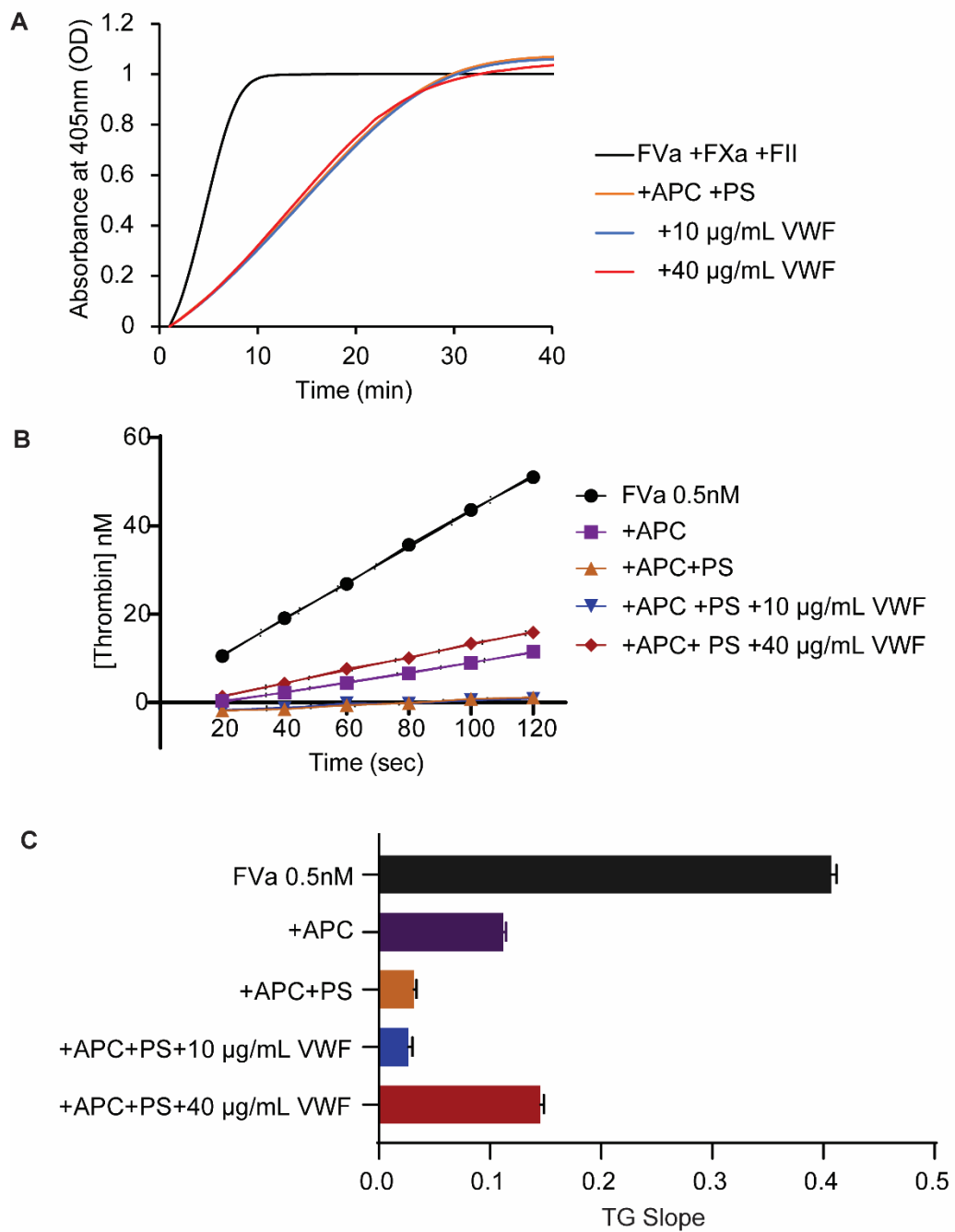


Figure 8.2. Sheared VWF had minimal impact on APC/PS prothrombinase inhibitory activity

Figure 8.2. Sheared VWF had minimal impact on APC/PS prothrombinase inhibitory activity

(A) Continuous and (B-C) discontinuous thrombin generation (TG) or prothrombinase activity was measured in the presence or absence of 0.5 nM FVa, 5 nM FXa, 1.4 μ M FII, 1 nM APC, 100 nM PS, and 10 or 40 μ g/mL VWF, sheared by vortexing (\sim 2,500 rpm for 30 s), using chromogenic enzyme activity assays. For each condition, shown are (B) thrombin concentration in respect to time and (C) the slope of TG. Every data point is the average of three replicates. Shown is representative image of at least three independent experiments.

3. The effect of sheared VWF on FVa-cleavage by APC/PS might be context dependent

We also investigated the impact of sheared VWF on FVa cleavage by APC/PS. APC with PS as its cofactor inactivates FVa, a cofactor component of prothrombinase complex, by cleavage at R506 and R306, which generates a ~30 kDa fragment. We monitored FVa cleavage with immunoblotting, in the context of a synthetic phospholipid surface (PC:PE:PS = 40:40:20) or on the activated platelet membrane. Plasma FVa is readily cleaved by APC while platelet-derived FVa is more resistant to APC inactivation on thrombin-activated platelets [367, 368]. We observed a slight enhancement of FVa cleavage in the presence of sheared VWF in the context of synthetic phospholipid vesicles using plasma-purified FVa (Figure 8.3B). On the contrary, we saw a slight inhibition of cleavage in the context of activated platelet membrane (Figure 8.3C), which displayed donor variability (n = 3).

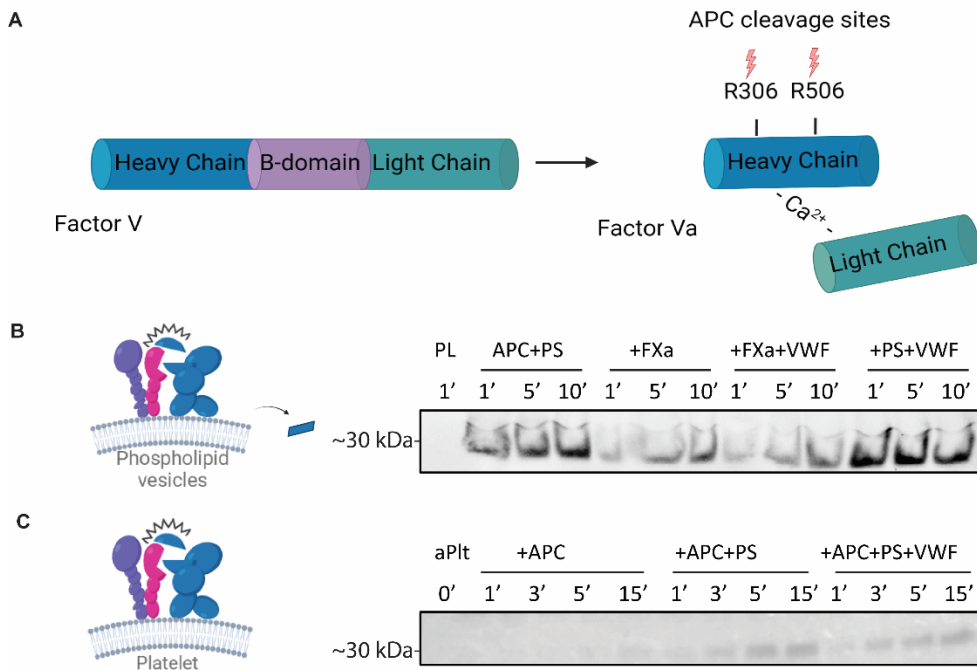


Figure 8.3. The impact of sheared VWF on FVa cleavage by APC/PS might be context dependent

(A) Schematic representation of FVa domain configuration and APC cleavage sites. (B-C) FVa cleavage was assayed by the generation of ~30 kDa cleavage product by immunoblotting, in the presence or absence of 1 nM APC, 100 nM PS, 5 nM FXa, or 10 µg/mL VWF, in the context of (B) 20 µM synthetic phospholipid vesicles (PC:PE:PS = 40:40:20) and (C) in 2×10^8 /mL thrombin-activated washed platelet from healthy human donor. Shown is representative image of at least three independent experiments.

4. The effect of sheared VWF on APC/PS prothrombinase inhibition on activated platelet surface shows donor variability

We measured the effect on thrombin generation or prothrombinase activity using activated washed platelet from healthy donors (n = 3). We observed donor variability to the effect consistent with previous results on FVa cleavage activity. These differences might be due to normal variation in the biology of platelet activation or secretion of the platelet's own FVa, VWF, or PS, among other things.

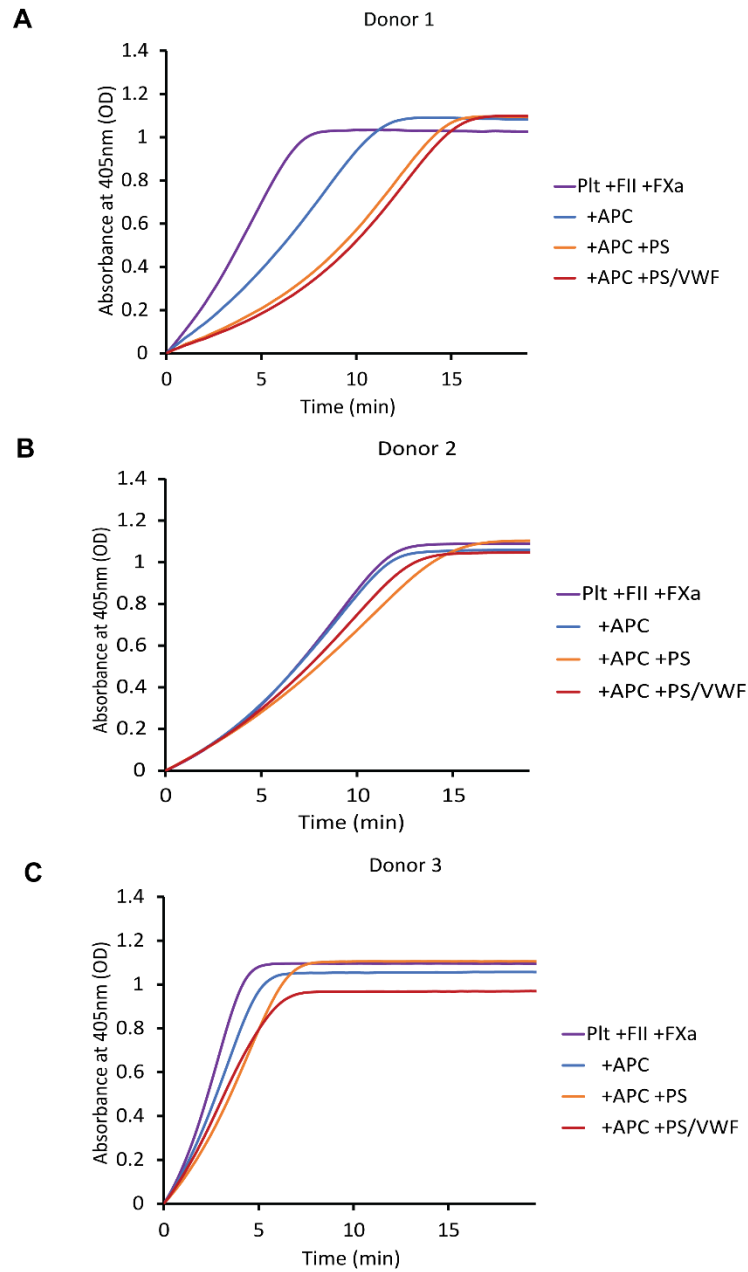


Figure 8.4. The effect of sheared VWF on APC/PS prothrombinase inhibition on platelet surface shows donor variability

Figure 8.4. The effect of sheared VWF on APC/PS prothrombinase inhibition on platelet surface shows donor variability

Prothrombinase activity was measured with a chromogenic thrombin generation assay in the presence or absence of 1 nM APC, 100 nM PS, or 10 $\mu\text{g}/\text{mL}$ VWF with shearing, incubated with 1.4 μM prothrombin (FII), $2 \times 10^8/\text{mL}$ activated washed platelet from three healthy human donors (A-C), initiated with 5 nM FXa and Spectrozyme TH.

Conclusions

Sheared VWF at least partially interferes with anticoagulant cofactor function of PS, significantly reversing TFPI α cofactor activity, suggesting a physiological relevance to the PS/VWF interaction. We continue to delineate these effects using various other modalities to gain more understanding regarding the role of PS/VWF interaction in circulation.

APPENDIX II. LONGITUDINAL OBSERVATIONS OF COVID-19 PATIENT STUDY

Introduction

Long COVID or Post-Acute Sequelae of COVID-19 (PASC) is a recognized long-term health problem affecting ~20-30% of COVID-19 survivors, in which post-acute symptoms including fatigue, shortness of breath, “brain fog,” chest pain, persistent loss of smell or taste, and various others, persist or arise months after the acute infection [168]. Viral persistence, autoimmunity, and persistent inflammation have been proposed as overlapping mechanisms that contribute to the pathogenesis of PASC [169], which we hypothesize to involve coagulation activation [314]. We are currently enrolling COVID-19 patients for longitudinal studies with approved IRB protocols. We aim to follow our patients longitudinally in order to evaluate coagulation parameters as well as the long-term thrombotic risk. Along with the laboratories of Drs. Whiteheart, Porterfield, and Garvy, we are part of the NIH RECOVER (Researching COVID-19 to Enhance Recovery Initiative) study, which separately recruits and follows COVID-19 patients in order to study the development and mechanisms of PASC. Through the VITAL (Virus-Induced Thrombosis Alliance), we have longitudinal cohorts of (1) ICU inpatients (n = 4) and outpatients (n = 10) who are observed at baseline and at 14, 28, and 40 days post-recruitment, and (2) healthy controls (n = 24) and outpatients (n = 25) who are observed at baseline and at 3, 6, and 12 months after. Here, preliminary data of these observations of the second cohort are shown. Outpatients in this cohort were mildly symptomatic PCR-test confirmed COVID-19 patients.

Results and discussion

1. Reduction in free PS recovers after three months, except in a subset of outpatients

We observed PS deficiency in a subset of outpatients at baseline, albeit the difference between groups not reaching significance. For the most part, this deficiency resolves at the 3-month follow up, except in a small subset of patients. This argues that acute inflammation is the main cause of PS deficiency.

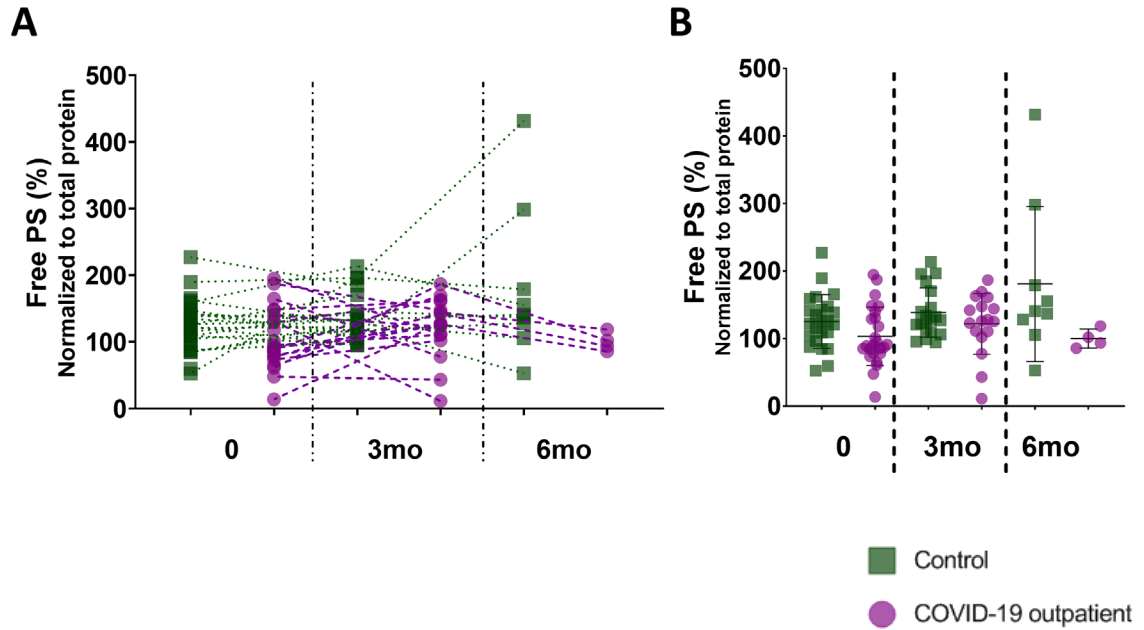


Figure 8.5. Longitudinal observation of free PS in COVID-19 outpatients

Free PS was measured with an ELISA in healthy controls (green square; $n = 24$) and COVID-19 outpatients (purple circle; $n = 25$) at baseline (0), 3 months (3mo), and 6 months (6mo) post recruitment. (A, B) Free PS measurements shown in a (A) before-after graph for every subject and (B) scatter dot graph of individual data points (error bar represents mean \pm SD). There is no statistical significance in the difference between groups at any time point. Every data point is an average of three measurements.

2. Elevation of the ETP ratio recovers after three months

We measured plasma thrombin generation using the fluorogenic calibrated automated thrombography and observed elevation of the endogenous thrombin potential (ETP) ratio in a subset of outpatients at baseline, albeit the difference between groups not reaching significance. The ratio of endogenous thrombin potential (ETP) values is defined as ETP with thrombomodulin (TM) divided by ETP without TM, in assays initiated with 4 μ M phospholipids and 1 μ M TF, with or without 20 nM TM supplementation. ETP ratio quantifies the contribution of APC/PS pathway activity in inhibiting thrombin generation, with higher ratio corresponding to lesser APC/PS pathway activity. We observed elevation of ETP ratio in several outpatients at baseline which, for the most part, resolves at the 3-month follow up, except in a small subset of patients. Due to a lack of clinical information, we could not explain the outlier controls at the 3-month time point. These data support the acute nature of COVID-19 immunothrombosis in the outpatients.

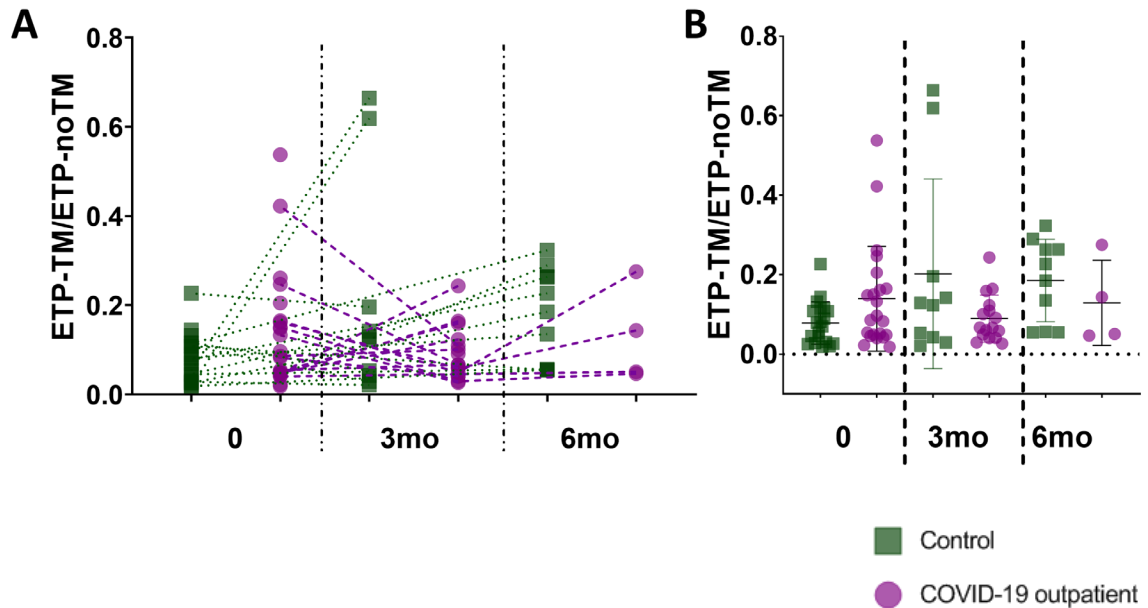


Figure 8.6. Longitudinal observation of ETP ratio in COVID-19 outpatients

Plasma thrombin generation is measured using fluorogenic substrate to thrombin according to the Calibrated Automated Thrombography (Thrombinoscope) method (Diagnostica Stago) in citrated plasma samples of healthy controls (green square; $n = 24$) and COVID-19 outpatients (purple circle; $n = 25$). (A,B) The ratio of endogenous thrombin potential (ETP) values, defined as ETP with thrombomodulin (TM) divided by ETP without TM, in assays initiated with $4 \mu\text{M}$ phospholipids and 1 pM TF, with or without 20 nM TM supplementation, shown in a (A) before-after graph for every subject and (B) scatter dot graph of individual data points (error bar represents mean \pm SD). There is no statistical significance in the difference between groups at any time point. Every data point is an average of three measurements.

Conclusions

Our preliminary data suggest that free PS deficiency and increased ETP ratio are observed at baseline in some COVID-19 outpatients compared to healthy controls. While both free PS deficiency and ETP ratio elevation resolve at the 3-month follow up, the former still persist in a subset of patients. We continue to observe our cohorts to up to a year post-infection to assess the coagulation and inflammatory changes and long term thrombotic risk, while also monitoring the development of long COVID symptoms.

REFERENCES

1. Palta, S., R. Saroa, and A. Palta, *Overview of the coagulation system*. Indian J Anaesth, 2014. 58(5): p. 515-23.
2. Heemskerk, J.W., E.M. Bevers, and T. Lindhout, *Platelet activation and blood coagulation*. Thromb Haemost, 2002. 88(2): p. 186-93.
3. Li, X., M.M.S. Sim, and J.P. Wood, *Recent Insights Into the Regulation of Coagulation and Thrombosis*. Arteriosclerosis, thrombosis, and vascular biology, 2020. 40(5): p. e119-e125.
4. Komiyama, Y., A. Pedersen, and W. Kisiel, *Proteolytic Activation of Human Factor IX and Factor X by Recombinant Human Factor VIII - Effects of Calcium, Phospholipids, and Tissue Factor*. Biochemistry, 1990. 29(40): p. 9418-9425.
5. Grover, S.P. and N. Mackman, *Intrinsic Pathway of Coagulation and Thrombosis*. Arteriosclerosis, Thrombosis, and Vascular Biology, 2019. 39(3): p. 331-338.
6. Barton, P.G., C.M. Jackson, and D.J. Hanahan, *Relationship between Factor V and Activated Factor X in the Generation of Prothrombinase*. Nature, 1967. 214(5091): p. 923-924.
7. Crawley, J.T.B., S. Zanardelli, C.K.N.K. Chion, and D.A. Lane, *The central role of thrombin in hemostasis*. Journal of Thrombosis and Haemostasis, 2007. 5(s1): p. 95-101.
8. Cesarman-Maus, G. and K.A. Hajjar, *Molecular mechanisms of fibrinolysis*. Br J Haematol, 2005. 129(3): p. 307-21.
9. Maroney, S.A., P.E. Ellery, J.P. Wood, J.P. Ferrel, N.D. Martinez, and A.E. Mast, *Comparison of the inhibitory activities of human tissue factor pathway inhibitor (TFPI) α and TFPI β* . Journal of Thrombosis and Haemostasis, 2013. 11(5): p. 911-918.
10. Wood, J.P., P. Ellery, S.A. Maroney, and A.E. Mast, *Biology of tissue factor pathway inhibitor*. Blood, 2014. 123(19): p. 2934-2943.
11. Hackeng, T.M., K.M. Seré, G. Tans, and J. Rosing, *Protein S Stimulates Inhibition of the Tissue Factor Pathway by Tissue Factor Pathway Inhibitor*. Proceedings of the National Academy of Sciences of the United States of America, 2006. 103(9): p. 3106-3111.
12. Wood, J.P., M.W. Bunce, S.A. Maroney, P.B. Tracy, R.M. Camire, and A.E. Mast, *Tissue factor pathway inhibitor-alpha inhibits prothrombinase during the initiation of blood coagulation*. Proceedings of the National Academy of Sciences of the United States of America, 2013. 110(44): p. 17838-17843.
13. Wood, J.P., M.W. Bunce, S.A. Maroney, P.B. Tracy, R.M. Camire, and A.E. Mast, *Tissue factor pathway inhibitor-alpha inhibits prothrombinase during the initiation of blood coagulation*. Proceedings of the National Academy of Sciences, 2013: p. 201310444.
14. Gierula, M. and J. Ahnström, *Anticoagulant protein S—New insights on interactions and functions*. Journal of Thrombosis and Haemostasis, 2020. 18(11): p. 2801-2811.

15. Peraramelli, S., S. Thomassen, A. Heinzmann, J. Rosing, T.M. Hackeng, R. Hartmann, F. Scheiflinger, and M. Dockal, *Inhibition of tissue factor:factor VIIa-catalyzed factor IX and factor X activation by TFPI and TFPI constructs*. *J Thromb Haemost*, 2014. 12(11): p. 1826-37.
16. Hamuro, T., Y. Kamikubo, Y. Nakahara, S. Miyamoto, and A. Funatsu, *Human recombinant tissue factor pathway inhibitor induces apoptosis in cultured human endothelial cells*. *FEBS Lett*, 1998. 421(3): p. 197-202.
17. Hembrough, T.A., G.M. Swartz, A. Papatthanassiu, G.P. Vlasuk, W.E. Rote, S.J. Green, and V.S. Pribluda, *Tissue factor/factor VIIa inhibitors block angiogenesis and tumor growth through a nonhemostatic mechanism*. *Cancer Res*, 2003. 63(11): p. 2997-3000.
18. Van De Wouwer, M.M., M.D. Collen, and M.E. Conway, *Thrombomodulin-Protein C-EPCR System: Integrated to Regulate Coagulation and Inflammation*. *Arteriosclerosis, Thrombosis, and Vascular Biology*, 2004. 24(8): p. 1374-1383.
19. Fuentes-Prior, P., Y. Iwanaga, R. Huber, R. Pagila, G. Rumennik, M. Seto, J. Morser, D.R. Light, and W. Bode, *Structural basis for the anticoagulant activity of the thrombin-thrombomodulin complex*. *Nature*, 2000. 404(6777): p. 518-25.
20. Gale, A.J., M.J. Heeb, and J.H. Griffin, *The autolysis loop of activated protein C interacts with factor Va and differentiates between the Arg506 and Arg306 cleavage sites*. *Blood*, 2000. 96(2): p. 585-93.
21. Gierula, M., C. Salles, II, S. Santamaria, A. Teraz-Orosz, J.T.B. Crawley, D.A. Lane, and J. Ahnström, *The roles of factor Va and protein S in formation of the activated protein C/protein S/factor Va inactivation complex*. *J Thromb Haemost*, 2019. 17(12): p. 2056-2068.
22. Norstrøm, E.A., S. Tran, M. Steen, and B. Dahlbäck, *Effects of factor Xa and protein S on the individual activated protein C-mediated cleavages of coagulation factor Va*. *J Biol Chem*, 2006. 281(42): p. 31486-94.
23. Wood, J.P., L.M. Baumann Kreuziger, P.E.R. Ellery, S.A. Maroney, and A.E. Mast, *Reduced Prothrombinase Inhibition by Tissue Factor Pathway Inhibitor Contributes to the Factor V Leiden Hypercoagulable State*. *Blood advances*, 2017. 1(6): p. 386-395.
24. Gale, A.J., T.J. Cramer, D. Rozenshteyn, and J.R. Cruz, *Detailed mechanisms of the inactivation of factor VIIIa by activated protein C in the presence of its cofactors, protein S and factor V*. *J Biol Chem*, 2008. 283(24): p. 16355-62.
25. Cramer, T.J., J.H. Griffin, and A.J. Gale, *Factor V is an anticoagulant cofactor for activated protein C during inactivation of factor Va*. *Pathophysiol Haemost Thromb*, 2010. 37(1): p. 17-23.
26. Shen, L. and B. Dahlbäck, *Factor V and protein S as synergistic cofactors to activated protein C in degradation of factor VIIIa*. *J Biol Chem*, 1994. 269(29): p. 18735-8.
27. D'Angelo, A., M.S. Lockhart, S.V. D'Angelo, and F.B. Taylor, Jr., *Protein S is a cofactor for activated protein C neutralization of an inhibitor of plasminogen activation released from platelets*. *Blood*, 1987. 69(1): p. 231-7.

28. Healy, L.D., J.A. Fernández, L.O. Mosnier, and J.H. Griffin, *Activated protein C and PAR1-derived and PAR3-derived peptides are anti-inflammatory by suppressing macrophage NLRP3 inflammasomes*. *J Thromb Haemost*, 2021. 19(1): p. 269-280.
29. Chattopadhyay, R., T. Sengupta, and R. Majumder, *Inhibition of intrinsic Xase by protein S: a novel regulatory role of protein S independent of activated protein C*. *Arterioscler Thromb Vasc Biol*, 2012. 32(10): p. 2387-93.
30. Chattopadhyay, R., T. Sengupta, and R. Majumder, *Inhibition of Intrinsic Xase by Protein S: A Novel Regulatory Role of Protein S Independent of Activated Protein C*. *Arteriosclerosis, Thrombosis, and Vascular Biology*, 2012. 32(10): p. 2387-2393.
31. Plautz, W.E., V.S. Sekhar Pilli, B.C. Cooley, R. Chattopadhyay, P.R. Westmark, T. Getz, D. Paul, W. Bergmeier, J.P. Sheehan, and R. Majumder, *Anticoagulant Protein S Targets the Factor IXa Heparin-Binding Exosite to Prevent Thrombosis*. *Arterioscler Thromb Vasc Biol*, 2018. 38(4): p. 816-828.
32. Olson, S.T. and I. Björk, *Regulation of thrombin activity by antithrombin and heparin*. *Semin Thromb Hemost*, 1994. 20(4): p. 373-409.
33. Perry, D.J., *Antithrombin and its inherited deficiencies*. *Blood Reviews*, 1994. 8(1): p. 37-55.
34. Broze, G.J., Jr. and J.P. Miletich, *Human Protein Z*. *J Clin Invest*, 1984. 73(4): p. 933-8.
35. Gacka, M.A., R. Małeckki, and R. Adamiec, *Participation of protein Z-dependent protease inhibitor and protein Z system in the pathomechanism of thrombotic complications*. *Int J Angiol*, 2010. 19(4): p. e120-5.
36. Di Scipio, R.G., M.A. Hermodson, S.G. Yates, and E.W. Davie, *A comparison of human prothrombin, factor IX (Christmas factor), factor X (Stuart factor), and protein S*. *Biochemistry*, 1977. 16(4): p. 698-706.
37. Majumder, R. and T. Nguyen, *Protein S: function, regulation, and clinical perspectives*. *Curr Opin Hematol*, 2021. 28(5): p. 339-344.
38. Pilli, V.S., W. Plautz, and R. Majumder, *The Journey of Protein S from an Anticoagulant to a Signaling Molecule*. *JSM Biochem Mol Biol*, 2016. 3(1).
39. Rigby, A.C. and M.A. Grant, *Protein S: a conduit between anticoagulation and inflammation*. *Crit Care Med*, 2004. 32(5 Suppl): p. S336-41.
40. Suleiman, L., C. Négrier, and H. Boukerche, *Protein S: A multifunctional anticoagulant vitamin K-dependent protein at the crossroads of coagulation, inflammation, angiogenesis, and cancer*. *Crit Rev Oncol Hematol*, 2013. 88(3): p. 637-54.
41. Dahlbäck, B., *The tale of protein S and C4b-binding protein, a story of affection*. *Thrombosis and haemostasis*, 2007. 98(1): p. 90-96.
42. Stavenuiter, F., N.F. Davis, E. Duan, A.J. Gale, and M.J. Heeb, *Platelet protein S directly inhibits procoagulant activity on platelets and microparticles*. *Thrombosis and haemostasis*, 2013. 109(2): p. 229-237.
43. Calzavarini, S., R. Prince-Eladnani, F. Saller, L. Bologna, L. Burnier, A.C. Brisset, C. Quarroz, M.D. Reina Caro, V. Ermolayev, Y. Matsumura, J.A. Fernández, T.M. Hackeng, J.H. Griffin, and A. Angelillo-Scherrer, *Platelet protein S limits venous but*

- not arterial thrombosis propensity by controlling coagulation in the thrombus.* Blood, 2020. 135(22): p. 1969-1982.
44. Schmidel, D.K., A.V. Tatro, L.G. Phelps, J.A. Tomczak, and G.L. Long, *Organization of the human protein S genes.* Biochemistry, 1990. 29(34): p. 7845-52.
 45. Furie, B., B.A. Bouchard, and B.C. Furie, *Vitamin K-dependent biosynthesis of gamma-carboxyglutamic acid.* Blood, 1999. 93(6): p. 1798-808.
 46. Walker, F.J., *Regulation of vitamin K-dependent protein S. Inactivation by thrombin.* J Biol Chem, 1984. 259(16): p. 10335-9.
 47. Dahlbäck, B., A. Lundwall, and J. Stenflo, *Localization of thrombin cleavage sites in the amino-terminal region of bovine protein S.* J Biol Chem, 1986. 261(11): p. 5111-5.
 48. Long, G.L., D. Lu, R.L. Xie, and M. Kalafatis, *Human protein S cleavage and inactivation by coagulation factor Xa.* J Biol Chem, 1998. 273(19): p. 11521-6.
 49. Stenberg, Y., S. Linse, T. Drakenberg, and J. Stenflo, *The high affinity calcium-binding sites in the epidermal growth factor module region of vitamin K-dependent protein S.* J Biol Chem, 1997. 272(37): p. 23255-60.
 50. Villoutreix, B.O., P. García de Frutos, M. Lövenklev, S. Linse, P. Fernlund, and B. Dahlbäck, *SHBG region of the anticoagulant cofactor protein S: secondary structure prediction, circular dichroism spectroscopy, and analysis of naturally occurring mutations.* Proteins, 1997. 29(4): p. 478-91.
 51. Lu, D., R.L. Xie, A. Rydzewski, and G.L. Long, *The effect of N-linked glycosylation on molecular weight, thrombin cleavage, and functional activity of human protein S.* Thromb Haemost, 1997. 77(6): p. 1156-63.
 52. Drakenberg, T., H. Ghasriani, E. Thulin, A.M. Thämlitz, A. Muranyi, A. Annala, and J. Stenflo, *Solution structure of the Ca²⁺-Binding EGF3-4 pair from vitamin K-dependent protein S: identification of an unusual fold in EGF3.* Biochemistry, 2005. 44(24): p. 8782-9.
 53. Sasaki, T., P.G. Knyazev, Y. Cheburkin, W. Göhring, D. Tisi, A. Ullrich, R. Timpl, and E. Hohenester, *Crystal structure of a C-terminal fragment of growth arrest-specific protein Gas6. Receptor tyrosine kinase activation by laminin G-like domains.* J Biol Chem, 2002. 277(46): p. 44164-70.
 54. Sanda, N., Y. Fujimori, T. Kashiwagi, A. Takagi, T. Murate, E. Mizutani, T. Matsushita, T. Naoe, and T. Kojima, *An Sp1 binding site mutation of the PROS1 promoter in a patient with protein S deficiency.* Br J Haematol, 2007. 138(5): p. 663-5.
 55. Suzuki, A., N. Sanda, Y. Miyawaki, Y. Fujimori, T. Yamada, A. Takagi, T. Murate, H. Saito, and T. Kojima, *Down-regulation of PROS1 gene expression by 17beta-estradiol via estrogen receptor alpha (ERalpha)-Sp1 interaction recruiting receptor-interacting protein 140 and the corepressor-HDAC3 complex.* J Biol Chem, 2010. 285(18): p. 13444-53.
 56. Lidegaard, Ø., I. Milsom, R.T. Geirsson, and F.E. Skjeldestad, *Hormonal contraception and venous thromboembolism.* Acta Obstet Gynecol Scand, 2012. 91(7): p. 769-78.

57. Hughes, Q., M. Watson, V. Cole, M. Sayer, R. Baker, and J. Staton, *Upregulation of protein S by progestins*. *J Thromb Haemost*, 2007. 5(11): p. 2243-9.
58. de Wolf, C.J., R.M. Cupers, R.M. Bertina, and H.L. Vos, *The constitutive expression of anticoagulant protein S is regulated through multiple binding sites for Sp1 and Sp3 transcription factors in the protein S gene promoter*. *J Biol Chem*, 2006. 281(26): p. 17635-43.
59. Tanaka, T., M. Narazaki, and T. Kishimoto, *IL-6 in inflammation, immunity, and disease*. *Cold Spring Harb Perspect Biol*, 2014. 6(10): p. a016295.
60. Pilli, V.S., A. Datta, S. Afreen, D. Catalano, G. Szabo, and R. Majumder, *Hypoxia downregulates protein S expression*. *Blood*, 2018. 132(4): p. 452-455.
61. Yasuma, T., Y. Yano, C.N. D'Alessandro-Gabazza, M. Toda, P. Gil-Bernabe, T. Kobayashi, K. Nishihama, J.A. Hinneh, R. Mifuji-Moroka, Z. Roen, J. Morser, I. Cann, I. Motoh, Y. Takei, and E.C. Gabazza, *Amelioration of Diabetes by Protein S*. *Diabetes*, 2016. 65(7): p. 1940-51.
62. Brinkman, H.J., K. Mertens, and J.A. van Mourik, *Proteolytic cleavage of protein S during the hemostatic response*. *J Thromb Haemost*, 2005. 3(12): p. 2712-20.
63. Andersson, H.M., M.J. Arantes, J.T. Crawley, B.M. Luken, S. Tran, B. Dahlbäck, D.A. Lane, and S.M. Rezende, *Activated protein C cofactor function of protein S: a critical role for Asp95 in the EGF1-like domain*. *Blood*, 2010. 115(23): p. 4878-85.
64. Mille-Baker, B., S.M. Rezende, R.E. Simmonds, P.J. Mason, D.A. Lane, and M.A. Laffan, *Deletion or replacement of the second EGF-like domain of protein S results in loss of APC cofactor activity*. *Blood*, 2003. 101(4): p. 1416-8.
65. He, X., L. Shen, and B. Dahlbäck, *Expression and functional characterization of chimeras between human and bovine vitamin-K-dependent protein-S-defining modules important for the species specificity of the activated protein C cofactor activity*. *Eur J Biochem*, 1995. 227(1-2): p. 433-40.
66. Evenäs, P., P. García de Frutos, G.A. Nicolaes, and B. Dahlbäck, *The second laminin G-type domain of protein S is indispensable for expression of full cofactor activity in activated protein C-catalysed inactivation of factor Va and factor VIIIa*. *Thromb Haemost*, 2000. 84(2): p. 271-7.
67. Nyberg, P., B. Dahlbäck, and P. García de Frutos, *The SHBG-like region of protein S is crucial for factor V-dependent APC-cofactor function*. *FEBS Lett*, 1998. 433(1-2): p. 28-32.
68. Heeb, M.J., R.M. Mesters, J.A. Fernández, T.M. Hackeng, R.K. Nakasone, and J.H. Griffin, *Plasma protein S residues 37-50 mediate its binding to factor Va and inhibition of blood coagulation*. *Thromb Haemost*, 2013. 110(2): p. 275-82.
69. Yegneswaran, S., T.M. Hackeng, P.E. Dawson, and J.H. Griffin, *The thrombin-sensitive region of protein S mediates phospholipid-dependent interaction with factor Xa*. *J Biol Chem*, 2008. 283(48): p. 33046-52.
70. Fernandes, N., L.O. Mosnier, L. Tonnu, and M.J. Heeb, *Zn²⁺-containing protein S inhibits extrinsic factor X-activating complex independently of tissue factor pathway inhibitor*. *J Thromb Haemost*, 2010. 8(9): p. 1976-85.

71. Evenäs, P., P. García De Frutos, S. Linse, and B. Dahlbäck, *Both G-type domains of protein S are required for the high-affinity interaction with C4b-binding protein*. Eur J Biochem, 1999. 266(3): p. 935-42.
72. Chatterjee, S., A. Sylvain, S. Pilli, W. Fant, D.R. Fricke, T. Watt, and R. Majumder, *Laminin G Domains of Protein S Bind and Inhibit FcγR1a*. Blood, 2019. 134: p. 3624.
73. Somajo, S., J. Ahnström, J. Fernandez-Recio, M. Gierula, B.O. Villoutreix, and B. Dahlbäck, *Amino acid residues in the laminin G domains of protein S involved in tissue factor pathway inhibitor interaction*. Thromb Haemost, 2015. 113(5): p. 976-87.
74. Teraz-Orosz, A., M. Gierula, A. Petri, D. Jones, R. Keniyopoullos, P.B. Folgado, S. Santamaria, J.T.B. Crawley, D.A. Lane, and J. Ahnström, *Laminin G1 residues of protein S mediate its TFPI cofactor function and are competitively regulated by C4BP*. Blood Adv, 2022. 6(2): p. 704-715.
75. Evenäs, P., B. Dahlbäck, and P. García de Frutos, *The first laminin G-type domain in the SHBG-like region of protein S contains residues essential for activation of the receptor tyrosine kinase sky*. Biol Chem, 2000. 381(3): p. 199-209.
76. Heeb, M.J., R.R. Koenen, J.A. Fernández, and T.M. Hackeng, *Direct anticoagulant activity of protein S-C4b binding protein complex in Heerlen heterozygotes and normals*. J Thromb Haemost, 2004. 2(10): p. 1766-73.
77. Rezende, S.M., R. Simmonds, and D. Lane, *Coagulation, inflammation, and apoptosis: different roles for protein S and the protein S-C4b binding protein complex*. Blood, 2004. 103(4): p. 1192-1201.
78. Reglińska-Matveyev, N., H.M. Andersson, S.M. Rezende, B. Dahlbäck, J.T. Crawley, D.A. Lane, and J. Ahnström, *TFPI cofactor function of protein S: essential role of the protein S SHBG-like domain*. Blood, 2014. 123(25): p. 3979-87.
79. Mahasandana, C., V. Suvatte, R.A. Marlar, M.J. Manco-Johnson, L.J. Jacobson, and W.E. Hathaway, *Neonatal purpura fulminans associated with homozygous protein S deficiency*. Lancet, 1990. 335(8680): p. 61-2.
80. Gandrille, S., D. Borgel, N. Sala, Y. Espinosa-Parrilla, R. Simmonds, S. Rezende, B. Lind, C. Mannhalter, I. Pabinger, P.H. Reitsma, C. Formstone, D.N. Cooper, H. Saito, K. Suzuki, F. Bernardi, et al., *Protein S deficiency: a database of mutations--summary of the first update*. Thromb Haemost, 2000. 84(5): p. 918.
81. Marlar, R.A. and J.N. Gausman, *Protein S abnormalities: A diagnostic nightmare*. American Journal of Hematology, 2011. 86(5): p. 418-21.
82. Mahasandana, C., G. Veerakul, V.S. Tanphaichitr, V. Suvatte, N. Opartkiattikul, and W.E. Hathaway, *Homozygous protein S deficiency: 7-year follow-up*. Thromb Haemost, 1996. 76(6): p. 1122.
83. Suchon, P., M. Germain, A. Delluc, D. Smadja, X. Jouven, B. Gyorgy, N. Saut, M. Ibrahim, J.F. Deleuze, M.C. Alessi, P.E. Morange, and D.A. Trégouët, *Protein S Heerlen mutation heterozygosity is associated with venous thrombosis risk*. Sci Rep, 2017. 7: p. 45507.
84. Hayashi, T., J. Nishioka, T. Shigekiyo, S. Saito, and K. Suzuki, *Protein S Tokushima: abnormal molecule with a substitution of Glu for Lys-155 in the second epidermal growth factor-like domain of protein S*. Blood, 1994. 83(3): p. 683-90.

85. ten Kate, M.K. and J. van der Meer, *Protein S deficiency: a clinical perspective*. Haemophilia, 2008. 14(6): p. 1222-8.
86. Adachi, T., *Protein S and congenital protein S deficiency: the most frequent congenital thrombophilia in Japanese*. Curr Drug Targets, 2005. 6(5): p. 585-92.
87. Ellery, P.E.R., I. Hilden, K. Sejling, M. Loftager, N.D. Martinez, S.A. Maroney, and A.E. Mast, *Correlates of plasma and platelet tissue factor pathway inhibitor, factor V, and Protein S*. Research and Practice in Thrombosis and Haemostasis, 2018. 2(1): p. 93-104.
88. Saller, F., A.C. Brisset, S.N. Tchaikovski, M. Azevedo, R. Chrast, J.A. Fernández, M. Schapira, T.M. Hackeng, J.H. Griffin, and A. Angelillo-Scherrer, *Generation and phenotypic analysis of protein S-deficient mice*. Blood, 2009. 114(11): p. 2307-14.
89. Angelillo-Scherrer, A., P. de Frutos, C. Aparicio, E. Melis, P. Savi, F. Lupu, J. Arnout, M. Dewerchin, M. Hoylaerts, J. Herbert, D. Collen, B. Dahlbäck, and P. Carmeliet, *Deficiency or inhibition of Gas6 causes platelet dysfunction and protects mice against thrombosis*. Nat Med, 2001. 7(2): p. 215-21.
90. Lu, Q. and G. Lemke, *Homeostatic regulation of the immune system by receptor tyrosine kinases of the Tyro 3 family*. Science, 2001. 293(5528): p. 306-11.
91. Jalbert, L.R., E.D. Rosen, L. Moons, J.C. Chan, P. Carmeliet, D. Collen, and F.J. Castellino, *Inactivation of the gene for anticoagulant protein C causes lethal perinatal consumptive coagulopathy in mice*. J Clin Invest, 1998. 102(8): p. 1481-8.
92. Huang, Z.F., D. Higuchi, N. Lasky, and G.J. Broze, Jr., *Tissue factor pathway inhibitor gene disruption produces intrauterine lethality in mice*. Blood, 1997. 90(3): p. 944-51.
93. Dahlbäck, B. and J. Stenflo, *High molecular weight complex in human plasma between vitamin K-dependent protein S and complement component C4b-binding protein*. Proc Natl Acad Sci U S A, 1981. 78(4): p. 2512-6.
94. Carlsson, S. and B. Dahlbäck, *Dependence on vitamin K-dependent protein S for eukaryotic cell secretion of the beta-chain of C4b-binding protein*. J Biol Chem, 2010. 285(42): p. 32038-46.
95. Dahlbäck, B., *Protein S and C4b-binding protein: components involved in the regulation of the protein C anticoagulant system*. Thromb Haemost, 1991. 66(1): p. 49-61.
96. García de Frutos, P., R.I. Alim, Y. Härdig, B. Zöller, and B. Dahlbäck, *Differential regulation of alpha and beta chains of C4b-binding protein during acute-phase response resulting in stable plasma levels of free anticoagulant protein S*. Blood, 1994. 84(3): p. 815-822.
97. Webb, J.H., A.M. Blom, and B. Dahlbäck, *Vitamin K-dependent protein S localizing complement regulator C4b-binding protein to the surface of apoptotic cells*. J Immunol, 2002. 169(5): p. 2580-6.
98. Furmaniak-Kazmierczak, E., C.Y. Hu, and C.T. Esmon, *Protein S enhances C4b binding protein interaction with neutrophils*. Blood, 1993. 81(2): p. 405-411.

99. Kask, L., L.A. Trouw, B. Dahlbäck, and A.M. Blom, *The C4b-binding protein-protein S complex inhibits the phagocytosis of apoptotic cells*. J Biol Chem, 2004. 279(23): p. 23869-73.
100. Trouw, L.A., S.C. Nilsson, I. Gonçalves, G. Landberg, and A.M. Blom, *C4b-binding protein binds to necrotic cells and DNA, limiting DNA release and inhibiting complement activation*. J Exp Med, 2005. 201(12): p. 1937-48.
101. van der Meer, J.H.M., T. van der Poll, and C. van 't Veer, *TAM receptors, Gas6, and protein S: roles in inflammation and hemostasis*. Blood, 2014. 123(16): p. 2460-2469.
102. Tsou, W.I., K.Q. Nguyen, D.A. Calarese, S.J. Garforth, A.L. Antes, S.V. Smirnov, S.C. Almo, R.B. Birge, and S.V. Kotenko, *Receptor tyrosine kinases, TYRO3, AXL, and MER, demonstrate distinct patterns and complex regulation of ligand-induced activation*. J Biol Chem, 2014. 289(37): p. 25750-63.
103. Fraineau, S., A. Monvoisin, J. Clarhaut, J. Talbot, C. Simonneau, C. Kanthou, S.M. Kanse, M. Philippe, and O. Benzakour, *The vitamin K-dependent anticoagulant factor, protein S, inhibits multiple VEGF-A-induced angiogenesis events in a Mer- and SHP2-dependent manner*. Blood, 2012. 120(25): p. 5073-83.
104. Che Mat, M.F., N.A. Abdul Murad, K. Ibrahim, N. Mohd Mokhtar, W.Z. Wan Ngah, R. Harun, and R. Jamal, *Silencing of PROS1 induces apoptosis and inhibits migration and invasion of glioblastoma multiforme cells*. Int J Oncol, 2016. 49(6): p. 2359-2366.
105. Gadiyar, V., G. Patel, and V. Davra, *Immunological role of TAM receptors in the cancer microenvironment*. Int Rev Cell Mol Biol, 2020. 357: p. 57-79.
106. Ginisty, A., L. Oliver, P. Arnault, F. Vallette, O. Benzakour, and V. Coronas, *The vitamin K-dependent factor, protein S, regulates brain neural stem cell migration and phagocytic activities towards glioma cells*. Eur J Pharmacol, 2019. 855: p. 30-39.
107. Elliott, M.R., K.M. Koster, and P.S. Murphy, *Efferocytosis Signaling in the Regulation of Macrophage Inflammatory Responses*. Journal of immunology (Baltimore, Md. : 1950), 2017. 198(4): p. 1387-1394.
108. Dransfield, I., A. Zagórska, E.D. Lew, K. Michail, and G. Lemke, *Mer receptor tyrosine kinase mediates both tethering and phagocytosis of apoptotic cells*. Cell Death Dis, 2015. 6(2): p. e1646.
109. Al Kafri, N. and S. Hafizi, *Tumour-Secreted Protein S (ProS1) Activates a Tyro3-Erk Signalling Axis and Protects Cancer Cells from Apoptosis*. Cancers, 2019. 11(12): p. 1843.
110. Jiang, L., X.Q. Chen, M.J. Gao, W. Lee, J. Zhou, Y.F. Zhao, and G.D. Wang, *The Pros1/Tyro3 axis protects against periodontitis by modulating STAT/SOCS signalling*. J Cell Mol Med, 2019. 23(4): p. 2769-2781.
111. Wang, X., A. Malawista, F. Qian, C. Ramsey, H.G. Allore, and R.R. Montgomery, *Age-related changes in expression and signaling of TAM receptor inflammatory regulators in monocytes*. Oncotarget, 2018. 9(11): p. 9572-9580.
112. Lumbroso, D., S. Soboh, A. Maimon, S. Schif-Zuck, A. Ariel, and T. Burstyn-Cohen, *Macrophage-Derived Protein S Facilitates Apoptotic Polymorphonuclear Cell*

- Clearance by Resolution Phase Macrophages and Supports Their Reprogramming.* Front Immunol, 2018. 9: p. 358.
113. Ubil, E., L. Caskey, A. Holtzhausen, D. Hunter, C. Story, and H.S. Earp, *Tumor-secreted Pros1 inhibits macrophage M1 polarization to reduce antitumor immune response.* J Clin Invest, 2018. 128(6): p. 2356-2369.
 114. Rothlin, C.V., S. Ghosh, E.I. Zuniga, M.B. Oldstone, and G. Lemke, *TAM receptors are pleiotropic inhibitors of the innate immune response.* Cell, 2007. 131(6): p. 1124-36.
 115. Lumbroso, D., S. Soboh, A. Maimon, S. Schif-Zuck, A. Ariel, and T. Burstyn-Cohen, *Macrophage-Derived Protein S Facilitates Apoptotic Polymorphonuclear Cell Clearance by Resolution Phase Macrophages and Supports Their Reprogramming.* Frontiers in immunology, 2018. 9: p. 358-358.
 116. Nepal, S., C. Tirupathi, Y. Tsukasaki, J. Farahany, M. Mittal, J. Rehman, D.J. Prockop, and A.B. Malik, *STAT6 induces expression of Gas6 in macrophages to clear apoptotic neutrophils and resolve inflammation.* Proceedings of the National Academy of Sciences of the United States of America, 2019. 116(33): p. 16513-16518.
 117. Carrera Silva, E.A., P.Y. Chan, L. Joannas, A.E. Errasti, N. Gagliani, L. Bosurgi, M. Jabbour, A. Perry, F. Smith-Chakmakova, D. Mucida, H. Cheroutre, T. Burstyn-Cohen, J.A. Leighton, G. Lemke, S. Ghosh, et al., *T cell-derived protein S engages TAM receptor signaling in dendritic cells to control the magnitude of the immune response.* Immunity, 2013. 39(1): p. 160-70.
 118. Chua, B.A., J.A. Ngo, K. Situ, C.M. Ramirez, H. Nakano, and K. Morizono, *Protein S and Gas6 induce efferocytosis of HIV-1-infected cells.* Virology, 2018. 515: p. 176-190.
 119. Ghosh Roy, S., *Chapter Five - TAM receptors: A phosphatidylserine receptor family and its implications in viral infections,* in *International Review of Cell and Molecular Biology*, V. Davra and L. Galluzzi, Editors. 2020, Academic Press. p. 81-122.
 120. Wang, Z.Y., P.G. Wang, and J. An, *The Multifaceted Roles of TAM Receptors during Viral Infection.* Virol Sin, 2021. 36(1): p. 1-12.
 121. Meertens, L., X. Carnec, M.P. Lecoin, R. Ramdasi, F. Guivel-Benhassine, E. Lew, G. Lemke, O. Schwartz, and A. Amara, *The TIM and TAM families of phosphatidylserine receptors mediate dengue virus entry.* Cell Host Microbe, 2012. 12(4): p. 544-57.
 122. Morizono, K., Y. Xie, T. Olafsen, B. Lee, A. Dasgupta, A.M. Wu, and I.S. Chen, *The soluble serum protein Gas6 bridges virion envelope phosphatidylserine to the TAM receptor tyrosine kinase Axl to mediate viral entry.* Cell Host Microbe, 2011. 9(4): p. 286-98.
 123. Miner, J.J., B.P. Daniels, B. Shrestha, J.L. Proenca-Modena, E.D. Lew, H.M. Lazear, M.J. Gorman, G. Lemke, R.S. Klein, and M.S. Diamond, *The TAM receptor Mertk protects against neuroinvasive viral infection by maintaining blood-brain barrier integrity.* Nat Med, 2015. 21(12): p. 1464-72.
 124. Giesen, P.L., U. Rauch, B. Bohrmann, D. Kling, M. Roqué, J.T. Fallon, J.J. Badimon, J. Himber, M.A. Riederer, and Y. Nemerson, *Blood-borne tissue factor: another*

- view of thrombosis*. Proceedings of the National Academy of Sciences of the United States of America, 1999. 96(5): p. 2311-2315.
125. Long, A.T., E. Kenne, R. Jung, T.A. Fuchs, and T. Renné, *Contact system revisited: an interface between inflammation, coagulation, and innate immunity*. J Thromb Haemost, 2016. 14(3): p. 427-37.
 126. Amara, U., M.A. Flierl, D. Rittirsch, A. Klos, H. Chen, B. Acker, U.B. Brückner, B. Nilsson, F. Gebhard, J.D. Lambris, and M. Huber-Lang, *Molecular intercommunication between the complement and coagulation systems*. J Immunol, 2010. 185(9): p. 5628-36.
 127. Brinkmann, V., U. Reichard, C. Goosmann, B. Fauler, Y. Uhlemann, D.S. Weiss, Y. Weinrauch, and A. Zychlinsky, *Neutrophil extracellular traps kill bacteria*. Science, 2004. 303(5663): p. 1532-5.
 128. Fuchs, T.A., A.A. Bhandari, and D.D. Wagner, *Histones induce rapid and profound thrombocytopenia in mice*. Blood, 2011. 118(13): p. 3708-14.
 129. Ammollo, C.T., F. Semeraro, J. Xu, N.L. Esmon, and C.T. Esmon, *Extracellular histones increase plasma thrombin generation by impairing thrombomodulin-dependent protein C activation*. J Thromb Haemost, 2011. 9(9): p. 1795-803.
 130. Medzhitov, R., P. Preston-Hurlburt, and C.A. Janeway, Jr., *A human homologue of the Drosophila Toll protein signals activation of adaptive immunity*. Nature, 1997. 388(6640): p. 394-7.
 131. Kawai, T. and S. Akira, *TLR signaling*. Semin Immunol, 2007. 19(1): p. 24-32.
 132. Ardoin, S.P., J.C. Shanahan, and D.S. Pisetsky, *The role of microparticles in inflammation and thrombosis*. Scand J Immunol, 2007. 66(2-3): p. 159-65.
 133. Fauci, A.S., G. Pantaleo, S. Stanley, and D. Weissman, *Immunopathogenic mechanisms of HIV infection*. Ann Intern Med, 1996. 124(7): p. 654-63.
 134. Deeks, S.G., S.R. Lewin, and D.V. Havlir, *The end of AIDS: HIV infection as a chronic disease*. Lancet, 2013. 382(9903): p. 1525-33.
 135. Jensen, B.-E.O., E. Knops, L. Cords, N. Lübke, M. Salgado, K. Busman-Sahay, J.D. Estes, L.E.P. Huyvoneers, F. Perdomo-Celis, M. Wittner, C. Gálvez, C. Mummert, C. Passaes, J.M. Eberhard, C. Münk, et al., *In-depth virological and immunological characterization of HIV-1 cure after CCR5Δ32/Δ32 allogeneic hematopoietic stem cell transplantation*. Nature Medicine, 2023.
 136. CDC. *HIV Surveillance Report: International Statistics*. 2019 April 12, 2019 [cited 2019 October 29]; Available from: <https://www.cdc.gov/hiv/statistics/overview/index.html>.
 137. May, T.M., T.M. Gompels, T.V. Delpech, T.K. Porter, T.C. Orkin, T.S. Kegg, T.P. Hay, T.M. Johnson, T.A. Palfreeman, T.R. Gilson, T.D. Chadwick, T.F. Martin, T.T. Hill, T.J. Walsh, T.F. Post, et al., *Impact on life expectancy of HIV-1 positive individuals of CD4+ cell count and viral load response to antiretroviral therapy*. AIDS, 2014. 28(8): p. 1193-1202.
 138. De Socio, G.V., G. Pucci, F. Baldelli, and G. Schillaci, *Observed versus predicted cardiovascular events and all-cause death in HIV infection: a longitudinal cohort study*. BMC infectious diseases, 2017. 17(1): p. 414-414.

139. Lijfering, W.M., H.G. Sprenger, R.R. Georg, P.A. Van Der Meulen, and J. Van Der Meer, *Relationship between progression to AIDS and thrombophilic abnormalities in HIV infection*. *Clinical Chemistry*, 2008. 54(7): p. 1226-1233.
140. Lijfering, W.M., M.K. Ten Kate, H.G. Sprenger, and J. Van Der Meer, *Absolute risk of venous and arterial thrombosis in HIV-infected patients and effects of combination antiretroviral therapy*. *Journal of thrombosis and haemostasis*, 2006. 4(9): p. 1928-1930.
141. Shen, Y.-M.P. and E.P. Frenkel, *Thrombosis and a hypercoagulable state in HIV-infected patients*. *Clinical and applied thrombosis/hemostasis : official journal of the International Academy of Clinical and Applied Thrombosis/Hemostasis*, 2004. 10(3): p. 277-280.
142. Brummel-Ziedins, K.E., M. Gissel, J. Neuhaus, Á.H. Borges, D.R. Chadwick, S. Emery, J.D. Neaton, R.P. Tracy, and J.V. Baker, *In silico thrombin generation: Plasma composition imbalance and mortality in human immunodeficiency virus*. *Research and Practice in Thrombosis and Haemostasis*, 2018. 2(4): p. 708-717.
143. Bibas, M., G. Biava, and A. Antinori, *HIV-Associated Venous Thromboembolism*. *Mediterr J Hematol Infect Dis*, 2011. 3(1): p. e2011030.
144. David, C.R., B. Myriam, A. Daniel, I. Uchenna, and G. Matthew Bidwell, *Association between Protease Inhibitor Use and Increased Cardiovascular Risk in Patients Infected with Human Immunodeficiency Virus: A Systematic Review*. *Clinical Infectious Diseases*, 2003. 37(7): p. 959-972.
145. Loelius, S.G., K.L. Lannan, N. Blumberg, R.P. Phipps, and S.L. Spinelli, *The HIV protease inhibitor, ritonavir, dysregulates human platelet function in vitro*. *Thrombosis Research*, 2018. 169: p. 96-104.
146. Alvarez, A., C. Rios-Navarro, M.A. Blanch-Ruiz, V. Collado-Diaz, I. Andujar, M.A. Martinez-Cuesta, S. Orden, and J.V. Esplugues, *Abacavir induces platelet-endothelium interactions by interfering with purinergic signalling: A step from inflammation to thrombosis*. *Antiviral Research*, 2017. 141: p. 179-185.
147. Khare, S., R. Kushwaha, A. Kumar, V. Venkatesh, H. Reddy, M. Jain, M. Yusuf, and U. Singh, *Prothrombotic state in HIV: A study on protein C, protein S, homocysteine and correlation with CD4 counts*. *Indian Journal of Medical Microbiology*, 2018. 36(2): p. 201-206.
148. Hassell, K.L., D.C. Kressin, A. Neumann, R. Ellison, and R.A. Marlar, *Correlation of antiphospholipid antibodies and protein S deficiency with thrombosis in HIV-infected men*. *Blood coagulation & fibrinolysis : an international journal in haemostasis and thrombosis*, 1994. 5(4): p. 455-462.
149. Sugerman, R., J. Church, J. Goldsmith, and G. Ens, *Acquired protein S deficiency in children infected with human immunodeficiency virus*. *Pediatric Infectious Disease Journal*, 1996. 15(2): p. 106-111.
150. Saif, M.W. and B. Greenberg, *HIV and thrombosis: a review*. *AIDS patient care and STDs*, 2001. 15(1): p. 15-24.
151. Funderburg, N.T., E. Mayne, S. Sieg, R. Asaad, W. Jiang, M. Kalinowska, A.A. Luciano, W. Stevens, B. Rodriguez, J. Brenchley, D.C. Douek, and M.M. Lederman, *Increased tissue factor expression on circulating monocytes in chronic HIV*

- infection: relationship to in vivo coagulation and immune activation.* Blood, 2010. 115: p. 161-167.
152. Muller, I., A. Klocke, M. Alex, M. Kotsch, T. Luther, E. Morgenstern, S. Zieseniss, S. Zahler, K. Preissner, and B. Engelmann, *Intravascular tissue factor initiates coagulation via circulating microvesicles and platelets.* FASEB Journal, 2003. 17(1).
 153. Zhu, N., D. Zhang, W. Wang, X. Li, B. Yang, J. Song, X. Zhao, B. Huang, W. Shi, R. Lu, P. Niu, F. Zhan, X. Ma, D. Wang, W. Xu, et al., *A Novel Coronavirus from Patients with Pneumonia in China, 2019.* N Engl J Med, 2020. 382(8): p. 727-733.
 154. Yesudhas, D., A. Srivastava, and M.M. Gromiha, *COVID-19 outbreak: history, mechanism, transmission, structural studies and therapeutics.* Infection, 2021. 49(2): p. 199-213.
 155. Cui, S., S. Chen, X. Li, S. Liu, and F. Wang, *Prevalence of venous thromboembolism in patients with severe novel coronavirus pneumonia.* J Thromb Haemost, 2020. 18(6): p. 1421-1424.
 156. Tang, N., D. Li, X. Wang, and Z. Sun, *Abnormal coagulation parameters are associated with poor prognosis in patients with novel coronavirus pneumonia.* J Thromb Haemost, 2020. 18(4): p. 844-847.
 157. Jiménez, D., A. García-Sánchez, P. Rali, A. Muriel, B. Bikdeli, P. Ruiz-Artacho, R. Le Mao, C. Rodríguez, B.J. Hunt, and M. Monreal, *Incidence of VTE and Bleeding Among Hospitalized Patients With Coronavirus Disease 2019: A Systematic Review and Meta-analysis.* Chest, 2021. 159(3): p. 1182-1196.
 158. Zhang, C., L. Shen, K.J. Le, M.M. Pan, L.C. Kong, Z.C. Gu, H. Xu, Z. Zhang, W.H. Ge, and H.W. Lin, *Incidence of Venous Thromboembolism in Hospitalized Coronavirus Disease 2019 Patients: A Systematic Review and Meta-Analysis.* Front Cardiovasc Med, 2020. 7: p. 151.
 159. Boonyawat, K., P. Chantrathammachart, P. Numthavaj, N. Nanthatanti, S. Phusanti, A. Phuphuakrat, P. Niparuck, and P. Angchaisuksiri, *Incidence of thromboembolism in patients with COVID-19: a systematic review and meta-analysis.* Thrombosis Journal, 2020. 18(1): p. 34.
 160. Conway, E.M., N. Mackman, R.Q. Warren, A.S. Wolberg, L.O. Mosnier, R.A. Campbell, L.E. Gralinski, M.T. Rondina, F.L. van de Veerdonk, K.M. Hoffmeister, J.H. Griffin, D. Nugent, K. Moon, and J.H. Morrissey, *Understanding COVID-19-associated coagulopathy.* Nature Reviews Immunology, 2022. 22(10): p. 639-649.
 161. Tang, N., D. Li, X. Wang, and Z. Sun, *Abnormal coagulation parameters are associated with poor prognosis in patients with novel coronavirus pneumonia.* Journal of thrombosis and haemostasis, 2020. 18(4): p. 844-847.
 162. Skendros, P., A. Mitsios, A. Chrysanthopoulou, D.C. Mastellos, S. Metallidis, P. Rafailidis, M. Ntinopoulou, E. Sertaridou, V. Tsironidou, C. Tsigalou, M. Tektonidou, T. Konstantinidis, C. Papagoras, I. Mitroulis, G. Germanidis, et al., *Complement and tissue factor-enriched neutrophil extracellular traps are key drivers in COVID-19 immunothrombosis.* J Clin Invest, 2020. 130(11): p. 6151-6157.
 163. Hottz, E.D., I.G. Azevedo-Quintanilha, L. Palhinha, L. Teixeira, E.A. Barreto, C.R.R. Pão, C. Righy, S. Franco, T.M.L. Souza, P. Kurtz, F.A. Bozza, and P.T. Bozza, *Platelet*

- activation and platelet-monocyte aggregate formation trigger tissue factor expression in patients with severe COVID-19.* Blood, 2020. 136(11): p. 1330-1341.
164. van de Veerdonk, F.L., M.G. Netea, M. van Deuren, J.W. van der Meer, Q. de Mast, R.J. Brüggemann, and H. van der Hoeven, *Kallikrein-kinin blockade in patients with COVID-19 to prevent acute respiratory distress syndrome.* Elife, 2020. 9.
165. Bayrakci, N., G. Ozkan, L.C. Mutlu, L. Erdem, I. Yildirim, D. Gulen, and A. Celikkol, *Relationship between serum soluble endothelial protein C receptor level and COVID-19 findings.* Blood Coagul Fibrinolysis, 2021. 32(8): p. 550-555.
166. Francischetti, I.M.B., K. Toomer, Y. Zhang, J. Jani, Z. Siddiqui, D.J. Brotman, J.E. Hooper, and T.S. Kickler, *Upregulation of pulmonary tissue factor, loss of thrombomodulin and immunothrombosis in SARS-CoV-2 infection.* EClinicalMedicine, 2021. 39: p. 101069.
167. Juneja, G.K., M. Castelo, C.H. Yeh, S.E. Cerroni, B.E. Hansen, J.E. Chessum, J. Abraham, E. Cani, D.J. Dwivedi, D.D. Fraser, M. Slessarev, C. Martin, S. McGilvray, P.L. Gross, P.C. Liaw, et al., *Biomarkers of coagulation, endothelial function, and fibrinolysis in critically ill patients with COVID-19: A single-center prospective longitudinal study.* J Thromb Haemost, 2021. 19(6): p. 1546-1557.
168. Xie, Y., B. Bowe, and Z. Al-Aly, *Burdens of post-acute sequelae of COVID-19 by severity of acute infection, demographics and health status.* Nature Communications, 2021. 12(1): p. 6571.
169. Mehandru, S. and M. Merad, *Pathological sequelae of long-haul COVID.* Nature Immunology, 2022. 23(2): p. 194-202.
170. Capizzi, A., J. Woo, and M. Verduzco-Gutierrez, *Traumatic Brain Injury: An Overview of Epidemiology, Pathophysiology, and Medical Management.* Medical Clinics of North America, 2020. 104(2): p. 213-238.
171. Park, E., J.D. Bell, and A.J. Baker, *Traumatic brain injury: can the consequences be stopped?* Cmaj, 2008. 178(9): p. 1163-70.
172. Lazaridis, C., C.G. Rusin, and C.S. Robertson, *Secondary brain injury: Predicting and preventing insults.* Neuropharmacology, 2019. 145: p. 145-152.
173. Hubbard, W.B., J.F. Dong, M.A. Cruz, and R.E. Rumbaut, *Links between thrombosis and inflammation in traumatic brain injury.* Thromb Res, 2021. 198: p. 62-71.
174. Zhang, J., F. Zhang, and J.-f. Dong, *Coagulopathy induced by traumatic brain injury: systemic manifestation of a localized injury.* Blood, 2018. 131(18): p. 2001-2006.
175. Stein, S.C. and D.H. Smith, *Coagulopathy in traumatic brain injury.* Neurocrit Care, 2004. 1(4): p. 479-88.
176. Moore, E.E., H.B. Moore, L.Z. Kornblith, M.D. Neal, M. Hoffman, N.J. Mutch, H. Schöchl, B.J. Hunt, and A. Sauaia, *Trauma-induced coagulopathy.* Nature Reviews Disease Primers, 2021. 7(1): p. 30.
177. Laroche, M., M.E. Kutcher, M.C. Huang, M.J. Cohen, and G.T. Manley, *Coagulopathy after traumatic brain injury.* Neurosurgery, 2012. 70(6): p. 1334-45.
178. Hulka, F., R.J. Mullins, and E.H. Frank, *Blunt brain injury activates the coagulation process.* Arch Surg, 1996. 131(9): p. 923-7; discussion 927-8.
179. Reiff, D.A., R.N. Haricharan, N.M. Bullington, R.L. Griffin, G. McGwin, Jr., and L.W. Rue, 3rd, *Traumatic brain injury is associated with the development of deep vein*

- thrombosis independent of pharmacological prophylaxis.* J Trauma, 2009. 66(5): p. 1436-40.
180. Greuters, S., A. van den Berg, G. Franschman, V.A. Viersen, A. Beishuizen, S.M. Peerdeman, C. Boer, and A.-B. investigators, *Acute and delayed mild coagulopathy are related to outcome in patients with isolated traumatic brain injury.* Critical Care, 2011. 15(1): p. R2.
 181. Oosting, J.D., R.H. Derksen, I.W. Bobbink, T.M. Hackeng, B.N. Bouma, and P.G. de Groot, *Antiphospholipid antibodies directed against a combination of phospholipids with prothrombin, protein C, or protein S: an explanation for their pathogenic mechanism?* Blood, 1993. 81(10): p. 2618-25.
 182. Recarte-Pelz, P., D. Tàssies, G. Espinosa, B. Hurtado, N. Sala, R. Cervera, J.C. Reverter, and P.G. de Frutos, *Vitamin K-dependent proteins GAS6 and Protein S and TAM receptors in patients of systemic lupus erythematosus: correlation with common genetic variants and disease activity.* Arthritis Res Ther, 2013. 15(2): p. R41.
 183. Suh, C.H., B. Hilliard, S. Li, J.T. Merrill, and P.L. Cohen, *TAM receptor ligands in lupus: protein S but not Gas6 levels reflect disease activity in systemic lupus erythematosus.* Arthritis Res Ther, 2010. 12(4): p. R146.
 184. Stahl, C.P., C.S. Wideman, T.J. Spira, E.C. Haff, G.J. Hixon, and B.L. Evatt, *Protein S deficiency in men with long-term human immunodeficiency virus infection.* Blood, 1993. 81(7): p. 1801-7.
 185. Bissuel, F., M. Berruyer, X. Causse, M. Dechavanne, and C. Trepo, *Acquired protein S deficiency: correlation with advanced disease in HIV-1-infected patients.* J Acquir Immune Defic Syndr (1988), 1992. 5(5): p. 484-9.
 186. Sim, M.M.S., M. Banerjee, T. Myint, B.A. Garvy, S.W. Whiteheart, and J.P. Wood, *Total Plasma Protein S Is a Prothrombotic Marker in People Living With HIV.* JAIDS Journal of Acquired Immune Deficiency Syndromes, 2022. 90(4).
 187. Nguyễn, P., J. Reynaud, P. Pouzol, M. Munzer, O. Richard, and P. François, *Varicella and thrombotic complications associated with transient protein C and protein S deficiencies in children.* Eur J Pediatr, 1994. 153(9): p. 646-9.
 188. Wills, B.A., E.E. Oragui, A.C. Stephens, O.A. Daramola, N.M. Dung, H.T. Loan, N.V. Chau, M. Chambers, K. Stepniewska, J.J. Farrar, and M. Levin, *Coagulation Abnormalities in Dengue Hemorrhagic Fever: Serial Investigations in 167 Vietnamese Children with Dengue Shock Syndrome.* Clinical Infectious Diseases, 2002. 35(3): p. 277-285.
 189. Stoichitoiu, L.E., L. Pinte, M.I. Balea, V. Nedelcu, C. Badea, and C. Baicus, *Anticoagulant protein S in COVID-19: low activity, and associated with outcome.* Rom J Intern Med, 2020. 58(4): p. 251-258.
 190. Baicus, C., L.E. Stoichitoiu, L. Pinte, and C. Badea, *Anticoagulant Protein S in COVID-19: The Low Activity Level Is Probably Secondary.* Am J Ther, 2021. 28(1): p. e139-e140.
 191. Bello, F.O., A.S. Akanmu, T.A. Adeyemo, B.M. Idowu, P. Okonkwo, and P.J. Kanki, *Derangement of protein S and C4b-binding protein levels as acquired*

- thrombophilia in HIV-infected adult Nigerians*. South Afr J HIV Med, 2021. 22(1): p. 1253.
192. Ferrari, E., B. Sartre, F. Squara, J. Contenti, C. Ocelli, F. Lemoel, J. Levraut, D. Doyen, J. Dellamonica, V. Mondain, D. Chirio, K. Risso, E. Cua, J.C. Orban, C. Ichai, et al., *High Prevalence of Acquired Thrombophilia Without Prognosis Value in Patients With Coronavirus Disease 2019*. J Am Heart Assoc, 2020. 9(21): p. e017773.
193. Ali, L., H. Jamoussi, N. Kouki, S. Fray, S. Echebbi, N. Ben Ali, and M. Fredj, *COVID-19 Infection and Recurrent Stroke in Young Patients With Protein S Deficiency: A Case Report*. Neurologist, 2021. 26(6): p. 276-280.
194. Lemke, G. and G.J. Silverman, *Blood clots and TAM receptor signalling in COVID-19 pathogenesis*. Nat Rev Immunol, 2020. 20(7): p. 395-396.
195. Martín-Rojas, R.M., G. Pérez-Rus, V.E. Delgado-Pinos, A. Domingo-González, I. Regalado-Artamendi, N. Alba-Urdiales, P. Demelo-Rodríguez, S. Monsalvo, G. Rodríguez-Macías, M. Ballesteros, S. Osorio-Prendes, J.L. Díez-Martín, and C. Pascual Izquierdo, *COVID-19 coagulopathy: An in-depth analysis of the coagulation system*. European Journal of Haematology, 2020. 105(6): p. 741-750.
196. Voicu, S., M. Delrue, B.G. Chousterman, A. Stépanian, P. Bonnin, I. Malissin, N. Deye, M. Neuwirth, C. Ketfi, A. Mebazaa, V. Siguret, and B. Mégarbane, *Imbalance between procoagulant factors and natural coagulation inhibitors contributes to hypercoagulability in the critically ill COVID-19 patient: clinical implications*. Eur Rev Med Pharmacol Sci, 2020. 24(17): p. 9161-9168.
197. Corrêa, T.D., R.L. Cordioli, J.C. Campos Guerra, B. Caldin da Silva, R. Dos Reis Rodrigues, G.M. de Souza, T.D. Midega, N.S. Campos, B.V. Carneiro, F.N.D. Campos, H.P. Guimarães, G.F.J. de Matos, V.F. de Aranda, and L.J. Rolim Ferraz, *Coagulation profile of COVID-19 patients admitted to the ICU: An exploratory study*. PLoS One, 2020. 15(12): p. e0243604.
198. Sehgal, T., N. Gupta, S. Kohli, A. Khurana, J. Dass, S. Diwan, J.M. A, M. Khan, M. Aggarwal, and A. Subramanian, *A Prospective Study of Specialized Coagulation Parameters in Admitted COVID-19 Patients and Their Correlation With Acute Respiratory Distress Syndrome and Outcome*. Cureus, 2021. 13(8): p. e17463.
199. Hardy, M., I. Michaux, S. Lessire, J. Douxfils, J.M. Dogné, M. Bareille, G. Horlait, P. Bulpa, C. Chapelle, S. Laporte, S. Testa, H. Jacqmin, T. Lecompte, A. Dive, and F. Mullier, *Prothrombotic hemostasis disturbances in patients with severe COVID-19: Individual daily data*. Data Brief, 2020. 33: p. 106519.
200. White, D., S. MacDonald, T. Edwards, C. Bridgeman, M. Hayman, M. Sharp, S. Cox-Morton, E. Duff, S. Mahajan, C. Moore, M. Kirk, R. Williams, M. Besser, and W. Thomas, *Evaluation of COVID-19 coagulopathy; laboratory characterization using thrombin generation and nonconventional haemostasis assays*. International Journal of Laboratory Hematology, 2021. 43(1): p. 123-130.
201. Fan, B.E., K. Ramanathan, C.L.L. Sum, D. Christopher, S.S.W. Chan, G.H. Lim, C.F. Bok, S.W. Wong, D.C. Lye, B.E. Young, J.Y. Lim, R.M. Lee, S.P. Lim, H.T. Tan, M.K. Ang, et al., *Global haemostatic tests demonstrate the absence of parameters of*

- hypercoagulability in non-hypoxic mild COVID-19 patients: a prospective matched study.* Journal of Thrombosis and Thrombolysis, 2022. 53(3): p. 646-662.
202. Bauer, W., N. Galtung, N. Neuwinger, L. Kaufner, E. Langer, R. Somasundaram, R. Tauber, and K. Kappert, *A Matter of Caution: Coagulation Parameters in COVID-19 Do Not Differ from Patients with Ruled-Out SARS-CoV-2 Infection in the Emergency Department.* TH Open, 2021. 5(1): p. e43-e55.
 203. Sarkar, M., I.V. Madabhavi, P.N. Quy, and M.B. Govindagoudar, *COVID-19 and coagulopathy.* Clin Respir J, 2021. 15(12): p. 1259-1274.
 204. Portier, I., R.A. Campbell, and F. Denorme, *Mechanisms of immunothrombosis in COVID-19.* Curr Opin Hematol, 2021. 28(6): p. 445-453.
 205. Devreese, K.M.J., *COVID-19-related laboratory coagulation findings.* Int J Lab Hematol, 2021. 43 Suppl 1(Suppl 1): p. 36-42.
 206. Morales, A., S. Rojo Rello, H. Cristóbal, A. Fiz-López, E. Arribas, M. Marí, A. Tutusaus, P. de la Cal-Sabater, G.A.F. Nicolaes, J.T. Ortiz-Pérez, D. Bernardo, and P. García de Frutos, *Growth Arrest-Specific Factor 6 (GAS6) Is Increased in COVID-19 Patients and Predicts Clinical Outcome.* Biomedicines, 2021. 9(4).
 207. Tonello, S., M. Rizzi, E. Matino, M. Costanzo, G.F. Casciaro, A. Croce, E. Rizzi, E. Zecca, A. Pedrinelli, V. Vassia, R. Landi, M. Bellan, L.M. Castello, R. Minisini, V.R. Mallela, et al., *Baseline Plasma Gas6 Protein Elevation Predicts Adverse Outcomes in Hospitalized COVID-19 Patients.* Dis Markers, 2022. 2022: p. 1568352.
 208. Tutusaus, A., M. Marí, J.T. Ortiz-Pérez, G.A.F. Nicolaes, A. Morales, and P. García de Frutos, *Role of Vitamin K-Dependent Factors Protein S and GAS6 and TAM Receptors in SARS-CoV-2 Infection and COVID-19-Associated Immunothrombosis.* Cells, 2020. 9(10).
 209. Ma, L., S.K. Sahu, M. Cano, V. Kuppuswamy, J. Bajwa, J. McPhatter, A. Pine, M.L. Meizlish, G. Goshua, C.H. Chang, H. Zhang, C. Price, P. Bahel, H. Rinder, T. Lei, et al., *Increased complement activation is a distinctive feature of severe SARS-CoV-2 infection.* Sci Immunol, 2021. 6(59).
 210. Ali, Y.M., M. Ferrari, N.J. Lynch, S. Yaseen, T. Dudler, S. Gragerov, G. Demopoulos, J.L. Heeney, and W.J. Schwaeble, *Lectin Pathway Mediates Complement Activation by SARS-CoV-2 Proteins.* Front Immunol, 2021. 12: p. 714511.
 211. Cugno, M., P.L. Meroni, R. Gualtierotti, S. Griffini, E. Grovetti, A. Torri, M. Panigada, S. Aliberti, F. Blasi, F. Tedesco, and F. Peyvandi, *Complement activation in patients with COVID-19: A novel therapeutic target.* J Allergy Clin Immunol, 2020. 146(1): p. 215-217.
 212. Carvelli, J., O. Demaria, F. Vély, L. Batista, N. Chouaki Benmansour, J. Fares, S. Carpentier, M.L. Thibault, A. Morel, R. Remark, P. André, A. Represa, C. Piperoglou, P.Y. Cordier, E. Le Dault, et al., *Association of COVID-19 inflammation with activation of the C5a-C5aR1 axis.* Nature, 2020. 588(7836): p. 146-150.
 213. Ikeda, K., K. Nagasawa, T. Horiuchi, T. Tsuru, H. Nishizaka, and Y. Niho, *C5a induces tissue factor activity on endothelial cells.* Thromb Haemost, 1997. 77(2): p. 394-8.
 214. Ramlall, V., P.M. Thangaraj, C. Meydan, J. Foox, D. Butler, J. Kim, B. May, J.K. De Freitas, B.S. Glicksberg, C.E. Mason, N.P. Tatonetti, and S.D. Shapira, *Immune*

- complement and coagulation dysfunction in adverse outcomes of SARS-CoV-2 infection.* Nat Med, 2020. 26(10): p. 1609-1615.
215. Reynolds, N.D., N.M. Aceves, J.L. Liu, J.R. Compton, D.H. Leary, B.T. Freitas, S.D. Pegan, K.Z. Doctor, F.Y. Wu, X. Hu, and P.M. Legler, *The SARS-CoV-2 SSHPS Recognized by the Papain-like Protease.* ACS Infect Dis, 2021. 7(6): p. 1483-1502.
 216. Shin, D., R. Mukherjee, D. Grewe, D. Bojkova, K. Baek, A. Bhattacharya, L. Schulz, M. Widera, A.R. Mehdipour, G. Tascher, P.P. Geurink, A. Wilhelm, G.J. van der Heden van Noort, H. Ovaa, S. Müller, et al., *Papain-like protease regulates SARS-CoV-2 viral spread and innate immunity.* Nature, 2020. 587(7835): p. 657-662.
 217. Ruzicka, J.A., *Identification of the antithrombotic protein S as a potential target of the SARS-CoV-2 papain-like protease.* Thromb Res, 2020. 196: p. 257-259.
 218. Zuo, Y., S.K. Estes, R.A. Ali, A.A. Gandhi, S. Yalavarthi, H. Shi, G. Sule, K. Gockman, J.A. Madison, M. Zuo, V. Yadav, J. Wang, W. Woodard, S.P. Lezak, N.L. Lugogo, et al., *Prothrombotic autoantibodies in serum from patients hospitalized with COVID-19.* Sci Transl Med, 2020. 12(570).
 219. Talotta, R. and E.S. Robertson, *Antiphospholipid antibodies and risk of post-COVID-19 vaccination thrombophilia: The straw that breaks the camel's back?* Cytokine Growth Factor Rev, 2021. 60: p. 52-60.
 220. Chatterjee, S., T. Sengupta, S. Majumder, and R. Majumder, *COVID-19: a probable role of the anticoagulant Protein S in managing COVID-19-associated coagulopathy.* Aging (Albany NY), 2020. 12(16): p. 15954-15961.
 221. Mast, A.E., A.S. Wolberg, D. Gailani, M.R. Garvin, C. Alvarez, J.I. Miller, B. Aronow, and D. Jacobson, *SARS-CoV-2 suppresses anticoagulant and fibrinolytic gene expression in the lung.* eLife, 2021. 10: p. e64330.
 222. Dofferhoff, A.S.M., I. Piscaer, L.J. Schurgers, M.P.J. Visser, J.M.W. van den Ouweland, P.A. de Jong, R. Gosens, T.M. Hackeng, H. van Daal, P. Lux, C. Maassen, E.G.A. Karssemeijer, C. Vermeer, E.F.M. Wouters, L.E.M. Kistemaker, et al., *Reduced Vitamin K Status as a Potentially Modifiable Risk Factor of Severe Coronavirus Disease 2019.* Clin Infect Dis, 2021. 73(11): p. e4039-e4046.
 223. Janssen, R. and J. Walk, *Vitamin K epoxide reductase complex subunit 1 (VKORC1) gene polymorphism as determinant of differences in Covid-19-related disease severity.* Med Hypotheses, 2020. 144: p. 110218.
 224. Janssen, R., M.P.J. Visser, A.S.M. Dofferhoff, C. Vermeer, W. Janssens, and J. Walk, *Vitamin K metabolism as the potential missing link between lung damage and thromboembolism in Coronavirus disease 2019.* Br J Nutr, 2021. 126(2): p. 191-198.
 225. Sim, M.M.S., H.R. Alfar, M. Hollifield, D.W. Chung, X. Fu, M. Banerjee, X. Li, A.C. Thornton, J.Z. Porterfield, J.L. Sturgill, G.A. Sievert, M. Barton-Baxter, K.S. Campbell, J.G. Woodward, J.A. Lopez, et al., *HIV-1 and SARS-CoV-2 Both Cause Protein S, but through Different Mechanisms [abstract].* Res Pract Thromb Haemost, 2021. 5.
 226. Mulder, R., J.K. de Vries, R.P.H.M. Müskens, A.B. Mulder, and M.V. Lukens, *High protein S activity due to C4b-binding protein deficiency in a 34-year-old*

- Surinamese female with ischemic retinopathy*. Clinical case reports, 2018. 6(5): p. 935-938.
227. Davidson, C.J., E.G. Tuddenham, and J.H. McVey, *450 million years of hemostasis*. J Thromb Haemost, 2003. 1(7): p. 1487-94.
228. Morawitz, P., *Beiträge zur Kenntnis der Blutgerinnung*. Beitr Chem Physio Pathol, 1904. 5: p. 133-141.
229. Hvatum, M. and H. Prydz, *Studies on tissue thromboplastin: I. Solubilization with sodium deoxycholate*. Biochimica et Biophysica Acta (BBA) - General Subjects, 1966. 130(1): p. 92-101.
230. Nemerson, Y., *The phospholipid requirement of tissue factor in blood coagulation*. J Clin Invest, 1968. 47(1): p. 72-80.
231. Nemerson, Y. and F.A. Pitlick, *Purification and characterization of the protein component of tissue factor*. Biochemistry, 1970. 9(26): p. 5100-5105.
232. Bjorklid, E. and E. Storm, *Purification and some properties of the protein component of tissue thromboplastin from human brain*. Biochem J, 1977. 165(1): p. 89-96.
233. Morrissey, J.H., *Tissue factor: an enzyme cofactor and a true receptor*. Thromb Haemost, 2001. 86(1): p. 66-74.
234. Spicer, E.K., R. Horton, L. Bloem, R. Bach, K.R. Williams, A. Guha, J. Kraus, T.C. Lin, Y. Nemerson, and W.H. Konigsberg, *Isolation of cDNA clones coding for human tissue factor: primary structure of the protein and cDNA*. Proceedings of the National Academy of Sciences of the United States of America, 1987. 84(15): p. 5148-5152.
235. Muller, Y.A., M.H. Ultsch, and A.M. de Vos, *The Crystal Structure of the Extracellular Domain of Human Tissue Factor Refined to 1.7 Å Resolution*. Journal of Molecular Biology, 1996. 256(1): p. 144-159.
236. David, W.B., D.A. Allan, C. Christiana, K.W. Fritz, G. Arabinda, H.K. William, N. Yale, and K. Daniel, *The crystal structure of the complex of blood coagulation factor VIIIa with soluble tissue factor*. Nature, 1996. 380(6569): p. 41.
237. Ahamed, J., H.H. Versteeg, M. Kerver, V.M. Chen, B.M. Mueller, P.J. Hogg, and W. Ruf, *Disulfide Isomerization Switches Tissue Factor from Coagulation to Cell Signaling*. Proceedings of the National Academy of Sciences of the United States of America, 2006. 103(38): p. 13932-13937.
238. Drake, T.A., J.H. Morrissey, and T.S. Edgington, *Selective cellular expression of tissue factor in human tissues. Implications for disorders of hemostasis and thrombosis*. The American journal of pathology, 1989. 134(5): p. 1087-1097.
239. Mackman, E.N., S.R. Tilley, and S.N. Key, *Role of the Extrinsic Pathway of Blood Coagulation in Hemostasis and Thrombosis*. Arteriosclerosis, Thrombosis, and Vascular Biology, 2007. 27(8): p. 1687-1693.
240. Riewald, M. and W. Ruf, *Mechanistic coupling of protease signaling and initiation of coagulation by tissue factor*. Proc Natl Acad Sci U S A, 2001. 98(14): p. 7742-7.
241. Schaffner, F. and W. Ruf, *Tissue factor and PAR2 signaling in the tumor microenvironment*. Arterioscler Thromb Vasc Biol, 2009. 29(12): p. 1999-2004.

242. Schulman, S., E. El-Darzi, M.H.C. Florido, M. Friesen, G. Merrill-Skoloff, M.A. Brake, C.R. Schuster, L. Lin, R.J. Westrick, C.A. Cowan, R. Flaumenhaft, W.H. Ouwehand, K. Peerlinck, K. Freson, E. Turro, et al., *A coagulation defect arising from heterozygous premature termination of tissue factor*. *The Journal of Clinical Investigation*, 2020. 130(10): p. 5302-5312.
243. Vladimir, Y.B., B. Viji, H. James, V. Oana, L. Mark, and N. Yale, *Alternatively spliced human tissue factor: a circulating, soluble, thrombogenic protein*. *Nature Medicine*, 2003. 9(4): p. 458.
244. Censarek, P., A. Bobbe, M. Grandoch, K. Schror, and A.A. Weber, *Alternatively spliced human tissue factor (asHTF) is not pro-coagulant*. *Thrombosis And Haemostasis*, 2007. 97(1): p. 11-14.
245. van Den Berg, Y.W., L.G. van Den Hengel, H.R. Myers, O. Ayachi, E. Jordanova, W. Ruf, C.A. Spek, P.H. Reitsma, V.Y. Bogdanov, and H.H. Versteeg, *Alternatively spliced tissue factor induces angiogenesis through integrin ligation*. *Proceedings of the National Academy of Sciences of the United States of America*, 2009. 106(46): p. 19497-19502.
246. Vladimir, Y.B., H. James, and N. Yale, *Active tissue factor in blood?* *Nature Medicine*, 2004. 10(11): p. 1156.
247. Rauch, U., B. Bohrmann, D. Kling, M. Roque, J.T. Fallon, J.J. Badimon, J. Himber, M.A. Riederer, and Y. Nemerson, *Blood-Borne Tissue Factor: Another View of Thrombosis*. *Proceedings of the National Academy of Sciences of the United States of America*, 1999. 96(5): p. 2311-2315.
248. Gregory, S.A., J.H. Morrissey, and T.S. Edgington, *Regulation of tissue factor gene expression in the monocyte procoagulant response to endotoxin*. *Molecular and cellular biology*, 1989. 9(6): p. 2752-2755.
249. Egorina, E.M., M.A. Sovershaev, G. Bjørkøy, F.X.E. Gruber, J.O. Olsen, B. Parhami-Seren, K.G. Mann, and B. Østerud, *Intracellular and surface distribution of monocyte tissue factor: application to intersubject variability*. *Arteriosclerosis, thrombosis, and vascular biology*, 2005. 25(7): p. 1493-1498.
250. del Conde, I., C.N. Shrimpton, P. Thiagarajan, and J.A. López, *Tissue-factor-bearing microvesicles arise from lipid rafts and fuse with activated platelets to initiate coagulation*. *Blood*, 2005. 106(5): p. 1604-1611.
251. Hoffman, M., H.C. Whinna, and D.M. Monroe, *Circulating tissue factor accumulates in thrombi, but not in hemostatic plugs*. *Journal of Thrombosis and Haemostasis*, 2006. 4(9): p. 2092-2093.
252. Day, S.M., J.L. Reeve, B. Pedersen, D.M. Farris, D.D. Myers, M. Im, T.W. Wakefield, N. Mackman, and W.P. Fay, *Macrovascular thrombosis is driven by tissue factor derived primarily from the blood vessel wall*. *Blood*, 2005. 105(1): p. 192-198.
253. Ni, H., C.V. Denis, S. Subbarao, J.L. Degen, T.N. Sato, R.O. Hynes, and D.D. Wagner, *Persistence of platelet thrombus formation in arterioles of mice lacking both von Willebrand factor and fibrinogen*. *The Journal of clinical investigation*, 2000. 106(3): p. 385-392.
254. Himber, J., C. Wohlgensinger, S. Roux, L.A. Damico, J.T. Fallon, D. Kirchhofer, Y. Nemerson, and M.A. Riederer, *Inhibition of tissue factor limits the growth of*

- venous thrombus in the rabbit*. Journal of Thrombosis and Haemostasis, 2003. 1(5): p. 889-895.
255. Zhou, L.J., I.L. May, I.P. Liao, I.P. Gross, and I.J. Weitz, *Inferior Vena Cava Ligation Rapidly Induces Tissue Factor Expression and Venous Thrombosis in Rats*. Arteriosclerosis, Thrombosis, and Vascular Biology, 2009. 29(6): p. 863-869.
256. Santucci, R.A., J. Erlich, J. Labriola, M. Wilson, K.J. Kao, T.S. Kickler, C. Spillert, and N. Mackman, *Measurement of tissue factor activity in whole blood*. Thrombosis and haemostasis, 2000. 83(3): p. 445-454.
257. Berckmans, R.J., R. Nieuwland, A.N. Böing, F.P. Romijn, C.E. Hack, and A. Sturk, *Cell-derived microparticles circulate in healthy humans and support low grade thrombin generation*. Thrombosis and haemostasis, 2001. 85(4): p. 639.
258. Le, D.T., S.I. Rapaport, and L.V. Rao, *Relations between factor VIIa binding and expression of factor VIIa/tissue factor catalytic activity on cell surfaces*. The Journal of biological chemistry, 1992. 267(22): p. 15447-15454.
259. Chen, V.M., J. Ahamed, H.H. Versteeg, M.C. Berndt, W. Ruf, and P.J. Hogg, *Evidence for activation of tissue factor by an allosteric disulfide bond*. Biochemistry, 2006. 45(39): p. 12020.
260. Liang, H., T.M. Brophy, and P. Hogg, *Redox properties of the tissue factor Cys(186)-Cys(209) disulfide bond*. Biochemical Journal, 2011. 437(3): p. 455-460.
261. Wang, P., Y. Wu, X. Li, X. Ma, and L. Zhong, *Thioredoxin and Thioredoxin Reductase Control Tissue Factor Activity by Thiol Redox-dependent Mechanism*. Journal Of Biological Chemistry, 2013. 288(5): p. 3346-3358.
262. Rothmeier, S.A., H.P. Marchese, M.F. Langer, M.Y. Kamikubo, M.F. Schaffner, M.J. Cantor, M.M. Ginsberg, M.Z. Ruggeri, and M.W. Ruf, *Tissue Factor Prothrombotic Activity Is Regulated by Integrin- α 6 Trafficking*. Arteriosclerosis, Thrombosis, and Vascular Biology, 2017. 37(7): p. 1323-1331.
263. Reinhardt, C., M.-L. Von Brühl, D. Manukyan, L. Grahl, M. Lorenz, B. Altmann, S. Dlugai, S. Hess, I. Konrad, L. Orschiedt, N. Mackman, L. Ruddock, S. Massberg, and B. Engelmann, *Protein disulfide isomerase acts as an injury response signal that enhances fibrin generation via tissue factor activation*. The Journal of clinical investigation, 2008. 118(3): p. 1110-1122.
264. Furlan-Freguia, C., P. Marchese, A. Gruber, Z.M. Ruggeri, and W. Ruf, *P2X7 receptor signaling contributes to tissue factor-dependent thrombosis in mice*. The Journal of clinical investigation, 2011. 121(7): p. 2932-2944.
265. Langer, F., B. Spath, C. Fischer, M. Stolz, F.A. Ayuk, N. Kröger, C. Bokemeyer, and W. Ruf, *Rapid activation of monocyte tissue factor by antithymocyte globulin is dependent on complement and protein disulfide isomerase*. Blood, 2013. 121(12): p. 2324-2335.
266. Chen, V.M.Y., *Tissue factor de-encryption, thrombus formation, and thiol-disulfide exchange*. Seminars in thrombosis and hemostasis, 2013. 39(1): p. 40-47.
267. Mulder, A.B., J.W. Smit, V.J. Bom, N.R. Blom, M.H. Ruiters, M.R. Halie, and J. van Der Meer, *Association of smooth muscle cell tissue factor with caveolae*. Blood, 1996. 88(4): p. 1306-1313.

268. Sevinsky, J.R., L.V. Rao, and W. Ruf, *Ligand-induced protease receptor translocation into caveolae: a mechanism for regulating cell surface proteolysis of the tissue factor-dependent coagulation pathway*. *The Journal of cell biology*, 1996. 133(2): p. 293-304.
269. Stark, M.K., J.I. Schubert, J.U. Joshi, J.B. Kilani, J.P. Hoseinpour, J.M. Thakur, J.P. Grünauer, J.S. Pfeiler, J.T. Schmidergall, J.S. Stockhausen, J.M. Bäumer, J.S. Chandraratne, J.M.-L. Von Brühl, J.M. Lorenz, J.R. Coletti, et al., *Distinct Pathogenesis of Pancreatic Cancer Microvesicle–Associated Venous Thrombosis Identifies New Antithrombotic Targets In Vivo*. *Arteriosclerosis, Thrombosis, and Vascular Biology*, 2018. 38(4): p. 772-786.
270. Butenas, S. and J. Krudysz-Amblo, *Decryption of tissue factor*. *Thrombosis Research*, 2012. 129(2): p. S18-S20.
271. Chen, V.M. and P.J. Hogg, *Encryption and decryption of tissue factor*. 2013. p. 277-284.
272. Folco, J.E., L.T. Mawson, W.A. Vromman, W.B. Bernardes-Souza, W.G. Franck, W.O. Persson, W.M. Nakamura, W.G. Newton, W.F. Luscinskas, and W.P. Libby, *Neutrophil Extracellular Traps Induce Endothelial Cell Activation and Tissue Factor Production Through Interleukin-1 α and Cathepsin G*. *Arteriosclerosis, Thrombosis, and Vascular Biology*, 2018. 38(8): p. 1901-1912.
273. Liang, T.W., E.Y. Fan, E.H. Lu, E.Z. Chang, E.W. Hu, E.J. Sun, E.H. Wang, E.T. Zhu, E.J. Wang, E.R. Adili, E.M. Garcia-Barrio, E.M. Holinstat, E.D. Eitzman, E.J. Zhang, and E.Y. Chen, *KLF11 (Krüppel-Like Factor 11) Inhibits Arterial Thrombosis via Suppression of Tissue Factor in the Vascular Wall*. *Arteriosclerosis, Thrombosis, and Vascular Biology*, 2019. 39(3): p. 402-412.
274. Baker, S.K., K.A. Kopec, G.A. Pant, L.L. Poole, S.H. Cline-Fedewa, P.D. Ivkovich, P.M. Olyae, P.B. Woolbright, P.A. Miszta, P.H. Jaeschke, P.A. Wolberg, and P.J. Luyendyk, *Direct Amplification of Tissue Factor: Factor VIIa Procoagulant Activity by Bile Acids Drives Intrahepatic Coagulation*. *Arteriosclerosis, Thrombosis, and Vascular Biology*, 2019. 39(10): p. 2038-2048.
275. Drake, T.A., J.H. Morrissey, and T.S. Edgington, *Selective cellular expression of tissue factor in human tissues. Implications for disorders of hemostasis and thrombosis*. *Am J Pathol*, 1989. 134(5): p. 1087-97.
276. Owens, A.P., 3rd and N. Mackman, *Tissue factor and thrombosis: The clot starts here*. *Thromb Haemost*, 2010. 104(3): p. 432-9.
277. Langer, F., B. Spath, C. Fischer, M. Stolz, F.A. Ayuk, N. Kröger, C. Bokemeyer, and W. Ruf, *Rapid activation of monocyte tissue factor by antithymocyte globulin is dependent on complement and protein disulfide isomerase*. *Blood*, 2013. 121(12): p. 2324-35.
278. Müller-Calleja, N., S. Ritter, A. Hollerbach, T. Falter, K.J. Lackner, and W. Ruf, *Complement C5 but not C3 is expendable for tissue factor activation by cofactor-independent antiphospholipid antibodies*. *Blood Adv*, 2018. 2(9): p. 979-986.
279. Willebrand, E.A., *Hereditär pseudohemofili*. *Finska Lakaresällskapets Handlingar*, 1926. 1(67): p. 7-112.

280. Zimmerman, T.S., O.D. Ratnoff, and A.E. Powell, *Immunologic differentiation of classic hemophilia (factor 8 deficiency) and von Willebrand's disease, with observations on combined deficiencies of antihemophilic factor and proaccelerin (factor V) and on an acquired circulating anticoagulant against antihemophilic factor*. J Clin Invest, 1971. 50(1): p. 244-54.
281. Meyer, D. and M.J. Larrieu, *Von Willebrand factor and platelet adhesiveness*. J Clin Pathol, 1970. 23(3): p. 228-31.
282. Lenting, P.J., C. Casari, O.D. Christophe, and C.V. Denis, *von Willebrand factor: the old, the new and the unknown*. J Thromb Haemost, 2012. 10(12): p. 2428-37.
283. Ruggeri, Z.M., *Structure and Function of von Willebrand Factor*. Thromb Haemost, 1999. 82(08): p. 576-584.
284. Hassan, M.I., A. Saxena, and F. Ahmad, *Structure and function of von Willebrand factor*. Blood Coagul Fibrinolysis, 2012. 23(1): p. 11-22.
285. Zhang, Q., Y.F. Zhou, C.Z. Zhang, X. Zhang, C. Lu, and T.A. Springer, *Structural specializations of A2, a force-sensing domain in the ultralarge vascular protein von Willebrand factor*. Proc Natl Acad Sci U S A, 2009. 106(23): p. 9226-31.
286. Skipwith, C.G., W. Cao, and X.L. Zheng, *Factor VIII and platelets synergistically accelerate cleavage of von Willebrand factor by ADAMTS13 under fluid shear stress*. J Biol Chem, 2010. 285(37): p. 28596-603.
287. Okhota, S., I. Melnikov, Y. Avtaeva, S. Kozlov, and Z. Gabbasov, *Shear Stress-Induced Activation of von Willebrand Factor and Cardiovascular Pathology*. Int J Mol Sci, 2020. 21(20).
288. Wu, Y.-P., P.G. de Groot, and J.J. Sixma, *Shear Stress-Induced Detachment of Blood Platelets From Various Surfaces*. Arteriosclerosis, Thrombosis, and Vascular Biology, 1997. 17(11): p. 3202-3207.
289. Bryckaert, M., J.P. Rosa, C.V. Denis, and P.J. Lenting, *Of von Willebrand factor and platelets*. Cell Mol Life Sci, 2015. 72(2): p. 307-26.
290. Huizinga, E.G., R. Martijn van der Plas, J. Kroon, J.J. Sixma, and P. Gros, *Crystal structure of the A3 domain of human von Willebrand factor: implications for collagen binding*. Structure, 1997. 5(9): p. 1147-56.
291. Morales, L.D., C. Martin, and M.A. Cruz, *The interaction of von Willebrand factor-A1 domain with collagen: mutation G1324S (type 2M von Willebrand disease) impairs the conformational change in A1 domain induced by collagen*. J Thromb Haemost, 2006. 4(2): p. 417-25.
292. Kawecki, C., P.J. Lenting, and C.V. Denis, *von Willebrand factor and inflammation*. J Thromb Haemost, 2017. 15(7): p. 1285-1294.
293. Fujimura, Y. and L.Z. Holland, *COVID-19 microthrombosis: unusually large VWF multimers are a platform for activation of the alternative complement pathway under cytokine storm*. Int J Hematol, 2022. 115(4): p. 457-469.
294. Plautz, W.E., V.S.S. Pilli, B.C. Cooley, R. Chattopadhyay, P.R. Westmark, T. Getz, D. Paul, W. Bergmeier, J.P. Sheehan, and R. Majumder, *Anticoagulant Protein S Targets the Factor IXa Heparin-Binding Exosite to Prevent Thrombosis*. Arteriosclerosis, Thrombosis, and Vascular Biology, 2018. 38(4): p. 816-828.

295. Rosenberg, J.B., S.L. Haberichter, M.A. Jozwiak, E.A. Vokac, P.A. Kroner, S.A. Fahs, Y. Kawai, and R.R. Montgomery, *The role of the D1 domain of the von Willebrand factor propeptide in multimerization of VWF*. *Blood*, 2002. 100(5): p. 1699-706.
296. Gralnick, H.R., S.B. Williams, L.P. McKeown, L. Magruder, K. Hansmann, M. Vail, and R.I. Parker, *Platelet von Willebrand factor*. *Mayo Clin Proc*, 1991. 66(6): p. 634-40.
297. McGrath, R.T., E. McRae, O.P. Smith, and J.S. O'Donnell, *Platelet von Willebrand factor--structure, function and biological importance*. *Br J Haematol*, 2010. 148(6): p. 834-43.
298. Zanardelli, S., J.T. Crawley, C.K. Chion, J.K. Lam, R.J. Preston, and D.A. Lane, *ADAMTS13 substrate recognition of von Willebrand factor A2 domain*. *J Biol Chem*, 2006. 281(3): p. 1555-63.
299. Bharati, K.P. and U.R. Prashanth, *Von Willebrand disease: an overview*. *Indian J Pharm Sci*, 2011. 73(1): p. 7-16.
300. Othman, M., *Platelet-type von Willebrand disease: a rare, often misdiagnosed and underdiagnosed bleeding disorder*. *Semin Thromb Hemost*, 2011. 37(5): p. 464-9.
301. Pottinger, B.E., R.C. Read, E.M. Paleolog, P.G. Higgins, and J.D. Pearson, *von Willebrand factor is an acute phase reactant in man*. *Thromb Res*, 1989. 53(4): p. 387-94.
302. Mancini, I., L. Baronciani, A. Artoni, P. Colpani, M. Biganzoli, G. Cozzi, C. Novembrino, M. Boscolo Anzoletti, V. De Zan, M.T. Pagliari, R. Gualtierotti, S. Aliberti, M. Panigada, G. Grasselli, F. Blasi, et al., *The ADAMTS13-von Willebrand factor axis in COVID-19 patients*. *J Thromb Haemost*, 2021. 19(2): p. 513-521.
303. Bernardo, A., C. Ball, L. Nolasco, J.F. Moake, and J.F. Dong, *Effects of inflammatory cytokines on the release and cleavage of the endothelial cell-derived ultralarge von Willebrand factor multimers under flow*. *Blood*, 2004. 104(1): p. 100-6.
304. Seth, R., T.A.J. McKinnon, and X.F. Zhang, *Contribution of the von Willebrand factor/ADAMTS13 imbalance to COVID-19 coagulopathy*. *American Journal of Physiology-Heart and Circulatory Physiology*, 2021. 322(1): p. H87-H93.
305. Gragnano, F., S. Sperlongano, E. Golia, F. Natale, R. Bianchi, M. Crisci, F. Fimiani, I. Pariggiano, V. Diana, A. Carbone, A. Cesaro, C. Concilio, G. Limongelli, M. Russo, and P. Calabrò, *The Role of von Willebrand Factor in Vascular Inflammation: From Pathogenesis to Targeted Therapy*. *Mediators Inflamm*, 2017. 2017: p. 5620314.
306. Rostami, M., H. Mansouritorghabeh, and M. Parsa-Kondelaji, *High levels of Von Willebrand factor markers in COVID-19: a systematic review and meta-analysis*. *Clin Exp Med*, 2022. 22(3): p. 347-357.
307. Li, H., Q. Wu, Z. Qin, X. Hou, L. Zhang, J. Guo, Y. Li, F. Yang, Y. Zhang, Q. Wu, L. Li, and H. Chen, *Serum levels of laminin and von Willebrand factor in COVID-19 survivors 6 months after discharge*. *Int J Infect Dis*, 2022. 115: p. 134-141.
308. Morrissey, J. *Morrissey Lab Protocol for Preparing Phospholipid Vesicles (SUV) by Sonication*. 2001 [cited 2019 September 27]; Available from: <http://tf7.org/suv.pdf>.
309. Banerjee, M., Y. Huang, S. Joshi, J. Popa Gabriel, D. Mendenhall Michael, J. Wang Qing, A. Garvy Beth, T. Myint, and W. Whiteheart Sidney, *Platelets Endocytose*

- Viral Particles and Are Activated via TLR (Toll-Like Receptor) Signaling. Arteriosclerosis, Thrombosis, and Vascular Biology, 2020. 40(7): p. 1635-1650.*
310. Hisada, Y. and N. Mackman, *Measurement of tissue factor activity in extracellular vesicles from human plasma samples. Research and Practice in Thrombosis and Haemostasis, 2019. 3(1): p. 44-48.*
 311. Key, N.S. and N. Mackman, *Tissue factor and its measurement in whole blood, plasma, and microparticles. Semin Thromb Hemost, 2010. 36(8): p. 865-75.*
 312. Amanat, F., D. Stadlbauer, S. Strohmeier, T.H.O. Nguyen, V. Chromikova, M. McMahon, K. Jiang, G.A. Arunkumar, D. Jurczynszak, J. Polanco, M. Bermudez-Gonzalez, G. Kleiner, T. Aydillo, L. Miorin, D.S. Fierer, et al., *A serological assay to detect SARS-CoV-2 seroconversion in humans. Nature medicine, 2020. 26(7): p. 1033-1036.*
 313. Stadlbauer, D., F. Amanat, V. Chromikova, K. Jiang, S. Strohmeier, G.A. Arunkumar, J. Tan, D. Bhavsar, C. Capuano, E. Kirkpatrick, P. Meade, R.N. Brito, C. Teo, M. McMahon, V. Simon, et al., *SARS-CoV-2 Seroconversion in Humans: A Detailed Protocol for a Serological Assay, Antigen Production, and Test Setup. Curr Protoc Microbiol, 2020. 57(1): p. e100.*
 314. Pretorius, E., C. Venter, G.J. Laubscher, M.J. Kotze, S.O. Oladejo, L.R. Watson, K. Rajaratnam, B.W. Watson, and D.B. Kell, *Prevalence of symptoms, comorbidities, fibrin amyloid microclots and platelet pathology in individuals with Long COVID/Post-Acute Sequelae of COVID-19 (PASC). Cardiovasc Diabetol, 2022. 21(1): p. 148.*
 315. Thomazini, C.M., R.P.S. Soares, T.R.F. da Rocha, A.T.A. Sachetto, and M.L. Santoro, *Optimization of von Willebrand factor multimer analysis in vertical mini-gel electrophoresis systems: A rapid procedure. Thromb Res, 2019. 175: p. 76-83.*
 316. Ott, H.W., A. Griesmacher, M. Schnapka-Koepf, G. Golderer, A. Sieberer, M. Spannagl, B. Scheibe, S. Perkhofer, K. Will, and U. Budde, *Analysis of von Willebrand factor multimers by simultaneous high- and low-resolution vertical SDS-agarose gel electrophoresis and Cy5-labeled antibody high-sensitivity fluorescence detection. Am J Clin Pathol, 2010. 133(2): p. 322-30.*
 317. Interlandi, G., O. Yakovenko, A.Y. Tu, J. Harris, J. Le, J. Chen, J.A. López, and W.E. Thomas, *Specific electrostatic interactions between charged amino acid residues regulate binding of von Willebrand factor to blood platelets. J Biol Chem, 2017. 292(45): p. 18608-18617.*
 318. St John, A., Y. Wang, J. Chen, W. Osborn, X. Wang, E. Lim, D. Chung, S. Stern, N. White, X. Fu, and J. López, *Plasma proteomic profile associated with platelet dysfunction after trauma. J Thromb Haemost, 2021. 19(7): p. 1666-1675.*
 319. Han, Y., J. Xiao, E. Falls, and X.L. Zheng, *A shear-based assay for assessing plasma ADAMTS13 activity and inhibitors in patients with thrombotic thrombocytopenic purpura. Transfusion, 2011. 51(7): p. 1580-91.*
 320. Herbig, B.A. and S.L. Diamond, *Pathological von Willebrand factor fibers resist tissue plasminogen activator and ADAMTS13 while promoting the contact pathway and shear-induced platelet activation. J Thromb Haemost, 2015. 13(9): p. 1699-708.*

321. National Research Council Committee for the Update of the Guide for the Care and Use of Laboratory Animals, C. and A. Use of Laboratory Animals, *The National Academies Collection: Reports funded by National Institutes of Health*, in *Guide for the Care and Use of Laboratory Animals*. 2011, National Academies Press (US)
322. Hubbard, W.B., C.L. Harwood, J.G. Geisler, H.J. Vekaria, and P.G. Sullivan, *Mitochondrial uncoupling prodrug improves tissue sparing, cognitive outcome, and mitochondrial bioenergetics after traumatic brain injury in male mice*. *J Neurosci Res*, 2018. 96(10): p. 1677-1688.
323. Vekaria, H.J., W.B. Hubbard, N.E. Scholpa, M.L. Spry, J.L. Gooch, S.J. Prince, R.G. Schnellmann, and P.G. Sullivan, *Formoterol, a $\beta(2)$ -adrenoreceptor agonist, induces mitochondrial biogenesis and promotes cognitive recovery after traumatic brain injury*. *Neurobiol Dis*, 2020. 140: p. 104866.
324. Hubbard, W.B., B. Joseph, M. Spry, H.J. Vekaria, K.E. Saatman, and P.G. Sullivan, *Acute Mitochondrial Impairment Underlies Prolonged Cellular Dysfunction after Repeated Mild Traumatic Brain Injuries*. *J Neurotrauma*, 2019. 36(8): p. 1252-1263.
325. Hubbard, W.B., C.L. Harwood, P. Prajapati, J.E. Springer, K.E. Saatman, and P.G. Sullivan, *Fractionated mitochondrial magnetic separation for isolation of synaptic mitochondria from brain tissue*. *Sci Rep*, 2019. 9(1): p. 9656.
326. Hubbard, W.B., M. Banerjee, H. Vekaria, K.S. Prakhya, S. Joshi, Q.J. Wang, K.E. Saatman, S.W. Whiteheart, and P.G. Sullivan, *Differential Leukocyte and Platelet Profiles in Distinct Models of Traumatic Brain Injury*. *Cells*, 2021. 10(3).
327. Shah, A.S.V., D. Stelzle, K.K. Lee, E.J. Beck, S. Alam, S. Clifford, C.T. Longenecker, F. Strachan, S. Bagchi, W. Whiteley, S. Rajagopalan, S. Kottlilil, H. Nair, D.E. Newby, D.A. McAllister, et al., *Global Burden of Atherosclerotic Cardiovascular Disease in People Living With HIV: Systematic Review and Meta-Analysis*. *Circulation*, 2018. 138(11): p. 1100-1112.
328. Walker, F.J., *Regulation of activated protein C by a new protein. A possible function for bovine protein S*. *The Journal of biological chemistry*, 1980. 255(12): p. 5521-5524.
329. Wood, P.J., R.P.E. Ellery, A.S. Maroney, and E.A. Mast, *Protein S Is a Cofactor for Platelet and Endothelial Tissue Factor Pathway Inhibitor- α but Not for Cell Surface-Associated Tissue Factor Pathway Inhibitor*. *Arteriosclerosis, Thrombosis, and Vascular Biology*, 2014. 34(1): p. 169-176.
330. Sutherland, M.R., A.Y. Simon, I. Shanina, M.S. Horwitz, W. Ruf, and E.L.G. Prydzial, *Virus envelope tissue factor promotes infection in mice*. *J Thromb Haemost*, 2019. 17(3): p. 482-491.
331. Walker, F.J., *Regulation of activated protein C by protein S. The role of phospholipid in factor Va inactivation*. *J Biol Chem*, 1981. 256(21): p. 11128-31.
332. Sim, M.M.S. and J.P. Wood, *Dysregulation of Protein S in COVID-19*. *Best Pract Res Clin Haematol*, 2022. 35(3): p. 101376.
333. Zhou, F., T. Yu, R. Du, G. Fan, Y. Liu, Z. Liu, J. Xiang, Y. Wang, B. Song, X. Gu, L. Guan, Y. Wei, H. Li, X. Wu, J. Xu, et al., *Clinical course and risk factors for mortality of*

- adult inpatients with COVID-19 in Wuhan, China: a retrospective cohort study.* The Lancet (British edition), 2020. 395(10229): p. 1054-1062.
334. Zhang, L., X. Yan, Q. Fan, H. Liu, X. Liu, Z. Liu, and Z. Zhang, *D-dimer levels on admission to predict in-hospital mortality in patients with Covid-19.* Journal of thrombosis and haemostasis, 2020. 18(6): p. 1324-1329.
335. Klok, F.A., M.J.H.A. Kruip, N.J.M. van der Meer, M.S. Arbous, D.A.M.P.J. Gommers, K.M. Kant, F.H.J. Kaptein, J. van Paassen, M.A.M. Stals, M.V. Huisman, and H. Endeman, *Incidence of thrombotic complications in critically ill ICU patients with COVID-19.* Thrombosis research, 2020. 191: p. 145-147.
336. Stitt, T.N., G. Conn, M. Gore, C. Lai, J. Bruno, C. Radziejewski, K. Mattsson, J. Fisher, D.R. Gies, P.F. Jones, and et al., *The anticoagulation factor protein S and its relative, Gas6, are ligands for the Tyro 3/Axl family of receptor tyrosine kinases.* Cell, 1995. 80(4): p. 661-70.
337. Pauls, J.E., M.F. Hockin, G.L. Long, and K.G. Mann, *Self-association of human protein S.* Biochemistry, 2000. 39(18): p. 5468-73.
338. Seré, K.M., M.P. Janssen, G.M. Willems, G. Tans, J. Rosing, and T.M. Hackeng, *Purified protein S contains multimeric forms with increased APC-independent anticoagulant activity.* Biochemistry, 2001. 40(30): p. 8852-60.
339. Li, F., C.Q. Li, J.L. Moake, J.A. López, and L.V. McIntire, *Shear stress-induced binding of large and unusually large von Willebrand factor to human platelet glycoprotein Ibalpha.* Ann Biomed Eng, 2004. 32(7): p. 961-9.
340. Ladikou, E.E., H. Sivaloganathan, K.M. Milne, W.E. Arter, R. Ramasamy, R. Saad, S.M. Stoneham, B. Philips, A.C. Eziefula, and T. Chevassut, *Von Willebrand factor (vWF): marker of endothelial damage and thrombotic risk in COVID-19?* Clin Med (Lond), 2020. 20(5): p. e178-e182.
341. Li, C.Q., J.F. Dong, and J.A. López, *The mucin-like macroglycopeptide region of glycoprotein Ibalpha is required for cell adhesion to immobilized von Willebrand factor (VWF) under flow but not for static VWF binding.* Thromb Haemost, 2002. 88(4): p. 673-7.
342. Chung, D.W., J. Chen, M. Ling, X. Fu, T. Blevins, S. Parsons, J. Le, J. Harris, T.R. Martin, B.A. Konkle, Y. Zheng, and J.A. López, *High-density lipoprotein modulates thrombosis by preventing von Willebrand factor self-association and subsequent platelet adhesion.* Blood, 2016. 127(5): p. 637-45.
343. Zhang, J., R. Jiang, L. Liu, T. Watkins, F. Zhang, and J.-f. Dong, *Traumatic brain injury-associated coagulopathy.* Journal of neurotrauma, 2012. 29(17): p. 2597-2605.
344. Morel, N., O. Morel, L. Petit, B. Hugel, J.F. Cochard, J.M. Freyssinet, F. Sztark, and P. Dabadie, *Generation of procoagulant microparticles in cerebrospinal fluid and peripheral blood after traumatic brain injury.* J Trauma, 2008. 64(3): p. 698-704.
345. Nekludov, M., F. Mobarrez, D. Gryth, B.-M. Bellander, and H. Wallen, *Formation of Microparticles in the Injured Brain of Patients with Severe Isolated Traumatic Brain Injury.* Journal of Neurotrauma, 2014. 31(23): p. 1927-1933.
346. Halpern, C.H., P.M. Reilly, A.R. Turtz, and S.C. Stein, *Traumatic coagulopathy: the effect of brain injury.* J Neurotrauma, 2008. 25(8): p. 997-1001.

347. Maegele, M., *Coagulopathy after traumatic brain injury: incidence, pathogenesis, and treatment options*. Transfusion, 2013. 53 Suppl 1: p. 28s-37s.
348. Gando, S., S. Nanzaki, and O. Kemmotsu, *Coagulofibrinolytic changes after isolated head injury are not different from those in trauma patients without head injury*. J Trauma, 1999. 46(6): p. 1070-6; discussion 1076-7.
349. Tian, Y., B. Salsbery, M. Wang, H. Yuan, J. Yang, Z. Zhao, X. Wu, Y. Zhang, B.A. Konkle, P. Thiagarajan, M. Li, J. Zhang, and J.-f. Dong, *Brain-derived microparticles induce systemic coagulation in a murine model of traumatic brain injury*. Blood, 2015. 125(13): p. 2151-2159.
350. Mondello, S., E.P. Thelin, G. Shaw, M. Salzet, C. Visalli, D. Cizkova, F. Kobeissy, and A. Buki, *Extracellular vesicles: pathogenetic, diagnostic and therapeutic value in traumatic brain injury*. Expert Review of Proteomics, 2018. 15(5): p. 451-461.
351. Sandsmark, D.K., A. Bashir, C.L. Wellington, and R. Diaz-Arrastia, *Cerebral Microvascular Injury: A Potentially Treatable Endophenotype of Traumatic Brain Injury-Induced Neurodegeneration*. Neuron, 2019. 103(3): p. 367-379.
352. Dentali, F., E. Nicolini, and W. Ageno, *Venous and arterial thrombosis associated with HIV infection*. Seminars in thrombosis and hemostasis, 2012. 38(5): p. 524-529.
353. Chatterjee, S., T. Sengupta, S. Majumder, and R. Majumder, *COVID-19: a probable role of the anticoagulant Protein S in managing COVID-19-associated coagulopathy*. Aging, 2020. 12(16): p. 15954-15961.
354. Jong, E., S. Louw, J.C.M. Meijers, M.D. de Kruif, H. Ten Cate, H.R. Büller, J.W. Mulder, and E.C.M. van Gorp, *The hemostatic balance in HIV-infected patients with and without antiretroviral therapy: partial restoration with antiretroviral therapy*. AIDS patient care and STDs, 2009. 23(12): p. 1001-1007.
355. Cunningham, M.T., J.D. Olson, W.L. Chandler, E.M. Van Cott, C.S. Eby, J. Teruya, S.C. Hollensead, D.M. Adcock, P.M. Allison, K.K. Kottke-Marchant, and M.D. Smith, *External quality assurance of antithrombin, protein C, and protein s assays: results of the College of American Pathologists proficiency testing program in thrombophilia*. Archives of pathology & laboratory medicine (1976), 2011. 135(2): p. 227-232.
356. Rönsholt, F.F., H. Ullum, T.L. Katzenstein, J. Gerstoft, and S.R. Ostrowski, *Persistent inflammation and endothelial activation in HIV-1 infected patients after 12 years of antiretroviral therapy*. PloS one, 2013. 8(6): p. e65182-e65182.
357. Blom, A.M., B.O. Villoutreix, and B. Dahlbäck, *Complement inhibitor C4b-binding protein-friend or foe in the innate immune system?* Mol Immunol, 2004. 40(18): p. 1333-46.
358. Zanardelli, S., A.C. Chion, E. Groot, P.J. Lenting, T.A. McKinnon, M.A. Laffan, M. Tseng, and D.A. Lane, *A novel binding site for ADAMTS13 constitutively exposed on the surface of globular VWF*. Blood, 2009. 114(13): p. 2819-28.
359. Zheng, Y., J. Chen, and J.A. López, *Flow-driven assembly of VWF fibres and webs in vitro microvessels*. Nat Commun, 2015. 6: p. 7858.
360. Zhou, F., T. Yu, R. Du, G. Fan, Y. Liu, Z. Liu, J. Xiang, Y. Wang, B. Song, X. Gu, L. Guan, Y. Wei, H. Li, X. Wu, J. Xu, et al., *Clinical course and risk factors for mortality of*

- adult inpatients with COVID-19 in Wuhan, China: a retrospective cohort study.* Lancet, 2020. 395(10229): p. 1054-1062.
361. Wu, C., X. Chen, Y. Cai, J. Xia, X. Zhou, S. Xu, H. Huang, L. Zhang, X. Zhou, C. Du, Y. Zhang, J. Song, S. Wang, Y. Chao, Z. Yang, et al., *Risk Factors Associated With Acute Respiratory Distress Syndrome and Death in Patients With Coronavirus Disease 2019 Pneumonia in Wuhan, China.* JAMA Intern Med, 2020. 180(7): p. 934-943.
362. Aibibula, M., K.M. Naseem, and R.G. Sturme, *Glucose metabolism and metabolic flexibility in blood platelets.* J Thromb Haemost, 2018. 16(11): p. 2300-2314.
363. Brown, A.C., E. Lavik, and S.E. Stabenfeldt, *Biomimetic Strategies To Treat Traumatic Brain Injury by Leveraging Fibrinogen.* Bioconjug Chem, 2019. 30(7): p. 1951-1956.
364. Johnson, V.E., M.T. Weber, R. Xiao, D.K. Cullen, D.F. Meaney, W. Stewart, and D.H. Smith, *Mechanical disruption of the blood–brain barrier following experimental concussion.* Acta Neuropathologica, 2018. 135(5): p. 711-726.
365. Muradashvili, N., R.L. Benton, K.E. Saatman, S.C. Tyagi, and D. Lominadze, *Ablation of matrix metalloproteinase-9 gene decreases cerebrovascular permeability and fibrinogen deposition post traumatic brain injury in mice.* Metab Brain Dis, 2015. 30(2): p. 411-26.
366. Jenkins, D.R., M.J. Craner, M.M. Esiri, and G.C. DeLuca, *Contribution of Fibrinogen to Inflammation and Neuronal Density in Human Traumatic Brain Injury.* J Neurotrauma, 2018. 35(19): p. 2259-2271.
367. Camire, R.M., M. Kalafatis, P. Simioni, A. Girolami, and P.B. Tracy, *Platelet-derived factor Va/Va Leiden cofactor activities are sustained on the surface of activated platelets despite the presence of activated protein C.* Blood, 1998. 91(8): p. 2818-29.
368. Gould, W.R., J.R. Silveira, and P.B. Tracy, *Unique in vivo modifications of coagulation factor V produce a physically and functionally distinct platelet-derived cofactor: characterization of purified platelet-derived factor V/Va.* J Biol Chem, 2004. 279(4): p. 2383-93.

VITA

Martha Mega Silvia Sim

Education and Training

- 2018 - 2023 Ph.D. program in Molecular and Cellular Biochemistry,
University of Kentucky, Lexington, KY, USA
- 2016 - 2018 M.Sc. in Medical Sciences, University of Kentucky, Lexington, KY, USA
- 2013 Board Certification of Primary Physician, Indonesia
- 2011 - 2013 Internship for Primary Physician, Lubuklinggau, Indonesia
- 2010 - 2011 Medical Doctor, Sriwijaya University, Palembang, Indonesia
- 2006 - 2010 B.Sc. in Medicine, Sriwijaya University, Indralaya, Indonesia

Professional Positions

- 2014 - 2016 Head of Quality Assurance Committee,
Myria General Hospital, Palembang, Indonesia
- 2014 - 2016 Member of Infection Control and Prevention Committee,
Myria General Hospital, Palembang, Indonesia
- 2013 - 2016 Medical Doctor, Emergency Department and ICU,
Myria General Hospital, Palembang, Indonesia
- 2013 Medical Doctor, Emergency Department,

Graha Mandiri Maternity Hospital, Palembang, Indonesia

- 2012 - 2013 Intern MD, Emergency Department and Clinic,
Siti Aisyah General Hospital, Lubuklinggau, Indonesia
- 2012 Intern MD, Puskesmas Simpang Priuk, Lubuklinggau, Indonesia

Awards and Honors

- 2022 Women in Science Award, 18th Midwest Platelet Conference
- 2022 Dr. Madhav and Dr. Radhika Devalaraja Outstanding Graduate Student
Thesis Award – University of Kentucky College of Medicine
- 2022 Abstract Achievement Award, 64th American Society of Hematology
Annual Meeting
- 2021 Outstanding Graduate Student Poster Presentation “The Deneys van der
Westhuyzen Award,” 23rd Gill Heart Institute Cardiovascular Research Day
- 2019 Travel Award, 21st Gill Heart Institute Cardiovascular Research Day
- 2016 - 2018 Fulbright award under Fulbright Indonesia for Research in Science and
Technology (FIRST) program
- 2007 - 2010 BBM scholarship during Bachelor of Medicine program, Sriwijaya
University
- 2006 - 2010 PPA scholarship during Bachelor of Medicine program, Sriwijaya
University

Scientific Publications

1. **Martha M.S. Sim**, Molly Mollica, Hammodah R. Alfar, Melissa Hollifield, Dominic W. Chung, Xiaoyun Fu, Daniëlle Coenen, Kanakanagavalli S. Prakhya, Siva Gandhapudi, Meenakshi Banerjee, Chi Peng, Xian Li, Alice C. Thornton, James Z. Porterfield, Jamie L. Sturgill, Gail A. Sievert, Marietta Barton-Baxter, Kenneth S. Campbell, Jerold G. Woodward, José A. López, Sidney W. Whiteheart, Beth A. Garvy, and Jeremy P. Wood. Von Willebrand Factor Contributes to Free Protein S Deficiency in Patients with SARS-CoV-2. (*Circulation Research*, submitted)
2. Xian Li, Xiaohong Song, Dlovan D. Mahmood, **Martha M.S. Sim**, Sara Bidarian, Jeremy P. Wood. Activated Protein C, Protein S, and Tissue Factor Pathway Inhibitor Cooperate to Inhibit Thrombin Activation. (*Journal of Thrombosis and Haemostasis*, submitted)
3. **Martha M.S. Sim** and Jeremy P. Wood. Dysregulation of Protein S in COVID-19. *Best Pract Res Clin Haematol*. 2022 Sep;35(3):101376
4. **Martha M.S. Sim**, Meenakshi Banerjee, Thein Myint, Beth A. Garvy, Sidney W. Whiteheart, and Jeremy P. Wood. Total Plasma Protein S Is A Prothrombotic Marker in People with HIV. *Journal of Acquired Immune Deficiency Syndrome*, 2022;90(4):463-471
5. W. Brad Hubbard, **Martha M.S. Sim**, KE Saatman, PG Sullivan, Jeremy P. Wood. Tissue factor release following traumatic brain injury drives thrombin generation. *Research Practice in Thrombosis and Haemostasis*, 2022 Jun 8;6(4):e12734
6. Tanya Myers-Morales, **Martha M.S. Sim**, Tanner J. DuCote, Erin C. Garcia. *Burkholderia multivorans* requires species-specific GltJK for entry of a contact-dependent growth inhibition system protein. *Molecular Microbiology*, 2021 Sep;116(3):957-973
7. Xian Li, **Martha M.S. Sim**, Jeremy P. Wood. Recent Insights into the Regulation of Coagulation and Thrombosis. *Arteriosclerosis, Thrombosis, and Vascular Biology*, 2020;40:e119–e125